12-2009

The role of O-GlcNAc signaling in acute myocardial ischemia.

Gladys Afor Ngoh
University of Louisville

THE ROLE OF *O*-GlcNAc SIGNALING IN ACUTE MYOCARDIAL ISCHEMIA

By

Gladys Afor Ngoh

B.S., University of Buea-Cameroon, 2004
M.S., University of Louisville, 2007

A Dissertation Submitted to the Faculty of the Graduate School of the University of Louisville in Partial Fulfillment of the Requirements for the Degree of

Doctor of Philosophy

Department of Physiology & Biophysics
University of Louisville
Louisville, Kentucky

December, 2009

THE ROLE OF *O*-GlcNAc SIGNALING IN ACUTE MYOCARDIAL ISCHEMIA

By

Gladys Afor Ngoh

B.S., University of Buea, 2004
M.S., University of Louisville, 2007

A Dissertation Approved on

October 21, 2009

By the following Dissertation Committee:

Dissertation director: Steven P. Jones, Ph.D.

Dissertation co-director: Irving G. Joshua, Ph.D

Stanley E. D'Souza, Ph.D

Suresh C. Tyagi, Ph.D

William L. Dean, Ph.D

DEDICATION

This dissertation is dedicated to my mother, Mrs. Ngoh nee Abiliwuh Ambe Jennet and my sister, Muriel Anonjei Ngoh. Mami, you helped me realize the importance of education as a child and made the sacrifices for me to achieve my greatest potential. Muriel, your example and sacrifice, helped me acquire the discipline necessary to pursue my dreams. I will be eternally grateful. Thank you both for the love, support and encouragement. Mami and Muriel, I am truly blessed to have you as a mother and sister respectively.

ACKNOWLEDGMENTS

I have many people to thank for helping me through this academic process. First, I want to thank Dr. Steven P. Jones, my research mentor for his support, guidance, and patience in the planning and execution of this great research project. I am truly privileged to have worked with Dr. Jones as my mentor. I will always be grateful to him for imparting in me the ability to think critically and encouraging me to believe in myself. We will work together again in the future.

I greatly appreciate the assistance of my dissertation committee, Drs. Irving Joshua, Suresh Tyagi, Stanley D'Souza and William Dean. I could not have asked for a more cooperative and supportive committee. Thank you so much for the many chances to learn.

My sincere gratitude goes to my extended mentors, Drs. Irving Joshua, William Wead, Ayotunde Adeagbo, and Tariq Hamid. Drs. Joshua and Wead, thank you for giving me an opportunity to succeed. You were all there with me from the beginning. You were always there to help, made sure I adjusted to my new environment and also adapted to life as a graduate student. Thanks for your continued support and counsel. Thanks Dr. Adeagbo for your encouragement and support. Thanks Dr. Hamid for all the technical support, critique, and for making me a better scientist.

I extend special and sincere thanks to my brother Ndumeya E. Ngoh and baby sisters, Yvette N. Ngoh and Barbara A. Ngoh for their love, support, and encouragement. You always called, texted or emailed to let me know you were praying for me all the time.

Special thanks to my dear friend, Nikia Myers. You helped me adjust to my new environment and taught me the basics of the American culture. You came in to my life just when I needed someone to support, love and trust. Nikia, you prayed with me and celebrated with me. I am blessed to have you as a friend.

Thanks to my lab mates; Linda T Harrison, Dr. Heberty Facundo, Lewis J. Watson and Eli Brainard for keeping this research experience an exciting and interesting challenge. I could not have asked for better Lab mates. I am especially grateful to Linda Harrison for teaching me the basics in the lab, proofing my abstracts and manuscripts, and for being patient even when I took forever to respond to her questions. Dr. Facundo, I am also very thankful for your critique, technical advice and for always listening to my numerous questions.

Thanks to my Intervarsity family especially the Throckmorton's and LeCompte's for making sure that even when I was overwhelmed with research, I could still make time to glorify God.

I am especially grateful for the support of my friend, late Stephen Nkabyo. You were there from the very first day I entered the US and you gave me my first lesson on American culture and what to expect.

Thank you to all Cameroonians (alumni and present) at the University of Louisville Health Science Center. You guys have been such a good and supportive family.

I wish to thank my classmates; Dorothea Rosenburger and Alex Porter for their friendship and kindness.

Finally, thanks to the entire faculty of the Department of Physiology and Biophysics for their continuous support and encouragement and the Integrated Programs in Biomedical Sciences (IPIBS), University of Louisville for giving me the opportunity to pursue a Ph.D in Physiology.

ABSTRACT

THE ROLE OF *O*-GlcNAc SIGNALING IN ACUTE MYOCARDIAL ISCHEMIA

Gladys Afor Ngoh

October 21, 2009

O-linked β-N-acetylglucosamine (*O*-GlcNAc) is an inducible, dynamically cycling, and reversible post-translational modification of serine/threonine amino acid residues of nucleocytoplasmic and mitochondrial proteins. *O*-GlcNAc transferase (OGT) adds, while *O*-GlcNAcase (GCA) removes *O*-GlcNAc from proteins. Albeit being a recruitable stress-induced signal in other tissues, the role of *O*-GlcNAc in the heart is unknown. Therefore, we hypothesized that *O*-GlcNAc is recruited in the heart during acute stress, and enhanced O-GlcNAc is cardioprotective. Subjecting neonatal rat cardiac myocytes (NRCMs) to hypoxia, or mice to myocardial ischemia reduced O-GlcNAc signaling. Augmented O-GlcNAc signaling attenuated, while diminished O-GlcNAc signaling exacerbated post-hypoxic cardiomyocyte death. To determine how O-GlcNAc protects, we identified numerous proteins including voltage dependent anionic channel (VDAC) to be O-GlcNAc-modified via mass spectrometry and immunoprecipitation. Since VDAC is a putative member of the mitochondrial

permeability transition pore (mPTP), we hypothesized that one mechanism of O-GlcNAc-mediated cardioprotection is by blocking mPTP formation. We ascertained if O-GlcNAc signaling affects key players in ischemic/hypoxic injury, Ca^{2+} overload and oxidative stress, both inducers of mPTP. Enhanced O-GlcNAc significantly mitigated, while, reduced O-GlcNAc aggravated post-hypoxic Ca^{2+} overload and ROS generation. Furthermore, augmented O-GlcNAc reduced, while, diminished O-GlcNAc sensitized mitochondria to mPTP formation according to Ca^{2+}-induced swelling. Since mPTP formation induces loss of mitochondrial membrane potential ($\Delta\psi_m$), we evaluated whether O-GlcNAc signaling affects post-hypoxic $\Delta\psi_m$ recovery. Enhanced O-GlcNAc significantly improved, while reduced O-GlcNAc minimized post-hypoxic $\Delta\psi_m$ recovery. Because ER stress contributes to ischemia-reperfusion injury, we evaluated whether inhibiting maladaptive ER stress reponse maybe another mechanism through which O-GlcNAc signaling cardioprotects. Indeed, augmented O-GlcNAc reduced maladaptive ER stress response according to diminished CHOP levels and PI positivity. To determine if such *in vitro* protection could be translated *in vivo*, we augmented O-GlcNAc levels (with PUGNAc) in adult, wild-type C57BL6 mice, subjected them to 40 minutes of left anterior descending coronary artery ligation, then reperfused for 24 hours, and assessed infarct size. Augmented O-GlcNAc levels significantly decreased infarct size. We conclude that O-GlcNAc mediates cardioprotection *in vitro* and *in vivo* via attenuating maladaptive ER stress response and recruitment of early events in the mitochondrial death pathway leading to mPTP formation.

TABLE OF CONTENTS

LIST OF TABLES

LISTS OF FIGURES

CHAPTER I

INTRODUCTION

According to the World Health Organization (WHO), ischemic heart disease is one of the leading causes of death worldwide, with about 3.8 million men and 3.4 million women dying yearly from this disease. In the United States, ischemic heart disease resulting from coronary artery disease is devastating, with 1.5 million US citizens developing myocardial infarctions that account for nearly 200,000 deaths per year (1, 2). The National Heart Lung and Blood Institute estimate that an average 14.2 years of life is lost due to a heart attack.

Nine easily measured and potentially modifiable risk factors account for over 90% of the risk of an initial acute myocardial infarction (MI). The effect of these risk factors is consistent in men and women, across different geographic regions, and by ethnic group, making the study applicable worldwide. These nine risk factors include cigarette smoking, abnormal blood lipid levels, high blood pressure, diabetes, abdominal obesity, a lack of physical activity, low daily fruit and vegetable consumption, alcohol overconsumption, and psychosocial index (329). Extensive clinical and statistical studies by the American Heart Association reveal that in addition to these nine factors, aging, gender, race, and stress also increase the risk of developing ischemic heart disease.

Despite prevalence of ischemic heart disease, better treatments for minimizing post-ischemic cardiac injury remain limited. A primary limitation to such advances may be our incomplete understanding of why cardiac myocytes die. Moreover, few ongoing efforts address the metabolic aspect of myocardial ischemia-reperfusion injury. The heart is an energy omnivore with energy requirements exceeding that of any of the body's other organs (274, 275). Despite its huge energy requirements, the heart has limited energy reserves and must therefore continually produce large amounts of ATP to sustain its function. In order to sustain this enormous energy demands, energy metabolism of the myocardium is coupled to ATP hydrolysis. It is widely accepted that alterations in cardiac energy substrate availability have significant effects on the energetic status of the heart. Therefore, it is likely that any imbalances to this tightly regulated system may contribute to the development and, perhaps exacerbate ischemic heart disease. Hence, a clear understanding of cardiac metabolism and its regulation under normal and pathological conditions is essential for the determination of how any potential treatment could be targeted in an attempt to alleviate the morbidities associated with ischemic heart disease.

Finally, an ongoing debate is whether the irreversible cardiomyocyte injury occurs primarily during ischemia or upon reperfusion. Understanding when irreversible myocardial injury occurs is relevant, because this would aid in the development of drugs and clinically allow the administration these cardioprotective drugs.

CHAPTER II

BACKGROUND AND LITERATURE REVIEW

1. Acute myocardial infarction (MI)

Commonly known as heart attack, MI is a manifestation of ischemic heart disease. It results from decreased or complete blockade of blood flow to the heart muscle. The resulting hypoxia decreases both aerobic fatty acid and glucose oxidation causing damage and potential death of heart tissue. Hypoxia reduces the oxygen supply to the myocardial cells leading to inhibition of oxidative reactions, diminished rate of ATP production by oxidative phosphorylation, modulation of protein kinase activities, and changes in the expression of specific genes (177). Because it is difficult to completely mimic the *in vivo* ischemic environment in isolated heart and/or cultured cardiomyocyte studies, hypoxia combined with procedures that inhibit aerobic glycolysis are frequently used, so that the main mechanical features of ischemia can be observed (235).

One hallmark of MI is a reduction in myocardial oxygen supply, i.e. there is a mismatch between oxygen supply and demand (Figure 1). This is manifested in a switch of myocardial energy substrate preference from fatty acid to glucose. Hence, there is a shift in heart metabolism from aerobic fatty acid metabolism to anaerobic glycolysis, which provides energy for critical myocardial cellular

processes (235). This alteration in substrate utilization results in the uncoupling between glycolysis and glucose oxidation. In aerobic glycolysis, glucose is broken down to pyruvate generating ATP and NADH in glycolysis. This pyruvate is further converted to acetyl CoA and more reducing molecules are generated in a process called glucose oxidation. Acetyl CoA then enters Krebs cycle, making more reducing molecules (NADH and $FADH_2$) through several enzyme catalyzed reactions. These reducing equivalents then enter the electron transport chain where they are utilized to generate electrons to reduce oxygen as well as a proton motive force necessary for ATP synthesis. However, in anaerobic metabolism, glucose oxidation is inhibited and glycolytic pyruvate is no longer converted to acetyl CoA. Instead glycolytic pyruvate is reduced to lactic acid which accumulates in the cytosol causing intracellular acidosis (99). This decrease in myocardial intracellular pH alters the sensitivity of contractile proteins and sarcoplasmic Ca^{2+} pump to Ca^{2+}. Decrease in glucose oxidation also diminishes oxygen-dependent oxidative phosphorylation. Therefore, the switch in substrate preference coupled with the change in substrate availability inhibits mitochondrial oxidative metabolism, forcing the heart to be more dependent on anaerobic glycolysis for energy its energy requirement (274).

Another consequence of myocardial ischemia is increased glucose utilization in cardiac tissues (235). The ischemia-mediated increase in glucose utilization is characterized by enhanced rates of exogenous glucose uptake *in vivo* (99, 266) due to increased GLUT 1(26) expression, GLUT 4(281) translocation to the plasma membrane, and increased hexokinase activity (212).

Because glucose transport is an essential metabolic function necessary for cell survival, alteration in glucose flux through the disruption of blood flow to the myocardium exerts profound metabolic dysfunction and intricately affects intracellular physiologic processes. Thus, MI may be considered an acute and direct metabolic insult.

During reperfusion (or reoxygenation), cardiac myocytes are subjected to abrupt biochemical and metabolic changes such as mitochondrial reenergization, generation of reactive oxygen species, intracellular and mitochondrial Ca^{2+} overload, restoration of cellular pH and activation of inflammation due to immediate resumption of oxidative functions as shown in Figure 1(245). During reoxygenation, damage of sarcolemmal membrane, reverse functioning Na^{+} - Ca^{2+} exchanger, and ROS-mediated sarcoplasmic reticulum dysfunction mediate further Ca^{2+} influx into the already Ca^{2+}-overloaded cardiac myocytes causing cardiomyocyte death via hypercontracture. Moreover, restoration of mitochondrial membrane potential drives Ca^{2+} entry into the mitochondria. This, together with the loss of the inhibitory effects of acidic pH on mitochondrial permeability transition pore (mPTP) and the generation of ROS, mediate mPTP opening (Figure 1). Opening of mPTP causes cardiac myocyte death by dissipating mitochondrial membrane potential, uncoupling oxidative phosphorylation, and inducing mitochondrial swelling.

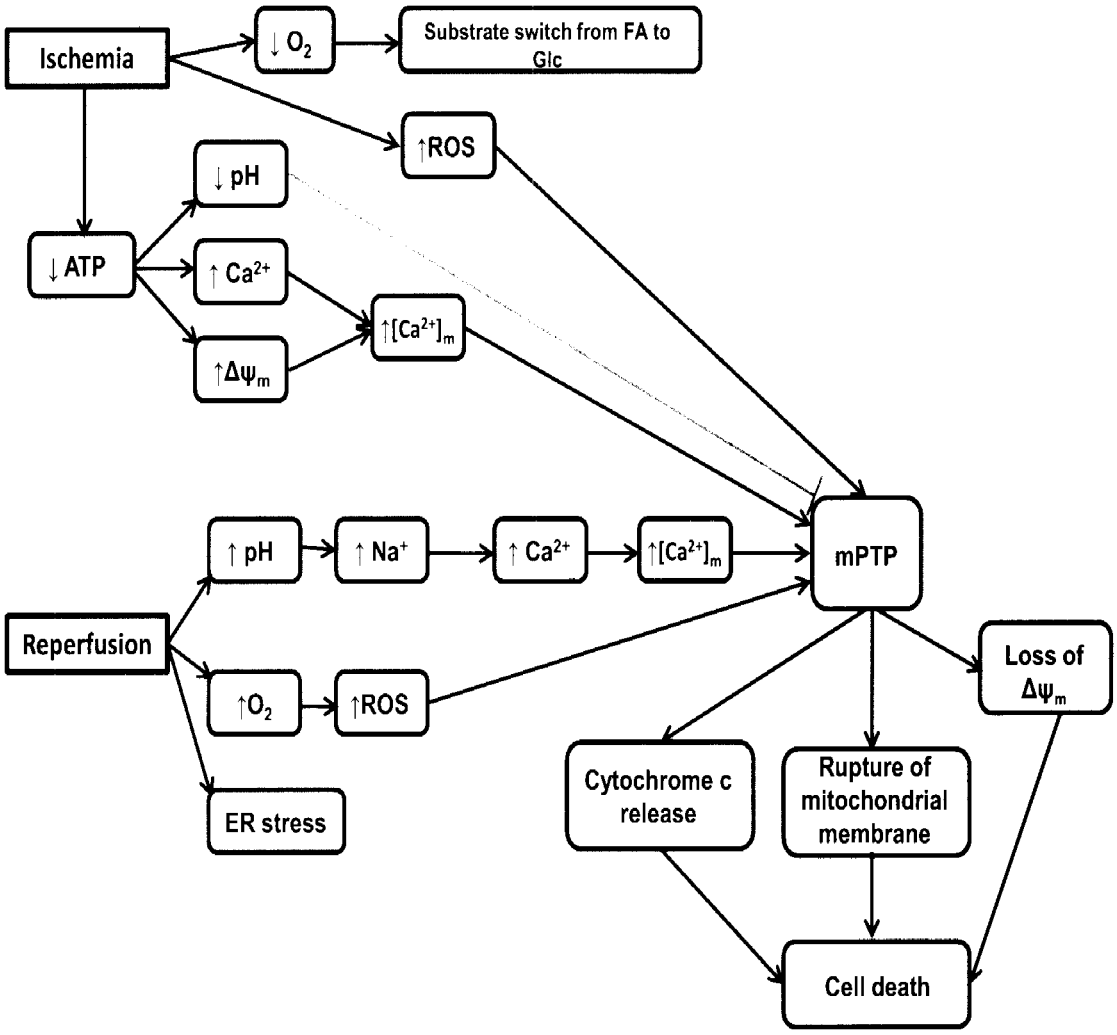

Figure 1. Molecular events occurring during myocardial ischemia-reperfusion injury. During myocardial reperfusion, the ischemic myocardium is subjected to abrupt biochemical and metabolic changes which adds to the changes generated during myocardial ischemia. These changes include mitochondrial reenergization ($\uparrow\Delta\psi_m$), generation of reactive oxygen species (ROS), intracellular ($[Ca^{2+}]_i$) and mitochondrial ($[Ca^{2+}]_m$) calcium overload and the restoration of intracellular pH. These factors interact with each other and mediate cardiomyocyte death via mitochondrial permeability transition pore (mPTP) formation. mPTP formation results in loss of mitochondrial membrane potential ($\Delta\psi_m$), massive matrix swelling, outer mitochondrial membrane rupture, and the release of the apoptotic signaling protein, cytochrome c, all culminating in cell death.

1. A. What causes cardiomyocyte death following MI?

1. A. I. Calcium Overload

Ca^{2+} primarily enters cardiac myocytes through L-type Ca^{2+} channels. Once in the cell, it induces Ca^{2+}-induced-Ca^{2+} release from the sarcoplasmic reticulum (SR). This increased intracellular calcium leads to cardiac myocyte contraction during systole. The Na^{+}-Ca^{2+} exchanger (NCX) and sarcolemmal Ca^{2+}-ATPase are responsible for removal of the cytosolic Ca^{2+} post contraction during diastole. NCX removed most of the Ca^{2+} that entered the myocyte via L-type Ca^{2+} channels while SR/Endoplasmic Reticulum ATPase (SERCA) removes the Ca^{2+} released by the SR (18, 77).

Ischemia causes intracellular ($[Ca^{2+}]_i$) and mitochondrial ($[Ca^{2+}]_m$) calcium overload (Figure 1)(94, 143, 218, 219, 224, 244, 260, 276-278). The primary source of the rise in $[Ca^{2+}]_i$ is via reverse functioning NCX. Ischemia causes metabolic acidosis that in turn activates the sodium-hydrogen exchanger (NHE) which facilitates the extrusion of H^{+} in exchange for Na^{+} thus, leading to high intracellular Na^{+} ($[Na^{+}]_i$)(219). Moreover, ischemia induces depolarization of the plasma membrane. Both the increased $[Na^{+}]_i$ and the depolarization of the plasma membrane result in the reversal of NCX to bring Ca^{2+} into the myocyte. Studies have shown that interventions that directly (via inhibition of L-type Ca^{2+} channel or NCX) or indirectly (blocking increased $[Na^{+}]_i$ via inhibition of NHE) attenuate the rise in $[Ca^{2+}]_i$, and reduce ischemia-reperfusion injury (37, 143, 162, 219, 224, 308). In the mitochondria, Ca^{2+} uptake is via the mitochondrial Ca^{2+} uniporter and it is driven by the mitochondrial membrane potential ($\Delta\psi_m$).

Hence, $[Ca^{2+}]_m$ uptake dissipates $\Delta\psi_m$ and unless electron transport continually resynthesizes this gradient, there will be no driving force for ATP synthesis in the mitochondria. Ca^{2+} is removed from the mitochondria primarily via the mitochondrial NCX. The rise in $[Ca^{2+}]_m$ observed during ischemia is mainly due to reverse functioning mitochondrial NCX (94). In fact, blocking mitochondrial NCX attenuates ischemia-induced $[Ca^{2+}]_m$ overload (94).

During reperfusion, there is a transient early increase in $[Ca^{2+}]_i$ as shown in Figure 1. This is because the slow return of intracellular pH to normal, facilitates $[Na^+]_i$ accumulation and subsequently $[Ca^{2+}]_i$ increase via reverse functioning NCX. If cardiac myocytes are not permanently damaged, $[Ca^{2+}]_i$ returns to near normal levels. But if cardiac myocytes are irreversibly damaged either due to dysfunction of Ca^{2+} handling proteins (262, 271), abnormal $[Na^+]_i$ levels (262), or abnormal ATP levels (229), $[Ca^{2+}]_i$ continues to rise throughout reperfusion. Since the reintroduction of oxygen during reperfusion, and resumption of oxidative metabolism regenerates $\Delta\psi_m$, one might expect significant $[Ca^{2+}]_m$ uptake. Indeed, studies have shown an additional rise in $[Ca^{2+}]_m$ during reperfusion (94).

1. A. II. Reactive Oxygen Species (ROS) generation

Reactive oxygen species are a class of radical and non-radical oxygen-containing molecules that display high reactivity with lipids, proteins and nucleic acids. Consequently, ROS are very unstable and highly reactive, and they tend to initiate chain reactions that result in irreversible chemical changes in lipids or

proteins. These potentially deleterious reactions can result in profound cellular dysfunction and even cytotoxicity. High levels of ROS can trigger cell death, whereas lower levels drive diverse and important cellular functions. The primary source of ROS in cardiac myocytes is the mitochondrial electron transport chain (ETC)(67, 142). Cardiac myocytes are rich in mitochondria, which in addition to providing the large amount of energy required to maintain cardiac output, can produce ROS that contribute to ischemia-reperfusion injury (183). The mitochondrial ETC produces ROS by the transfer of unpaired electrons from complex I and from ubisemiquinone of complex III to molecular oxygen (100, 159). Also, "electron leakage" may contribute to ROS generation. It is estimated that approximately 5% of the oxygen consumed by myocytes are transformed into ROS. Because of this, mitochondria are targets for ROS damage. Additional sources of ROS generation include neutrophils, oxyradical generation from xanthine oxidase, autooxidation of catecholamines, activation of various NAD(P)H oxidases and reactive nitrogen species. These additional sources become the primary source of ROS generation when prolonged ischemia irreversibly disrupts ETC (75, 87). Basally generated ROS are efficiently detoxified by endogenous enzymatic antioxidants, such as superoxide dismutase, glutathione peroxidase, and catalase (211, 314). However, under conditions associated with excess ROS generation, such as ischemia-reperfusion injury, the flux of ROS generated by tissues can exceed the capacity of endogenous oxidant defense mechanisms to detoxify ROS and prevent deleterious ROS-mediated reactions.

Ischemia/hypoxia augments ROS generation in the intact myocardium and isolated cardiac myocytes (9, 14, 166). In fact, Zweier *et al.* demonstrated using electron spin resonance of frozen ground hearts that 20 minutes of ischemia increased ROS production (340). Interventions that prevent ischemia-mediated rise in ROS regeneration reduce myocardial ischemia-reperfusion injury. Indeed, Lesnefsky *et al.* showed that inhibition of electron transport during ischemia protects cardiac mitochondria and reduces ischemia-reperfusion injury (186).

During reperfusion, a large burst of ROS has been consistently shown to occur (Figure 1)(166, 302, 339). This burst in ROS generation during reoxygenation has been attributed to damage of electron transport chain components resulting in inefficient electron transfer. Several studies have shown that addition of antioxidants or scavengers delay irreversible myocardial damage or attenuate ischemia-reperfusion injury (7, 43, 168). Overexpression of manganese superoxide dismutase reduces infarct size in mice (157). Moreover, treatment of *in vivo* or *in vitro* hearts with antioxidants reduced ROS generation (22).

1. A. III. Mitochondrial permeability transition pore (mPTP) formation

The mPTP is a non-specific pore spanning both the outer mitochondrial membrane (OMM) and inner mitochondrial membrane (IMM) shown in Figure 2. This pore allows molecules <1.5kDa to enter and exist the mitochondria. Even though the molecular composition of mPTP is still debatable, mPTP may reflect

interaction of several proteins that would connect the mitochondrial matrix to the cytosolic space. A relatively simple model was first proposed to constitute cyclophilin D (CyP-D) in the matrix, adenine nucleotide translocase (ANT) in the IMM and voltage dependent anionic channel (VDAC) in the OMM (104, 259). This simplistic model was later made complex by the addition of several other proteins such as the benzodiazepine receptor (BdR), hexokinase (HK) and creatine kinase (CK) to accommodate the variety of effectors acting on the mPTP (205, 259). An alternative model of mPTP proposes that mPTP would be formed by clusters of misfolded proteins.

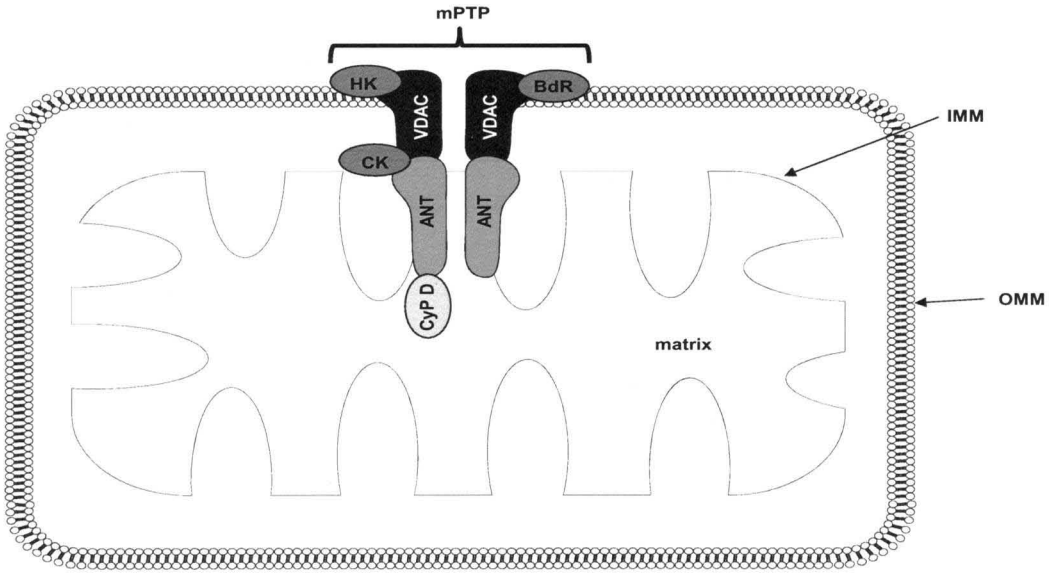

Figure 2. Mitochondrial permeability transition pore complex (mPTP). mPTP is a non-specific pore that allows molecules <1.5kDa to pass in and out of the mitochondria. As described in the text, mPTP is thought to constitute cyclophilin D (CyP D) in the matrix, adenine nucleotide translocase (ANT) in the inner mitochondrial membrane (IMM) and voltage dependent anionic channel (VDAC) in the outer mitochondrial membrane (OMM). Other components thought to regulate mPTP include benzodiazepine receptor (BdR), Hexokinase (HK) and creatine kinase (CK). IMS refers to the intermembranous space.

Voltage dependent anionic channel (VDAC) proteins are the most abundant protein in the OMM (Figure 2) and exist as three isoforms (VDAC-1, VDAC-2, and VDAC-3). VDAC was first discovered over 30 years ago as a channel protein more permeable to Cl^- than to K^+ (263). Later, VDAC was shown to be a single channel with ion selectivity that reacts to membrane potential (51). Recently, VDAC was shown to transport ATP and interact with molecules that need to be in close proximity to ATP (258). VDAC interacts with hexokinase (206), creatine kinase (265) and members of the Bcl family (Bcl-2, Bak and Bax)(269, 270, 304). Hence, VDAC serves as a binding partner for proteins that mediate and regulate the integration of mitochondrial functions with other cellular activities. VDAC is thought to play a critical role in mitochondrial death pathways. The role of VDAC in mPTP and mitochondrial-mediated apoptosis is still being debated. Earlier reports indicated that VDAC might be required for cytochrome c release from the mitochondria during apoptosis (269, 270). Indeed, there is evidence that VDAC-2 plays an important role in suppressing apoptosis in mice by sequestering Bak and that VDAC-2 null MEFs are more susceptible to apoptosis (38). Additionally, several lines of evidence suggested that the OMM protein involved in mPTP formation might be VDAC: purified VDAC incorporated into planar phospholipid bilayers formed a channel with electrophysiological properties similar to those of mPTP; VDAC channel properties changed in the presence of NADH, glutamate or Ca^{2+}; and finally chromatography of mitochondrial extracts on a CyP-D matrix allowed for the purification of VDAC and ANT, which in the presence of CyP-D catalyzed the

CsA-sensitive permeabilization of liposomes to solutes. Recently, work by Krauskopf *et al* (171) and Baines *et al* (11) dispute the role of VDAC in mPTP and apoptosis. Baines *et al.* showed that VDACs are dispensable for mPTP formation (11). Moreover, eliminating VDAC isoforms by genetic knockout or knockdown using small interfering RNAs, did not affect mPTP formation. Furthermore, VDAC-deficient mouse embryonic fibroblast exhibited similar cellular response and mitochondrial response to Ca^{2+} overload, oxidative stress and Bax-Bid activation as control cells (11).

In addition to their normal physiological function of exchanging mitochondrial ATP for cytosolic ADP, ANTs has been implicated in cell death. There exist three ANT isoforms (ANT1, ANT2, and ANT3) in humans and two isoforms (ANT1 and ANT2) in mice. ANTs operate as gated pores located in the inner mitochondrial membrane (Figure 2) such that when occupied by transportable substrates, they alternate between two conformations in which the ADP/ATP-binding site is either on the matrix side of the IMM (m-state) or on the cytoplasmic side (c-state). ANT ligands that bind to the m-state (e.g. bongkrekic acid, BKA) inhibit mPTP formation while c-state ligands (e.g. carboxyatractyloside (CAT), pyridoxal phosphate) activate mPTP. The involvement of ANT in mPTP formation was first demonstrated in studies in which ATP and BKA inhibited opening of the mPTP by decreasing its sensitivity to Ca^{2+} while CAT and adenine nucleotide depletion both triggered pore opening by sensitizing the pores to Ca^{2+}. This notion is now questionable following a recent study by Kokoszka *et al.* showing that liver mitochondria from mice lacking

ANT were sensitive to CsA inhibitable mPTP (169). Moreover, Konkoszka and Wallace studies revealed that the mPTP in ANT-null mitochondria were insensitive to opening by atracyloside and to closure by ADP, all compounds that affect PTP opening through ANT (102, 169).

CyP D, a product of the *Ppif* gene, is a member of the cyclophilin family. CyP-D is located in mitochondrial matrix (Figure 2) and exhibits peptidyl-prolyl cis-trans isomerase (PPIase) activity. The involvement of CyP-D in mPTP formation was first suggested when similar concentration of CsA was found to inhibit mitochondrial cyclophilin activity and block mPTP opening (106, 213). Moreover, mitochondrial cyclophilin and mPTP showed comparable sensitivities to CsA analogues (93, 231). CyP-D favors mPTP opening by facilitating the Ca^{2+}-induced conformational change. Such earlier findings were later confirmed by studies using CyP-D knockout mice from several groups (10, 12, 58, 106, 223, 264, 267). These studies revealed that CyP-D regulates mPTP, CyP-D null mitochondria were not responsive to Ca^{2+}, and CyP-D is a relevant factor for mPTP modulation but not required for its formation and opening. Additionally, mPTP formation in CyP-D null mitochondria is not inhibited by the mPTP blocker cyclosporine A (CsA) and mPTP opening is essential for mitochondrial-mediated necrotic cell death but dispensable for mitochondrial-mediated apoptotic cell death (10, 12, 58, 106, 223, 264, 267).

Factors that regulate mPTP can be classified as matrix or membrane effectors (Table 1). Matrix effectors such as mitochondrial Ca^{2+} overload (16, 17), oxidized pyridine nucleotides (40, 61, 63), high inorganic phosphate and

increased mitochondrial ROS (31, 40, 60, 61, 107) favor PTP, while CsA (24, 64), bongkrekate (140, 180), and matrix pH below 7(16, 17, 104, 141) inhibit mPTP formation. Membrane effectors including amphipathic anions (like fatty acids produced by phospholipase A_2) favor mPTP (25, 242), while polycations (spermine)(179), amphipathic cations (sphingosine, trifluoperazine)(25) and positively charged peptides (253) inhibit mPTP opening.

Table 1: Known inducers and inhibitors of mPTP

	Matrix Effectors	**Membrane Effectors**
Favor mPTP	Mitochondrial calcium overload	Amphipathic anions
	Oxidized pyridine nucleotides	
	High inorganic phosphates	
	Increased mitochondrial ROS generation	
	carboxyatractyloside	
Inhibit mPTP	Cyclosporine A (CsA)	Polycations e.g. Spermine
	Bongkrekate	Amphipathic cations e.g. spingosine
	Matrix pH < 7	Positively charged peptides

Agents that prevent mPTP formation attenuate ischemia-reperfusion injury. In fact, known mPTP inhibitors, cyclosporine A (CsA) and it analog sanglifehrin A, have been shown to protect cardiac myocytes against reoxygenation injury (95, 227, 320) and decrease infarct size in various species

(122, 123) . CsA has also recently been shown to reduce infarct size in humans during percutaneous coronary intervention procedure (243). Furthermore, cardioprotective interventions such as ischemic preconditioning, ROS scavengers, inhibitors of the Na^+-H^+ exchanger and Ca^{2+} antagonists have been shown to inhibit mPTP formation as part of the mechanisms through which they confer cytoprotection (68, 101, 104). In addition, mice lacking CyP-D, a putative mPTP component are less susceptible to ischemia-reperfusion injury (10, 223). The inhibitory effect of CsA and its analogs involves interaction with CyP-D that reduces sensitivity of pore opening to Ca^{2+}.

1. A. IV. Endoplasmic Reticulum (ER) stress

Proper protein synthesis, folding, and transport are essential for cell survival. The rough endoplasmic reticulum (ER) is involved with maintaining proper synthesis, folding, and transport of proteins targeted to membranes and organelles (20). Conditions that alter the ionic balance, molecular chaperones, protein glycosylation machinery, and/or redox status of the ER lumen cause ER stress and trigger an intracellular signaling system called the unfolded protein response (UPR, Figure 3)(23, 36, 163, 195, 261). Initially, the UPR promotes adaptation to reestablish normal ER function. Such adaptation occurs by reducing the quantity of protein synthesized in the ER, inducing the expression of genes that enhance protein folding capacity of the ER, promoting ER-associated protein degradation to remove misfolded proteins, and reestablishing the ER luminal environment to that suitable for new protein synthesis and folding (Figure

3). Such initial responses are designed to resolve the stress and ultimately enhance the chances of survival, but if the ER stress is prolonged, the maladaptive arm of the UPR is activated causing cell death as shown Figure 3 (284).

ER stress has been implicated in the pathogenesis of several diseases including ischemia-reperfusion injury (249, 293). One study showed that numerous UPR genes are induced within 24 hours of myocardial infarction in mice (117). Moreover, several studies have shown that interventions that inhibit ER stress in the heart attenuate ischemia-reperfusion injury in mice or hypoxic injury in cultured cardiac myocytes (230, 249, 286, 289).

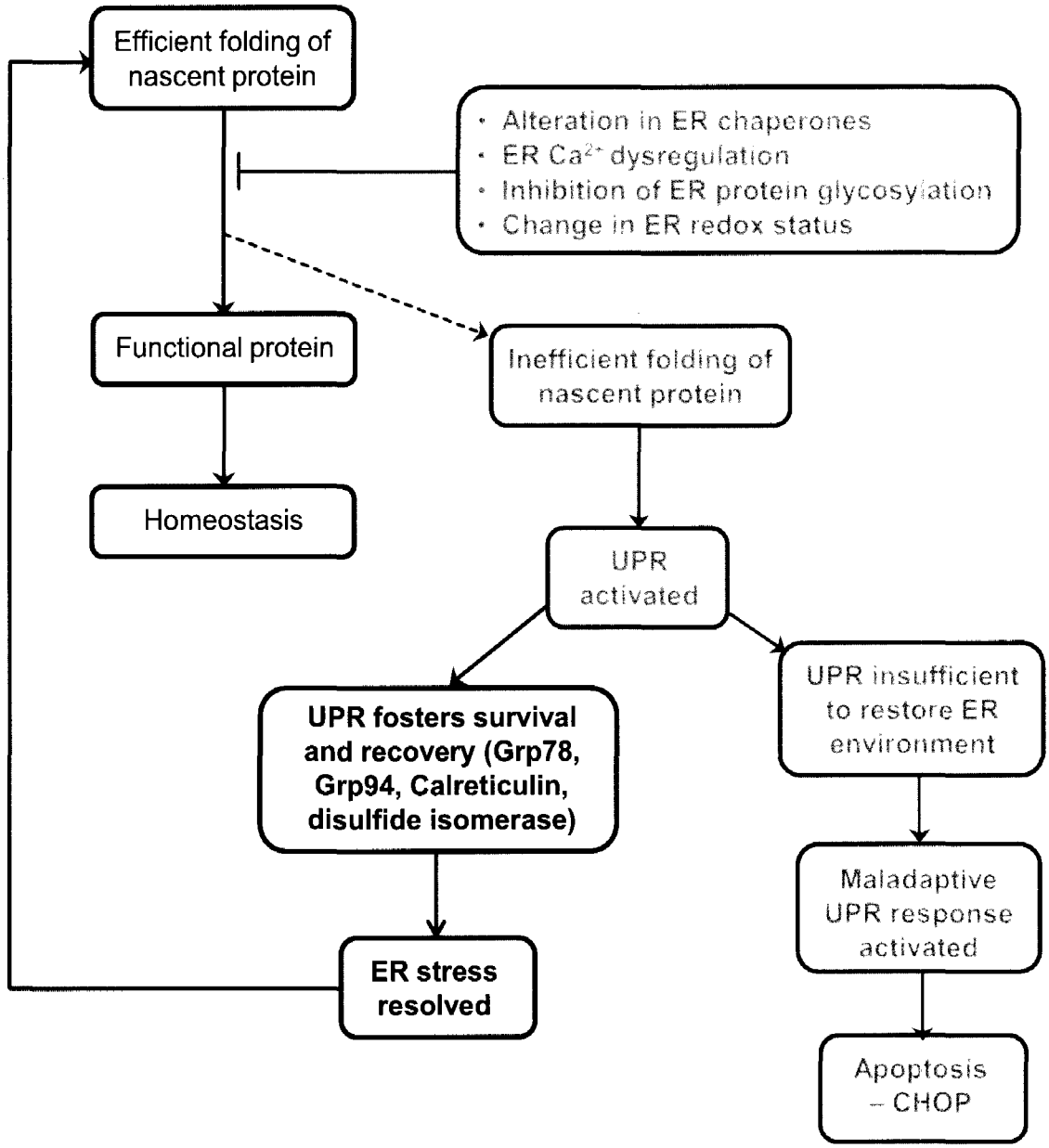

Figure 3. Unfolded protein response (UPR). Under non-stressed conditions, proteins synthesized in the ER are efficiently folded. Stressors that perturb the ER protein glycosylation machinery, ER Ca^{2+} levels, and/or redox status results in accumulation of misfolded proteins in the ER and initiates the unfolded protein response (UPR). The initial action of the UPR is geared towards restoring normal ER environment via increased synthesis of ER chaperones (e.g. glucose regulated peptides 94(Grp 94) and 78 (Grp 78)), calcium binding proteins (e.g.calreticulin) and protein disulfide isomerases (PDI)). If ER stress is not resolved during the prosurvival phase, maladaptive UPR is activated leading to apoptosis. CHOP/GADD153 - growth arrest and DNA damage 153.

1. B. Cardioprotective mechanisms

1. B. I. Ischemic Preconditioning

Inducing brief non-lethal episodes of ischemia and reperfusion to the heart prior to an episode of sustained lethal myocardial ischemia has the capacity to dramatically reduce myocardial ischemia-reperfusion injury. This phenomenon, termed ischemic preconditioning (IPC), is a transient, self-defense mechanism present in the heart and many other organs including the kidney, liver, and brain (220). IPC significant and reproducible and serves as the gold standard for studies of cardioprotection (152). IPC reduces myocardial infarct size, lactate generation and rate of fall of ATP. There are two "windows" of protection afforded by preconditioning, "early" and "late" preconditioning. The protective effect of early IPC is mediated by posttranslational modification and is lost if the time between the initial IPC protocol and the sustained ischemia is greater than one hour (292). The late or second window of preconditioning involves gene up regulation and occurs 24 hours after preconditioning.

Intense investigation of the mechanisms responsible for the protective effects of preconditioning has revealed numerous potential mediators and downstream effectors of preconditioning (Figure 4), but cause and effect relationships have not been fully delineated. However, Tong *et al.* and others have successfully demonstrated that ischemic preconditioning enhances glucose uptake (147, 296, 309). Moreover, preconditioned hearts have less anaerobic glycolysis, hence make less lactate and have less acidic pH during ischemia (221, 278). Interestingly, the rate of ATP consumption is slower for PC hearts

(221, 278). Two hypotheses have been put forward to explain why PC hearts have reduced ATP hydrolysis: 1. IPC might inhibit ATP breakdown by reverse mode functioning of mitochondrial ATP synthase confirmed by *in vitro* and *in vivo* data from several groups (69, 97, 149, 187, 207, 328). 2. The ATPase inhibitor subunit might bind to and inhibit the mitochondrial ATPase during IPC. Data from several groups show that IPC and diazoxide enhance early binding of ATPase inhibitor subunit to mitochondrial ATPase (6, 52, 59). Contrarily, Grover's (89) and Jennings' (303) groups found no evidence supporting inhibition of ATP synthase in PC hearts. IPC has also been shown to decrease Ca^{2+} overload (218), oxidative stress (301), and PTP formation (123, 148).

Recent studies suggest that IPC also activates several signaling pathways (Figure 4). The most prominent is the activation of G-protein coupled receptors. Activation of GPCRs leads to activation of the phosphoinositide-3-kinase (PI3K) pathway. The action of PI3K is attributed to the generation of phosphatidylinositol 3,4,5-phosphate (PIP_3). PIP_3 facilitates phosphoinositide-dependent protein kinase 1 (PDK1) phoshorylation and activation of substrates like Akt (PKB), p70S6K, Protein Kinase C (PKC), extracellular regulated kinase (ERK), p38 MAPK, JNK, PKC-ε, and eNOS/NO to mediate cardioprotection. In fact, Tong *et al* showed PC induced PI3K-mediated cardioprotection was via activation of targets upstream of PKC (297). Moreover, phosphatase and tensin homolog deleted chromosome ten (PTEN) which regulates PIP_3, is degraded during PC and might be involved in GPCR recycling (30, 73, 298).

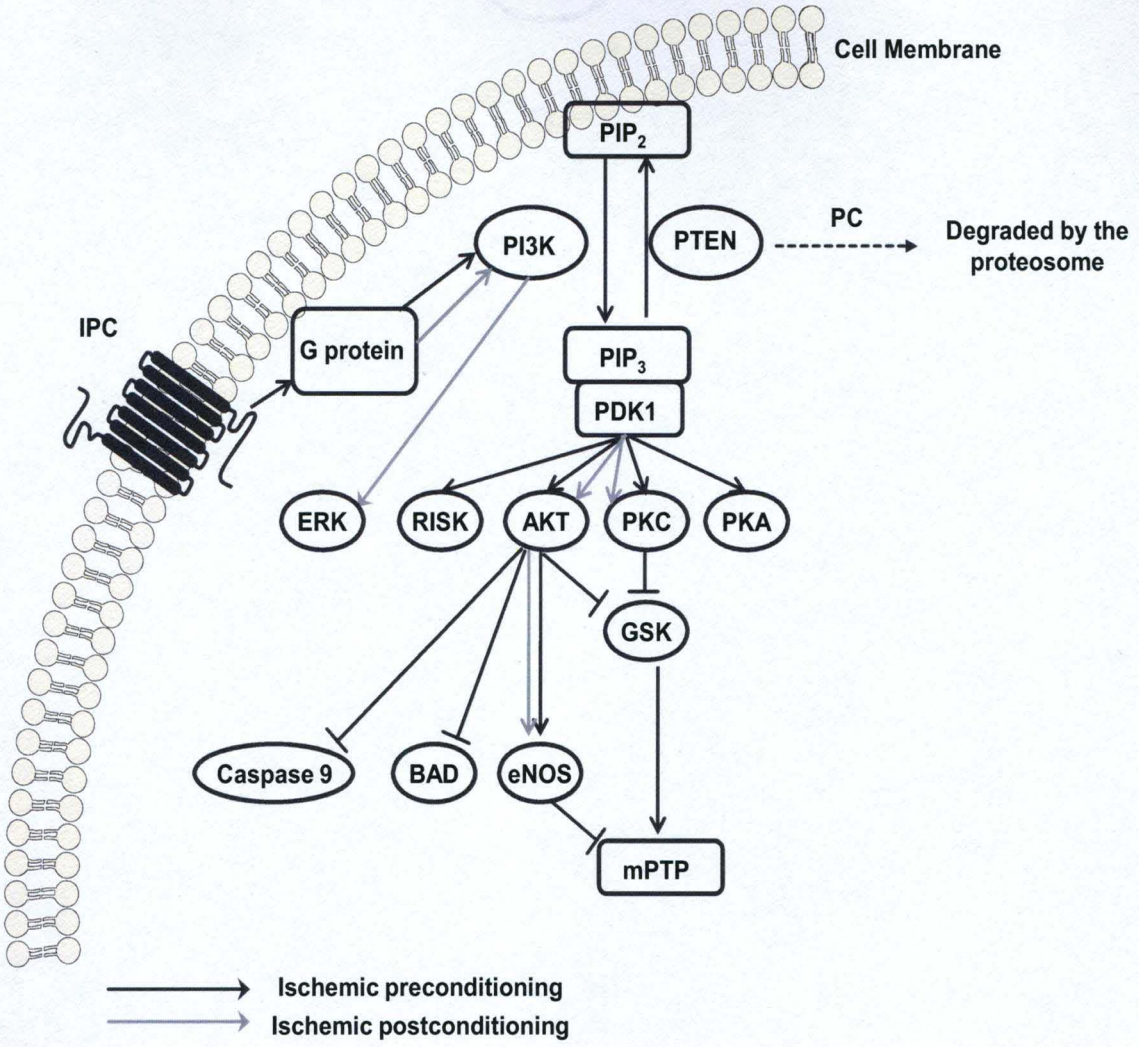

Figure 4. Summary of signaling pathways activated by ischemic preconditioning and postconditioning. IPC leads to release of agonists that activate G proteins coupled receptor (GPCR), leading to activation of phosphoinositide 3-kinase which in turn activates protein kinase B (PKB or AKT), PKA, PKC, and extracellular regulated kinase (ERK) signaling pathways. These pathways converge on the mitochondrial where they inhibit mitochondrial permeability transition pore (mPTP) formation. PIP2 – phosphatidylinositol 3,4-diphoshpate, PIP3 – phosphatifylinositol3,4,5-triphoshate, PDK1 – protein dependent kinase 1, PTEN - phosphatase and tensin homolog deleted on chromosome ten, GSK-glycogen synthase kinase, eNOS – endothelial nitric oxide synthase.

1. B. II. Reperfusion Injury Survival Kinases (RISK pathway)

The RISK pathway refers to a group of protein kinases that when activated during myocardial reperfusion confers cardioprotection (126, 327). Extensive preclinical data have amassed showing that pharmacologic preconditioning (126, 127), IPC, or postconditioning(124) activation of RISK pathway reduces infarct size by up to 50%. Indeed, Hausenloy *et al.* showed that ERK and Akt were activated at the start of reperfusion and blockade of ERK and Akt at the start of reperfusion blocks PC-mediated protection in PC hearts (124). RISK pathway is thought to reduce myocardial ischemia-reperfusion injury by inhibiting mPTP formation(66), improving SR calcium uptake (3, 246) and by activation of antiapoptotic pathways (327).

1. B. III. Postconditioning

Interrupting myocardial reperfusion with brief cycles of myocardial ischemia and reperfusion reduces infarct size. This phenomenon, termed ischemic postconditioning, was first reported by Zhao *et al* in 2003 (335). In this study, after 45 minutes of sustained myocardial ischemia in dogs, the interruption of reperfusion with three 30 second cycles of ischemia and reperfusion reduced myocardial infarct size from 47% to 11% (335). Thus, the myocardial reperfusion phase could be a target of cardioprotection. Although the exact mechanisms through which postconditioning confers protection are not fully understood, postconditioning has been shown to inhibit lethal reperfusion injury through the same mechanisms as IPC (Figure 4)(124). Postconditioning activates PI3K

pathway which results in the activation of downstream targets like PKC, PKG/NO, and MAPK to mediate cardioprotection. Ischemic postsconditioning also targets important mediators of ischemia-reperfusion injury such as oxidative stress, $[Ca^{2+}]_i$ overload, neutrophil accumulation (336) and cellular pH (49). Moreover, ischemic postconditioning activates the RISK pathway (126) and blocks opening of the mPTP (125).

2. Hexosamine Biosynthetic Pathway (HBP)

Intracellular glucose normally provides substrate for metabolic processes. In general, upon entering the cell, glucose is rapidly phosphorylated by hexokinase to glucose-6-phosphate which either enters glycogen metabolism or reversibly converted to fructose-6-phosphate for primarily glycolysis (Figure 5). Thus, glycogen synthesis and glycolysis uses ≈90-95% of cellular glucose. Less than 5% of the remaining cellular glucose is shunted to a unique accessory pathway, the hexosamine biosynthetic pathway (208). This pathway involves a series of enzyme catalyzed reactions ending with the formation of uridine diphosphate-N-acetylglucosamine (UDP-GlcNAc, Figure 5). HBP begins with the rate limiting conversion of fructose-6-phosphate to glucosamine-6-phosphate by *L*-glutamine: fructose-6-phosphate amidotransferase (GFAT) using glutamine as the amide donor (Figure 5). The next critical reaction involves the modification of the hexosamine core in the conversion of glucosamine-6-phosphate to N-acetylglucosmaine-6-phosphate by glucosamine-6-phosphate acetyltranseferase (Emeg32) using acetyl-coenzyme A (CoA, Figure 5). The final step involves

exergonic pyrophosphorylation of glucosamine-1-phosphate to uridine diphosphate-β-N-acetylglucosamine (UDP-GlcNAc) by UDP-GlcNAc pyrophosphorylase (Figure 5). Once formed, UDP-GlcNAc serves as the glycosidic precursor for glycoproteins, glycolipids, proteoglycans, and more germane to this research project, serves as the nucleotide sugar for the post-translational glycosylation of nuclear, cytoplasmic and mitochondrial proteins (O-GlcNAc). Despite using less than 5% of cellular glucose, UDP-GlcNAc, is second only to ATP in terms of the intracellular concentration of high energy compounds (209). Flux through HBP can be increased by adding exogenous glucosamine. Glucosamine enters the cell via a glucose transporter and is phosphorylated by hexokinase to glucosamine-6-phosphate, thus by-passing GFAT and rapidly increasing UDP-GlcNAc levels(204).

Data on how the critical enzymes of the HBP are regulated is unexpectedly very limited. GFAT activity is glutamine-dependent and can be inhibited by the glutamine analogues 6-azido-5-oxo-*L*-norleucine (DON) and O-diazoacetyl-*L*-serine (azaserine)(215). There are two isoforms of GFAT; GFAT1 and GFAT2 transcribed from separate genes. GFAT1 is highly expressed in the pancreas, placenta and testes while, GFAT2 is more abundant in the heart and central nervous system. Eukaryotic GFAT is highly conserved and regulated transcriptionally (241), post-translationally by cAMP-dependent protein kinase(35, 136) and by UDP-GlcNAc feedback inhibition (88). Phosphorylation of GFAT1 decreases its activity while phosphorylation of GFAT2 increases its

activity. Emeg32, another critical enzyme of the HBP, is important for maintaining proper intracellular UDP-GlcNAc concentration (21).

The diverse nature of the precursors of UDP-GlcNAc potentially links HBP to several metabolic pathways (Figure 5). First, less than 5% cellular glucose siphoned to the HBP (203). Second, glutamine, a nonessential amino acid highly abundant in muscle cells enters the HBP at the rate limiting step, potentially linking HBP to amino acid metabolism. Third, acetyl-CoA, produced primarily from fatty acid and pyruvate oxidation in the mitochondria, enters HBP during the acetylation of the glucosamine core to form N-acetylglucosamine-6-phosphate, possibly links HBP to fatty acid metabolism. Finally, ATP enters the HBP at the final step i.e. the conversion of N-acetylglucosamine-1-phosphate to UDP-GlcNAc by UDP-GlcNAc pyrophosphorylase, linking HBP to nucleotide metabolism. Therefore, UDP-GlcNAc and hence O-GlcNAc might act as a nutrient and/or metabolic sensor.

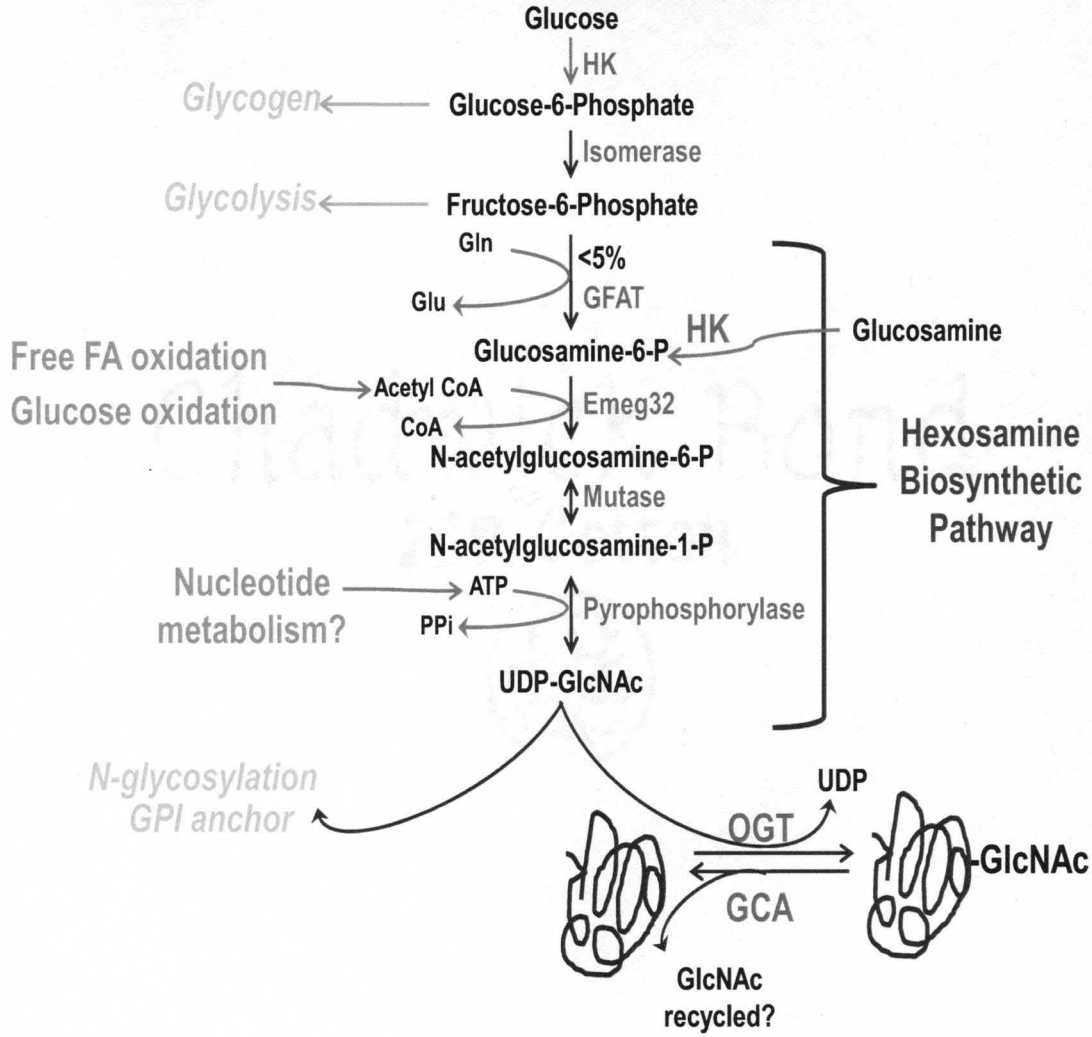

Figure 5. Hexosamine biosynthetic pathway (HBP). Once cells take up glucose, it is first phosphorylated by hexokinase. This phosphorylated glucose either enters glycogen synthetic pathway or is further converted to fructose-6-phosphate by glucose-6-phosphate isomerase. The majority of fructose-6-phosphate is channeled to glycolysis. Of the remainder, between <5% is channeled to an accessory pathway for glucose metabolism, the hexosamine biosynthetic pathway (HBP). This pathway begins with the rate limiting conversion of fructose-6-phosphate to glucosamine-6-phosphate by L-glutamine:D-fructose-6-phosphate amidotransferase (GFAT). The next critical reaction involves acetylation of gluocsamine-6-Phosphate by glucosamine-6-phosphate acetyltransferase (Emeg32) to for N-acetylglucosamine-6-phosphate (GlcNAc-6-P). Next are two reversible reactions: first the conversion of GlcNAc-6-P to GlcNAc-1-P by phosphate-acetylglucosamine mutase, and then the formation uridine diphosphate- GlcNAc (UDP-GlcNAc) by UDP-GlcNAc pyrophosphorylase.

3. What is O-GlcNAc

3. A. O-GlcNAc biology

Beta-O-linked N-acetylglucosamine (*O*-GlcNAc) is a post-translational sugar modification of eukaryotic proteins (Figure 6) first described in 1984 by Torres and Hart in a study in which soluble β-1-4 galactosyltransferase was used to probe lymphocyte plasma membrane for surface glycans (300). This study was ground breaking at that time because not only were glycosylated proteins thought to exist only in luminal compartments and on cell surfaces, but, also all glycosylation processes were thought to be largely static. The addition of *O*-GlcNAc to proteins from UDP-GlcNAc stores is a metabolic post-translational modification occurring in the cytoplasm, nucleus, and potentially mitochondria.

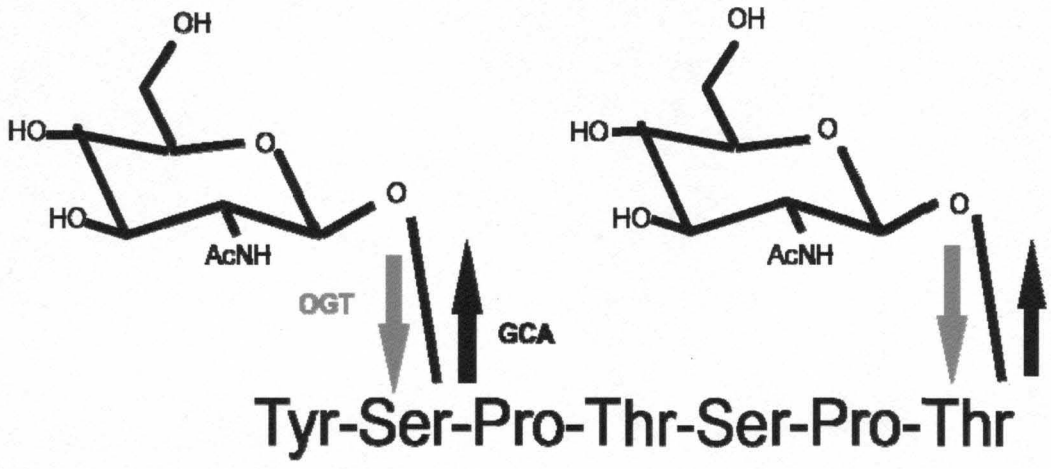

Figure 6. O-GlcNAc transferase (OGT) adds, while O-GlcNAcase (GCA) removes GlcNAc molecule from Ser/Thr residues of mature nuclear, cytoplasmic and mitochondrial proteins.

O-GlcNAcylation is in many ways distinct from the "classical" protein glycosylation in that: 1. O-GlcNAc modified proteins are found mostly within the nucleus, cytoplasm or mitochondria versus cell surfaces, the lumen of membranous organelles, the endoplasmic reticulum and Golgi apparatus for N-glycosylation (118, 138). 2. O-GlcNAc is not elongated into complex structures or further modified (with the exception of nuclear pore protein) unlike the extraordinarily complex array of glycans found on extracellular glycoproteins (131, 132, 300). 3. O-GlcNAc rapidly cycles on and off proteins on a time scale similar to that for phosphorylation/dephosphorylation, unlike extracellular complex glycans, which are static (70, 79, 176, 255). 4. There is no obvious consensus sequence for the addition of O-GlcNAc to proteins while N-glycosylation has Asn-X-Ser/Thr sequence (where X could be any amino acid other than proline or aspartic acid). 5. GlcNAc is added to proteins through an O-linkage on the hydroxyl group of Ser/Thr while in N-glycosylation the monosaccharide is added through an N-linkage on the amide group of Asn.

Akin to phosphorylation, O-GlcNAcylation is one of the most common post-translational modifications. O-GlcNAc is similar to a protein phosphorylation in that: 1. Both O-GlcNAcylation and phosphorylation post-translational modifications are found on serine and threonine residues (119, 120). 2. Both modifications are dynamically added and removed from proteins in response to cellular signals (44, 45, 160). 3. Both alter the functions and associations of the modified protein. Conversely, O-GlcNAc differs from protein phosphorylation in that only two enzymes control the addition and removal of the O-GlcNAc post-

translational modification from proteins, while over 600 genetically distinct kinases and phosphatases exist in mammalian cells.

O-GlcNAc modified proteins do not have a consensus sequence, but most of the sites of *O*-GlcNAc addition mapped so far have a Pro-Val-Ser motif similar to that recognized by proline-directed kinases. Moreover, many phosphorylation sites are also known glycosylation sites (44, 45). O-GlcNAc and O-phosphate site-mapping studies so far suggest that there are at least four different types of dynamic interplay between O-GlcNAc and O-phosphate. There is evidence of competitive occupancy at the same site; for example, that which occurs in the transcription factor c-Myc(46, 47, 160), estrogen receptor-β(39), oncoprotein SV-40 large T-antigen(214) and endothelial nitric oxide synthase(74). In competitive occupancy, O-GlcNAcylation and O-phosphorylation compete for the same site and have antagonistic effects. Next, there exist competitive and alternative occupancy occurring at adjacent sites, such as in tumor suppressor p53(323) and synapsin I(50). Hence, it is possible that O-GlcNAcylation can inhibit phosphorylation at adjacent sites by steric hindrance or modulation of protein structure. Another, interplay between O-GlcNAc and O-phosphate described is a complex interplay whereby some O-phosphate attachment sites on a given protein are the same as some O-GlcNAc sites, whereas others are adjacent to, or even distant from each other, as on the C-terminal domain of RNA polymerase II(53) and on cytokeratins 8 and 18(45). The finally type of interplay involves proteins in which this relationship has yet to be clearly defined. The interplay between O-GlcNAc and O-phosphate is also underscored by the recent finding

that OGT transiently forms complexes containing the catalytic subunit of protein phosphatase 1 (PP1c)(311), hence there may exist a single enzyme complex for the addition of GlcNAc and removal of phosphate. Additionally, many known *O*-GlcNAc sites have the PEST sequence (Pro-Glu-Ser-Thr), a sequence associated with rapid degradation suggesting that *O*-GlcNAcylation at these sites might slow or prevent protein degradation(113). O-GlcNAcylation affects protein trafficking and localization for example c-Myc (160), Tau(182), and Stat5a(85, 225) have a larger portion of the O-GlcNAcylated form located in the nucleus than cytoplasm.

3. B. Enzymatic regulation of O-GlcNAc cycling

Modulation of protein O-GlcNAcylation is achieved by the concerted action of two highly evolutionarily conserved enzymes, a uridine diphospho-N-acetylglucosamine: peptide β-N-acetylglucosaminyl transferase (OGT) and O-β-N-acetylglucosaminidase (O-GlcNAcase aka GCA, OGA, or MGEA5).

O-GlcNAc transferase (OGT) is a soluble, ubiquitously expressed, and highly conserved enzyme in all multicellular eukaryotic organisms involved with the addition of a single β-N-acetylglucosamine (GlcNAc) moiety (from UDP-GlcNAc) via an O-linkage to serine/theronine amino residues of mature nuclear, cytoplasmic and mitochondrial proteins as shown in Figure 6(110, 112, 173, 199). OGT is expressed in all examined tissue types and is most abundant in the glucose-sensing cells of the pancreas and in the brain. OGT is primarily located in the nucleus and has an optimum pH of about 6(173, 199). OGT is encoded by a single copy X-linked gene in mammals while plants have two OGT homologs

spy and secret agents (121, 173, 199, 268). Even though OGT is coded by a single gene in mammals, alternative splicing of OGT mRNA leads to three potential isoforms, nucleocytoplasmic OGT (ncOGT), mitochondrial OGT (mOGT) and short OGT (sOGT)(173, 199, 232). These isoforms share an identical C-terminal catalytic domain but have distinct N-terminal domains contributing to their differential localization and unique targeting sequences (115, 198, 232). Structurally, OGT contains an N-terminal tetratricopeptide repeat (TPR), a linker region and C-terminal catalytic domains (173, 199). TPR domain consists of a 34 amino acid repeat varying from 3-12 involved in inter-subunit interaction, protein-protein interaction, subcellular targeting, substrate recognition, cell cycle regulation and transcriptional control (13, 144, 145, 151, 174, 199, 326). The linker region is the least conserved sequence of OGT. The catalytic domain of OGT is thought to have a UDP-GlcNAc binding site and is involved with the glycosylation of proteins (319). Post-translational modification of OGT by tyrosine phosphorylation and O-GlcNAc modification, UDP-GlcNAc concentration and protein-protein interaction are thought to regulate OGT activity (42, 173, 199). Recently, insulin signaling was shown to regulate OGT (316, 324). In these studies, insulin increased post-translational OGT phosphorylation and O-GlcNAcylation, OGT activity and transient translocation from nucleus to the cytoplasm (316, 324). In neuro-2a neuroblastoma cells, OGT mRNA and protein expression are regulated in an AMP-activated protein kinase-dependent manner, whereas OGT enzymatic activity is regulated in a p38 MAPK-dependent manner (41). Moreover, activated p38 has been shown to interact with OGT and

recruit it to specific substrates, such as neurofilament H during glucose deprivation in neuroblastoma cells (41). Tissue specific OGT mutation causes disturbance in somatic cell function(234) while OGT deletion is embryonically lethal(268), hence O-GlcNAc is important for cellular viability.

O-β-N-acetylglucosaminidase (O-GlcNAcase, aka GCA, OGA, or *MGEA5*) is a soluble, highly conserved enzyme, expressed in all eukaryotic organisms involved with the removal of O-GlcNAc modification from proteins (Figure 6)(84). O-GlcNAcase is primary located in the cytoplasm with an optimum pH of 5.5-7 and coded for by a single gene. Structurally, O-GlcNAcase is a 917 amino acid protein with an N-terminal hexosaminidase and a C-terminal histone acetyltransferase domain (HAT)(56, 78, 84, 130, 295). The N-terminal domain is similar to hyaluronidase and was originally identified as a meningioma expressed antigen 5(56, 78, 84, 130). While there may be some activity against hyaluronan, the preferred substrate for O-GlcNAcase is O-GlcNAc (84, 310). The C-terminal histone acetyltransferase domain acetylates free histones and nucleosomal histone proteins (295). O-GlcNAcase is cleaved by caspase 3 into HAT and hexosaminidase domains with no change in the activity of each domain. Protein-protein interaction and phosphorylation are thought to regulate O-GlcNAcase activity (84, 310). Two splice variants of O-GlcNAcase have been reported in rats, both lacked O-GlcNAcase activity but retained HAT activity. The spliced variant detected in Goto-Kakizaki rats (~90kDa) lacks exon 8 while the spliced variant in Sprague-Dawley (~84kDa) lacks both exons 8 and 9.

The fact that OGT is known to associate with histone deacetylase complexes(326) and promote transcriptional silencing (326), while O-GlcNAcase has a HAT domain(295), has led to the hypothesis that O-GlcNAcylation plays a role in the regulation of transcription. Such hypothesis has been supported by studies identifying numerous transcription factors to be regulated by O-GlcNAc-modification (146, 165, 178, 325). O-GlcNAcylation can either suppress or enhance transcription, depending on the promoter involved and other associated proteins. The transcription factor STAT5A is known to alter gene activation by preferentially binding to the co-activator of transcription, CREB-binding protein when O-GlcNAc modified (85). O-GlcNAc modification of Sp1 has multiple effects on the function of the transcription factor (146). Augmented O-GlcNAc modification of SP1 has been shown to drive the transcription of plasminogen activator and extracellular matrix proteins that have an important role in diabetic cardiovascular disease while reduction of Sp1 glycosylation led to an increase in Sp1 proteasome susceptibility (113).

3. C. Pharmacologic regulation of O-GlcNAc cycling

Pharmacological approaches to better understand the role of enzymes controlling the presence of *O*-GlcNAc on proteins in biological and pathological processes have been limited due to lack of specific high-affinity inhibitors (Table 2). Alloxan, a uracil and UDP-GlcNAc analog, may be an irreversible inhibitor of OGT (170). The drawbacks of this compound include its ability to inhibit many other enzymes using uridine as substrate, its reactivity with many cellular

components like DNA (285) and also, its ability to inhibit O-GlcNAcase(181). Compounds "4" (aka TT04) and "5" (aka TT40) inhibit OGT by competing with UDP-GlcNAc for the same site on OGT(96); however, there are relatively few reports of their use in biological systems. *O*-GlcNAcase, unlike OGT, has several known pharmacologic inhibitors. Streptozotocin (STZ), a diabetogenic compound and GlcNAc analog, inhibits *O*-GlcNAcase by binding to its active site, leading to the formation of energetically more stable transition state ligands (254, 294). Results from studies using STZ as an *O*-GlcNAcase inhibitor should be interpreted with caution because of its cytotoxic effects on pancreatic cells and its ability to reduce cellular NAD levels (27). Whether the STZ-mediated increase in *O*-GlcNAc levels is due to secondary or other toxic effects remains debatable. Furthermore, Macualey *et al.* showed that STZ had no effect on *O*-GlcNAcase activity *in vitro* (200). PUGNAc, a GlcNAc analog, prevents the binding of *O*-GlcNAcase to GlcNAc (134). Even though PUGNAc lacks the cytotoxic effects of STZ(111), it inhibits other lysosomal hydrolases and shows little specificity for *O*-GlcNAcase over hexosaminidase (200). 1,2-dideoxy-2-methyl-D-glucopyranoso[2,1-*d*]-2-thiazoline (NAG-thiazoline) and its derivatives inhibit *O*-GlcNAcase and have 1500-fold greater specificity for *O*-GlcNAcase over hexosaminidase than PUGNAc(200). GlcNAcstatin, a glucoimidazole-based inhibitor, has been shown to inhibit *O*-GlcNAcase in the picomolar range with 100,000-fold selectivity over lysosomal hexosaminidase in human embryonic kidney 293 and SH-SY5Y neuroblastoma cell lines but has not been as widely studied as PUGNAc (71). This may be more selective and potent than PUGNAc

and NAG-thiazoline. Thiamet-G, another *O*-GlcNAcase inhibitor, has also recently been developed (330). Again, few studies have addressed the role of *O*-GlcNAcase inhibition beyond the use of PUGNAc or NButGT. As with inhibitors of OGT, concern remains regarding the off-target effects of PUGNAc, STZ, and other putative inhibitors of *O*-GlcNAcase. Thus, the use of other approaches, such as RNA interference or adenoviruses, could clarify some of the off-target effects of the aforementioned pharmacologic approaches.

Table 2: Common pharmacologic inhibitors of OGT and GCA

O-GlcNAc Transferase (OGT)	O-GlcNACase (GCA)
Alloxan (Konrad et al., 2002)	PUGNAc (Horsch et al., 1991)
Compound 4 (Gross et al., 2005)	Streptozotocin (Roos et al., 1998)
Compound 5 (Gross et al., 2005)	Alloxan (Lee et al., 2006)
	NButGT (Macauley et al., 2005)
	GlcNAcstatin (Dorfmueller et al., 2006)
	Thiamet-G (Yuzwa et al., 2008)

3. D. Detection tools and methods

Despite its abundance and discovery two decades ago, few protein targets have been unequivocally and site-specifically identified as carrying an O-GlcNAc modification. This is due to the lack of specific and sensitive methods, which are further limited by the relatively labile nature of the modification, its limited mass,

its fast turnover(45, 255) and its lack of charge(315). One of the earlier developed approaches relied upon enzymatic labeling of terminal O-GlcNAc residues with radioactive uridine diphospho-galactose (UDP[^{3}H]Gal) using galactosyltransferase (114, 133, 256, 299). Since O-linkage of GlcNAc to protein is resistant to peptide/N-glycosidase F (PNGase F), nonspecifically UDP[^{3}H]Gal tagged N-linked oligosaccharides were cleaved by PNGase F treatment. The main limitation of this technique was that O-GlcNAc is not readily accessible to galactosyltransferase. Hence, galactosyltransferase will recognize any terminal GlcNAc residue, such as those found in many N-linked oligosaccharides. Consequently, definitive identification of O-GlcNAc modification requires further carbohydrate characterization. In addition, the donor sugar UDP–[3H]galactose has a very low specific activity (17–20 Ci/mmol), making this method insensitive compared to radiolabeling techniques with other isotopes, such as [32P]phosphate, with specific activities as high as 6000 Ci/mmol. Such a low specific activity of the sugar donor may require several weeks of exposure to detect O-GlcNAc.

Plant lectins like wheat germ agglutinin (WGA) or succinylated WGA have also been used for the detection and purification of O-GlcNAc-containing proteins (41, 288, 321). WGA does not recognize GlcNAc in a linkage-specific manner and therefore, samples must first be treated with peptide: N-glycosidase F (PNGase F) to remove the N-linked sugars. Another disadvantage of this method is that sWGA is less sensitive and only proteins with multiple O-GlcNAc residues are readily detected. Sensitivity may be improved by using sWGA-

conjugated sepharose column to isolate and enrich O-GlcNAc–modified proteins from cell extracts. Thus, the identification of *O*-GlcNAc by this existing method requires further carbohydrate analysis for confirmation.

Several monoclonal antibodies that recognize O-GlcNAc are commercially available, the most commonly used of these antibodies are referred to as RL2(133, 239, 272) and CTD110.6(54). RL2, generated against nuclear pore glycoproteins, recognizes a limited subset of O-GlcNAc proteins and requires protein determinants in addition to O-GlcNAc. CTD110.6, a murine monoclonal IgM raised against the O-GlcNAc–modified C-terminal domain of the RNA polymerase II large subunit, specifically recognizes single O-GlcNAc residues in β-O-glycosidic linkage to serine and threonine. CTD110.6 shows no apparent cross-reactivity with peptide determinants and apparently does not react with other closely related carbohydrate antigens. All of the antibodies are somewhat restrictive in their target specificity and may require more than one site of modification. Despite their limitations, these antibodies have proven invaluable in both early and ongoing studies of O-GlcNAc biology.

Several chemical approaches have also been developed to analyze O-GlcNAc residues(315). Alkaline ß-elimination can be used to generate radiochemically labeled O-GlcNAc moieties (114, 299) and introduce a radiochemical label if borotritide is used instead of borohydride in the reduction stage of the reaction. Another more recent approach, mild ß-elimination followed by Michael addition with dithiothreitol (BEMAD), is useful for mass spectrometry (312). Bertozzi's group (306) recently developed a purely chemical means of

detection involving the incorporation of an azido derivative of GlcNAc (GlcNAz) into protein targets of O-GlcNAc. Because the enzymes of O-GlcNAc modification (OGT and O-GlcNAcase) tolerate analogs of their natural substrates in which the *N*-acyl side chain has been modified to a bio-orthogonal azide moiety (GlcNAz), cells can be metabolically labeled or the reaction can be performed *in vitro* with recombinant galactosyltransferase. These O-azidoacetylglucosamine–modified proteins can be covalently derivatized with various biochemical probes at the site of protein glycosylation using Staudinger ligation. This strategy should have general application for both the identification of O-GlcNAc–modified proteins and mapping protein target sites that bear O-GlcNAc modification. Because UDP-GlcNAc is incorporated into several classes of glycoconjugates, specificity must be demonstrated with properly controlled experiments. Tagging-via-substrate (TAS)(226) and Click-chemistry(98) also use the same principle. These techniques are highly sensitive and especially useful for lower molecular weight proteins. Despite the development of such techniques, the lack of a recognizable consensus motif somewhat complicates the analyses of O-GlcNAc function and limits predictive capabilities.

3. E. How does *O*-GlcNAc signaling affect cellular function in disease?

Since its discovery two decades ago, *O*-GlcNAc has been implicated in a variety of pathological processes such as neurological diseases, cancer, diabetes, and insulin signaling. Genes encoding both OGT and *O*-GlcNAcase map to chromosomal regions associated with neurodegenerative diseases.

Neurodegenerative disorders result from disease-specific protein aggregates due to accumulation of certain major proteins (116, 161, 287). This protein accumulation may be due to defects in these proteins, accelerated rate of synthesis or defects in protein degradation. Since the ubiquitin-proteosome system (UPS) disposes of some of these protein aggregates (185, 202, 233), it is plausible that failure of the UPS would contribute to the pathogenesis of neurodegenerative disorders. Numerous studies have shown that proteosomal function is controlled by post-translational modification of its cap by O-GlcNAc (113, 279, 280, 334). Moreover, augmented O-GlcNAc modified proteosome is less active proteosome(334). Recently, Kan *et al.* showed that augmented O-GlcNAc modification in the brain (with streptozotocin) reduced cerebral function and induced neuronal apoptosis (192). Alzheimer's disease, a neurodegenerative disease is characterized by the aggregation of β-amyloid and microtubule-associated protein, tau in affected neurons. β-amyloid and tau proteins are *O*-GlcNAc-modified and the degree of *O*-GlcNAcylation has been shown to change in Alzheimer's disease(8, 90, 91). Moreover, the gene encoding O-GlcNAcase, the enzyme involved with the removal of O-GlcNAc modification, has been mapped to a region on chromosome 10q24.1 linked to Alzheimer's disease (55).

Altered protein glcosylation is known to correlate with tumorigenesis, but the role of O-GlcNAc in the pathogenesis of tumors is still to be determined. Many oncogene and tumor suppressor gene products, such as c-Myc, SV40 large T antigen, and p53, have been shown to be modified by O-GlcNAc. The oncogen, c-Myc is O-GlcNAc-modified at Thr-58, a known phosphorylation site.

O-GlcNAcylation of tumor suppressor gene p53 is known to increase DNA binding and transcriptional activity. The O-GlcNAcylation of oncogenes and tumor suppressor proteins emphasizes the critical roles of O-GlcNAcylation in cancer.

The vast majority of the data amassed so far on O-GlcNAc and cellular function are in the context of diabetes and dysregulation of insulin signaling. There is significant evidence suggesting that prolonged augmentation of O-GlcNAc levels either via increasing HBP flux(129, 257), overexpression of OGT(324), or inhibition of O-GlcNAcase(307), impair insulin signaling a hallmark of type II diabetes. Flux through HBP can be regulated by cellular glucose levels, GFAT or glucosamine. Adipocytes and muscles cells exposed to chronic high levels of glucose in the presence of insulin develop insulin resistance. Moreover, inhibition of GFAT (with DON) blocked the hyperglycemia-mediated insulin resistance while glucosamine treatment (enters HBP down stream of GFAT) restored the insulin resistant phenotype (129, 203, 208, 210, 257). Blockade of insulin-stimulated GLUT4 translocation and subsequent glucose uptake have been proposed as possible mechanisms through which hyperglycemia and glucosamine induce insulin resistance (29, 129). Direct manipulation of OGT and GCA, the enzymes involved with the regulation of O-GlcNAc modification, is associated with the pathogenesis of diabetic complications and insulin resistance. Interestingly, genetic studies reveal that mutation of GCA gene is associated with susceptibility to the development of diabetes in the Mexican American population (139, 184). In addition, nematodes (*C. elegans*) expressing

GCA null allele exhibited a phenotype metabolically similar to that of human type II diabetes (80). Overexpression of OGT in cardiac myocytes impaired calcium cycling via inhibition of SERCA, a phenotype reversed by ectopic overexpression of GCA(48). Also, pharmacologic augmentation of O-GlcNAc signaling (via GCA inhibition with PUGNAc) causes insulin resistance in 3T3-L1 adipocytes (307). Hence, alteration of post-translational protein glycosylation is influential in the pathogenesis of insulin resistance and the development of other diabetic complications.

This project explores the role of O-GlcNAc signaling in the pathogenesis of acute myocardial ischemia. It provides evidence that O-GlcNAc signaling is endogenously recruited during acute stress events in the heart. Moreover, it highlights O-GlcNAc signaling as an emerging cardioprotective signal and identifies potential mechanisms of O-GlcNAc-mediated cardioprotection.

CHAPTER III

HYPOTHESIS AND SPECIFIC AIMS

Physiological or chemical stress normally induces signal transduction events that end with the activation and/or production of molecules and proteins that diminish the effects of deleterious signaling pathways (167, 172). Protein phosphorylation is typically the mechanism associated with these signal transduction pathways but in 2004, *Zachara et al.* showed that the post-translational sugar protein modification, *O*-GlcNAc, may be a stress induced signal. In this study, exposing multiple cell lines to diverse stressors (heat shock, ethanol, UV, hypoxia, reductive, oxidative and osmotic stress), results in a rapid and global increase in *O*-GlcNAc levels (332). This response was one of the earliest responses. Moreover, interventions that reduced *O*-GlcNAc levels resulted in post-stress lethality while interventions that augmented *O*-GlcNAc levels resulted in more stress tolerant cells raising the possibility that increasing *O*-GlcNAc modification acts as a short-term survival signal (331, 332). In addition, it has been proposed that stress-induced glucose uptake results in elevated pools of UDP-GlcNAc and, hence, increased *O*-GlcNAc in cells(216).

O-GlcNAc is intricately linked to glucose because its donor, UDP-GlcNAc is the end product of HBP which uses less than 5% of cellular glucose. Several

Studies have shown that cells subjected to stress rapidly take up glucose (188, 201, 217). Moreover, this increased glucose uptake has been associated with increased tolerance to stress either by maintaining membrane potential, stabilizing redox state and/or maintaining cellular ATP levels(109, 188, 201, 240, 282).

In a healthy functioning adult heart, about 60-70% of myocardial energy is obtained from the metabolism of fatty acids, while the remainder comes from non-lipid sources like carbohydrates, ketone bodies, and amino acids (196, 247, 248). This is supported by data showing that cardiomyocytes remain viable and beat synchronously when cultured in glucose-free media for several days(248). Nevertheless, during ischemia or hypoxia, the primary source for maintenance of myocardial viability is glucose (251, 252, 273). Hypoxia/ ischemia induced the translocation of the major glucose transporter GLUT-4(281), increased GLUT-1 expression (26), and increased hexokinase activity(212). Multiple studies have suggested that augmented glucose uptake and glycolytic flux can reduce ischemic/hypoxic injury in cardiomyocyte *in vivo* or *in vitro* (15, 76, 236). In fact, *Malhotra et al.* showed that glucose uptake and metabolism through glycolysis protected cardiomyocytes from hypoxia-induced apoptosis(201). Taken together, these events serve to enhance glucose uptake and metabolism.

More interesting is the fact that glycolysis is not the only glucose metabolic pathway implicated in glucose-mediated protection. Studies have shown that blocking glucose flux via the hexosamine biosynthetic pathway (HBP) using azaserine (a GFAT inhibitor), reduced glucose-induced JNK1 activity[193], and

ablated hyperglycemia-mediated decrease in angiotensin II induced hypertrophy (237) resulting in decreased cell survival. The end product of HBP serves as the monosaccharide donor for the post-translational glycosylation of proteins, *O*-GlcNAc, raising the possible involvement of *O*-GlcNAc signaling in glucose-mediated cytoprotection.

Knowing that ischemia/hypoxia is a stress event, we sought to determine if *O*-GlcNAc signaling is involved with the lethality associated with neonatal cardiac myocytes subjected to oxidative stress, hypoxia-reoxygenation, ER stress and adult mice subjected to myocardial ischemia. Hence I proposed the general hypothesis that *O*-GlcNAc signaling confers cardioprotection against acute stress (Figure 6). After identifying potential proteins *O*-GlcNAc-modified in the heart, I further hypothesized that one potential mechanism of *O*-GlcNAc-mediated cardioprotection is attenuating mitochondrial death pathway. Moreover, since ER stress is known to contribute to the pathogenesis of post-hypoxic or post-ischemic injury, I hypothesized that mitigating the activation of maladaptive ER stress response is another possible mechanism through which O-GlcNAc mediates cardioprotection. To test this hypothesis, I addressed the following specific aims.

<u>Specific Aim I:</u> Determine if *O*-GlcNAc modification is protective in the heart

a. Determine the role of *O*-GlcNAc transferase in cardiomyocytes following hypoxia-reoxygenation and ER stress.

b. Determine the role of *O*-GlcNAcase in cardiomyocytes following oxidative stress, hypoxia-reoxygenation, and ER stress.

Specific Aim II: To identify metabolic proteins modified by *O*-GlcNAc in the heart

a. Use a gel based approach to discover potential candidate proteins in cardiomyocytes
b. Incorporate a focused approach to interrogate discrete protein subsets within mitochondria

Specific Aim III: To evaluate the influence of *O*-GlcNAc on mitochondrial mediated death pathway.

a. Determine whether manipulation of O-GlcNAc signaling affects post-hypoxic ROS generation
b. Determine whether manipulation of O-GlcNAc affects post-hypoxic Ca^{2+} overload.
c. Determine whether manipulation of O-GlcNAc affects post-hypoxic recovery of mitochondrial trans inner membrane potential.
d. Characterize potential modulation of mitochondrial permeability transition pore.

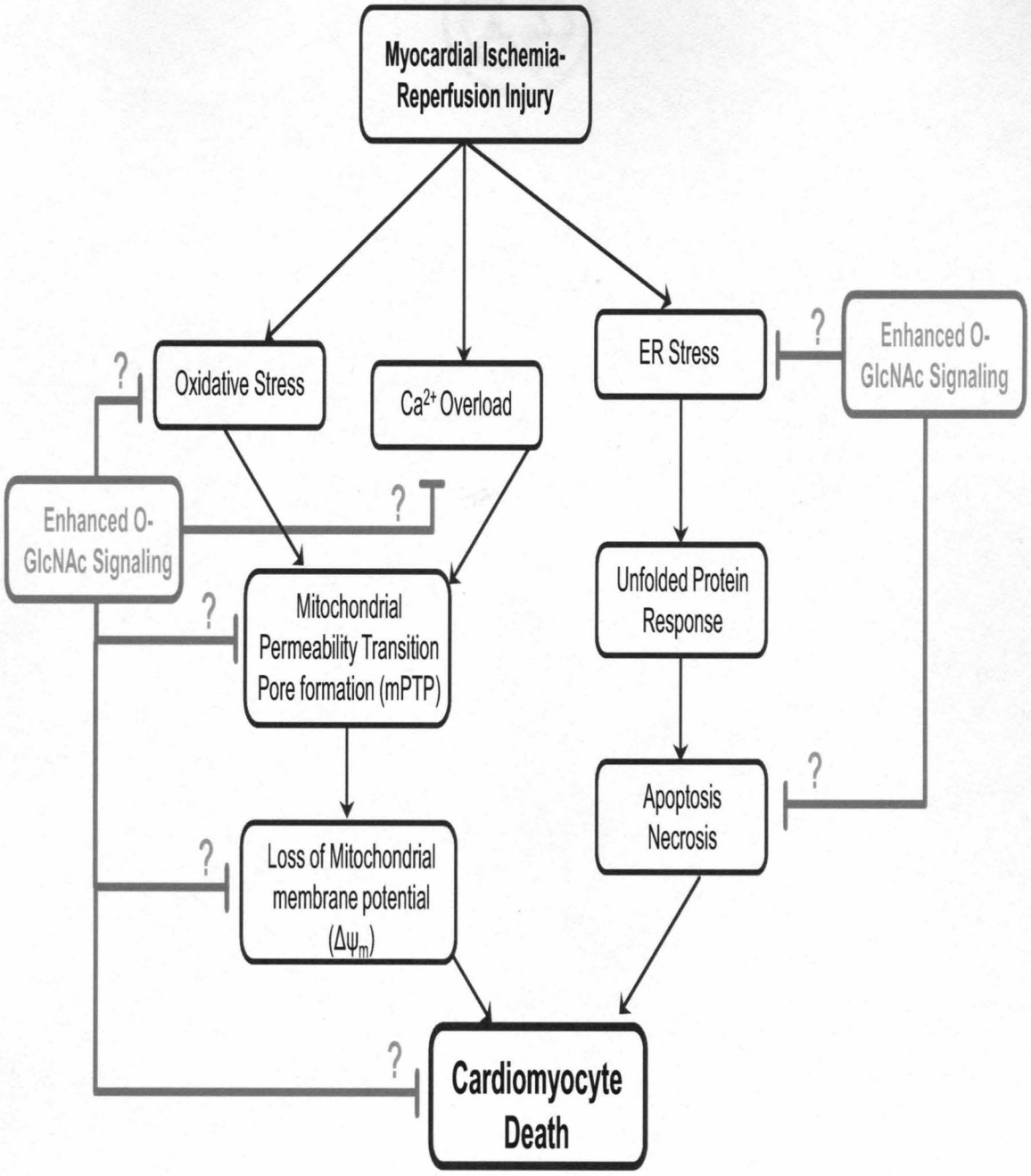

Figure 7. Hypothesis scheme

CHAPTER IV

MATERIALS AND METHODS

All animals were used in compliance with the Guide for the Care and Use of Laboratory Animals, published by the National Institutes of Health (Department of Health and Human Services, publication NO. [NIH] 86-23). The experimental protocol for the present study was reviewed and approved by the Institutional Animal Care and Use Committee of the University of Louisville.

Neonatal rat cardiac myocyte isolation and culture: Neonatal rat cardiac myocytes (NRCMs) were isolated from 1-2 day old Sprague-Dawley rats and cultured according to a well characterized protocol (4, 158, 290, 291). Mice were decapitated, hearts removed, rinsed and minced in calcium- and bicarbonate-free Hank's buffer with HEPES. The tissue fragments were digested by stepwise trypsin (10 mL) dissociation. The dissociated cells were mixed with 7mL FBS, and centrifuged at 180g at room temperature for 5 minutes. The pellet was resuspended in 30mL of warm fortified DMEM containing 5% fetal bovine serum, penicillin/streptomycin, and vitamin B_{12}, and centrifuged at 180g for 5 minutes. Pellet was then resuspended in 50 mL of warm fortified DMEM, and then preplated in 100mm dishes for one hour to allow fibroblast to adhere and enrich

culture with myocytes. The nonadherent myocytes were then plated at a density of 0.8-1.0x 10^6 cells/mL. BrdU (0.1mmol/L) was added to the medium the first four days of culture to inhibit fibroblast growth. The cells were maintained at 37°C in the presence of 5% CO_2 in a humidified incubator. Twenty-four hours prior to experimentation, medium was changed to serum-free DMEM.

Mouse genotyping: At 6-8 weeks of age, mice were ear tagged and tail snips were taken. Total DNA was isolated from tail snips using the Qiagen DNAeasy Tissue Kit. The DNA was stored at -20°C until PCR was performed. PCR was performed using the Taq PCR Core Kit from Qiagen. Mixes were created as follows: tube 1 contained 1 µL DNTP, 1ul of 20 µmol/L Primer oIMR3203 (5'-CAT CTC TCC AgC CCC ACA AAC Tg-3'), 1 µL of 20 µmol/L Primer oIMR3204 (5'-gAC gAA gCA ggA ggg gAg AgC AC-3'), 10 µL Enzyme Q, and 7 µL water per sample. Tube 2 contained 5 µL 10X buffer, 0.5 µL Taq, and 14.5 µL water per sample. 20 uL of each tube were added to PCR tube containing 10 µL of purified DNA. PCR was performed at the following conditions: 1 cycle of 94°C for 3 min, 35 cycles of 94°C for 30 sec, 61°C for 1 min and 72°C for 1 min, 1 cycle of 72°C for 2 min then hold at 4°C ad infinitum. PCR samples were run on a 2% agarose gel with SYBER Safe stain (Invitrogen). Gels were visualized under UV light using a Fuji LAS-3000 imaging system. Once the line was taken to OGT-loxP flanked homozygosity, neonatal mouse cardiac myocytes were isolated and cultured as described below.

Neonatal mouse cardiac myocyte isolation and culture: Neonatal mouse cardiac myocytes (NMCMs) were isolated from 1-2 day old homozygous loxP-flanked OGT mice using a modified protocol for NRCM isolation. Mice were decapitated, hearts removed, rinsed and minced in calcium- and bicarbonate-free Hank's buffer with HEPES. The tissue fragments were digested by stepwise trypsin (2 mL) dissociation. The dissociated cells were mixed with 3mL FBS, and centrifuged at 180g at room temperature for 5 minutes. The pellet was resuspended in 6mL of warm fortified DMEM containing 5% fetal bovine serum, penicillin/streptomycin, and vitamin B_{12}, and centrifuged at 180g for 5 minutes. Pellet was then resuspended in 10 mL of warm fortified DMEM, and then preplated in 100mm dishes for one hour to allow fibroblast to adhere and enrich culture with myocytes. The nonadherent myocytes were then plated at a density of 0.6-1.0x 10^6 cells/mL. BrdU (0.1mmol/L) was added to the medium the first four days of culture to inhibit fibroblast growth. The cells were maintained at 37°C in the presence of 5% CO_2 in a humidified incubator.

Gene transfer: NRCMs were infected with replication-deficient adenoviruses carrying OGT gene (AdOGT), *O*-GlcNAcase (Ad*GCA*), green fluorescent protein (AdGFP), or empty virus (AdNull) for 48 hours as described previously(291). Doses used include 0 and 100 multiplicity of infection (MOI). NMCMs were infected with replication-deficient adenovirus carrying the CRE recombinase gene (0 or 50 MOI AdCRE) for 72 hours to remove the loxP-flanked OGT gene (Fgure 7). Twenty-four hours prior to experimentation, medium was changed to

serum-free DMEM. An initial aliquot of AdOGT and AdGCA (48) was subsequently expanded and purified using cesium chloride gradients, yielding adequate concentrations (10^{10}-10^{11} plaque forming units/milliliter) while AdCRE, AdGFP, and AdNull were purchased from Vector Biolabs. Functional expression was confirmed by appropriate immunoblot analysis.

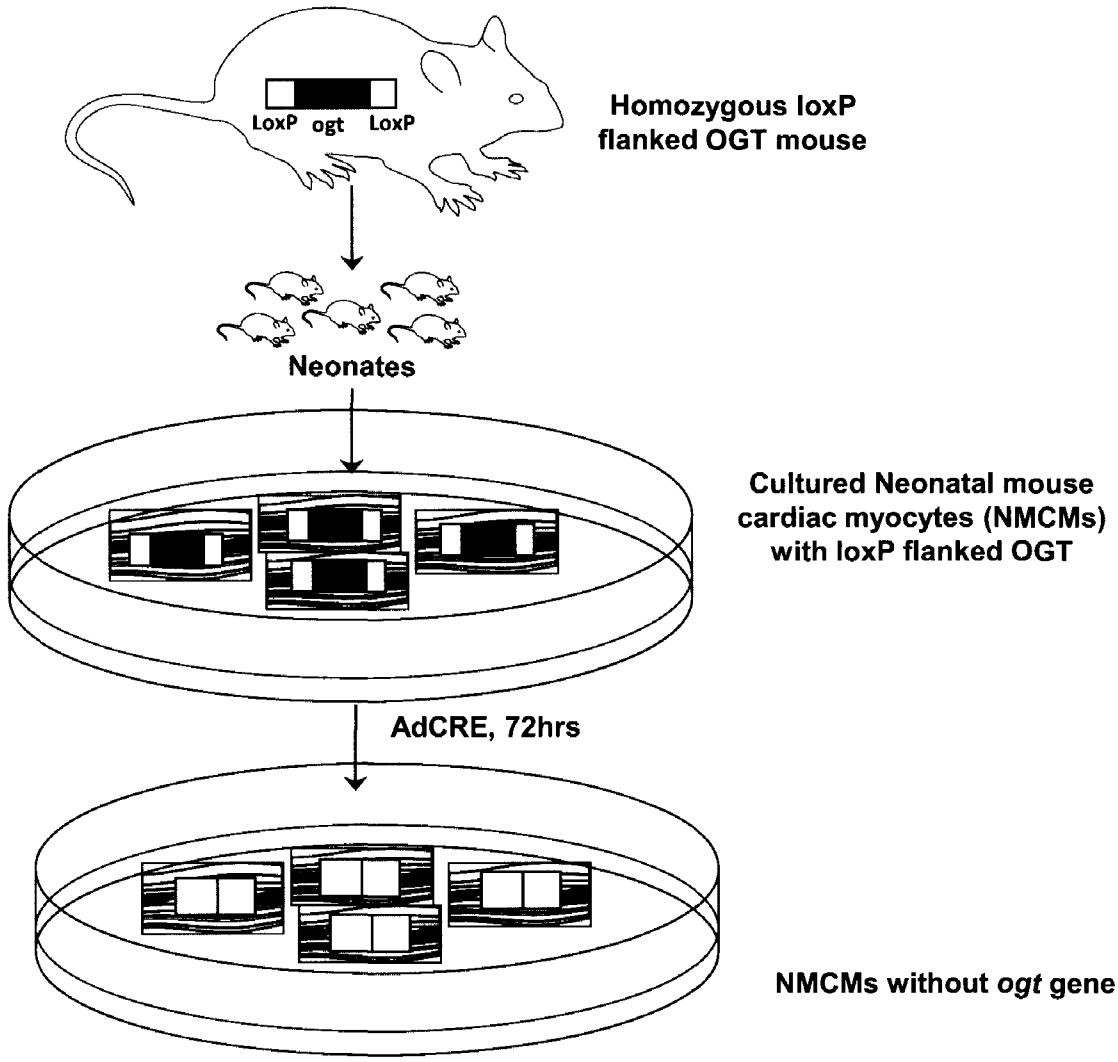

Figure 8. OGT knockout protocol. Neonatal mouse cardiac myocyte (NMCM) OGT knockout. Mice carrying loxP flanked OGT gene were bred to homozygousity on the C57 background. NMCMs were isolated and cultured. NMCMs were infected with adenovirus carrying the CRE recombinase gene (AdCRE) for 72hrs. Because CRE recombinase drives the fusion of lox P sites, infecting NMCMs with AdCRE results in deletion of ogt gene.

Enzyme inhibition: NRCMs were treated with Vehicle (0.1% DMSO or ethanol), [2H-1, 3-thiazine-6-carboxylic acid, 2-[(4-chlorophenyl) imino] tetrahydro-4-oxo-3- (2-tricyclo [3.3.1.13, 7] dec-1-ylethyl-)] (i.e. compound 4 or TT04: 1 mol/L) or 3(2H)-bensoxazolecarboxylic acid, 5-chloro-2-oxo-phenyl ester (i.e. compound 5 or TT40: 10 µmol/L) dissolved in DMSO (96) prior to hypoxia/reoxygenation or two hours before protein harvest for western blotting to inhibit OGT. TT04 and TT40 compete with UDP-GlcNAc for binding to OGT thereby blocking the addition of GlcNAc to protein (96). TT04 is toxic to cells above 1 µmol/L during normoxia, thus the reason for short treatment time and concentrations used. *O*-GlcNAcase activity was blocked using *O*-(2-acetamido-2-deoxy-d-glucopyranosylidene) amino-N-phenylcarbamate (111, 317) in 0.1% ethanol (i.e., PUGNAc: 200µmol/L, overnight) and subjected to hypoxia/reoxygenation or total protein isolated for western blotting. Sample size was equal to six per group per treatment.

RNA Interference: Cultured NRCMs were transfected with short interfering (si) RNA directed against OGT (30nmol/L, siRNA ID # 173150; 5'-GCCUGACAAUACUGGUGGUGUUtt-3'), short interfering (si) RNA directed against *O*-GlcNAcase (60nmol/L, siRNA ID # 190811; with sense strand 5'-GCAACUUAUGACUCCAUCtt-3' and antisense strand 3'-GAUGAGAGUCAUAAGUUGCtc-5') or control sequence fluorescently tagged as a non-silencing control (Cy^{TM}3-labeled negative control, Applied Biosystems). Myocytes were transfected with Ambion's SiPORT NeoFX transfection reagent

according to manufacturer's instructions. Thirty-six or seventy-two hours following transfection, myocytes were subjected to H/R or whole cell lysates were harvested for assessment of OGT protein, O-GlcNAcase and O-GlcNAc levels as described below. Sample size is equal to six per group per treatment.

ER stress induction: Normoxic NRCMs treated as mentioned above were subjected to ER stress by treatment with 1μg/mL of Brefeldin A (BfA) or 0.5 μg/mL of Tunicamycin (TM) for 24 hours. TM inhibits N-glycosylation of nascent ER proteins by preventing UDP-GlcNAc-dolichol phosphate GlcNAc-phosphate transferase activity (72) while BfA interferes with anterograde protein transport from the ER to the Golgi apparatus by inhibiting transport in Golgi, which leads to proteins accumulating inside the ER (81).

Reverse Transcription Real-Time PCR: DNA-free total RNA was extracted with Trizol reagent (Invitrogen) from NRCMs treated with AdGFP (100 MOI, 48 hours), AdOGT (100 MOI, 48 hours), AdGCA (100 MOI, 48 hours), Vehicle or PUGNAc (200μmol/L, overnight). Manufacturer's instructions. Total RNA concentration was determined by measuring the absorbance at 260nm (A_{260}). The ratios of readings at 260nm and 280nm (A_{260}/A_{280}) or 260nm and 230nm (A_{260}/A_{230}) provided an estimated of protein/ phenol and DNA contaminants respectively. For purity, the ratio A_{260}/A_{280} should be above 1.8 and the A_{260}/A_{230} ratio should be a close to 2. Total RNA (1 μg) according was subjected to reverse transcriptase reaction to synthesize the cDNA using IScript™ cDNA synthesis kit

(BioRad). Sequences for GCA, SOD1, SOD2, GPX, Cat, 18s, and GAPDH, used are shown in Table 3. The relative levels of GCA, SOD1, SOD2, GPX, Cat, 18s and GAPDH mRNA transcripts were quantified by real-time PCR using SYBR® Green (Applied Biosystems). The data generated were normalized to GAPDH or 18s threshold cycle (C_T) values by using the ΔΔCT comparative method (194).

Table 3: Primers for real time PCR

gene	Sense (5'-3')	Anti-sense (3'-5')
gca	tggaagaccttgggttatgg	tgctcagcttcttccactga
sod1	ccactgcaggacctcatttt	caatcacaccacaagccaag
sod2	ggccaagggagatgttacaa	gaaccttggactcccacaga
gpx	tcagttcggacatcaggaga	cattcacctcgcacttctca
catalase	gtggttttcaccgacgagat	catgtcagggtccttcaggt
gapdh	tgatgacatcaagaaggtggtgaag	tccttggaggccatgtgggccat
18s	aaacggctaccacatccaag	cctccaatggatcctcgtta

Protein expression: Total cellular proteins were isolated from NRCMs as follows. NRCMs were washed with PBS, harvested in ice-cold lysis buffer (containing 68 mmol/L sucrose, 200 mmol/L mannitol, 50 mmol/L KCl, 1mmol/L EGTA, 1mmol/L DTA and 5 mmol/L HEPES) with freshly added 0.2 μmol/L DTT, 0.1v/v% protease inhibitor stock, 0.4% (v/v) NP-40, 0.4% (v/v) Triton-X and post translational modification inhibitor stock. Extracts were sonicated and the

resulting lysates centrifuged at 15000xg for 5 minutes at 4°C to remove cell debris. Forty micrograms of protein (according to Bradford assay) was applied to each lane of a 6% SDS-PAGE electroblotted onto PVDF membranes for *O*-GlcNAcase, while fifty micrograms of protein was applied to each lane of a 4-12% or 10% gradient NuPAGE Bis-Tris gel (Invitrogen) or 7% NuPAGE Tris-acetate gel (Invitrogen) and electroblotted onto nitrocellulose membranes (Invitrogen) for OGT, *O*-GlcNAc levels and α-tubulin. Reagent-grade nonfat milk (BioRAD) 5% (w/v) in Tris buffered saline was used for blocking. Blots were incubated with anti-OGT (1:1000, SIGMA), anti-*O*-GlcNAcase (1:200, a gift from Dr Zachara of Johns Hopkins), anti-*O*-GlcNAc antibodies (1:1000 CTD 110.6; Covance or 1:2000 RL2; Affinity BioReagents), anti-Grp 94 (1:1000, SCBT), anti-Grp 78 (1:1000, SCBT), anti-PARP (1:1000, SCBT), anti-CHOP (1:1000, SCBT), anti-calreticulin (1:1000, SCBT) or anti-α-tubulin (1:1000, SCBT), as primary antibodies for 12 minutes at 25°C or overnight at 4°C. Blots were then incubated for 12 minutes or one hour with 0.05μg/mL of appropriate HRP-conjugated secondary antibody (goat anti-rat IgG, goat anti-rabbit IgG, goat anti-mouse IgM, goat anti-mouse IgG, donkey anti-goat IgG or anti-chicken IgG) and detected with an enhanced chemiluminescent detection system (Pierce).

Glycoprotein staining: Total cellular protein was isolated from NRCMs treated with either Vehicle, OGT inhibitor (1μmol/L TT04) or infected with adenovirus overexpressing OGT as described above. Following SDS-PAGE, gels were fixed by incubation in 50% methanol and 5% glacial acetic acid for 2 hours at 25°C.

The fixed gels were then washed by gentle agitation three times with 3% glacial acetic acid solution for 10minutes, oxidized with periodic acid for one hour at room temperature, stained with Pro-Q emerald for 1hour in the dark and imaged using a 488 laser and 520 /BP 40 emission filter on TYPHOON 9400.

Enzymatic labeling of O-GlcNAc-modified proteins: *O*-GlcNAc modified proteins were labeled using Invitrogen's Click-iT enzymatic labeling kit according to manufacturer's instructions (Figure 8). Detergents were precipitated out of 200µg whole cell lysate (n=6/group) or 50µL of immunoprecipitated protein (VDAC or O-GlcNAc modified proteins) using the chloroform/methanol precipitation method by adding 600 µL of methanol, 150 µL of chloroform and 400 µL of distilled water and centrifuging at 14000g for 5mins at 4°C. The interface layer containing the protein precipitate was washed twice with methanol and centrifuged at 14000g for 5mins at 4°C. The resulting pellet was then covered with lint-free paper and allowed to dry for 15mins in fume hood. The dried pellet was resuspended in 40 µL of 1% SDS and 20mM HEPES buffer pH 7.9, boiled at 90°C for 5mins, vortexed briefly and allowed to cool on ice for 3mins. 49 µL of distilled water, 80 µL of labeling buffer and 11 µL of $MgCl_2$ were added and the mixture vortexed briefly. 10 µL of UDP-GalNAz (azide-modified UDP-N-Acetylgalactosamine) and 7.5 µL of mutant β-1-4-galactosyltransferase were added. The mixture was vortexed briefly and incubated at 4°C overnight. The next day, the GalNAz-labeled *O*-GlcNAc-modified protein mixture was precipitated using the chloroform/methanol precipitation method and

resuspended in 50 µL of buffer containing 1% SDS, 50mM Tris-HCl, and pH 8. The azide-labeled proteins were tagged with a fluorescent dye, TAMRA, by adding 100 µL of TAMRA in 2x click-iT reaction buffer, 10 µL of distilled water, 10 µL of $CuSO_4$, 10 µL of click-iT reaction buffer additive 1 and 20 µL of Click-iT reaction buffer additive 2. The mixture was vortexed for 5secs after the addition of each component. The mixture was then rotated for 1 hour at 4°C for the conversion of the azide group to a stable triazole conjugate. 25mM DTT was added, incubated at 4°C for 15mins to stop the reaction and proteins precipitated using the chloroform/methanol precipitation method. The dried-labeled protein sample was resuspended in SDS-PAGE buffer for electrophoresis. The gel was then imaged by excitation using a 532nm laser on a TYPHOO 9400 imager.

SYPRO Ruby staining: Gels were stained for total protein using SYPRO ruby gel stain according to manufacturer's instructions. Briefly, gels were first washed 3 times using distilled water, fixed by incubation in 50% methanol and 5% glacial acetic acid for 15 minutes at 25ºC, and washed by gentle agitation three times with distilled water for 10minutes.The fixed gels were then rapid stained with SYPRO ruby for 1hour in the dark by microwaving and agitating for 30 seconds, microwaving for 30 seconds and agitating for 5minutes and microwaving for 30 seconds and agitating for 23 minutes. The stained gels were then destained by gentle agitation in 7% glacial acetic acid and 10% methanol solution for 30minutes, washed by gentle agitation three times with distilled water for 5

minutes, and imaged using a 488 laser and 610 /BP 30 emission filter on TYPHOON 9400.

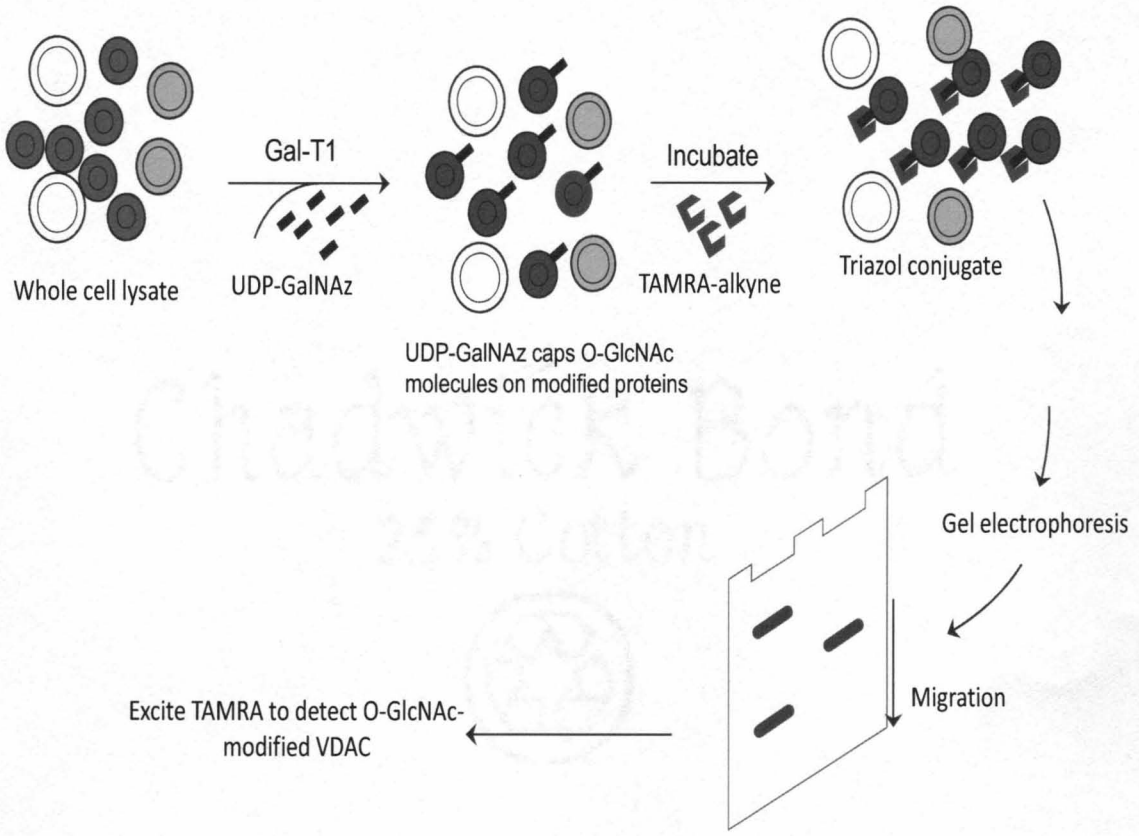

Figure 9. Enzymatic labeling of *O*-GlcNAc-modified proteins. Exogenous galactosyltransferase (Gal-T1) was used to cap O-GlcNAc molecules on modified proteins with azide-modified galactosamine (UDP-GalNAz) overnight. GalNAz capped proteins were then incubated with a fluorescently tagged alkyne (TAMRA-alkyne) to convert the "azide" group into a stable triazol conjugate. Proteins were then separated by SDS-PAGE and imaged on TYPHOON 9400.

Identification of *O*-GlcNAc-modified Proteins: Proteins from Vehicle and PUGNAc-treated samples were precipitated with 10% trichloroacetic acid (v/v) and centrifuged at 14,055 x g for 15 minutes at 4°C. The protein pellets were washed with acetone and dried under a gentle stream of nitrogen gas. Two-

dimensional electrophoresis (2DE) sample buffer (20 mmol/L Tris, pH 6.8, containing 8 mol/L urea, 2% CHAPS, 1 mmol/L EDTA, and 50 mmol/L DTT) was then added and proteins were allowed to solubilize for 2 hours at room temperature with gentle vortexing. Samples were again centrifuged at 14,055 x g for 15 minutes at 4 °C and the protein concentration in the supernatant was assayed by a modified method of Bradford using bovine serum albumin in 8mol/L urea as a standard. DTT was added to a final concentration of 50 mmol/L, ampholytes were added to 1%, and 40 µg of protein from the Vehicle and PUGNAc-treated samples were loaded for passive rehydration (12 hours incubation) onto 3-10 NL and 7-10 IPG strips (Bio-Rad). The proteins were isoelectrically focused (Figure 9) for 26000 V/hrs at 25°C and strips were then equilibrated with base rehydration buffer containing DTT and iodoacetamide, respectively. IPG strips were then loaded on a 12% polyacrylamide gel and electrophoresed for 90 minutes at 140 V for protein separation in the second dimension. Proteins were then transferred to PVDF membranes by electroblotting overnight at 30 mA. Parallel gels were silver-stained using the EMBL silver-staining protocol. For western analysis, O-GlcNAc-modified proteins were probed using 4 µg/ml anti-O-GlcNAc monoclonal antibodies (CTD110.6) followed by 0.1 µg/ml goat anti-mouse secondary antibodies. Membranes were developed using ECL Plus reagents and analyzed with a Typhoon 9400 Variable Mode Imager (Amersham Biosciences). To obtain peptides for MS analysis, protein spots of interest were excised from parallel silver-stained gels and digested with trypsin using a modified version of the method described by Jensen

et al(150). Briefly, the excised gel pieces were incubated for 15 minutes in 100 mmol/L NH_4HCO_3 and 50% acetonitrile and dried by vacuum centrifugation. Proteins were then reduced by incubation with 20 mmol/L DTT at 56°C for 45 min, followed by alkylation with 65 mmol/L iodoacetamide in the dark at room temperature for 30 min. After alkylation, gel pieces were incubated for 15 min in 50 mmol/L NH_4HCO_3 and 50% acetonitrile and dried by vacuum centrifugation. Proteins were hydrolyzed by incubation in 20 ng of modified trypsin (Promega) per ml at 37°C overnight. Trypsin-generated peptides were applied on stainless steel targets by thin-film spotting using α-cyanohydroxycinnamic acid (Aldrich) as a matrix. Mass spectral data were obtained with a TOF-Spec 2E instrument (Micromass) and a 337 nm N_2 laser at 20 to 35% power in the reflector mode. Spectral data were obtained by averaging 10 spectra, each of which was the composite of 10 laser firings. Mass axis calibrations were accomplished by using peaks from tryptic auto-hydrolysis. Peptide masses obtained by MALDI-TOF/MS analysis were analyzed with Protein Probe software (MassLynx) to identify intact proteins. Additionally, the National Center for Biotechnology Information (NCBI) database was also used for protein identification(238). Peptides displaying masses consistent with *O*-GlcNAc modification (monoisotopic mass = 203.079) were ascribed as potentially modified protein fragments.

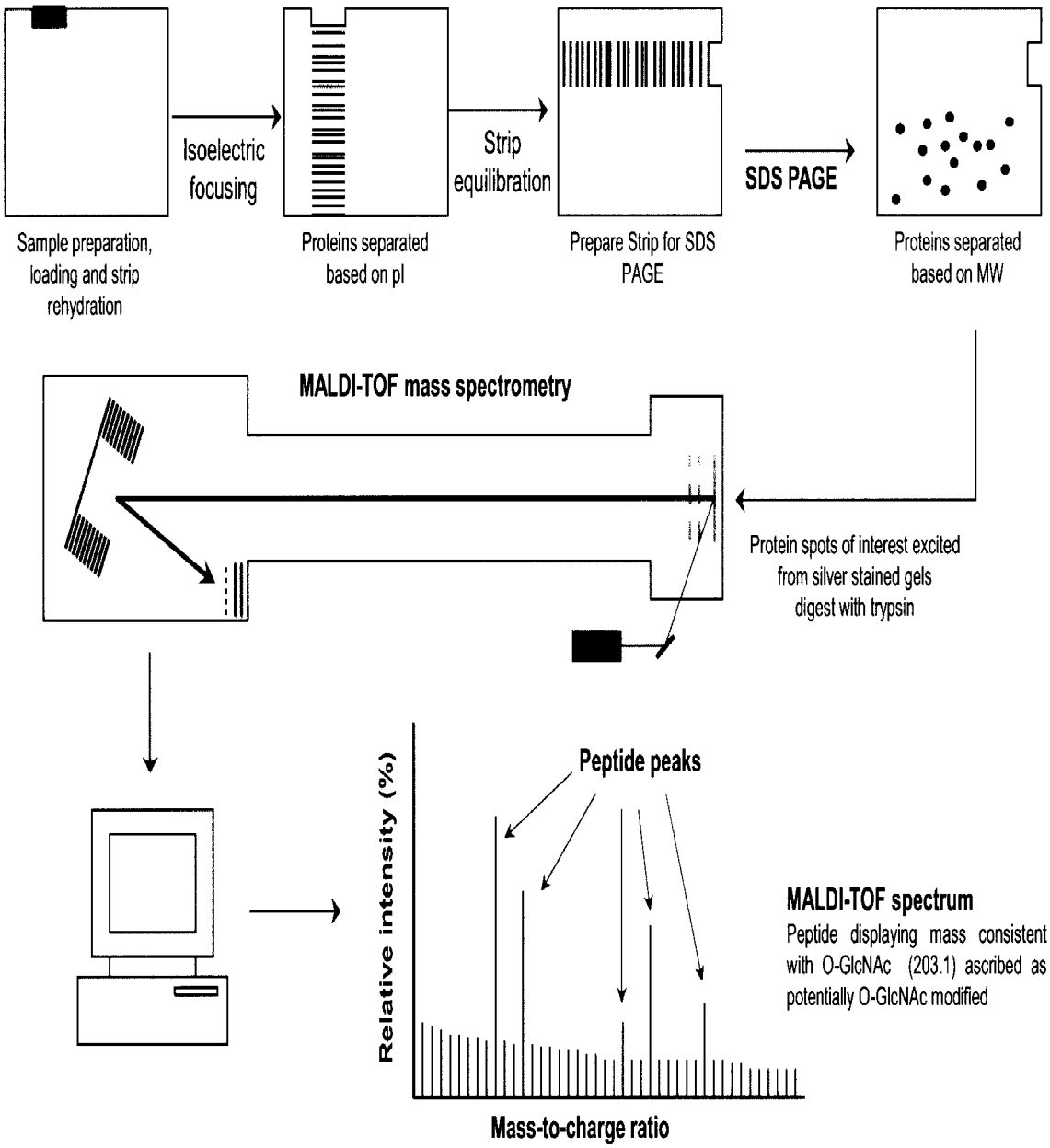

Figure 10. Protocol for identifying O-GlcNAc modified proteins by 2-D gel electrophoresis followed by MALDI-TOF.

Mitochondrial isolation: C57BL/6 mice were injected (intraperitoneal) with Vehicle (0.1% w/v DMSO or 0.1% ethanol), 10 mg/kg TT04, or 50mg/kg of PUGNAc. After 18 h, the mice were anesthetized with 100 mg/kg pentobarbital. Hearts were harvested, immediately rinsed with PBS, and placed in Kontes Duall homogenizer containing 4 mL sucrose buffer A (300 mmol/L sucrose, 10 mmol/L Tris–HCl, 2 mmol/L EGTA and 5 mg/mL BSA, pH 7.4) on ice. Hearts were homogenized using 12 strokes. The homogenate was centrifuged at 2000 ×g for 2 min at 4 °C to remove cell debris. The supernatant was further centrifuged at 10,000 ×g for 5 min 4 °C to sediment impure mitochondria. Mitochondria were washed twice with 1 mL of sucrose buffer A (minus BSA)(92) and purified by adding 19% Percoll and centrifuging at 14,000 ×g for 10 min at 4 °C. Mitochondrial pellet was washed twice with 0.5 mL of sucrose buffer B (300 mmol/L sucrose, 10 mmol/L Tris–HCl, pH 7.4)(103). Purified mitochondrial pellet was resuspended in 0.5 mL of sucrose buffer B. 100µL of mitochondrial stock was used for protein concentration determination using BIO-RAD protein assay buffer according to the Bradford method. Adult mouse hearts were used to confirm the insights from the neonatal rat cardiomyocytes in the adult myocardium, and more importantly, because of the relatively high yield of intact mitochondria from the adult mouse heart.

Co-immunoprecipitation: Co-immunoprecipitation was performed with Protein G immunoprecipitation kit (Sigma) according to manufacturer's instructions on adult mouse cardiac mitochondrial proteins from DMSO, TT04 (OGT inhibitor),

HCl or PUGNAc treated mice as shown on Figure 10. Briefly, 5 µL of the anti-*O*-GlcNAc antibody (RL2) or 10 µL of the anti-VDAC antibody and 245 µL of 1× IP buffer were added to 50 µL of sample and rotated in an end-to-end fashion at 4 °C for 1 h. 50 µL of washed Protein-G-sepharose beads was added to antibody-sample mixture and rotated in a head-to-tail fashion at 4 °C overnight. The antibody-sample-bead mixture was then washed five times with 300 µL of 1× IP buffer and once with 0.1× IP buffer centrifuging at 12,000 000 ×g at 4 °C for 30 s between washes. 1× sample buffer, reducing agent and 1× TBS were added and the mixture was heated at 95 °C for 5 min. Samples were then immunoblotted for VDAC using anti-VDAC (1:2000, Santa Cruz) or *O*-GlcNAc using RL2 (1:1000, Affinity BioReagents). Standard densitometry was performed and the value for the Vehicle (DMSO or HCl) group was set at 100%. All samples were normalized to their total VDAC levels (which were not different between the two groups).

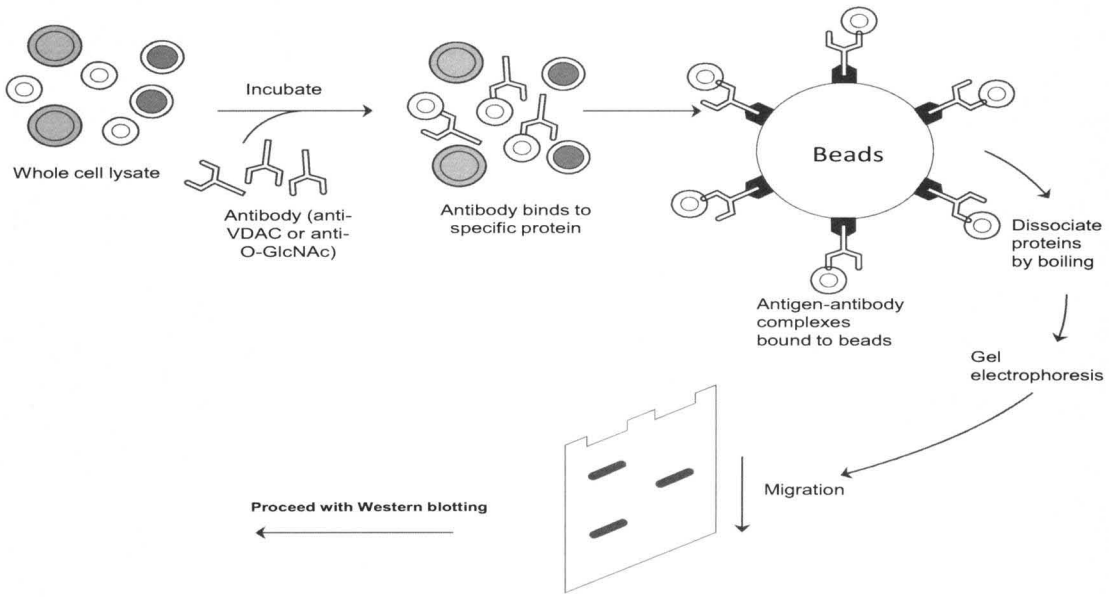

Figure 11. Immunoprecipitation protocol.

Densitometry: Densitometry was performed using non-saturated chemiluminescent membranes exposed and quantitated using Fuji LAS-3000 bio-imaging analyzer. Multiple exposures from every experiment were used to confirm that the signal was within the linear range. Densitometric analysis of *O*-GlcNAc levels using CTD 110.6 and RL2 antibodies were performed on the entire lane. *O*-GlcNAc levels were normalized to the appropriate control (Ponceau stain), and then expressed as a percentage of control (set at 100%).

***In vitro* hypoxia-reoxygenation injury in cardiac myocytes:** Cardiac myocytes were subjected to hypoxia using Esumi lethal ischemic media, pH 6.2 (containing 117 mmol/L NaCl, 12 mmol/L KCl, 0.9 mmol/L $CaCl_2$, 0.49 mmol/L $MgCl_2$, 4 mmol/L HEPES, 20 mmol/L sodium lactate, and 5.6 mmol/L L-glucose) by sealing the plated myocytes in humidified hypoxic chambers (Billups-Rothenberg, Inc) (164), flushing each chamber with a gas mixture consisting of 5% CO_2 and 95% N_2 for fifteen minutes, and incubating the hypoxic chamber in a modular incubator at 37°C for three hours. Following hypoxia, the media was changed to 1x Esumi control media (pH 7.4, 137 mmol/L NaCl, 3.8 mmol/L KCl, 0.9 mmol/L $CaCl_2$, 0.49 mmol/L $MgCl_2$, 4 mmol/L HEPES, and 5.6 mmol/L D-glucose) and culture dishes reoxygenated for one or six hours in the modular incubator or on the fluorescent microscope during imaging as appropriate. Similarly treated NRCMs were subjected to four or 9 hours of normoxia in 1x Esumi control media to serve as normoxic/aerobic controls.

Cell death: Cell death was assessed for NRCM treated as mentioned above and subjected to hypoxia/reoxygenation by measuring normoxic or post-hypoxic LDH release using a commercially available kit (Sigma). Data was expressed as LDH release relative total LDH in the cells and normalized to the appropriate controls (1hr reoxygenation data) or normoxic untreated control (for 6hrs reoxygenation data). Similarly treated NRCMs were stained with the fluorescent DNA-binding dyes Hoechst 33342, 5μg/mL and propidium iodide, 5μg/mL (Invitrogen) during the last 30 minutes of reoxygenation(19). The stained nuclei were then visualized using a 20x objective on a Nikon-TE2000E2 fluorescence microscope and Xcite 120 Fluor light source (level of 12%). Filters used included 350/50 nm excitation and 470/40 nm emission filters for Hoechst and 560/40 nm excitation and 630/60 nm emission filters for PI. Neutral density filter setting was set at ND4 and binning of 2x for all image acquisition. Exposure duration was set at 100ms for Hoechst and 200ms for PI. Four fields per treatment were counted and data were expressed as % PI positive nuclei/total nuclei. Because the nuclear stain Hoechst 33342 is membrane permeable, it was used to determine total cells in each field and not as an index of apoptosis. Sample size of at least four per group was used.

Apoptosis: Apoptosis was assessed by measuring Caspase 3/7 activity in whole cell lysates using Caspase Glo kit (PROMEGA) according to manufacturer's instructions. Briefly, equal volumes of whole cell lysate (50μg) and caspase reagent were mixed and incubated in the dark for one hour at room temperature.

Bioluminescence was measure using Modulus luminometer (Turner Biosystems) and expressed in relative luminescent units (RLUs). Sample size is equal to at least five per group per treatment.

Fluorescence Microscopy: NRCMs were imaged in imaging medium (Dulbecco's Modified Eagle Medium (with HEPES and minus phenol red and pyruvate). Images were captured using a Photometric CoolSNAP ES camera attached to a Nikon-TE2000E2 fluorescence microscope with a T-PFS Perfect Focus Unit all controlled with MetaMorph 6.3r2 software. The Perfect Focus System was used to prevent minute defocusing caused by changes over time during time-lapse imaging. Xcite 120 Fluor light source (level of 12%) was used and a Plan Apo 60xA/oil (NA=1.4) objective were used for magnification. Neutral density filter setting was set at ND4 and binning of 2x for all image acquisition. Images were captured every 90 seconds for 60 minutes. Exposure duration was set at 100ms for all fluorescent dyes except for rhod-2 which was set at 50ms. Excitation and emission filters varied depending on the fluorescent dye as mentioned below.

Assessment of Calcium Overload: NRCMs treated with AdGFP, AdNull, AdOGT, AdGCA, vehicle, or PUGNAc were loaded with 2μmol/L of rhod-2(290, 291) (used to assess mitochondrial calcium, Invitrogen) and subjected to 3 hours of hypoxia. Calcium levels were assessed by following the changes in rhod-2 fluorescence during reoxygenation using time-lapse fluorescent microscopy.

Imaging was initiated during reoxygenation by exciting rhod-2 through 560/28 nm and 646/38 nm emission filter. All experimental groups were repeated in six separate NRCM cultures.

Assessment of reactive oxygen species (ROS) production: ROS levels were assessed in NRCMs using time-lapse fluorescence microscopy by following the changes in 5-(and-6)-carboxy-2',7'-dichlorodihydrofluorescein diacetate (DCF) fluorescence(291). NRCMs treated with AdNull, AdOGT, AdGCA, Vehicle, or PUGNAc were loaded with 2μmol/L DCF and subjected to 3 hours of hypoxia as mentioned above. During reoxygenation, imaging was initiated immediately by exciting DCF through 470/40 nm bandpass filter and emission through 522/40 nm bandpass filters. All experimental groups were repeated in at least four separate isolations.

Assessment of mitochondrial membrane potential: Using time-lapse fluorescence microscopy (4, 5, 158, 290, 291), detection of mitochondrial membrane potential changes were performed by following changes in tetramethylrhodamine methyl ester (TMRM) fluorescence. NRCMs treated with AdGFP, AdOGT, AdGCA, vehicle, PUGNAc, Control siRNA or GCA siRNA were loaded with 100 nmol/L TMRM and subjected to 3 hours of hypoxia. Imaging was initiated during reoxygenation by exciting TMRM through a 546/11 nm bandpass filter and emission assessed through a 567/15 nm bandpass filter.

Exposure duration was set at 100ms and all experimental groups were repeated in at least four separate isolations.

Mitochondrial swelling assay: The mitochondrial swelling assay was performed similar to previous reports. Two mg/ml cardiac mitochondria from Vehicle- (0.1% DMSO or 0.1% ethanol), TT04- (OGT inhibitor), or PUGNAc- (GCA inhibitor) treated mice in buffer B was loaded on a 96-well plate and allowed to warm to room temperature. $CaCl_2$ (100 µmol/L) was used to induce mitochondrial swelling and the change in absorbance measured spectrophotometrically at 520 nm. A decrease in absorbance indicated an increase in swelling (i.e. mitochondrial permeability transition pore opening).

Murine *in vivo* ischemia-reperfusion: Three- to four-month-old male SV129 (mean body weight 25±1g) were randomized to PUGNAc or isovolumetric Vehicle treatment groups. Mice were subjected to *in vivo* coronary artery ischemia-reperfusion for assessment of O-GlcNAc levels or myocardial infarct size according to well characterized protocol (Figure 11)(156, 158). Mice were anesthetized with intraperitoneal injections of ketamine hydrochloride (50 mg/kg) and sodium pentobarbital (50 mg/kg). The animals were then attached to a surgical board with their ventral side up. The mice were orally intubated with polyethylene (PE)-60 tubing connected to a rodent ventilator (Harvard Apparatus) with tidal volume and breathing rate set by standard allometric equations. The mice were supplemented with 100% oxygen via the ventilator side port. Body

temperature was maintained between 36.5 and 37.5 using a rectal probe and a heat lamp. A left thoracotomy was performed using a thermal cautery, and the proximal left main coronary artery was visualized with the aid of a dissecting microscope and completely occluded for 40 minutes with 7-0 silk suture mounted on a tapered needle (BV-1, Ethicon). After 40 minutes, the suture was removed and reperfusion was initiated and visually confirmed. The chest was closed in layers using 4.0 silk suture. The skin was closed using 4-0 nylon suture. Ketoprofen was given as analgesia prior to closing the chest. Upon recovery of spontaneous breathing, mice were removed from the ventilator, extubated and allowed to recover in a warm, clean cage supplemented with 100% oxygen.

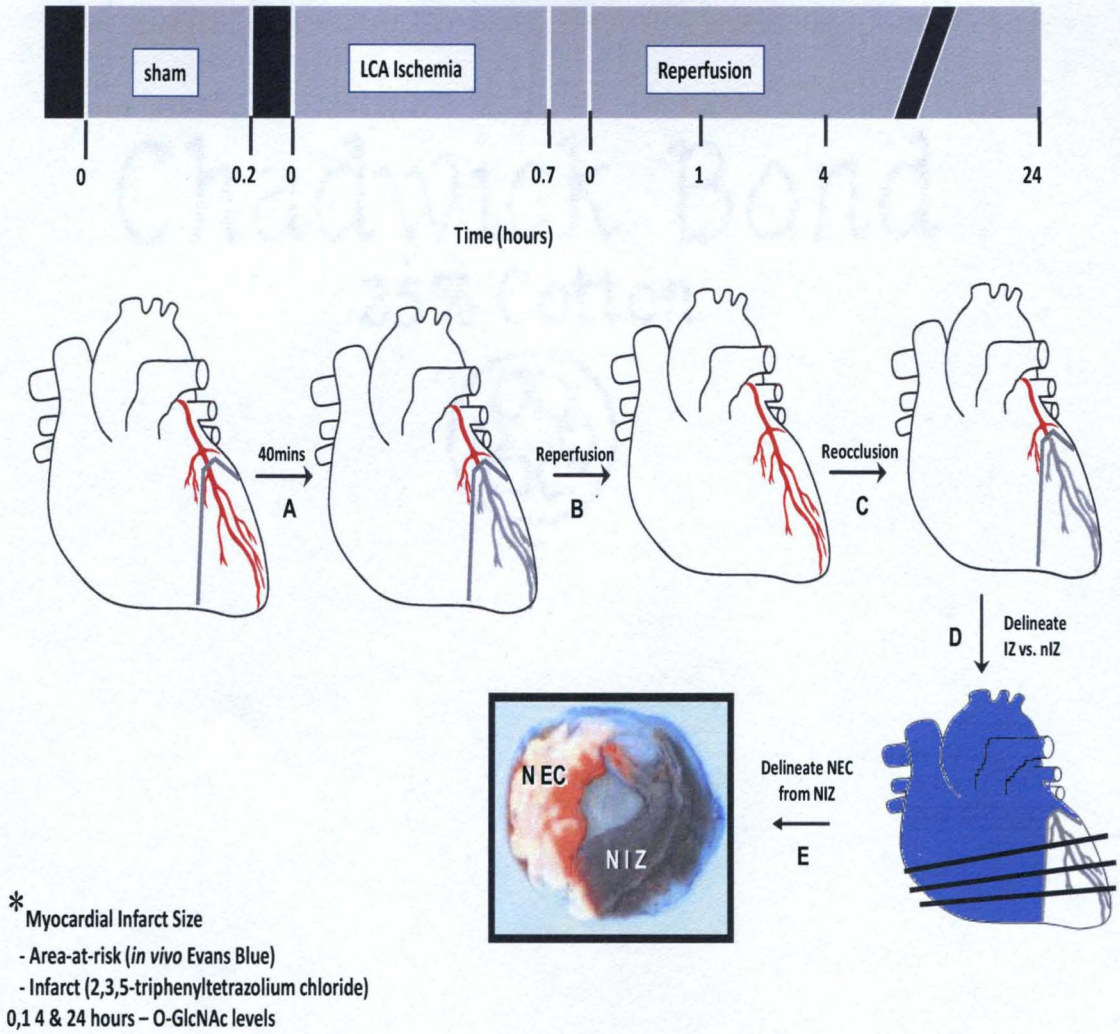

Figure 12. Murine myocardial ischemia-reperfusion protocol. **A** – 40mins of left anterior descending coronary artery ligation. **B** – Suture cut and reperfusion initiated. **C** – Reocclusion of LAD. **D** – Injection of Evans blue dye into the right carotid artery to delineate the ischemic zone and the non-ischemic zone. **E** – Heart cross sections incubated in TTC to delineate viable and non viable tissue. NEC: necrotic tissue and NIZ: non-ischemic zone.

Myocardial ischemic/non-ischemic zone determination: Following 40minutes ligation of left anterior descending coronary artery in C57BL6 mice described above, reperfusion was initiated. After 0, 1, 4 and 24 h of reperfusion, the mice were anesthetized with isoflurane. A tracheotomy was performed and mice were

ventilated as described above. A catheter (PE-10 tubing) was placed in the common carotid artery to allow for Evans blue dye injection. A median sternotomy was performed, and the left main coronary artery was relegated in the same location as before. Evans blue dye (1.2 ml of a 2% solution) was injected into the carotid artery catheter into the heart to delineate the ischemic zone from the non ischemic zone (Figure 11). The heart was rapidly excised and serially sectioned along the long axis in 1-mm-thick sections. With the aid of a dissecting microscope, the non-ischemic and ischemic zone was separated and O-GlcNAc levels were assessed.

Myocardial infarct size determination: Myocardial infarct size was determined according to well characterized protocol (153, 155). After 24 h of reperfusion, the mice were anesthetized as with isoflurane and Evans blue dye (1.2 ml of a 2% solution) used to delineate the ischemic zone from the non ischemic zone as described above. The heart was rapidly excised and serially sectioned along the long axis in 1-mm-thick sections, which were then incubated in 1.0% 2,3,5-triphenyltetrazolium chloride for five minutes at 37°C to demarcate the viable and nonviable myocardium within the risk zone (Figure 11). Digital pictures of the basal of each section were taken. Each of the five 1-mm-thick myocardial slices was weighed. A blinded observer assessed the areas of infarct, risk, and non-ischemic zone using computer-assisted planimetry (Image J, version 1.38x).

Evaluation of blood pressure, heart rate, and left ventricular function: In order to assess the closed-chest hemodynamic status, mice were anesthetized with ketamine (50 mg/kg, intraperitoneal) and pentobarbital (50 mg/kg, intraperitoneal) and supplemented with oxygen via a nasal cone. A fluid-filled polyethylene catheter was inserted into the right common carotid artery and advanced to the aorta left ventricle via (197). Data were recorded for 10 seconds. Offline assessment of these data yielded mean arterial blood pressure, and heart rate (HR). The catheter was then advanced through the aortic valve into the left ventricle (LV). Data were recorded for 10 seconds. *In vivo* transthoracic echocardiography of the left ventricle using a 15 MHz linear array transducer (15L8s) interfaced with a Sequoia C512 (Acuson) was performed (154, 156). Ventricular parameters were measured according to the leading-edge technique. M-mode (frame rate=30 Hz; sweep speed=200 mm/s) echocardiograms were captured from short-axis views of the LV at the mid-papillary level. Data for each animal were calculated from at least 10 seconds of chart recording. All data were calculated from 10 independent cardiac cycles per experiment. Short axis views at the midpapillary level yielded left ventricular (LV) end diastolic diameter (EDD), end systolic diameter (ESD), heart rate (HR), and fractional shortening (%FS). LV fractional shortening (LVFS) was calculated according to the following equation: LVFS= ([LVEDD-LVESD]/ LVEDD)x100.

Cardiac troponin-I assessement: cardiac Troponin-I release was measured in plasma from mice subjected to sham surgery or ischemia-reperfusion protocol

described above according to manufacturer's instructions. First, a 1:4 dilution of plasma samples in plasma diluents was made and loaded on to a 96 well plate in triplicate. Diluted plasma samples were allowed to react simultaneously with two affinity purified antibodies (one used for solid phase immobilization and the other and conjugated to HRP) on the microtiter wells by incubating plate at room temperature on a plate shaker. Wells were washed with water to remove any unbound HRP-conjuated antibody. HRP substrate, tetramethylbezidine was added and plate incubated for 20 minutes at room temperature fordevelopment of color. 1mol/L HCl was added to each well to stop color development and absorbance measured on a spectrophotometer at 450nm. cTnI concentration of the samples were determined from standard curve and in ng/mL.

Statistical analysis: Data were analyzed using GraphPad Prism 4 software. One-way ANOVA was employed for three or more experimental groups and Dunnett's *t* tests for post hoc analysis. Unpaired student's *t* test was used to analyze data containing two experimental groups. Data are reported as mean ± standard error of the mean with differences between treatment groups accepted as significant when $p < 0.05$.

CHAPTER V

RESULTS

A. O-GlcNAc levels are altered following oxidative stress: *O*-GlcNAc levels were assessed via Western blot analysis in isolated cardiomyocytes treated with Vehicle or PUGNAc (a GCA inhibitior) and exposed to various durations of hydrogen peroxide (H_2O_2, 0.1 mmol/L) in serum-free media. Cardiomyocytes experience a significant ($p<0.05$) decrement in *O*-GlcNAc levels at about 40 minutes (Figure 12A). Myocytes treated with PUGNAc showed markedly ($p<0.05$) higher levels of *O*-GlcNAc throughout the time course compared with Vehicle-treated myocytes (Figure 12A). Furthermore, the oxidative stress-mediated decrement in *O*-GlcNAc levels was retarded in the PUGNAc- compared with the Vehicle-treated group (Figure 12A). To determine whether reversal of the decrement in *O*-GlcNAc levels could attenuate cell death, cardiomyocytes were treated with PUGNAc or Vehicle, exposed to H_2O_2, and coincubated with propidium iodide and annexin V. At the end of 150 minutes of H_2O_2 exposure, the percentage of propidium iodide–positive cells was significantly ($p<0.05$) augmented compared with control (Figure 12B). Moreover, exposure to H_2O_2 induced a significant ($p<0.05$) increase in annexin V fluorescence positivity compared with control (Figure 12C). PUGNAc treatment significantly ($p<0.05$)

attenuated H_2O_2-induced cell death according to PI and annexin V positivity. Saponin permeabilization was used at the end of the experimental protocol to confirm equal numbers of cells per field (Figure 12B).

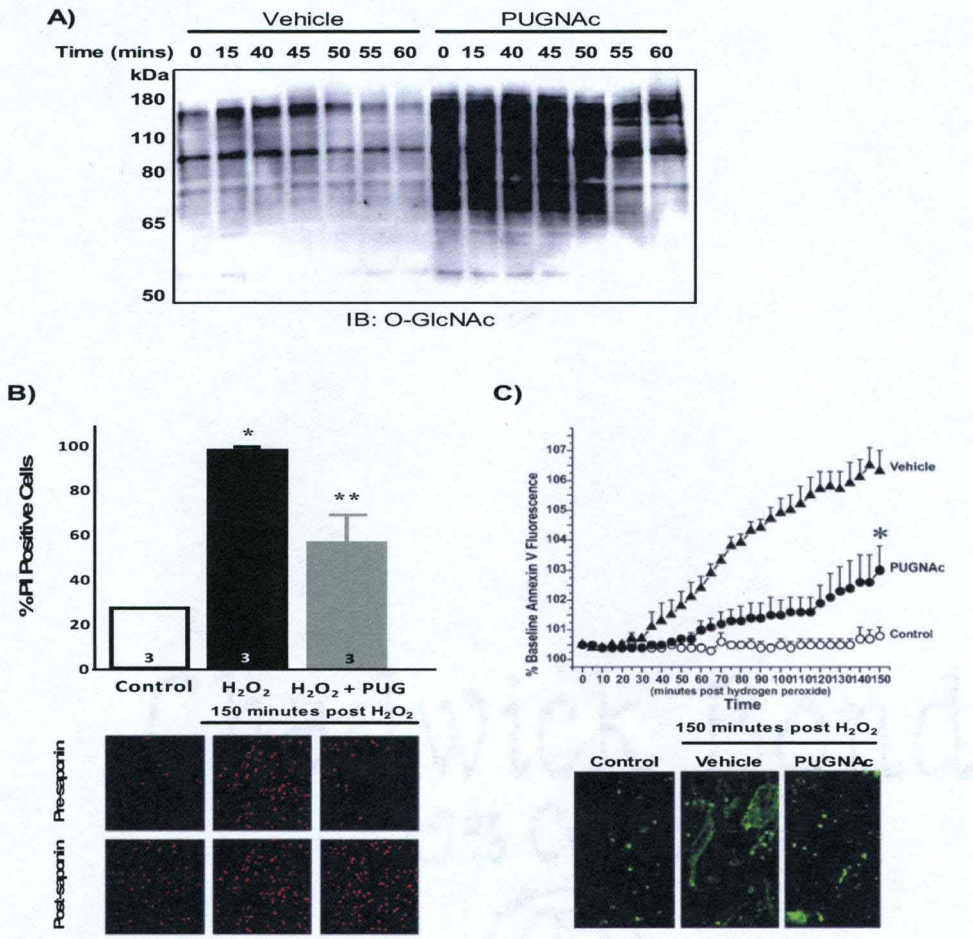

Figure 13. Effects of augmented O-GlcNAc levels on oxidative stress-induced cardiomyocyte death. **A)** Representative immunoblot (IB) of time course of O-GlcNAc levels in cardiac myocytes treated with Vehicle or PUGNAc and subjected to oxidative stress for 60 minutes (n=4 per group). O-GlcNAc levels are significantly elevated in PUGNAc-treated myocytes compared with Vehicle. **B)** After 150 minutes of oxidative stress, most Vehicle-treated myocytes become PI positive, a phenomenon inhibited by PUGNAc (n=3/group). Representative confocal images of myocytes from each treatment group at the end of the experiment (pre-saponin) or after saponin permeabilization, indicating equivalent number of cells per field. **C)** During the time course of oxidative stress, annexin V positivity increases in Vehicle-treated myocytes, an effect attenuated by PUGNAc. Representative confocal images of myocytes from each treatment group at the end of the experiment (n=3/group).

B. *O*-GlcNAc levels are altered following hypoxia-reoxygenation: To determine if *O*-GlcNAc levels change during hypoxia and reoxygenation, isolated neonatal rat cardiac myocytes (NRCMs) were subjected to hypoxia and reoxygenated for different durations (0, 1 and 6 hours). Hypoxia significantly decreased *O*-GlcNAc levels compared to normoxia (Figure 13A-B). During reoxygenation, we observed a time dependent increase in *O*-GlcNAc levels peaking after 6 hours (Figure 13A-B) and falling to minimal levels by 18 hours of reoxygenation (data not shown).

Hypoxia damaged cardiac myocytes as reflected in increased post-hypoxic LDH release compared to normoxia. Reoxygenation further exacerbated the hypoxia-mediated myocytes injury mirrored by the time dependent increase in post-hypoxic LDH release for hypoxic myocytes compared to normoxia (Figure 13C).

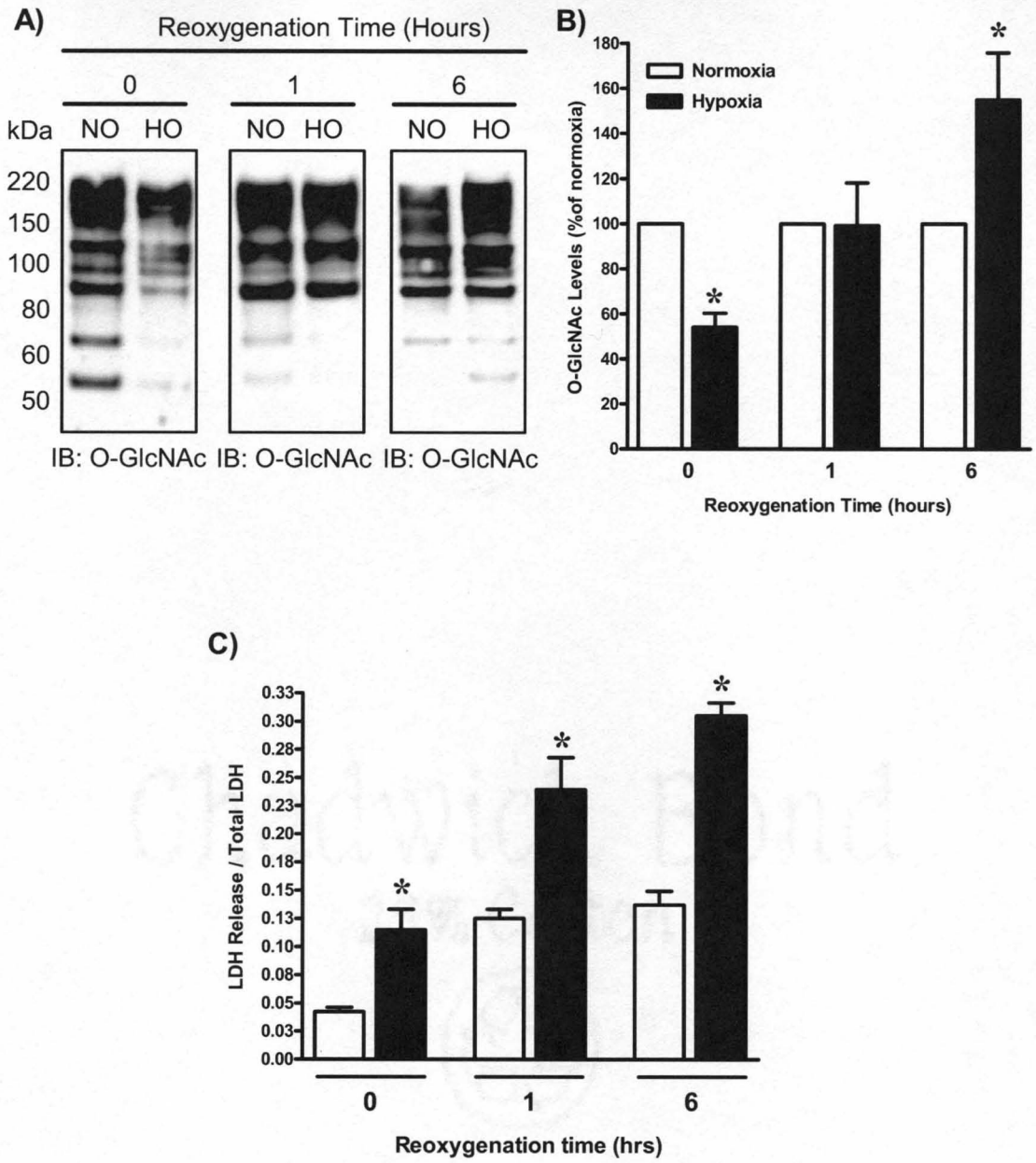

Figure 14. Effects of hypoxia-reoxygenation on O-GlcNAc levels. Myocytes were subjected to hypoxia for three hours and reoxygenated for zero, one or six hours. O-GlcNAc levels were assessed on whole cell lysates or cell injury assessed by measuring post-hypoxic LDH release in the media. **B)** Representative immunoblots of time course of O-GlcNAc levels in cardiac myocytes. **B)** Densitometric quantification of O-GlcNAc immunoblots expressed as percent of normoxic control. **C)** Hypoxia induced cell injury according to post-hypoxic LDH release.

C. ROLE OF OGT IN POST-HYPOXIC CARDIOMYOCYTE INJURY

C.1. OGT overexpression attenuates post-hypoxic cardiac myocyte death: Adenovirus carrying the OGT gene was used to study gain-of-function for *O*-GlcNAc transferase (AdOGT). Forty eight hours after infecting isolated neonatal rat cardiac myocytes (NRCMs) with AdOGT, total cellular proteins were harvested and OGT protein and *O*-GlcNAc levels assessed via western blot analysis. Infection of NRCMs with AdOGT augmented OGT levels (349 ± 86% of 0 MOI, n=3/group, Figure 14A). Assessment of the functional readout, *O*-GlcNAc, showed significant ($p < 0.05$) increase in *O*-GlcNAc levels (145 ± 19% of 0 MOI, n>/=6/group, Figure 14B). To confirm this finding, two additional approaches were used. First, the same samples were evaluated using another *O*-GlcNAc antibody (RL2), which showed a significant (n=5/group, $p < 0.05$, Figure 14B) increase in *O*-GlcNAc levels at 100 MOI compared to 0 MOI AdOGT. Second, additional samples were prepared for evaluation using a non-immune technique (enzymatic labeling of *O*-GlcNAc with TAMRA fluorophore; i.e. click-chemistry based approach). The enzymatic labeling technique also showed a significant augmentation of *O*-GlcNAc levels with 100 MOI AdOGT (155 ± 9%) compared to 0 MOI AdOGT (Figure 14B). Immunoblots/gels for *O*-GlcNAc levels show multiple positive bands because *O*-GlcNAc is a post-translational modification, not a single protein (Figure 14B). In addition to the significant increases in *O*-GlcNAc levels, there was no significant difference in total glycoprotein levels following OGT overexpression according proQ emerald

staining (Figure 14C). Equal protein loading was confirmed by densitometric analysis of Ponceau-stained membranes or SYPRO ruby stained gels.

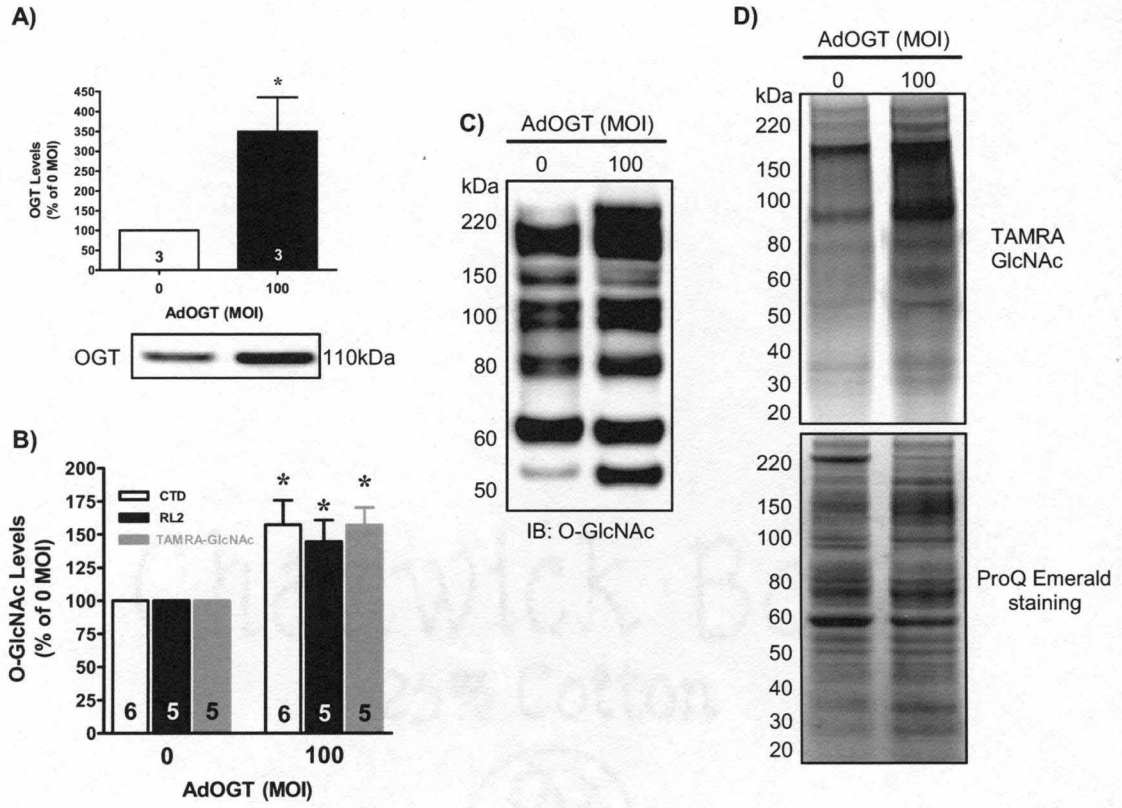

Figure 15. Effects of OGT overexpression (using AdOGT) on post-hypoxic cardiomyocyte injury. Myocytes were infected with AdOGT 48 hours prior to protein harvest or hypoxia-reoxygenation. **A)** Summary densitometric analysis (n=3/group) and immunoblot of OGT (using SQ17) show significant ($p<0.05$) increase in OGT protein with 100 MOI compare to 0 MOI of AdOGT. **B)** Densitometric analysis (n=5-6/group) and of the functional readout of OGT, O-GlcNAc. Significant increase in O-GlcNAc levels (n=6/group) is seen with the CTD110.6 and RL2 antibodies as well as TAMRA fluorescence. As expected, multiple immunopositive bands appear because the O-GlcNAc modification occurs on numerous proteins throughout the cell. **C)** Representative immunoblot show significantly augmented O-GlcNAc levels with AdOGT. **D)** Representative TAMRA-GlcNAc gel showing augmented O-GlcNAc levels despite no change in total glycoprotein levels (ProQ gel staining, n=3/group) with AdOGT *$p<0.05$ vs. 0 MOI AdOGT.

To evaluate the effects of OGT overexpression on post-hypoxic cardiac myocyte survival, similarly-treated cardiac myocytes were subjected to hypoxia (three hours) and reoxygenation (one hour). Post-hypoxic media were harvested and assayed for LDH release and cells were evaluated for PI positivity. A significant ($p < 0.05$) decrease in post-hypoxic LDH release was seen with 100 MOI (67 ± 15% of 0 MOI) compared with 0 MOI AdOGT treated NRCMs (Figure 15A). Also, we observed a significant reduction in PI positivity at 100 MOI (66 ± 7% of AdGFP) compared with AdGFP treated NRCMs (Figure 15B).

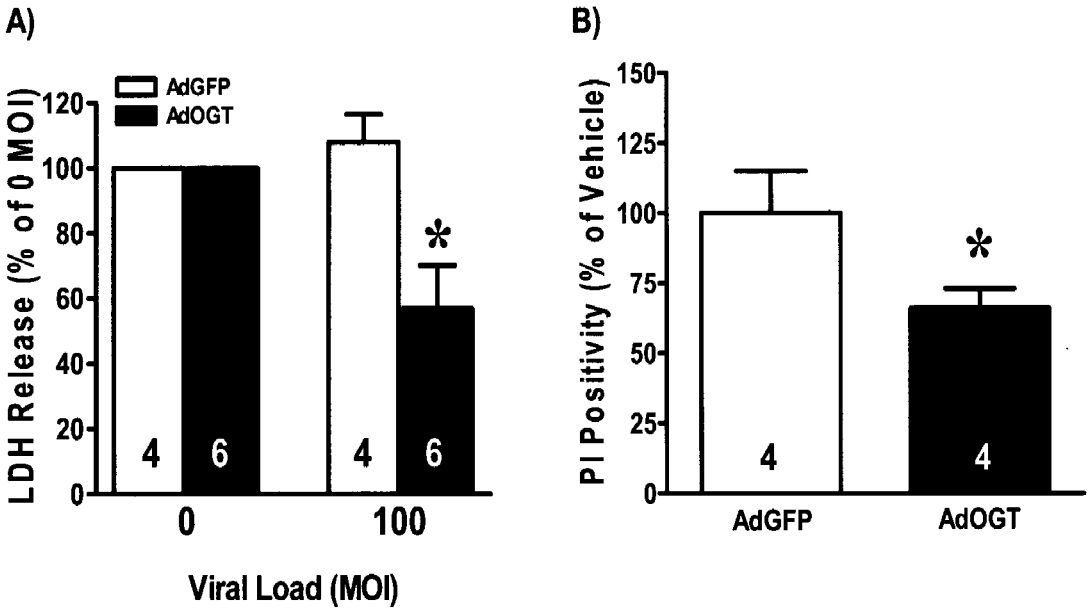

Figure 16. **A)** OGT overexpression improved post-hypoxic cardiac myocyte survival. LDH release was spectrophotometrically determined from the media following hypoxia-reoxygenation (n=4-6/group). **B)** OGT overexpression attenuated post-hypoxic injury according to propidium iodide staining. *p<0.05 vs. 0 MOI AdOGT or 100 MOI AdGFP.

C.2. OGT inhibition exacerbates post-hypoxic cardiac myocyte injury: Loss-of-function for OGT was evaluated by incubating cultured NRCMs (n = 6/group) with Vehicle (0.1% DMSO) or OGT inhibitors (1.0 μmol/L TT04 or 10 μmol/L TT40) for two hours prior to protein harvest and immunoblotting for *O*-GlcNAc levels. The concentrations of TT04 and TT40 used were not toxic to the cells under normoxic conditions. Significant reductions (65 ± 7%, $p < 0.05$) in *O*-GlcNAc levels were observed with TT04 treatment compared to Vehicle (Figure 16A). We observed similar results with RL2, an additional *O*-GlcNAc antibody as shown in bar graph (Figure 16A). A similar phenomenon was observed with a related OGT inhibitor, TT40 (Figure 16B). There was no significant difference in glycoprotein levels following OGT inhibition (100 ± 8% of Vehicle, p = NS) compared with Vehicle (100 ± 4%) according to Pro-Q Emerald staining (Figure 16C) demonstrating that the OGT inhibitor (TT04) does not alter other glycosylation processes. As with virtually all known compounds, no absolute and exclusive claims can be made regarding potential non-specific effects.

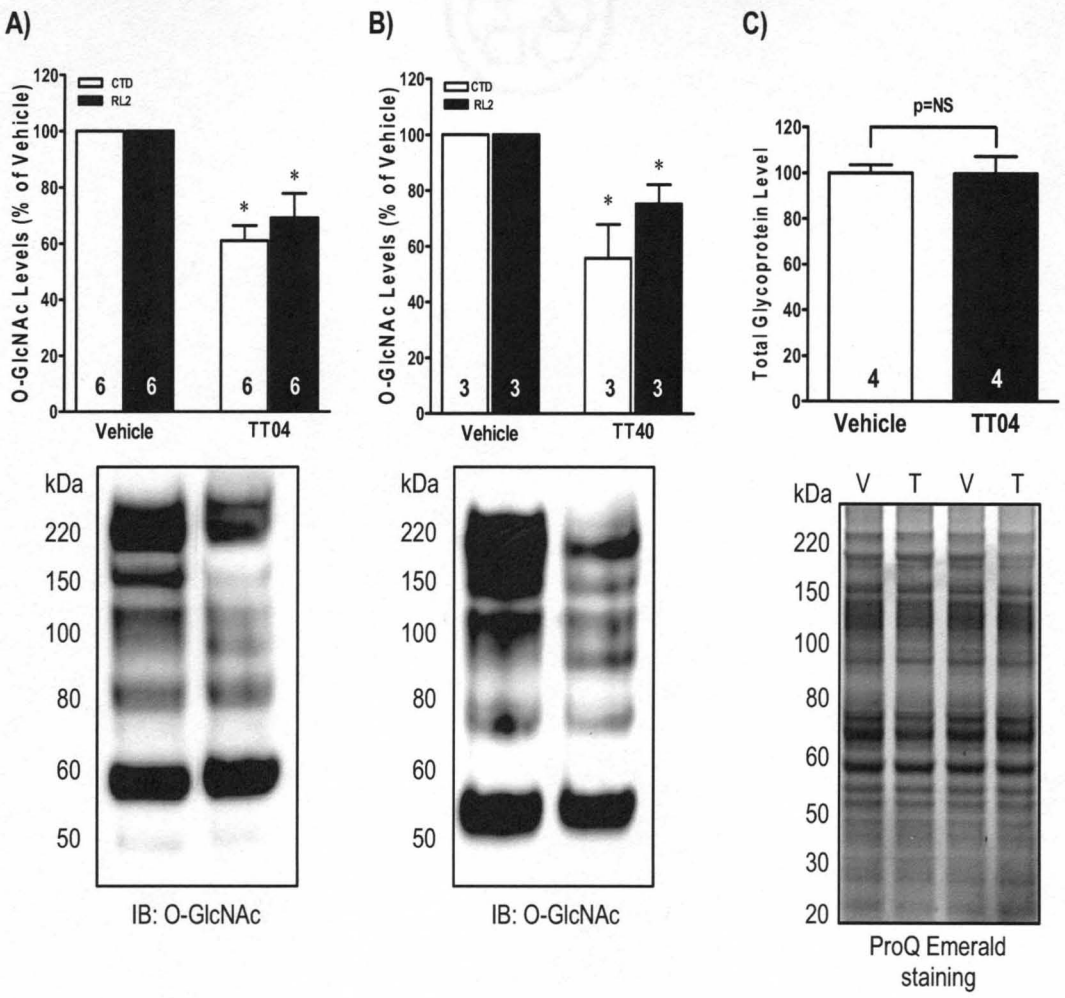

Figure 17. Evaluation of effects of OGT inhibition on post-hypoxic cardiac myocyte survival. NRCMs were treated with the OGT inhibitor, TT04 or TT40, prior to protein harvest or H/R. **A)** Densitometric analysis and representative immunoblots for O-GlcNAc levels following TT04 treatment show significant reduction in O-GlcNAc levels. Multiple bands occur because O-GlcNAc is a post-translational modification occurring on a plethora of intracellular proteins (n=6/group). **B)** Densitometric analysis and representative immunoblots for O-GlcNAc levels following TT40 treatment show significant decrease in O-GlcNAc levels (n=3/group). **C)** Densitometric analysis and representative ProQ emerald stained gel for glycoprotein levels following TT04 treatment show no change in glycoprotein levels (n=4/group).

To evaluate the effects of OGT inhibition on cardiac myocyte survival post-hypoxia, cardiac myocytes (n = 6/group) were treated with TT04, subjected to hypoxia-reoxygenation, and media harvested to measure LDH release. Inhibition

of OGT with TT04 (172 ± 18%, p<0.05) or TT40 (227±30%, p<0.05) significantly augmented post-hypoxic LDH release compared to vehicle (Figure 17A). Moreover, PI positivity was significantly more following OGT inhibition with TT04 (132 ± 10%, $p < 0.05$) compared to Vehicle (Figure 17B).

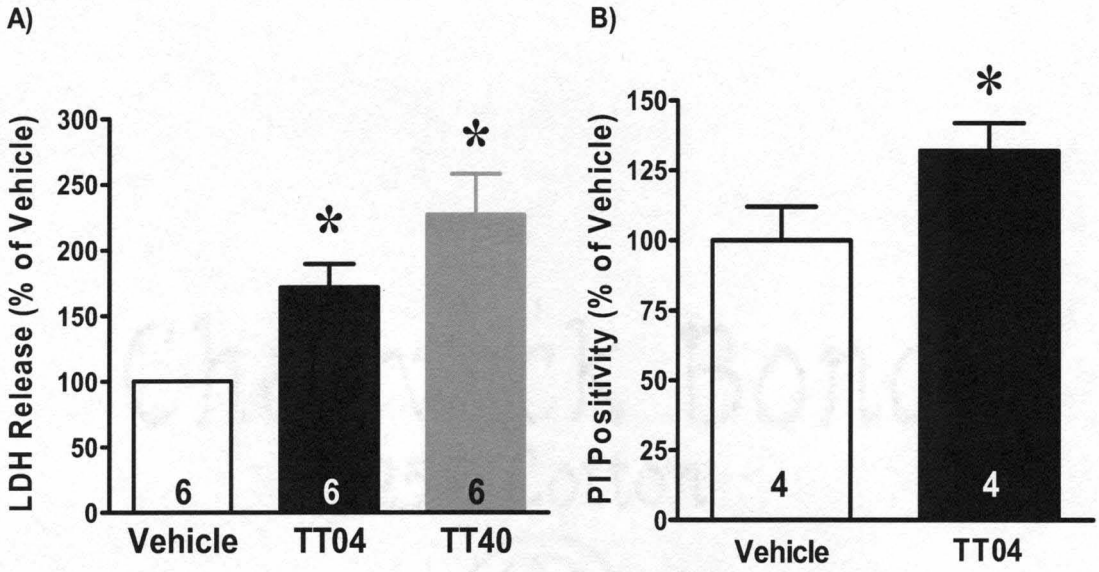

Figure 18. A) OGT inhibition (with TT04 and TT40) significantly exacerbated post-hypoxic cardiac myocyte survival. LDH release was spectrophotometrically determined from the media following hypoxia-reoxygenation (n=6/group). **B)** OGT inhibition via TT04 worsens post-hypoxic injury reflected by the significant increase in PI positive cells (n=4/group). *p<0.05 vs. Vehicle.

C.3. Knockdown of OGT sensitizes cardiac myocytes to post-hypoxic death: NRCMs (n ≥ 4/group) were treated with OGT siRNA or Control siRNA for 36 hours to knockdown OGT expression at the mRNA level. The transfection efficiency for the siRNA was estimated to be greater than 90% (Figure 18A). Whole cell lysates immunoblotted for OGT and *O*-GlcNAc showed significant reductions in OGT levels (49 ± 8% of Control, $p < 0.05$) and *O*-GlcNAc levels (64 ± 5% of Control, $p < 0.05$) for OGT siRNA-treated NRCMs compared with

control siRNA-treated NRCMs (Figure 18B-C). There was no difference in α-tubulin levels between OGT siRNA- and Control siRNA-treated myocytes according to western blot (Figure 18B).

To investigate the effects of OGT gene knockdown on cardiac myocyte survival post-hypoxia, cardiac myocytes (n=6/group) were treated with 30 nmol/L OGT siRNA or Control siRNA for 36 hours, subjected to hypoxia-reoxygenation, and media harvested to measure LDH release. There was a significant (120 ± 2% of control $p < 0.05$) augmentation in post-hypoxic LDH release in OGT siRNA-treated NRCMs compared to Control siRNA-treated NRCMs (Figure 18D).

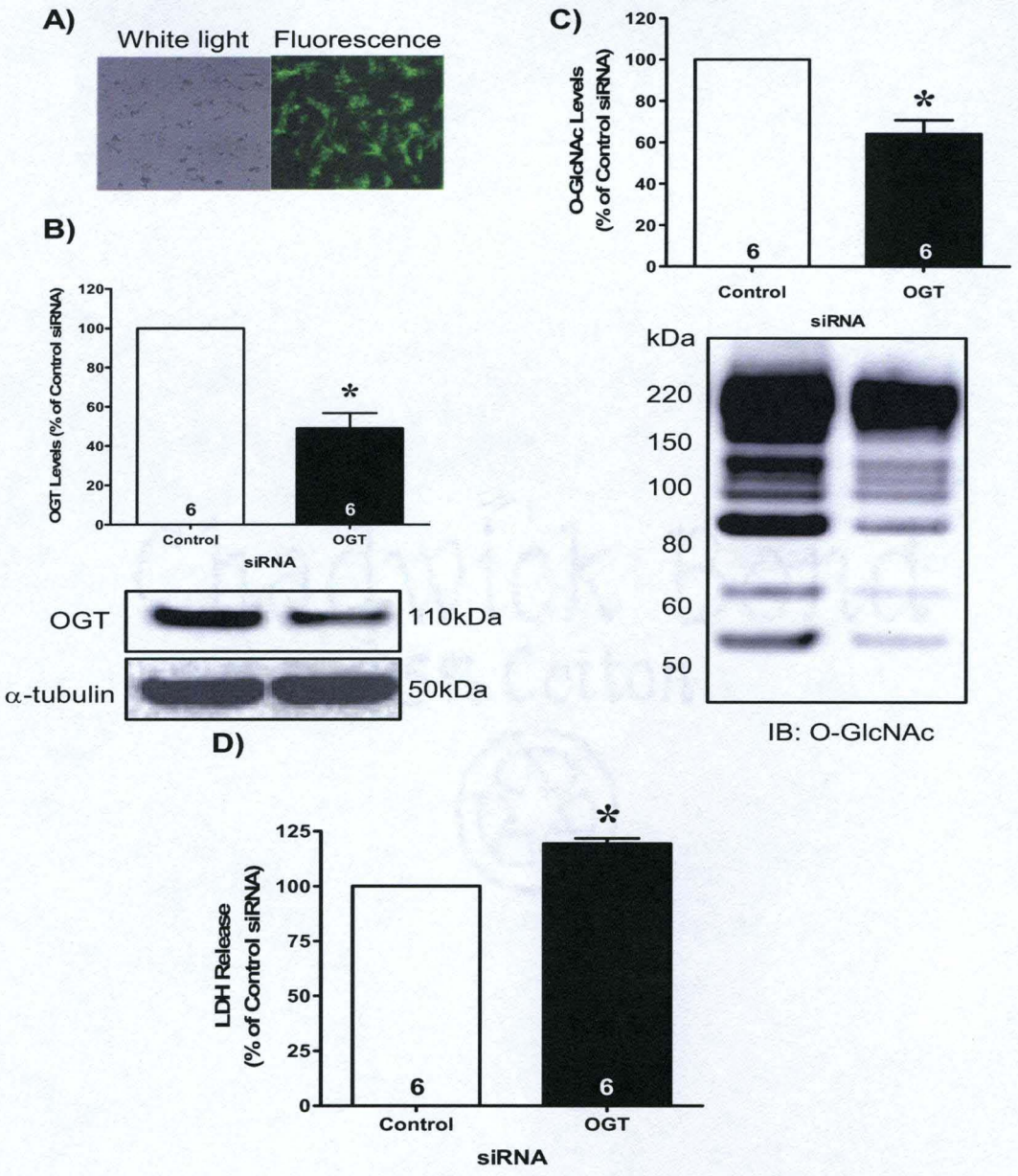

Figure 19. Effects of OGT gene knockdown on post-hypoxic NRCM survival (n=6/group). **A)** NRCMs transfected with fluorescently tagged control siRNA showing a transfection efficiency of more than 90%. **B)** Knockdown of OGT significantly reduces OGT protein levels according to immunoblotting in OGT siRNA-treated compared with Control siRNA treated NRCMs. **C)** Whole cell lysates from OGT siRNA-treated NRCMs showed a significant decrease in O-GlcNAc levels compared with those from Control siRNA-treated NRCMs according to western blotting. **D)** NRCMs treated with OGT siRNA were more sensitive to hypoxia-induced injury (according to LDH release) compared with NRCMs treated with Control siRNA. *$p < 0.05$ vs. Control siRNA.

C.4. Deletion of OGT gene sensitizes cardiac myocytes to hypoxic injury: Neonatal mouse cardiac myocytes (NMCMs, n=3/group) carrying only loxP-flanked copies of the OGT gene (Figure 19A) were infected with adenovirus expressing CRE-recombinase for 72 hours. Whole cell lysates were immunoblotted for CRE-recombinase, OGT, and *O*-GlcNAc modification. NMCMs expressing CRE-recombinase (Figure 19B) showed significant reductions in OGT (44 ± 16% of control, Figure 19C) and *O*-GlcNAc levels (28 ± 5% of control, Figure 19D). To assess the effect of OGT deletion on cardiac myocyte survival following hypoxia, 72 hour post-AdCRE infection, NMCMs were subjected to 3 h of hypoxia and 1 h of reoxygenation and media harvested for LDH assay. A significant ($p < 0.05$) elevation in LDH release was observed at 50 MOI (122 ± 12% of control) compared with 0 MOI AdCRE (Figure 19E).

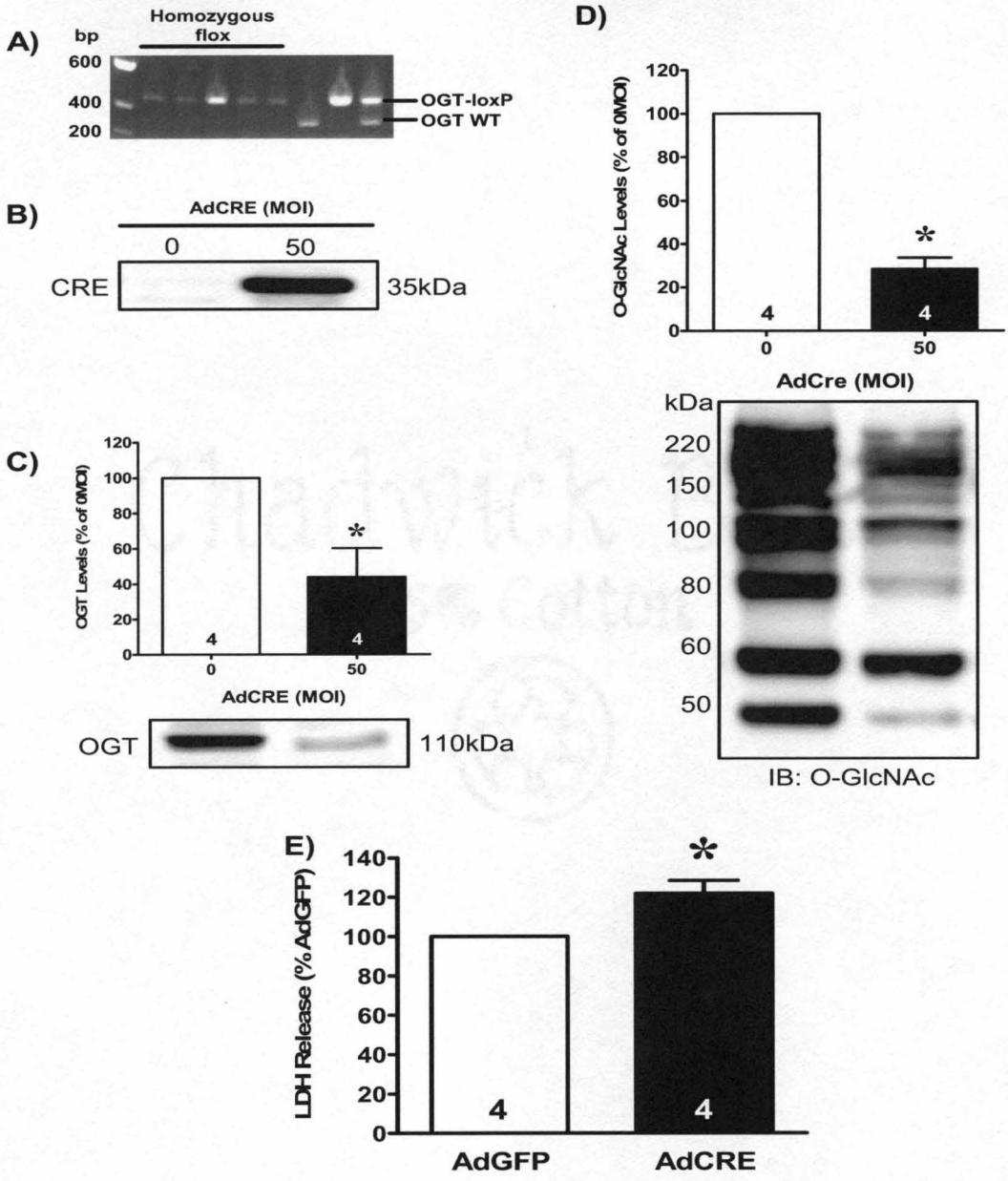

Figure 20. Effects of OGT deletion on survival following hypoxia in cardiac myocytes. NMCMs were infected with AdCRE 72 hours prior to protein harvest or H/R. **A)** Representative genotyping PCR results showing loxP-flanked or WT OGT gene. **B)** Cardiac myocytes from homozygous litters were exposed to AdCRE or no virus. There was a significant ($p<0.05$) increase in CRE-recombinase expression (n=4/group) and **C)** a significant ($p<0.05$) decrease in OGT levels with 50 MOI compared with 0 MOI AdCRE (n=4/group). **D)** O-GlcNAc levels were markedly decreased at 50 MOI compared with 0 MOI AdCRE (n=4/group). **E)** LDH release was significantly ($p<0.05$) elevated at 50 MOI compared with 0 MOI AdCRE following hypoxia-reoxygenation (n=4/group). *$p<0.05$ vs. 0 MOI AdCRE.

D. ROLE OF GCA IN HYPOXIA-INDUCED CARDIAC MYOCYTE INJURY

D.1. GCA (AdGCA) overexpression exacerbates post-hypoxic cardiac myocyte death: Forty-eight hours following AdGCA infection of isolated NRCMs (n>/=5 per group), total cellular proteins were isolated for GCA protein and *O*-GlcNAc levels (via western blot analysis). Adenoviral overexpression of GCA significantly ($p<0.05$) augmented GCA protein levels (Figure 20A). Such elevation corresponded with a significant ($p<0.05$) reduction in *O*-GlcNAc levels (48±7% of 0 MOI AdGCA) (Figure 20B). Similar findings were seen with another *O*-GlcNAc antibody, RL2 (65±8% of 0 MOI AdGCA; Figure 20B). Immunoblots for *O*-GlcNAc levels show multiple immunopositive bands because *O*-GlcNAc is a posttranslational modification, not a single protein (Figure 20B). Other studies have demonstrated similar findings in various cell lines (333) and NRCMs(33, 34). Equal protein loading was confirmed by densitometric analysis of Ponceau-stained membranes.

To evaluate the effects of GCA overexpression on post-hypoxic cardiac myocyte survival, similarly treated cardiac myocytes were subjected to hypoxia (3 h) and reoxygenation (1 or 6 h). Post-hypoxic media was harvested for LDH release, and additional post-hypoxic NRCMs were stained with PI to assess cell death. Myocytes infected with AdGCA were more sensitive to hypoxia-induced injury by the first hour of reoxygenation according to LDH release (150±23% of 0 MOI AdGCA, $p<0.05$; Figure 20C). To determine whether the detrimental effect of AdGCA on post-hypoxic cardiac myocytes was short-lived, similarly treated NRCMs were reoxygenated for 6 hours after 3 hours of hypoxia. The longer

duration of reoxygenation (6 hours) still showed exacerbated cellular injury in AdGCA NRCMs, according to LDH release (179±14% versus 136±8% for AdGFP, $p<0.05$; Figure 20C). Another index of cell death i.e. PI positivity confirmed our one hour (17±2% versus 10±1% for AdGFP; Figure 20D) and six hour (34±3% versus 24±2% for AdGFP, $p<0.05$; Figure 20D) post-post-hypoxic LDH data compared to 0 MOI AdGCA or AdGFP.

Cell damage was not significantly different among AdGCA, AdGFP, or uninfected NRCMs under normoxia according to LDH release (109±3% of control versus 93±3% of control, $p>0.05$) and PI positivity (14±1% for GCA versus 13±1% for AdGFP versus 12±1% for control, $p>0.05$). Such results confirm that viral infection does not affect cell survival or *O*-GlcNAc levels in this system.

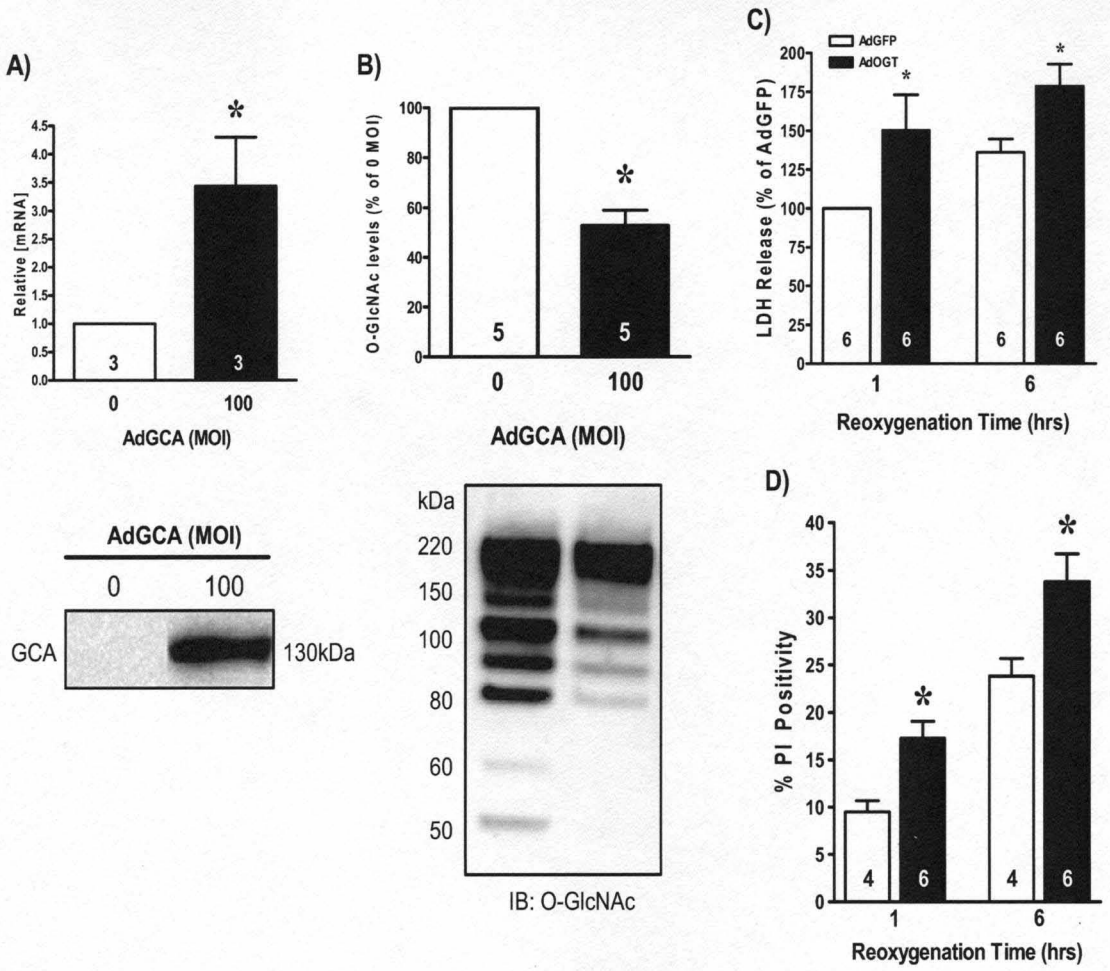

Figure 21. Myocytes were infected with AdGFP or AdGCA (0 or 100 MOI) 48 hours before protein isolation or hypoxia/reoxygenation. **A)** Bar graph of real time PCR showing significantly augmented GCA mRNA levels at 100 MOI compared to 0 MOI AdGCA (n=3/group). **B)** Representative immunoblot of GCA protein shows significant elevation in GCA levels following AdGCA infection. **C)** Densitometric analysis and representative immunoblot of *O*-GlcNAc levels. AdGCA significantly reduced *O*-GlcNAc levels. As expected, multiple immunopositive bands appear because the *O*-GlcNAc modification occurs on numerous proteins throughout the cell (n=5/group). **D)** GCA overexpression exacerbated post-hypoxic cardiac myocyte damage according to LDH release (n=5/group). **E)** GCA overexpression aggravated post-hypoxic injury according to propidium iodide positivity (n=4-5 /group). *P<0.05 vs. 0 MOI AdGCA or 100 MOI AdGFP.

D.2. GCA inhibition attenuates post-hypoxic cardiac myocyte injury: NRCMs (n=6/ group) were treated with PUGNAc (GCA inhibitor) overnight before protein harvest, then immunoblotted for *O*-GlcNAc levels. PUGNAc significantly increased *O*-GlcNAc levels (878±215% of control, $p<0.05$) compared to vehicle (Figure 21A).

Additional NRCMs (n=6/ group) were treated with PUGNAc, subjected to hypoxia/reoxygenation, and media harvested to measure LDH release. Inhibition of GCA (with PUGNAc) (70±10% of Vehicle, $p<0.05$; Figure 21B) significantly attenuated post-hypoxic LDH release at the end of the first hour of reoxygenation. The protective effect of augmented *O*-GlcNAc levels (with PUGNAc) was still seen at 6 hours of reoxygenation according to LDH release (133±11% for PUGNAc, $p<0.05$ versus 177±14% for Vehicle; Figure 21B). Similar protective effects were observed using PI positivity as another index of cell death at both one (9±1% versus 13±1% for vehicle, $p<0.05$; Figure 21C) and six hour (21±2% versus 36±2% of Vehicle, $p<0.05$; Figure 21C) reoxygenation time points. PI positivity and PI positivity. PUGNAc or Vehicle treatment did not significantly alter normoxic/aerobic cellular viability compared with untreated NRCMs under normoxia according to LDH release ($p>0.05$, 90±8% of control versus 104±8% of Control) and PI positivity ($p>0.05$, 12±1% for PUGNAc versus 13±1% for Vehicle versus 13±1% for Control).

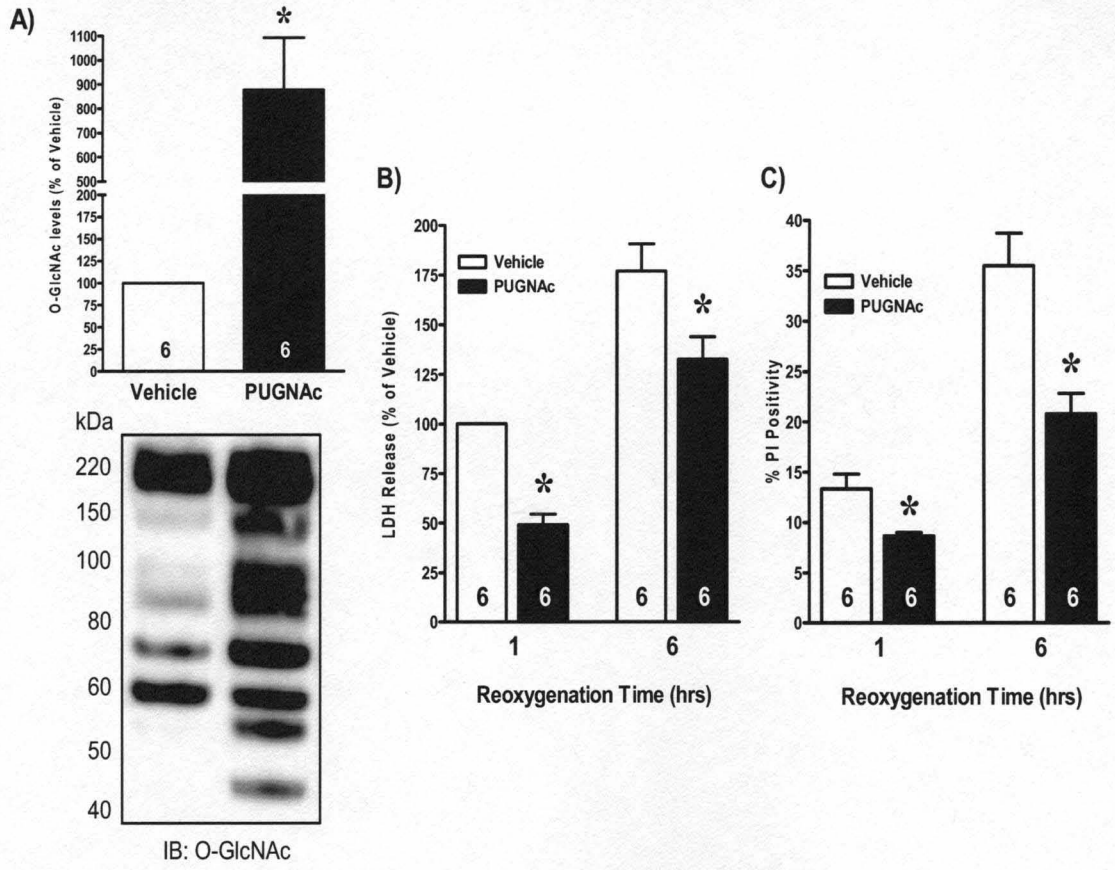

Figure 22. NRCMs were subjected to pharmacological repression of GCA activity (n=6/group). **A)** Densitometric analyses of *O*-GlcNAc Western blots show significantly elevated *O*-GlcNAc levels compared to Vehicle. Representative immunoblots for *O*-GlcNAc levels following PUGNAc treatment show a significant increase in *O*-GlcNAc levels compared to Vehicle. Multiple bands occur because *O*-GlcNAc is a posttranslational modification. **B)** GCA inhibition with PUGNAc diminished post-hypoxic injury in NRCMs (according to LDH release) compared with Vehicle. **C)** GCA inhibition with PUGNAc reduced post-hypoxic injury (per PI positivity) compared with Vehicle. **P*<0.05 vs. Vehicle.

D.3. Knockdown of GCA reduces post-hypoxic cardiac myocyte injury: NRCMs (n=6/group) were treated with 60 nmol/L GCA siRNA or Control siRNA for 72 h to knockdown GCA expression. GCA knockdown significantly ($p<0.05$) reduced GCA protein levels compared to Control siRNA, despite no change in α-tubulin levels (Figure 22A). GCA siRNA significantly ($p<0.05$) augmented O-GlcNAc levels (132±12% of Control, $P<0.05$) compared to Control siRNA (Figure 22A & B).

Additional NRCMs were treated with GCA or Control siRNA, subjected to hypoxia/reoxygenation, and media harvested to measure LDH release. GCA siRNA significantly ($p<0.05$) reduced post-hypoxic LDH release after 1 h (72±10% of Control siRNA; Figure 22C) and 6 hours (130±4% for GCA siRNA versus 170±26% for Control siRNA; Figure 22C) of reoxygenation compared to Control siRNA. In addition, GCA siRNA significantly diminished PI positivity at 6 hours (22±2% for GCA siRNA versus 33±2% for Control siRNA, $p<0.05$; Figure 22D) compared with Control siRNA. GCA (102±5%) or Control siRNA (97±5%) treatment did not cause significant cell damage compared with untreated NRCMs under normoxia/aerobic conditions.

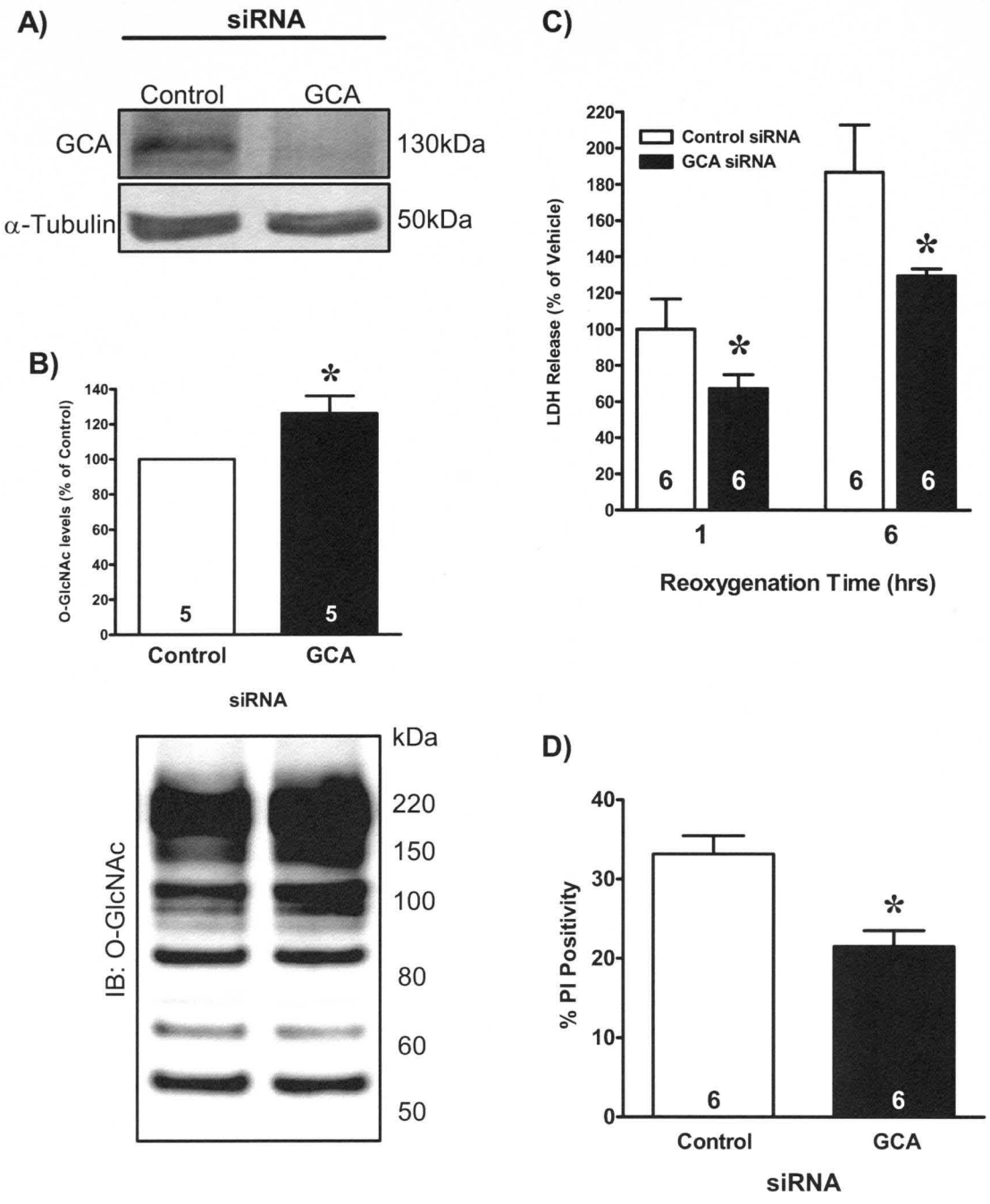

Figure 23. A) GCA message knockdown (siRNA) significantly reduced GCA protein levels compared with Control siRNA (n=5-6/group). **B)** Densitometric analysis of O-GlcNAc immunoblots showed a significant increase in O-GlcNAc levels for GCA siRNA compared with Control siRNA. Representative immunoblot for lysates from GCA siRNA-treated NRCMs showing augmented O-GlcNAc levels compared to Control siRNA. **C)** GCA siRNA-treated NRCMs were more resistant to hypoxia-induced injury according to LDH release and **D)** PI positivity compared to Control siRNA. *P<0.05 vs. Control siRNA.

E. ROLE OF O-GlcNAc IN ER STRESS-INDUCED CARDIOMYOCYTE DEATH

E.1. Hypoxia induces ER stress: ER stress markers were evaluated to confirm that hypoxia induces ER stress. Cardiac myocytes subjected to six hours of hypoxia and six hours of reoxygenation then immunoblotted for ER stress proteins showed significantly ($p<0.05$) augmented UPR-inducible proteins, Grp 94 (169+/-14% of Normoxia), Grp 78 (136+/-16% of Normoxia), and calreticulin (135+/-15% of Normoxia) as shown in Figure 23A and B. Moreover, hypoxia induced apoptosis according to significant ($p<0.05$) PARP cleavage (50+/-16% of normoxia) despite no change in α-tubulin protein levels (Figure 23A & B). These results indicate that hypoxia induces ER stress in cultured neonatal cardiac myocytes and confirms previous findings by other groups (283, 293). Because hypoxia/ischemia exact multiple insults on cardiac myocytes, we wanted to isolate one such pathology (ER stress) and ask whether O-GlcNAc signaling could interfere with this specific pro-death pathway.

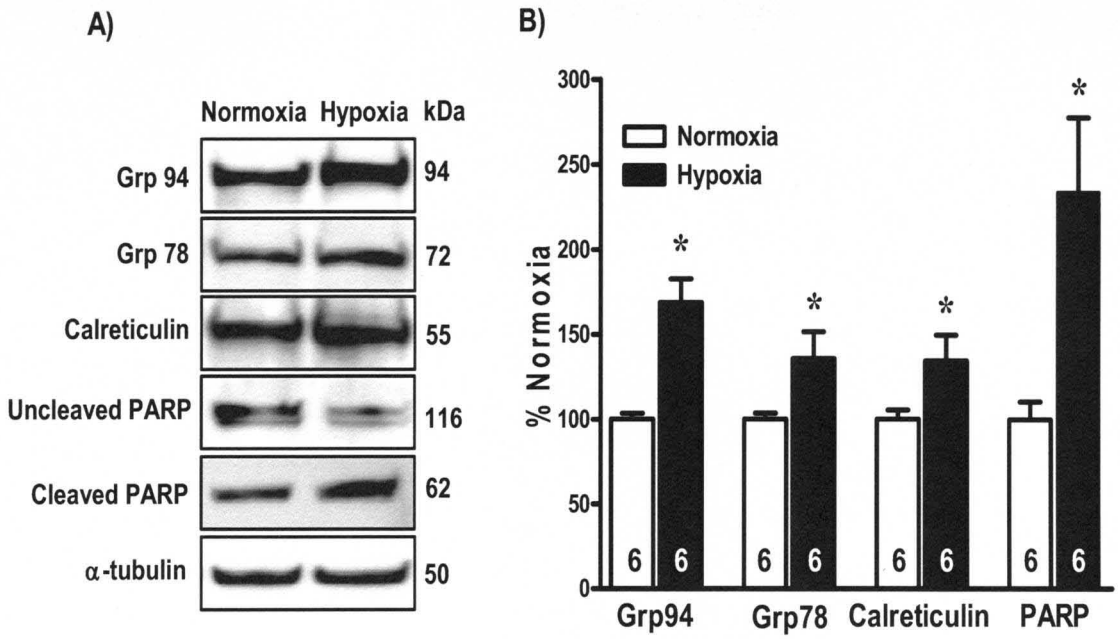

Figure 24. Cardiac myocytes (n=6/group) were subjected to hypoxia-reoxygenation and activation of ER stress evaluated. **A)** Hypoxia activated ER stress as reflected by immunoblots showing augmented Grp 94, Grp 78, and calreticulin levels. **B)** Densitometric quantification of immunoblots showed significant post-hypoxic upregulation of Grp 94, Grp 78, Calreticulin (Cal), and PARP cleavage (expressed as cleaved/uncleaved PARP in bar graph). * $p<0.05$ vs. Normoxia.

E.2. Genetic manipulation of O-GlcNAc signaling alters maladaptive ER stress signaling: As shown above and supported by other groups, augmented O-GlcNAc levels attenuate post-hypoxic cardiac myocyte death (33, 34), post-ischemic contractile dysfunction in isolated perfused hearts (189-191), and hemorrhagic shock-mediated inflammation (337, 338). Because numerous studies have implicated ER stress in the pathogenesis of post-ischemia/hypoxic injury(249, 283, 293), we evaluated whether genetic manipulation of O-GlcNAc signaling affects ER stress-induced cardiac myocyte death, *per se*, under normoxic conditions.

Cardiac myocytes infected with replication deficient adenovirus carrying GFP, OGT, or GCA gene for 24 hours, were treated with prototypical ER stress inducers, Tunicamycin (TM)(72) or Brefeldin A (BfA)(250), for 24 hours. O-GlcNAc levels and the levels of several UPR inducible proteins were assessed by immunoblotting. BfA treatment significantly ($p<0.05$) augmented O-GlcNAc levels (206±19% of AdGFP, Figure 24A). OGT overexpression significantly (296±32% for AdOGT + BfA vs. 206 ±19% for AdGFP + BfA, $p<0.05$) increased O-GlcNAc levels over the levels already induced by ER stress (Figure 24A). Although induction of ER stress in GCA overexpressed cells augmented O-GlcNAc levels, it was still less than baseline O-GlcNAc levels (Figure 24A). Similar changes in O-GlcNAc signaling were observed following induction of ER stress with TM (Figure 24B).

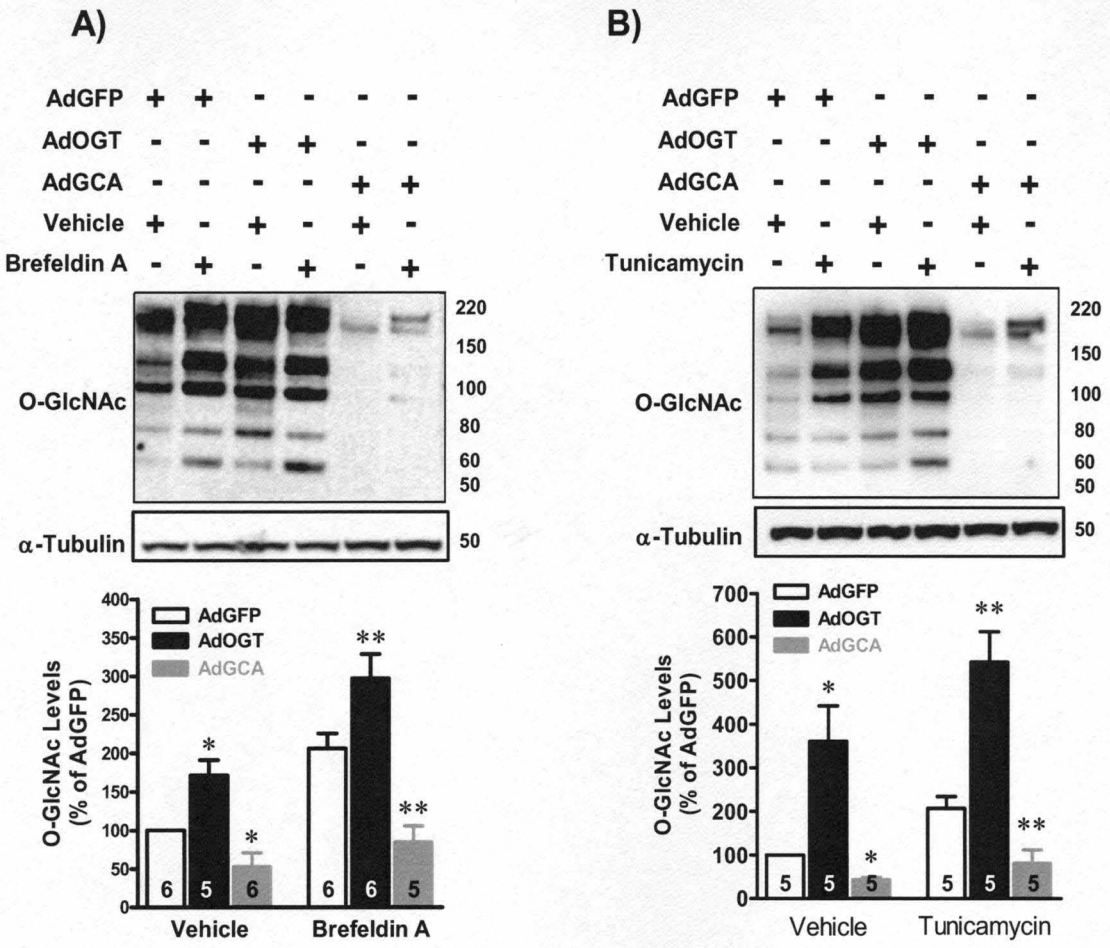

Figure 25. Normoxic cardiac myocytes (n=6/group) were treated with AdGFP, AdOGT, or AdGCA, subjected to ER stress with Brefeldin A (BfA, inhibit ER-golgi protin transport) or Tunicamycin (TM, inhibits *N*-glycosylation). Whole cell lysates was immunoblotted for O-GlcNAc and α-tubulin. **A)** BfA treatment augmented O-GlcNAc levels. OGT overexpression significantly augmented O-GlcNAc levels over that induced by BfA as shown in immunoblot and densitometric quantification of immunoblots. **B)** TM treatment augmented O-GlcNAc levels. OGT overexpression significantly augmented O-GlcNAc levels over that induced by TM. n=6/group. * $p<0.05$ vs. AdGFP, ** $p<0.05$ vs. AGFP + BfA or AdGFP + TM.

BfA-induced ER stress stimulated significant ($p<0.05$) increase in ER chaperones, Grp 94 (185±14% AdGFP), Grp 78 (491±56% AdGFP), and Calreticulin (155±34% AdGFP) as shown in Figure 25A & B. Moreover, BfA treatment activated the maladaptive arm of ER stress response according to PARP cleavage (231±29% AdGFP) and CHOP activation (839±29% AdGFP) as shown in Figure 25A & B. OGT overexpression significantly reduced BfA-mediated ER stress reflected by reduced Grp 94 (144±10% for AdOGT + BfA vs. 185±14% for AdGFP + BfA) and Grp 78 (303±28% for AdOGT + BfA vs. 491±56% for AdGFP + BfA) protein levels (Figure 25A & B). Furthermore, OGT overexpression significantly ($p<0.05$) attenuated BfA-induced activation of maladaptive ER stress response according to diminished CHOP activation (400±77% for AdOGT + BfA vs. 839±29% for AdGFP + BfA, Figure 25A & B).

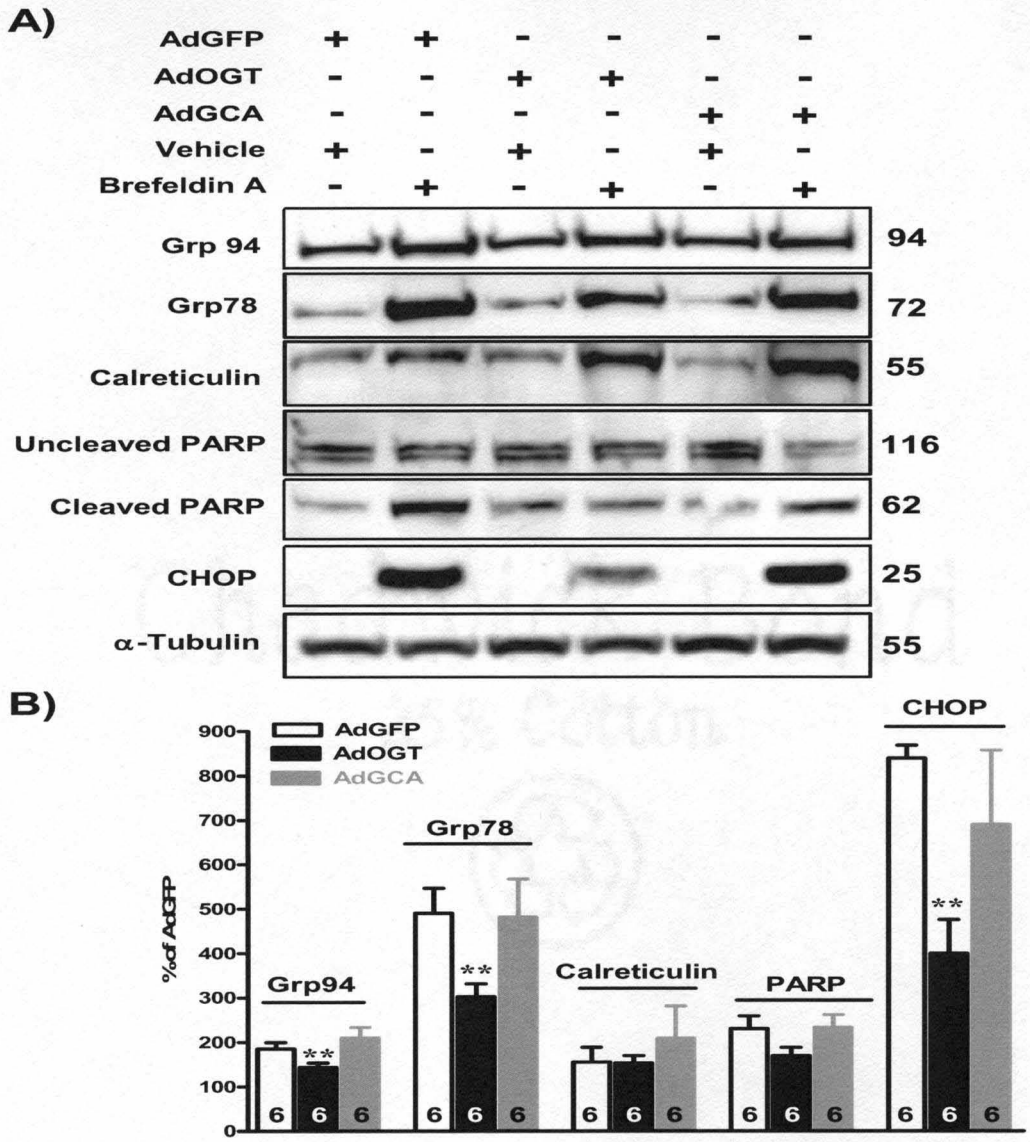

Figure 26. Normoxic cardiac myocytes (n=6/group) were treated with AdGFP, AdOGT or AdGCA, subjected to ER stress with BfA and whole cell lysates immunoblotted for Grp 94, Grp 78, Calreticulin, PARP and CHOP. **A)** Total protein was isolated from selected cultures and immunoblotted for ER stress indicators. OGT overexpression significantly attenuated, while GCA overexpression did not change BfA-induced ER stress according to immunoblotting. **B)** Densitometric quantification of immunoblots showed significant reduction in BfA-induced increase in Grp 94, Grp 78, and CHOP levels with OGT overexpression. OGT overexpression did not affect Calreticulin expression or PARP cleavage (expressed as cleaved PARP/uncleaved PARP). GCA overexpression did not significantly change BfA-induced Grp94, grp78, Calreticulin, PARP cleavage and CHOP levels. * $p<0.05$ vs. AdGFP, ** $p<0.05$ vs. AGFP + BfA.

To confirm the protective effects of augmented O-GlcNAc levels (via OGT overexpression) on the activation of maladaptive unfolded protein response, we examined whether OGT overexpression affects ER stress induced by Tunicamycin (TM), an inhibitor of N-glycosylation of nascent ER proteins. OGT overexpression significantly ($p<0.05$) reduced the TM-induced ER stress according to Grp 94 (320±33% for AdOGT + TM vs. 421±18% for AdGFP + TM), Grp 78 (322±47% for AdOGT + TM vs. 536±31% for AdGFP + TM), and CHOP activation (1549±239% for AdOGT + TM vs. 3065±585% for AdGFP + TM) as shown in Figures 26A & B. In both BfA and TM treatments, OGT overexpression did not affect ER stress-mediated increase in calreticulin protein level or PARP cleavage (Figure 26A-B). GCA overexpression did not alter BfA or TM-mediated increases in the ER chaperones: Grp94, Grp78 and calreticulin (Figure 26A-B). Finally, AdGCA did not affect ER stress mediated apoptosis according to CHOP activation and PARP cleavage (Figures 25 and 26). These results demonstrate that known ER stress inducers (BfA and TM) augment protein levels of three well-characterized UPR-inducible proteins in cardiomyocytes, consistent with other groups(283, 293).

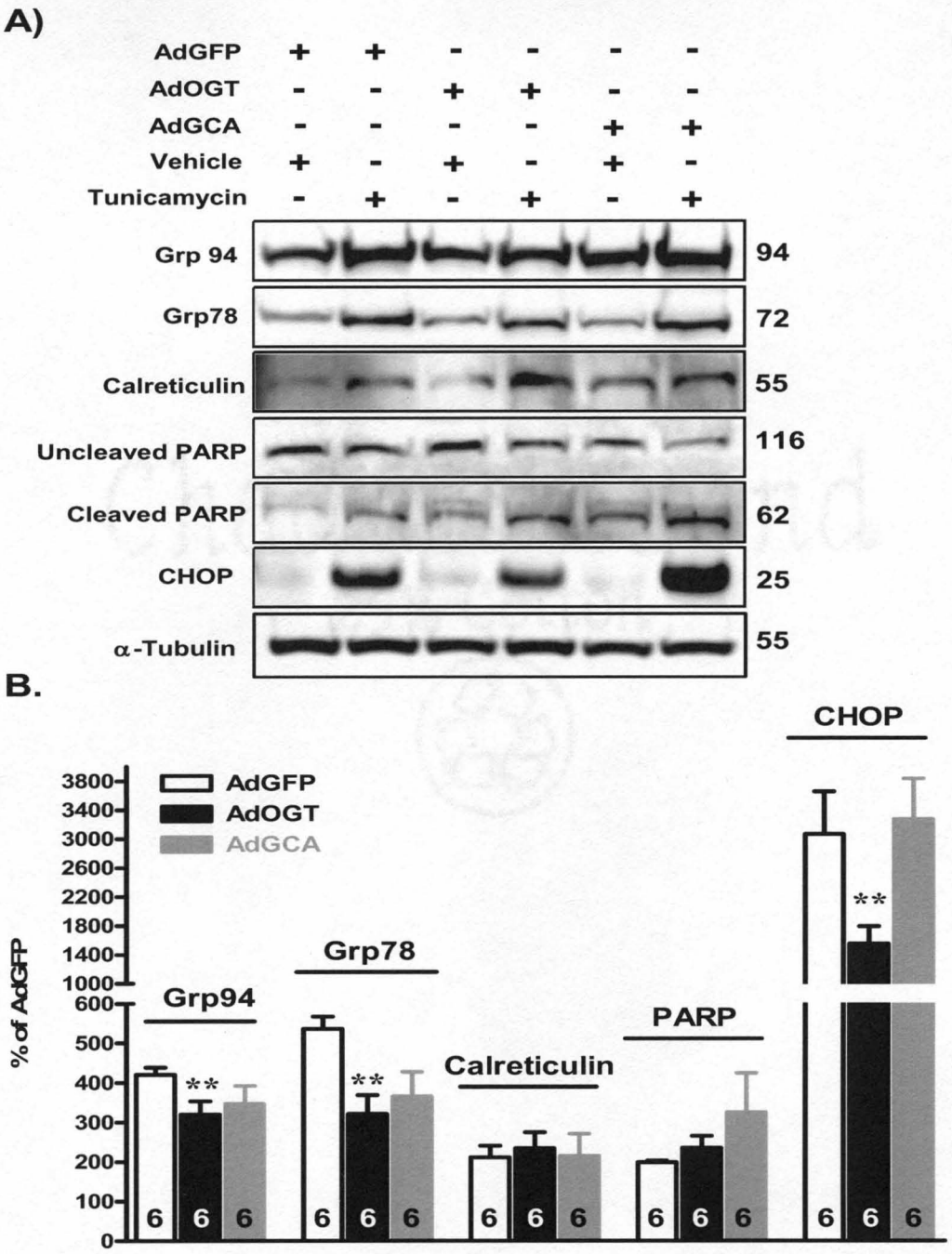

Figure 28. Normoxic cardiac myocytes (n=6/group) were treated with AdGFP, AdOGT, or AdGCA, subjected to ER stress with TM and whole cell lysates immunoblotted for O-GlcNAc, Grp 94, Grp 78, Calreticulin, PARP and CHOP. **A)** OGT overexpression significantly mitigated, while GCA overexpression did not change TM-induced ER stress according to immunoblotting. **B)** Densitometric quantification of immunoblots showed significant reduction in TM-induction of Grp 94, Grp 78, and CHOP with OGT overexpression despite no change with GCA overexpression. * $p<0.05$ vs. AdGFP, ** $p<0.05$ vs. AdGFP + TM.

E.3. Genetic manipulation of O-GlcNAc signaling affects ER stress-mediated cardiac myocyte death: During prolonged or severe ER stress, the cell death pathways can be activated. Therefore, we questioned whether genetic manipulation of the two enzymes involved with O-GlcNAc signaling affects ER stress-induced cardiac myocyte death. In the absence of ER stress, neither OGT overexpression nor GCA overexpression altered cellular viability according to PI positivity (Figure 27A). OGT overexpression significantly (38±3% for AdOGT + BfA vs. 47±3% for AdGFP + BfA, $p<0.05$) attenuated, while GCA overexpression exacerbated (60±2% for AdGCA + BfA, $p<0.05$) BfA-induced cell death according to PI positivity (Figure 27A). Neither OGT nor GCA overexpression significantly altered BfA mediated cardiomyocyte apoptosis according to Caspase 3/7 activity (Figure 27B).

Similarly, OGT overexpression significantly mitigated TM-induced cardiomyocyte death (21±3% for AdOGT + TM vs. 34±3% for AdGFP + TM, $p<0.05$, Figure 27C). GCA overexpression did not alter TM-mediated cardiomyocyte death (Figure 27C). Moreover, both OGT and GCA overexpression did not significantly alter TM-mediated cardiomyocyte apoptosis according to Caspase 3/7 activity (Figure 27D). Taken together, these results indicate that augmented O-GlcNAc levels are protective against ER stress-induced cell death.

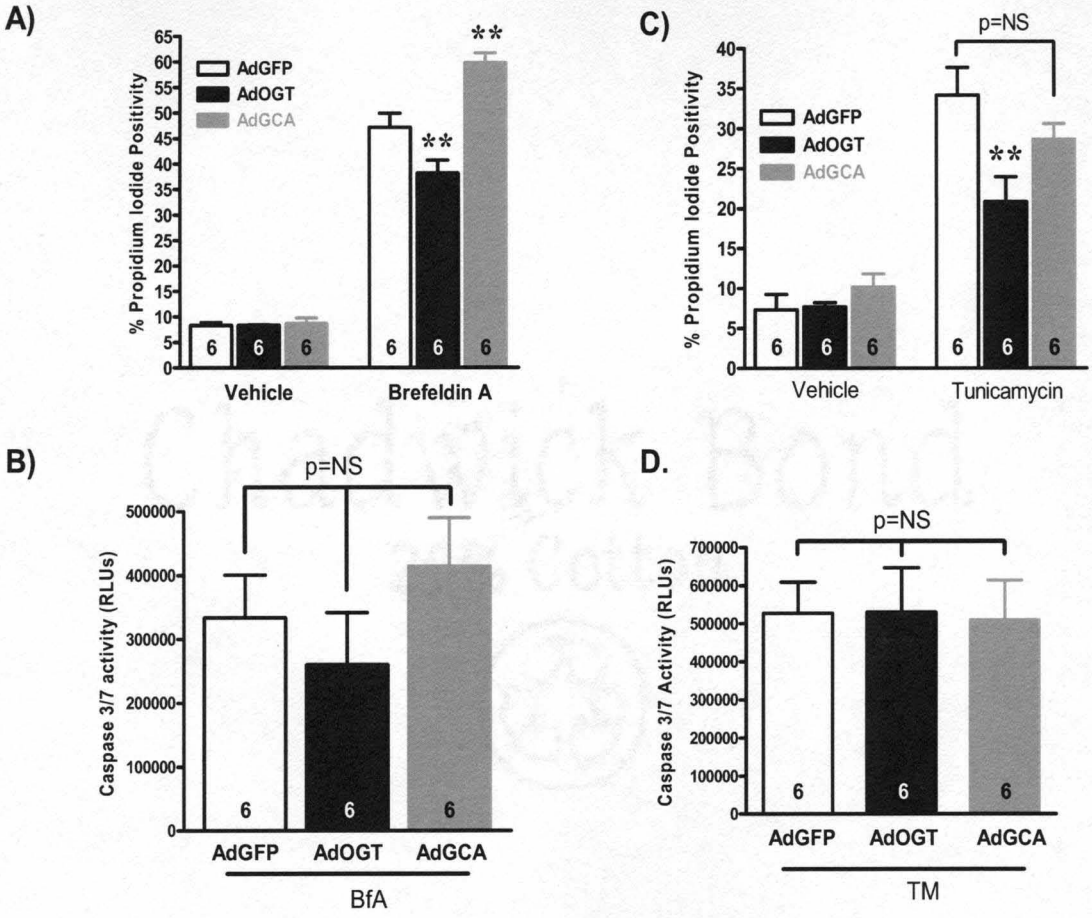

Figure 28. Normoxic cardiac myocytes ((n=6/group) were treated with AdGFP, AdOGT or AdGCA, subjected to ER stress with BfA and cell death evaluated using the nuclear stain, PI or measuring caspase activity. **A)** OGT overexpression significantly attenuated, while GCA overexpression exacerbated ER stress-induced cardiac myocyte death according to PI positivity. **B)** OGT or GCA overexpression did not change ER stress-induced cardiomyocyte apoptosis. **C)** OGT overexpression also significantly reduced TM-induced cardiac myocyte death despite no change with GCA overexpression according to PI positivity. **D)** Neither OGT nor GCA overexpression affected TM-induced cardiomyocyte apoptosis. n>/=5/group. * $p<0.05$ vs. AdGFP, ** $p<0.05$ vs. AdGFP + BfA or TM.

E.4. O-GlcNAcase inhibition reduces pro-death UPR signaling: Next, we used a complementary approach to elevate O-GlcNAc levels by inhibiting O-GlcNAcase with PUGNAc(111). Cardiac myocytes were treated with PUGNAc or Vehicle (0.1% ethanol) three hours prior to ER stress induction (with TM or BfA, 24 hours) and whole cell lysates immunoblotted for O-GlcNAc levels and ER stress indicators. Inhibition of O-GlcNAcase significantly augmented O-GlcNAc levels above that induced by BfA (Figure 28A) or TM (Figure 28B) alone.

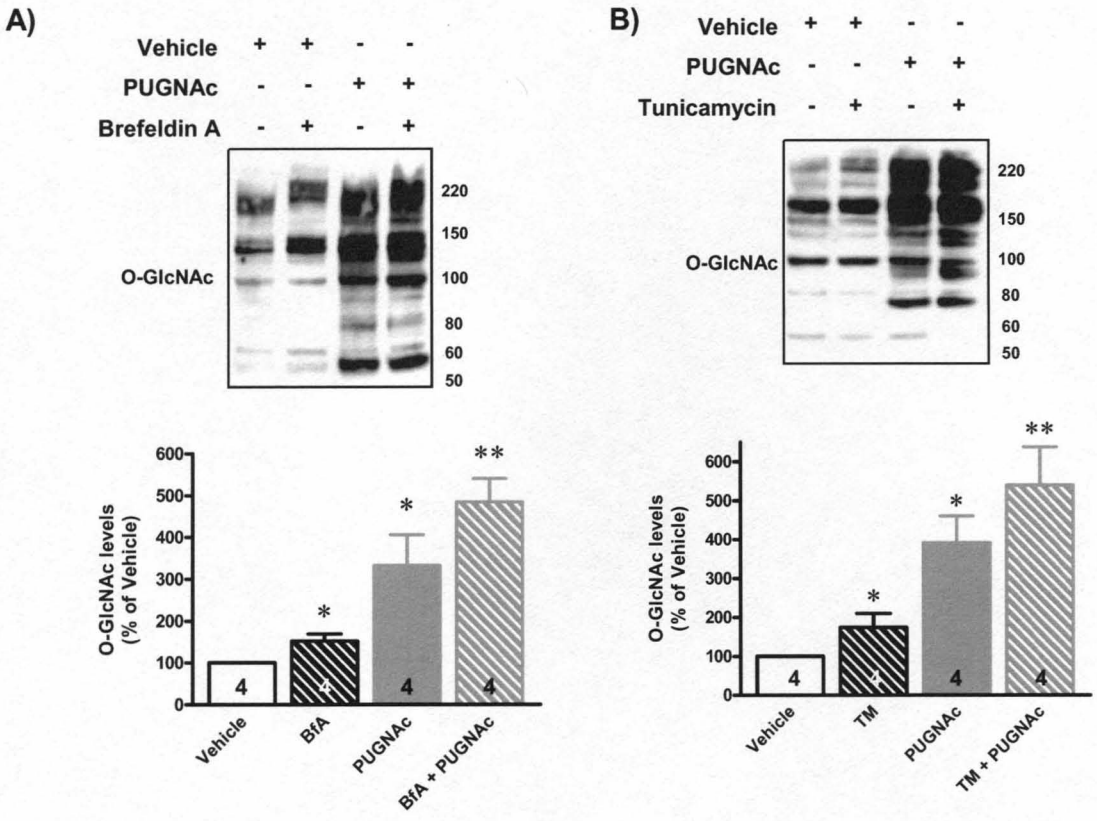

Figure 29. Normoxic cardiac myocytes were treated with either Vehicle or O-GlcNAcase inhibitor (PUGNAc) and subjected to ER stress (with BfA or TM). **A)** Western blots of whole cell lysates showed augmented O-GlcNAc levels with O-GlcNAcase inhibition compared to Vehicle. O-GlcNAcase inhibition augmented O-GlcNAc levels above that induced by BfA. **B)** O-GlcNAcase inhibition significantly increased O-GlcNAc levels above that induced by TM. n=4/group. *p<0.05 vs. Vehicle, ** p<0.05 vs. BfA or TM.

Moreover, O-GlcNAcase inhibition significantly ($p<0.05$) reduced BfA-induced ER stress according to Grp 94 (124±12% for PUGNAc + BfA vs. 179±18% for BfA alone), Grp 78 (136±7% for PUGNAc + BfA vs. 224±51% for BfA alone), and calreticulin (148±26% PUGNAc + BfA vs. 268±6% for BfA alone) shown in Figure 29. Additionally, O-GlcNAcase inhibition significantly ($p<0.05$) blocked the activation of maladaptive ER stress response as reflected by diminished CHOP activation (579±76% for BfA + PUGNAc vs. 1474±216% for BfA alone, Figure 29). Similar findings were observed with TM. PUGNAc treatment significantly attenuated TM-induced ER stress according to Grp 94 (171±3% for PUGNAc + TM vs. 285±73% for TM alone, $p<0.05$), Grp 78 (164±12% for PUGNAc + TM vs. 293±40% for TM alone, $p<0.05$), Calreticulin (174±15% PUGNAc + TM vs. 260±49% for TM alone, $p<0.05$) as represented in Figure 30. Finally, O-GlcNAcase inhibition reduced TM-induced CHOP activation, but did not affect BfA or TM induced PARP cleavage (Figure 30).

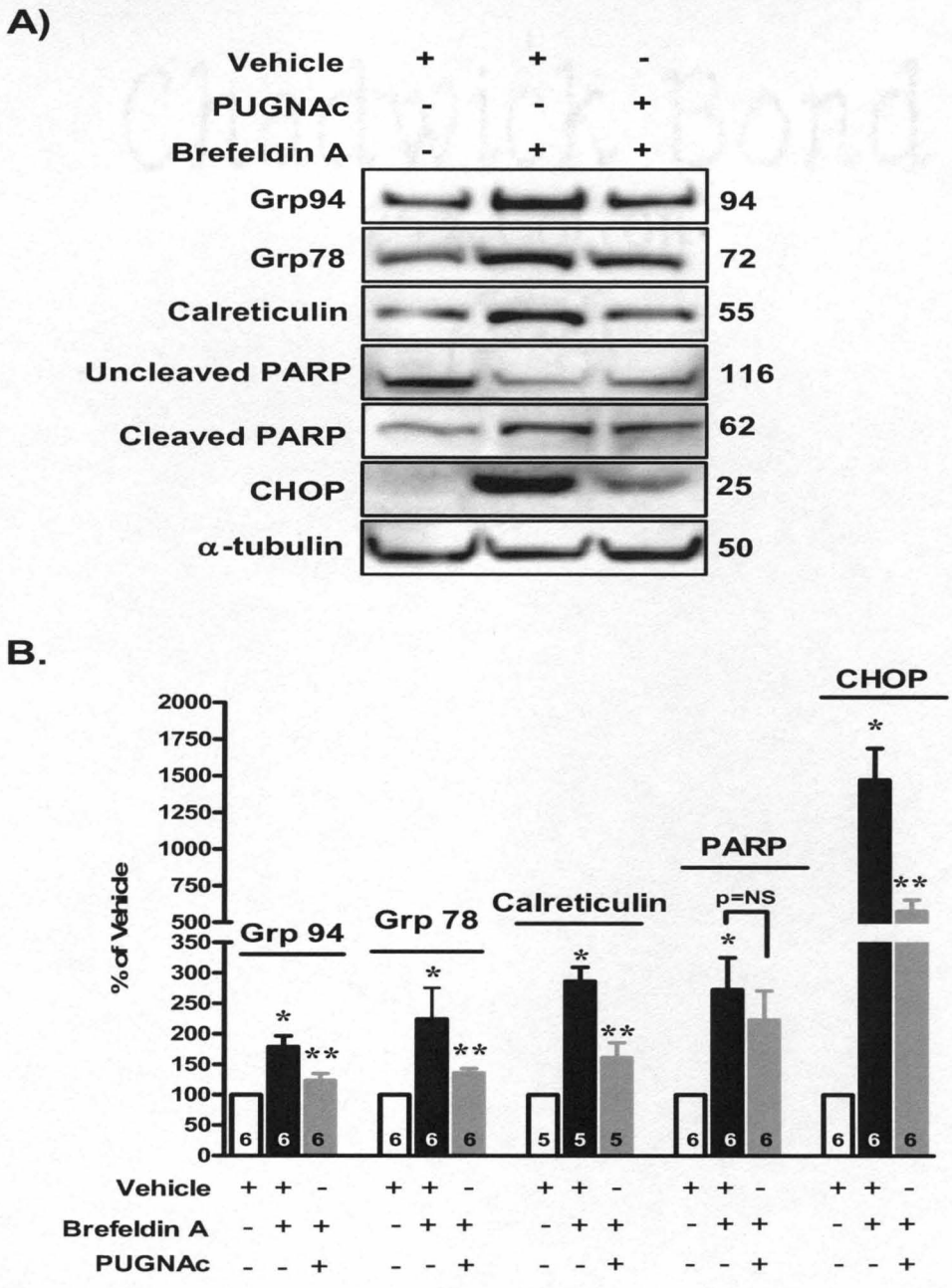

Figure 30. Normoxic cardiac myocytes ((n=5-6/group) were pre-treated with either Vehicle or O-GlcNAcase inhibitor (PUGNAc) and subjected to ER stress with BfA. **A)** Western blots of whole cell lysates showed significant reduction in BfA-mediated activation of Grp 94, Grp 78, Calreticulin and CHOP protein levels with O-GlcNAcase inhibition. **B)** Densitometric quantification of immunoblots showed significantly reduced Grp 94, Grp 78, Calreticulin, and CHOP protein levels with O-GlcNAcase inhibition. PUGNAc treatment did not affect BfA-mediated PARP cleavage (expressed as cleaved PARP/uncleaved PARP). * $p<0.05$ vs. Control, ** $p<0.05$ vs. BfA.

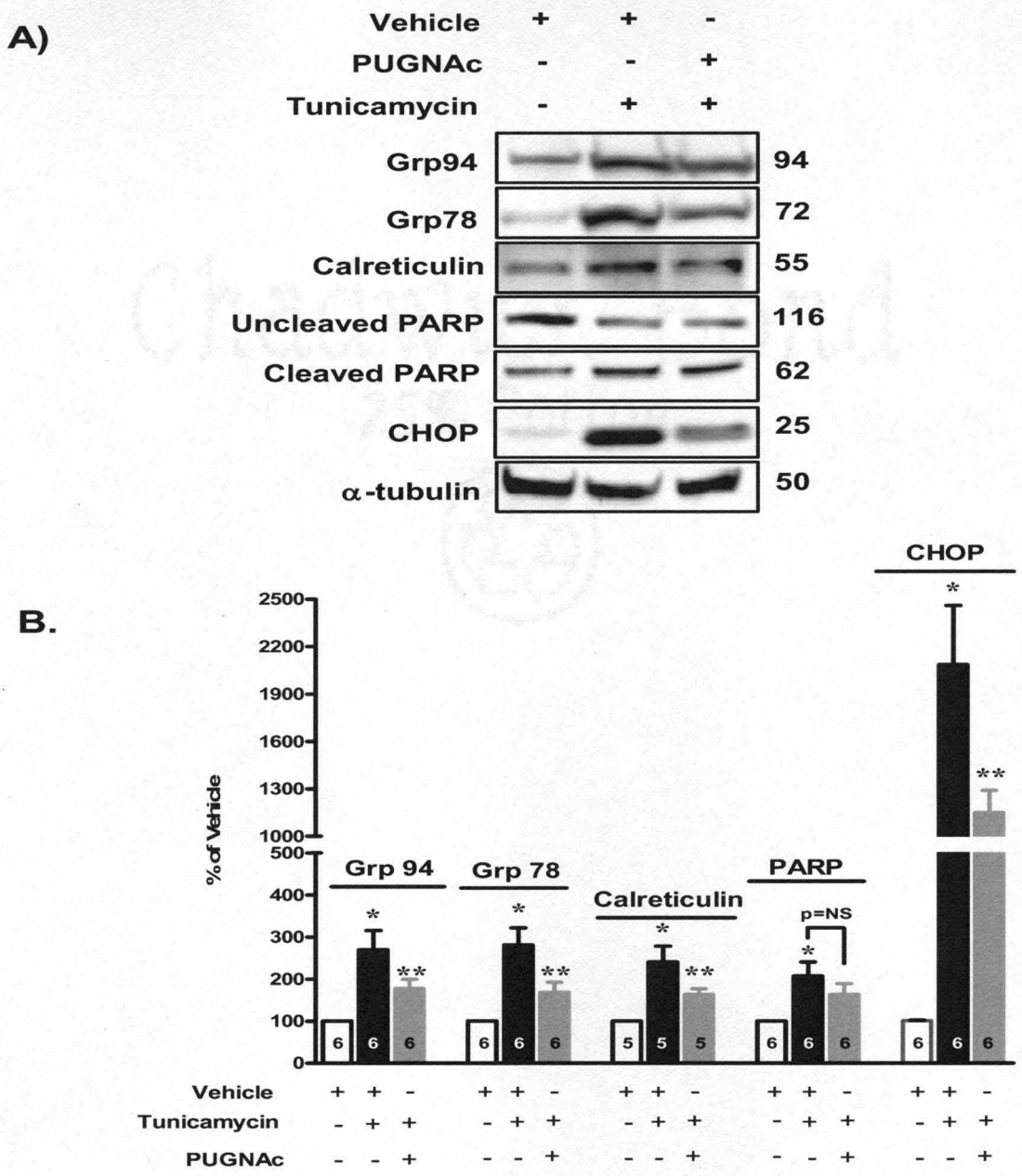

Figure 31. Normoxic cardiac myocytes (n=5-6/group) were pre-treated with either Vehicle or O-GlcNAcase inhibitor (PUGNAc) and subjected to ER stress with TM. Whole cell lysates were immunoblotted for ER chaperones (Grp 94, Grp 78 and Calreticulin) and pro-apoptotic (CHOP and PARP) proteins. **A)** O-GlcNAcase inhibition showed significant reduction in BfA-mediated activation of Grp 94, Grp 78, Calreticulin and protein levels. Moreover, GCA inhibition significantly reduced the TM mediated increase in CHOP protein levels despite no effect on PARP cleavage compared to TM alone according to representative immunoblots and **B)** densitometric quantification. * $p<0.05$ vs. Control, ** $p<0.05$ vs.TM.

E.4. O-GlcNAcase inhibition mitigates ER stress-induced cardiac myocyte death: Like OGT overexpression, O-GlcNAcase inhibition (with PUGNAc) has been shown to be cytoprotective during hypoxia, ischemia and oxidative stress(190). Here, O-GlcNAcase inhibition with PUGNAc significantly attenuated BfA-induced cardiomyocyte death (18±7% for PUGNAc + BfA vs. 41±7% for BfA alone, $p<0.05$, Figure 31A). Such results were further supported by significantly attenuated TM-induced ER stress with O-GlcNAcase inhibition with PUGNAc (15±3% PUGNAc + TM vs. 33±6% for TM alone, $p<0.05$, Figure 31B). Thus, shifting the cellular balance in favor of O-GlcNAcylation via genetic or pharmacologic means mitigates ER stress-induced cell death. Inhibition of O-GlcNAcase did not significantly alter BfA or TM-induced apoptosis according to Caspase 3/7 activity (Figure 31C and D).

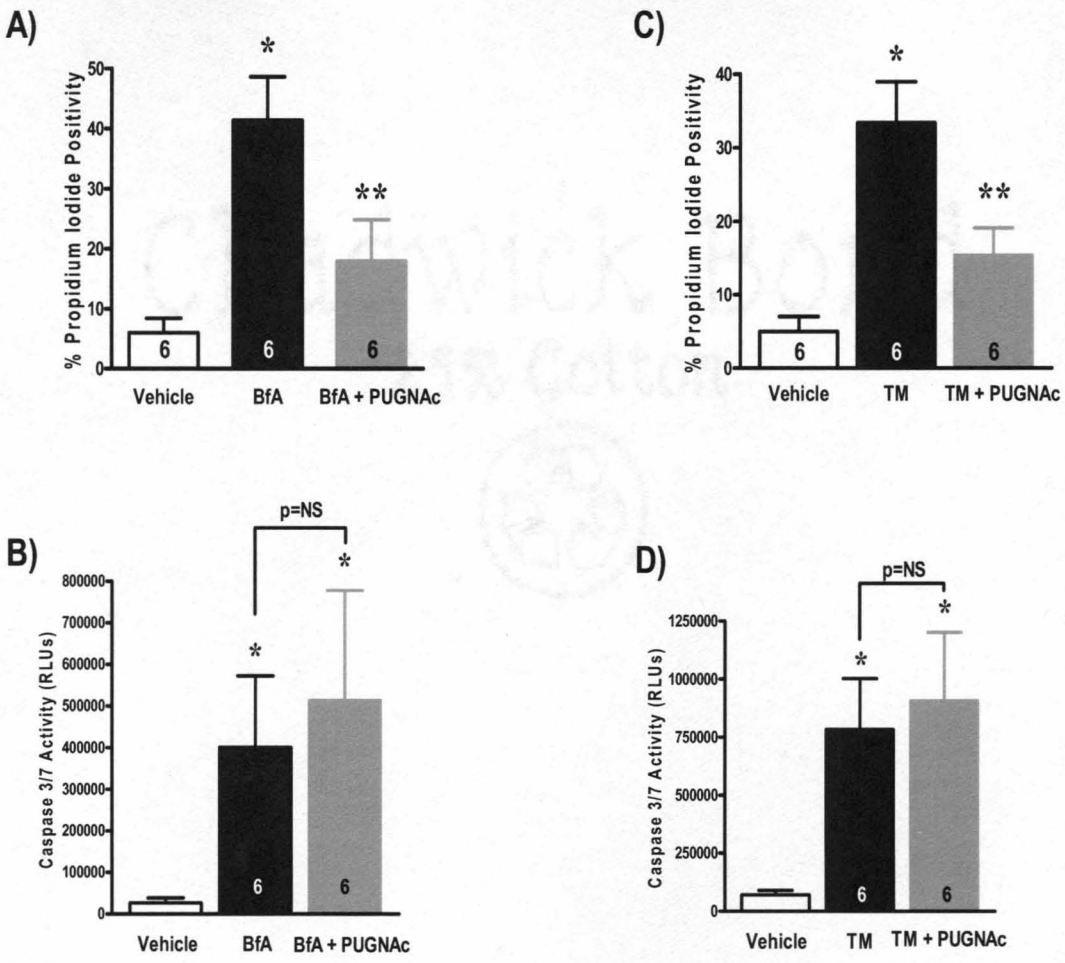

Figure 32. Normoxic cardiac myocytes were pre-treated with either Vehicle or O-GlcNAcase inhibitor (PUGNAc), subjected to ER stress with BfA or TM and cell death evaluated via PI or caspase activity. **A)** O-GlcNAcase inhibition attenuated BfA-induced cardiomyocyte death. **B)** O-GlcNAcase inhibition did not affect BfA-induced cardiomyocyte apoptosis. **C)** O-GlcNAcase inhibition attenuated TM-induced cardiomyocyte death. **D)** O-GlcNAcase inhibition did not affect TM-induced cardiomyocyte apoptosis. n=6/group. * $p<0.05$ vs. Control, ** $p<0.05$ vs. BfA or TM.

F. PROTEIN MODIFICATION BY *O*-GlcNAc

Numerous studies have documented an ever-growing list of proteins modified by *O*-GlcNAc. However, sparse information exists on specific cardiac proteins modified by *O*-GlcNAc. According to the immunoblotting data in Figures above, it appears that several proteins are modified by *O*-GlcNAc in cardiac myocytes. In Figure 32, we attempted to specifically identify some of these as potential candidates for cardioprotection. Proteins isolated from cultured cardiac myocytes treated with vehicle or PUGNAc were harvested as described above. Two-dimensional gel electrophoresis revealed at least 13 spots on which the *O*-GlcNAc modification (as evidenced by CTD antibody positivity) was augmented after PUGNAc treatment (Figure 32A). Analysis of these 13 spots (Table 4) by Matrix Assisted Laser Desorption /Ionization- Time Of Flight (MALDI-TOF) mass spectrometry revealed several proteins involved in metabolism and one (VDAC) that piqued our interest because of its participation in the mitochondrial permeability transition pore (mPTP). Next, we performed an immunoprecipitation experiments to confirm that VDAC was modified by pulling down the *O*-GlcNAc–modified proteins and performing an immunoblot against VDAC. Indeed, the band corresponding to ≈30 kDa was also augmented in the PUGNAc sample compared with vehicle (Figure 32B).

Table 4: List of MALDI-TOF protein ID

Spot No.	Protein Identity	Accession No.	Molecular Weight, Da	Isoelectric Point	Sequence Coverage, %
1	HSP60	CAA38564	60 965	6.1	32
2	HSP60	CAA38564	60 965	6.1	39
3	Desmin	P48675	53 325	5.3	39
4	-Actin	Q61264	37 729	5.4	24
5	HSP27	NP_114176	22 865	6.1	28
6	**VDAC**	**AAH60558**	**32 060**	**8.4**	**54**
7	Malate dehydrogenase	AAH63165	36 117	8.9	35
8	Malate dehydrogenase	P04636	35 655	9.1	34
9	Glyceraldehyde 3-phosphate dehydrogenase	P04797	35 705	8.6	28
10	Glyceraldehyde 3-phosphate dehydrogenase	P04797	35 705	8.6	27
11	Fructose-bisphosphate aldolase	NP_036627	39 220	8.5	40
12	Fructose-bisphosphate aldolase	NP_036627	39 220	8.5	28
13	Pyruvate kinase	P11980	57 649	7.6	21

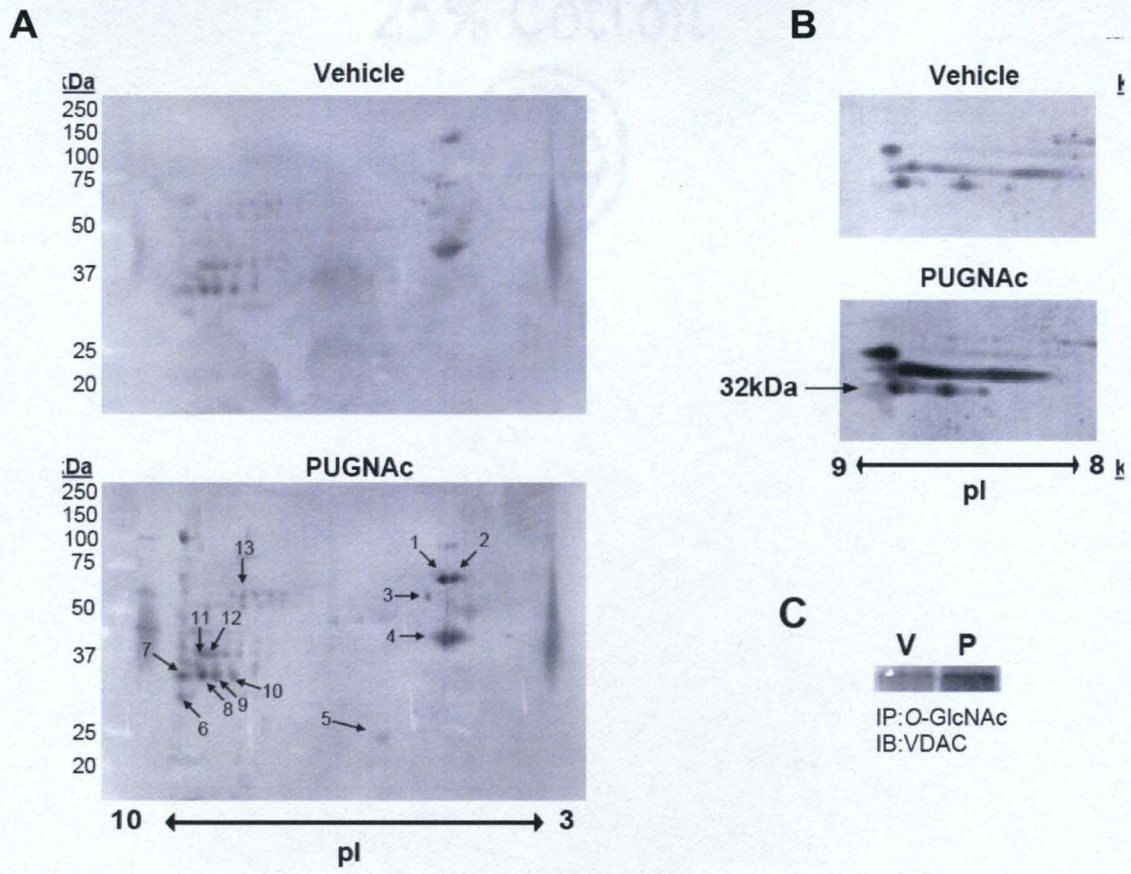

Figure 33. Cardiomyocytes were treated with Vehicle or PUGNAc, whole cell lysate isolated and O-GlcNAc-modified proteins identified via two-dimensional immunoblotting and MALDI-TOF. **A)** 2D immunoblotting for *O*-GlcNAc identified several proteins with enhanced immunoreactivity, which was subsequently submitted for mass spectrometry analysis via parallel silver-stained gels. Several proteins displayed augmented *O*-GlcNAc modification after PUGNAc treatment, including VDAC (spot 6); n=2. See the Table 4 for protein identities. pI indicates isoelectric point. **B)** Additional samples separated on narrower isoelectric point and molecular weight ranges to enhance the ability to identify the VDAC spot. **C)** Additional protein isolates were subjected to immunoprecipitation (IP) with an antibody against *O*-GlcNAc, then immunoblotted (IB) for VDAC.

F.1. VDAC is a mitochondrial target of *O*-GlcNAc: Our focus on VDAC is based on its identity as a putative element in formation of the mPTP, which represents a significant and proximal event in the commitment to cell death. Although this serves only as an initial foray into the likely numerous proteomic changes associated with *O*-GlcNAc in this system, this singular finding is intriguing and consistent with the *in vitro* evidence for *O*-GlcNAc–mediated cardioprotection. It is important to note that lower-molecular-weight proteins are not shown in the 1-dimensional gels earlier in this study because the Western blots were not optimized for lower-molecular-weight ranges. Nevertheless, the appearance of the lower-molecular-weight bands appeared after the saturation of some of the higher-molecular-weight bands (by which time the exposure was stopped for the analyses shown in the earlier Figures).

Because our MALDI-TOF data identified VDAC as a target of *O*-GlcNAc modification, we assessed O-GlcNAc-modified VDAC levels following inhibition OGT (with TT04) or GCA (via PUGNAc) as a possible mechanistic link between *O*-GlcNAc signaling and the mitochondria. Adult wild-type mice were treated with TT04 (10mg/kg), PUGNAc (50 mg/kg IP) or isovolumic Vehicle (0.1% DMSO or 0.1% Ethanol) intraperitoneally, and cardiac mitochondrial proteins were evaluated to ascertain whether such changes in VDAC modification suggested by the 2-dimensional gels (Figure 32) also occurred in the adult myocardium. Fractionation of hearts from Vehicle-, TT04- and PUGNAc-treated mice yielded clean, largely intact mitochondria (Figure 33A). Further examination of the mitochondrial fraction revealed that cardiac mitochondria from TT04-treated mice

contained reduced *O*-GlcNAc-modified-VDAC compared with those from Vehicle-treated mice (Figure 33B). Moreover, an immune-independent technique further confirmed the co-IP findings showing reduction in *O*-GlcNAc modification of VDAC with OGT inhibition (Figure 33C). Conversely, more VDAC was *O*-GlcNAc modified after PUGNAc treatment compared with Vehicle and such change occurred without a difference in total VDAC according to immunoblotting (Figure 33D). Again, VDAC is not the only *O*-GlcNAc modified protein.

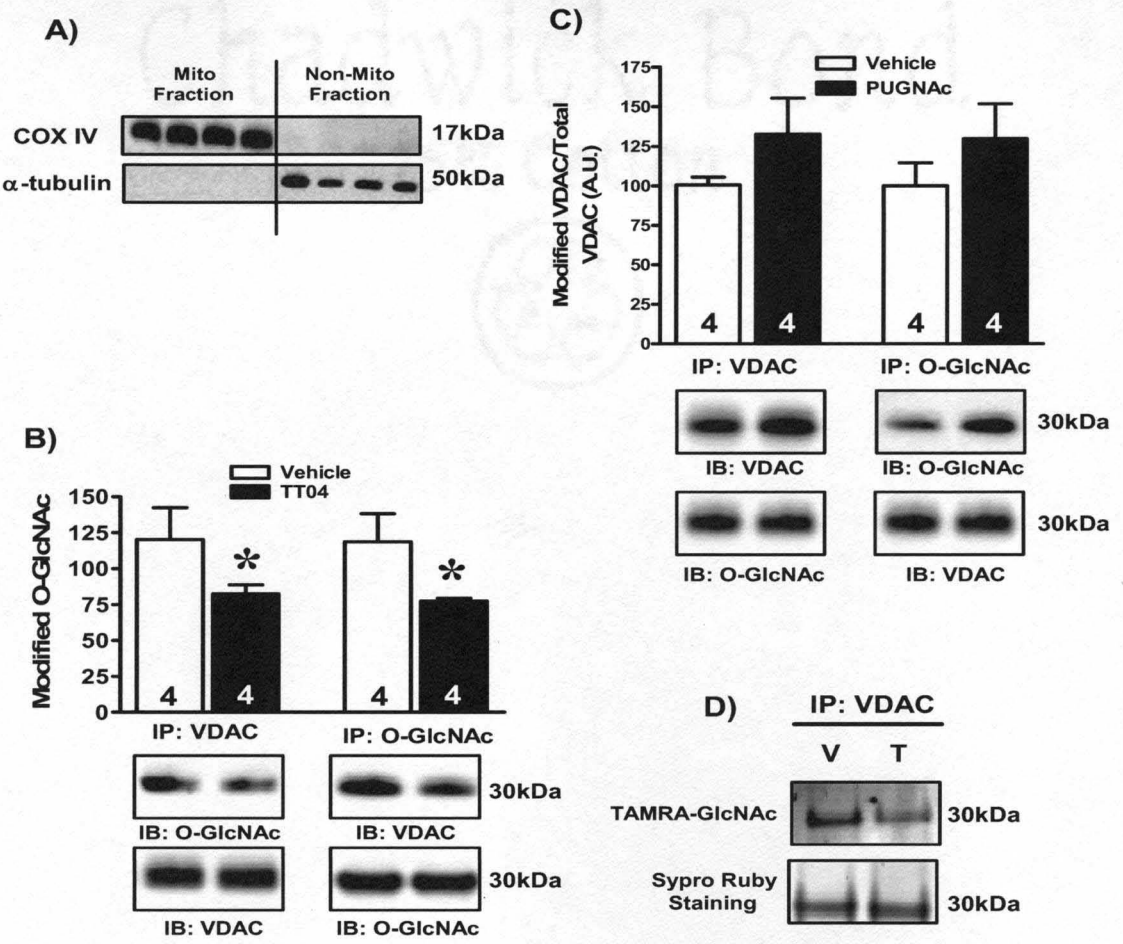

Figure 34. Adult mice were treated with vehicle (V; n=4), TT04 (n=4) or PUGNAc (P; n=4), and cardiac mitochondria were isolated. **A)** Total protein was isolated from mitochondrial and non-mitochondrial aliquots. Immoblotting for cytochrome *c* oxidase subunit 4 (COX IV) and α-tubulin in the mitochondrial non-mitochondrial lysates confirmed sound mitochondrial isolation. **B)** OGT inhibition (via TT04) reduced O-GlcNAc levels on at least one mitochondrial protein (VDAC). Co-immunoprecipitation for O-GlcNAc-modified-VDAC showed a reduction in O-GlcNAc-modified-VDAC in adult cardiac mitochondria from TT04-treated mice compared with Vehicle-treated mice, despite no difference in total VDAC levels from both groups (n = 4/group). **C)** GCA inhibition (via PUGNAc) augmented O-GlcNAc levels on at least one mitochondrial protein (VDAC). Co-immunoprecipitation for O-GlcNAc-modified-VDAC showed an increase in O-GlcNAc-modified-VDAC in adult cardiac mitochondria from PUGNAc-treated mice compared with Vehicle-treated mice, despite no difference in total VDAC levels from both groups (n = 4/group). **D)** Immunoprecipitation for VDAC and enzymatic labeling of O-GlcNAc-modified proteins confirmed the reduction in O-GlcNAc-modified-VDAC in cardiac mitochondria from TT04-treated compared with Vehicle-treated mice. There was no difference in protein loading according to SYPRO ruby staining. *$p < 0.05$ vs. Vehicle.

F.2. Effects of manipulation of O-GlcNAc levels on expression of mPTP components: To determine if baseline manipulation of O-GlcNAc levels altered the protein levels of mPTP components, whole cell lysates from normoxic NRCMs treated with AdGFP, AdGCA, Vehicle, PUGNAc, Control siRNA or GCA siRNA were immunoblotted for CyP D, ANT and VDAC. Neither augmented O-GlcNAc levels (PUGNAc or GCA siRNA) nor diminished O-GlcNAc levels (AdGCA) significantly ($p>0.05$) changed CyP D, ANT and VDAC protein levels (Figure 34).

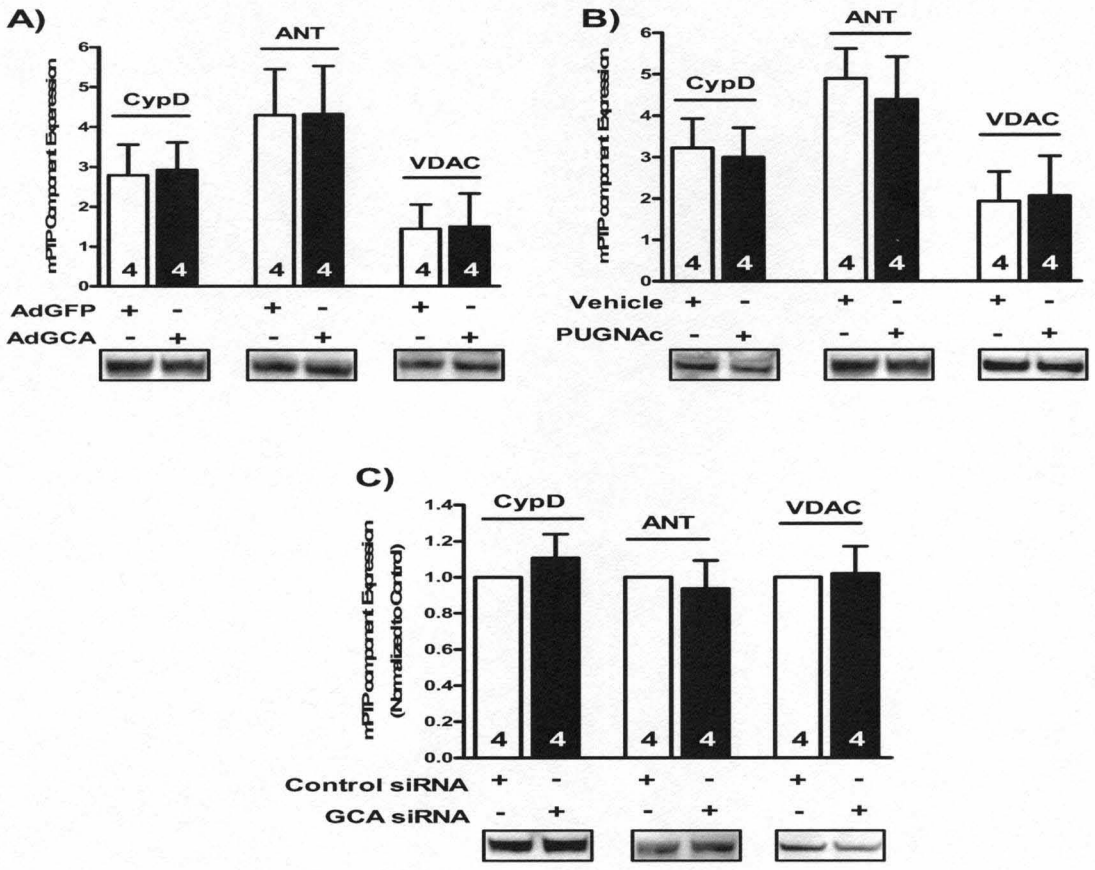

Figure 35. Expression of putative molecular components of mitochondrial permeability transition pore (mPTP). Expression of CypD, ANT, and VDAC were not significantly affected by **A)** genetic overexpression (n=4/group), **B)** pharmacological inhibition (n=4/group), or **C)** siRNA knockdown of GCA according to western blotting (n=4/group). P=NS for all comparisons.

G. O-GlcNAc MODIFICATION AND MITOCHONDRIAL-MEDIATED DEATH PATHWAY

G.1. Effects of altered O-GlcNAc levels on hypoxia-induced Ca^{2+} overload

G.1.i. Effects of OGT overexpression on hypoxia-induced Ca^{2+} overload: Several studies have implicated Ca^{2+} overload as a key contributor to mitochondrial permeability transition leading to ischemia-reperfusion injury and interventions that reduce or delay the rise in [Ca^{2+}] block or delay myocardial death (219, 244, 276, 277). In addition, inhibiting the rise in mitochondrial [Ca^{2+}] has been shown to confer cardioprotection following acute MI or IRI (94, 218). Moreover, dysregulation of mitochondrial Ca^{2+} is known to induce mPTP formation (63, 141). Accordingly, we assessed whether OGT overexpression affects Ca^{2+} overload following hypoxia in NRCMs. OGT overexpression did not alter baseline mitochondrial Ca^{2+} levels but significantly attenuated hypoxia-induced mitochondrial Ca^{2+} overload according to rhod-2 fluorescence (n=5/group, Figure 35).

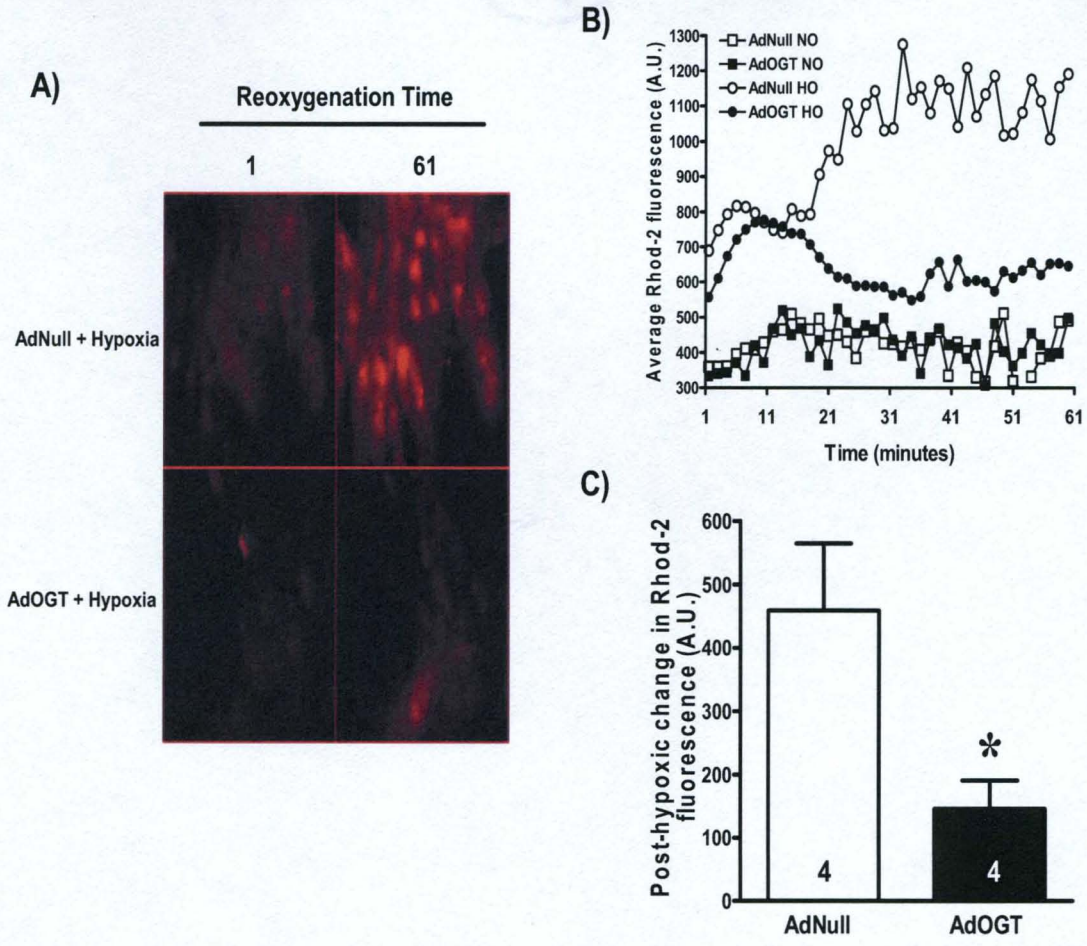

Figure 36. Evaluation of calcium overload in post-hypoxic cardiac myocytes using Rhod-2AM (n=5/group). Myocytes were treated with AdNull or AdOGT. Following hypoxia, myocytes undergo progressive calcium overload. Genetic overexpression of OGT attenuates post-hypoxic calcium overload according **A)** representative montage **B)** reoxygenation time-lapse graph and **C)** bar graph representation of the change in rhod-2 fluorescence.

G.1.ii. Effects of GCA manipulation on hypoxia-mediated Ca^{2+} overload: To determine if manipulation of GCA levels affects hypoxia-induced Ca^{2+} overload, cardiac myocytes were treated with either AdGFP (48 hours, 100 MOIs), AdGCA (48 hours, 100 MOI), Vehicle (overnight), or PUGNAc (overnight, 200 µmol/L), loaded with the mitochondrial calcium indicator rhod-2 (2 µmol/L) and subjected to three hours of hypoxia and one of reoxygenation. Time-lapse fluorescence microscopy was initiated at the beginning of reoxygenation for changes in mitochondrial Ca^{2+} levels. Augmentation of Ca^{2+} levels is reflected by an increase in rhod-2 fluorescence. Hypoxia sensitized myocytes to Ca^{2+} overload. GCA overexpression (AdGCA) exacerbated hypoxia-induced calcium overload during reoxygenation reflected by a significant increase in rhod-2 fluorescence (Figure 36A-B), whereas GCA inhibition (PUGNAc) attenuated hypoxia-induced calcium overload compared to Vehicle (Figure 36A & C).

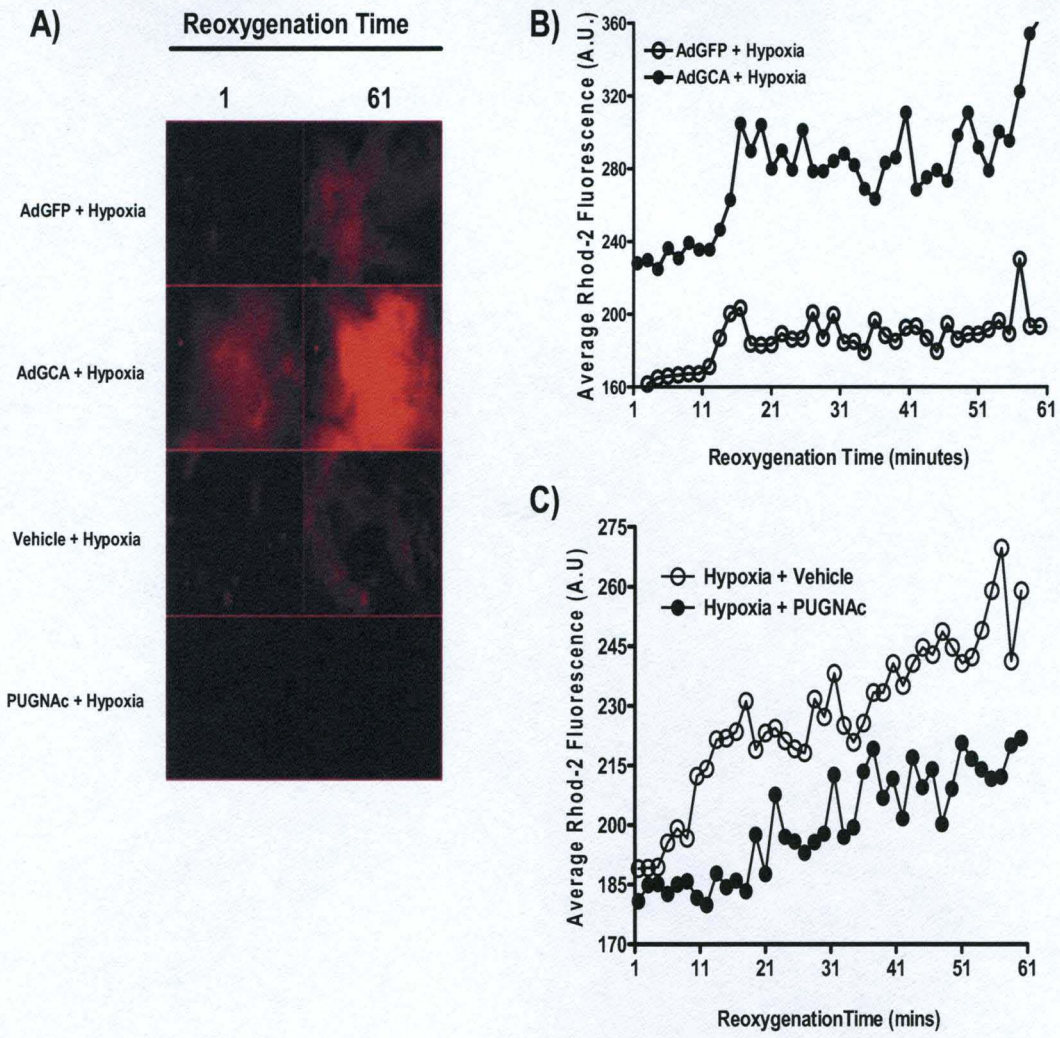

Figure 37. Assessment of calcium overload in post-hypoxic cardiac myocytes using Rhod-2AM (n>/=4/ group). Myocytes were treated with AdGFP or AdGCA (**A** and **B**) or vehicle or PUGNAc (**A** and **C**). Following hypoxia, myocytes undergo progressive calcium overload. Genetic overexpression of GCA exaggerates, whereas pharmacological inhibition of GCA attenuates, post-hypoxic calcium overload. *P<0.05 vs. AdGFP or Vehicle.

G.2. Effects of altered O-GlcNAc levels on hypoxia-induced ROS generation

G.2.i. Effects of OGT overexpression on hypoxia-induced ROS production: Reactive oxygen species (ROS) are important contributors to ischemia-reperfusion injury. In fact, studies have shown that addition of antioxidants or ROS scavengers delay the onset or attenuate ischemia-reperfusion injury (7, 43, 168). Therefore, I evaluated the effects of overexpressing OGT to augment O-GlcNAc levels on hypoxia-induced ROS generation. NRCMs infected with 100 MOI of AdNull or AdOGT for 48h were loaded with DCF (2 μmol/L) and subjected to hypoxia for three hours. Time-lapse fluorescence microscopy was initiated at the beginning of reoxygenation for changes in ROS levels. Augmentation of ROS levels is reflected by an increase in DCF fluorescence. Hypoxia augmented myocytes ROS generation which was significantly attenuated by OGT overexpression. OGT ovexpression did not change baseline ROS levels (Figure 37).

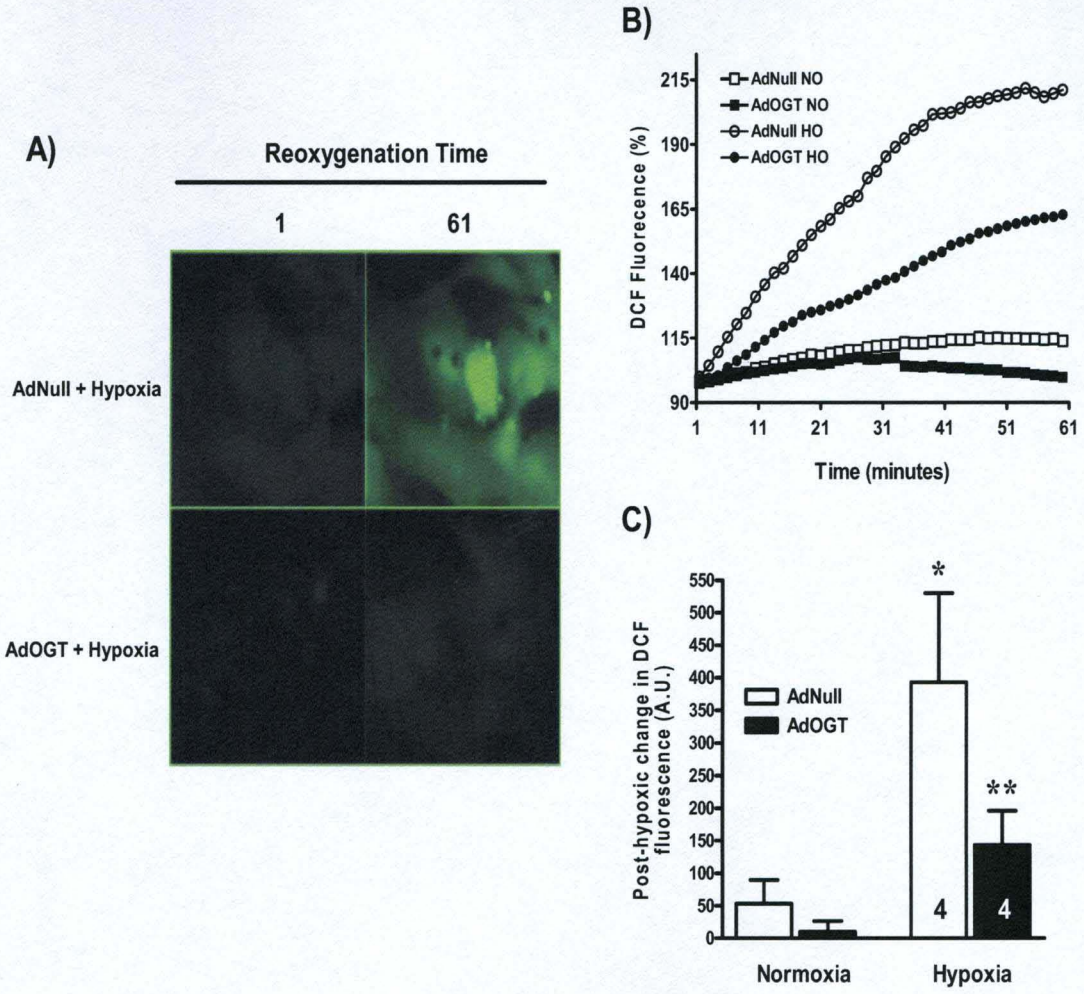

Figure 38. Evaluation of post-hypoxic ROS production in NRCMs treated with AdNull or AdOGT using DCF (n=4 per group). Subjecting myocytes to hypoxia augmented ROS production. An effect attenuated by genetic overexpression of OGT. **A)** Representative montage showing DCF fluorescence. **B)** Quantitative changes in mean DCF fluorescence (expressed as %) in NRCMs using time-lapse fluorescent microscopy. **C)** Bar graph showing the change in DCF fluorescent intensity between 1 minute and 61 minutes. *P<0.05 vs. AdNull.

G.2.ii. Effects of GCA manipulation on hypoxia-mediated ROS production: To determine the effect of GCA manipulation on post-hypoxic ROS generation, NRCMs treated with AdGFP, AdGCA, Vehicle or PUGNAc, were loaded with DCF, and then subjected to hypoxia (3h) and reoxygenation (one hour). Imaging was initiated at the beginning of reoxygenation for changes in ROS levels. GCA overexpression (AdGCA) exacerbated hypoxia-induced ROS production during reoxygenation reflected by a significant ($p<0.05$) increase in DCF fluorescence (Figure 38A-C), whereas GCA inhibition (PUGNAc) attenuated hypoxia-induced ROS generation compared to Vehicle (Figure 38A, D-E).

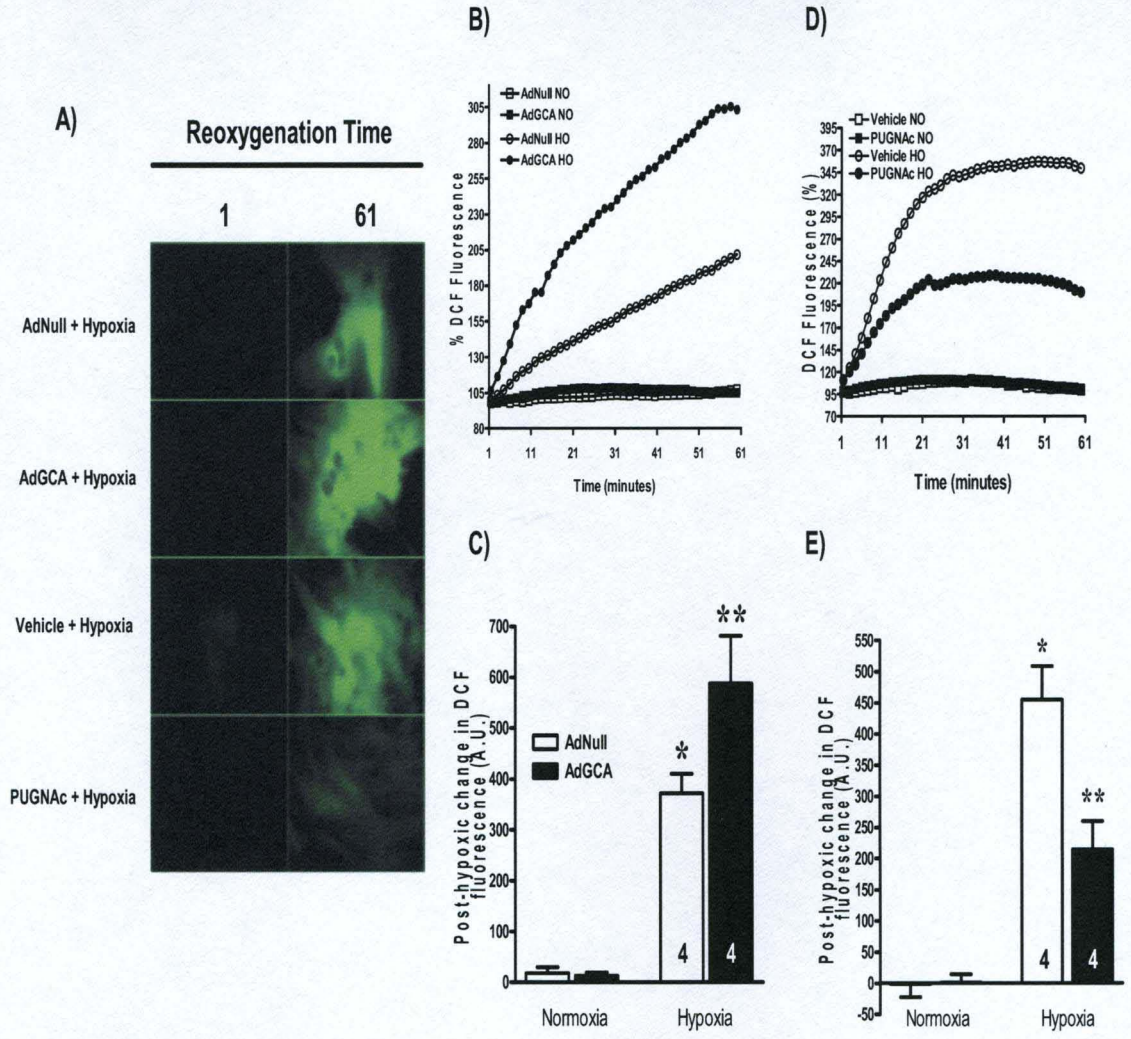

Figure 39. Evaluation of post-hypoxic ROS production in NRCMs treated with AdNull, AdGCA, Vehicle or PUGNAc using DCF (n=4 per group). Hypoxia induced ROS production. Genetic overexpression of GCA exaggerated, while pharmacologic inhibition of GCA (PUGNAc) mitigated post-hypoxic ROS production. **A)** Representative montage showing DCF fluorescence. **B)** Quantitative changes in mean DCF fluorescence (expressed as %) in NRCMs infected with AdNull or AdGCA using time-lapse fluorescent microscopy **C.** Bar graph showing the change in DCF fluorescent intensity between 1 and 61 minutes in NRCMs infected with AdNull or AdGCA. **D)** Quantitative changes in mean DCF fluorescence (expressed as %) in NRCMs treated with Vehicle or PUGNAc using time-lapse fluorescent microscopy **E)** Bar graph showing the change in DCF fluorescent intensity between 1 and 61 minutes in NRCMs infected with Vehicle or PUGNAc. *P<0.05 vs. AdNull or Vehicle, **p<0.05 vs. AdNull + Hypoxia or Vehicle + hypoxia.

G.2.iii. Effects of O-GlcNAc manipulation on catalase, SOD and GPX expression: To determine if alteration in the expression of oxidative stress response enzymes, glutathione peroxidase, superoxide dismutase and catalase was responsible for the O-GlcNAc mediated decrease in post-hypoxic ROS generation, real time PCR for Cat, GPX, and SOD mRNA levels was performed on RNA from normoxic NRCMs treated with AdGFP, AdGCA, Vehicle or PUGNAc. OGT overexpression (AdOGT) did not significantly altered ($p>0.05$) GPX, SOD, and Cat expression (Figure 39A). Moreover, neither overexpression of GCA (AdGCA) nor inhibition of GCA (PUGNAc) significantly changed GPX and SOD expression (Figure 39A & B). GCA overexpression (AdGCA) significantly diminished while GCA (Figure 39A) inhibition significantly augmented Cat expression despite no change in protein levels (Figure 39B).

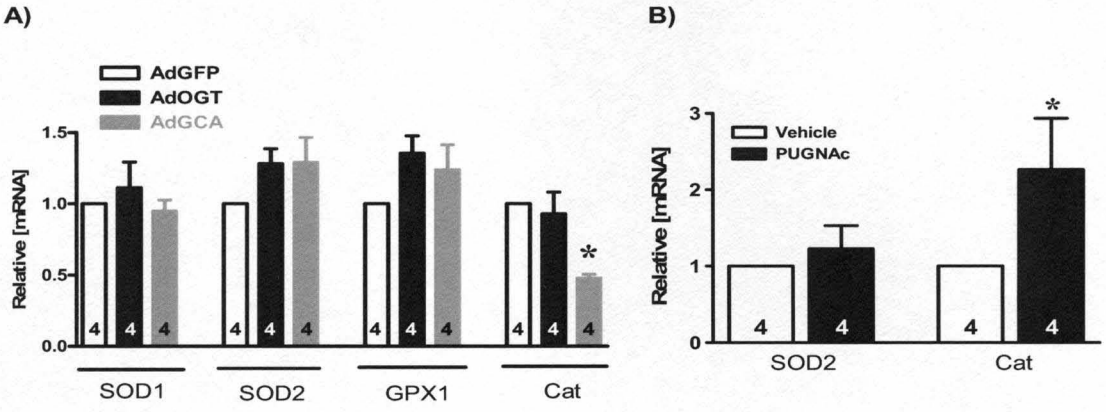

Figure 40. Expression of antioxidant enzymes: superoxide dismutase (SOD1 & SOD2), glutathione peroxidase (GPX) and Catalase (Cat), evaluated via real time PCR in NRCMs treated AdGFP, AdOGT, AdGCA, Vehicle or PUGNAc (n=4/group). **A)** Genetic overexpression of OGT did not affect SOD1, SOD2, GPX and Cat expression. Even though SOD1, SOD2, and GPX expression were not significantly affected by overexpression of GCA, Cat expression was significantly reduced. **B)** Pharmacological inhibition of GCA activity did not affect SOD2 expression but significantly augmented Cat expression.

G.3. Effects of O-GlcNAc manipulation on Ca^{2+}-induced mPTP formation

Because a hallmark of mPTP is the massive swelling of the mitochondria, we assessed sensitivity to calcium-induced mitochondrial swelling following manipulation of O-GlcNAc levels. To test the potential link between *O*-GlcNAc modification and a functional biochemical assessment of mitochondrial function within the mechanistic context of cell survival, cardiac mitochondria isolated from TT04-, PUGNAc- and Vehicle-treated adult mouse hearts were subjected to calcium-induced mitochondrial swelling. Exposure of isolated mitochondria to supra-physiological concentrations of Ca^{2+} permeabilizes the mitochondrial inner membrane to small solutes (< 1.5 kDa) (108). Mitochondria isolated from vehicle- PUGNAc- and TT04-treated mice were intact (Figure 40A), were free of cellular debris (Figure 40B), and maintained stable, calcium-free absorbance levels throughout the assay (Figure 40C). Cardiac mitochondria from TT04-, PUGNAc or Vehicle-treated mice were challenged with 0.1 mmol/L calcium chloride and the change in absorbance measured at 520 nm every 2 s. The mPTP inhibitors, Cyclosporine A and Sanglifehrin A, significantly inhibited calcium-induced swelling in mitochondria from Vehicle- treated mice (Figure 40C) showing that the swelling was mPTP dependent. Similar results were observed with mitochondria from TT04- or PUGNAc-treated mice (data not shown).

Adult cardiac mitochondria from TT04-treated mice were significantly (178 ± 10% of Vehicle) more sensitive to $CaCl_2$ induced swelling compared with Vehicle (Figure 40D). Conversely, cardiac mitochondria isolated from PUGNAc-treated mice revealed resistance to the induction of mPTP. The rate of swelling

in Figure 40D was calculated as a simple change in absorbance with respect to time and normalized to the Vehicle group. Such functional data complement the biochemical data in Figure 32. These data provide a novel molecular link between the identity of an *O*-GlcNAc-modified protein and a potential direct mechanism of cytoprotection.

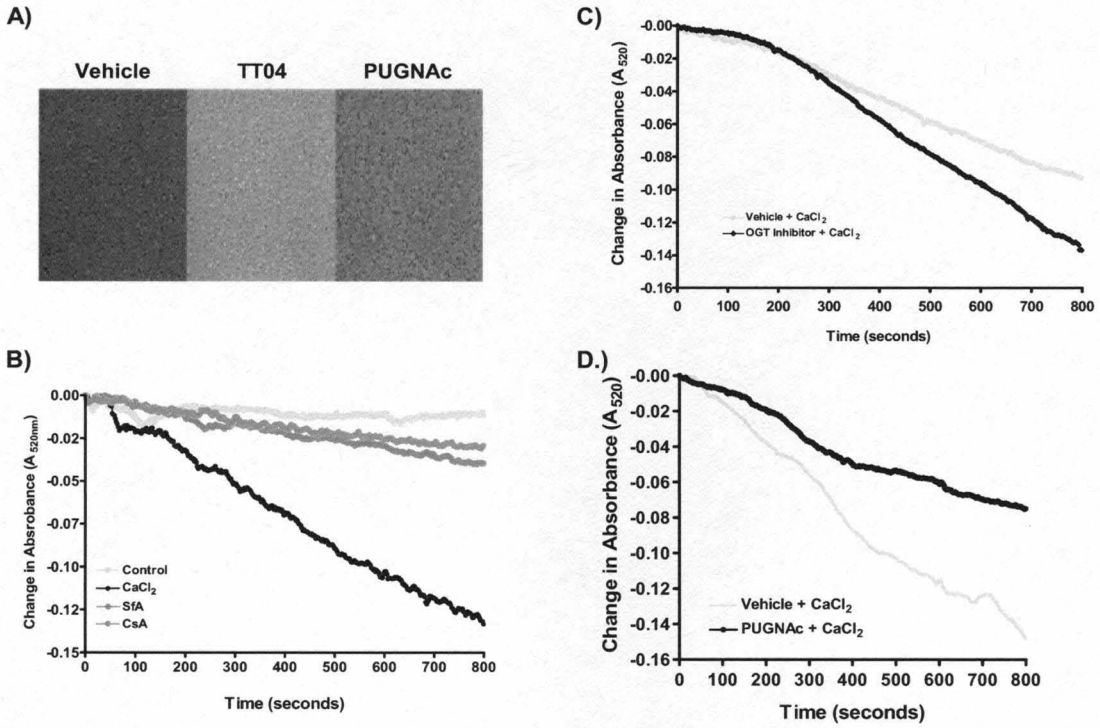

Figure 41. Assessment of sensitivity to mPTP formation according to calcium-induced mitochondrial swelling. Adult mouse cardiac mitochondria were subjected to time control or challenged with 100 µmol/L $CaCl_2$. Change in absorbance (at 520 nm) was measured over time every two seconds using a spectrophotometer. **A)** Gross transmitted light evaluation of Percoll-purified cardiac mitochondria from vehicle-, TT04- and PUGNAc-treated hearts (respectively) demonstrating structures of ≈1 µm in diameter, with no apparent cellular debris (image size 100x75 µm). **B)** Challenge with 0.1 mmol/L calcium chloride significantly reduced absorbance (520 nm) in the cardiac mitochondria. An effect significantly inhibited by mPTP inhibitors; CsA or SfA **C)**. Cardiac mitochondria from TT04-treated mice were significantly more sensitive to calcium-induced swelling compared with those from Vehicle-treated mice (n=4/group). **D)** Cardiac mitochondria from PUGNAc-treated mice were significantly less sensitive to calcium-induced swelling compared with those from Vehicle-treated mice (n=4/group). *p< 0.05 vs. Vehicle.

G.4. Effects of OGT manipulation on post-hypoxia $\Delta\psi_m$ recovery

Specifically motivated by the importance of maintaining mitochondrial integrity to enhance cell survival, we ascertained whether hypoxia-induced loss of mitochondrial membrane potential was affected by alterations in O-GlcNAc levels. Such an avenue is particularly attractive given the early decline in O-GlcNAc levels shown above.

G.4.i Effects of OGT manipulation on post-hypoxia $\Delta\psi_m$ recovery: Because mitochondria are arbiters of cell fate and the present data support the role of OGT as a pro-survival enzyme, we assessed the effects of blocking endogenous OGT activity on post-hypoxic mitochondrial membrane potential. NRCMs were treated with AdGFP (100 MOI, 48 hour), AdOGT (100 MOI 48 hour), TT04 (OGT inhibitor; prior to H/R, 1 μmol/L) or equal volume of DMSO, and loaded with the mitochondrial membrane potential indicator, tetramethylrhodamine methylester (TMRM; 50 nmol/L). Cardiac myocytes were then subjected to three hours of hypoxia and one hour of reoxygenation. During the reoxygenation period, myocytes were evaluated for changes in mitochondrial membrane potential using time-lapse fluorescence microscopy. Dissipation of mitochondrial membrane potential is reflected by a loss of TMRM fluorescence. For reference purposes, the normoxic group averaged between 205 and 225 A.U. Thus, the mitochondria are not 'increasing' their fluorescence, more precisely, they are 'recovering'.

AdGFP-infected NRCMs loaded with TMRM maintained mitochondrial membrane potential under normoxia and showed no significant difference in

mitochondrial membrane potential over time (Figure 41B). Overexpression of OGT (AdOGT) attenuated the loss of mitochondrial membrane potential compared to AdGFP as shown by increased TMRM fluorescence and thus protected myocytes from cell death following hypoxia (Figure 41A, B & D). Inhibition of OGT (via TT04) exacerbated the loss of mitochondrial membrane potential compared to H/R alone as shown by a further reduction in TMRM fluorescence and thus sensitized myocytes to mitochondrial damage (Figure 41A, C-D). Such findings support a role for OGT at the level of the mitochondrial permeability transition pore.

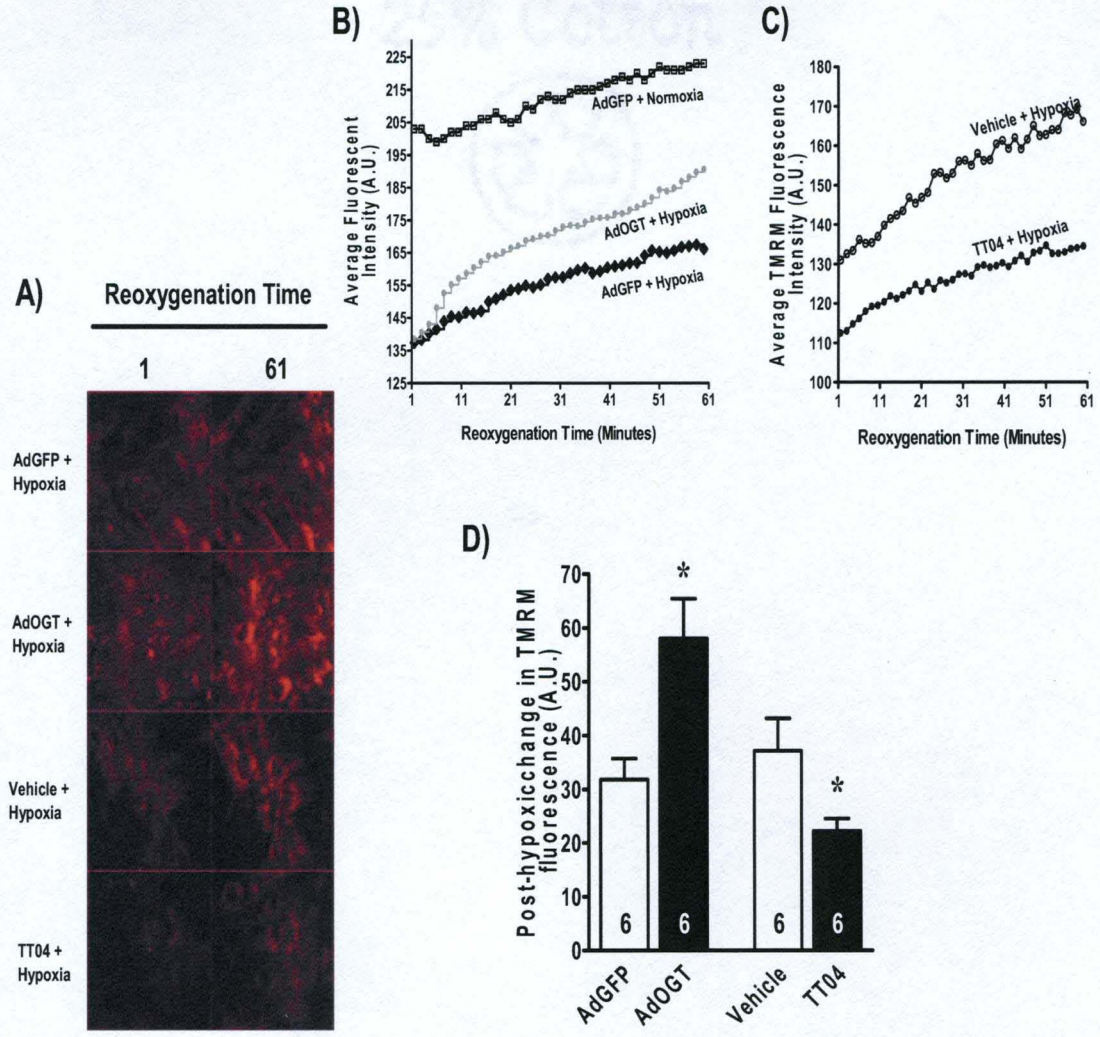

Figure 42. Assessment of post-hypoxic mitochondrial membrane potential recovery in NRCMs following manipulation of OGT. TMRM fluorescence was used to indicate mitochondrial membrane potential (n=6/group) beginning at post-hypoxic reoxygenation and continuing through the first hour of reoxygenation. OGT overexpression improved the recovery of mitochondrial membrane potential compared to AdGFP while OGT inhibition (via TT04) repressed the recovery of mitochondrial membrane potential compared to Vehicle. **A)** Representative montages of post-hypoxic TMRM fluorescence in cardiomyocytes. **B)** Graph showing average TMRM fluorescence for AdGFP and AdOGT infected myocytes over 60 minutes of reoxygenation as index of recovery of mitochondrial membrane potential. **C)** Graph showing average TMRM fluorescence for Vehicle and TT04 treated myocytes over 60 minutes of reoxygenation. **D)** Quantification of the change in relative fluorescent intensity for AdGFP, AdOGT, Vehicle and TT04 treated myocytes. *P<0.05 vs. AdGFP or Vehicle

G.4.ii. Effects of GCA manipulation on post-hypoxia $\Delta\psi_m$ preservation: Loss of mitochondrial membrane potential ($\Delta\psi_m$) commits cells to death pathways (4, 175). Consequently, we examined the effects of GCA knockdown on hypoxia-induced loss of mitochondrial membrane potential using TMRM. We assessed the effects of altered GCA activity on post-hypoxic mitochondrial membrane potential. NRCMs were treated with either AdGFP (48 hours, 100 MOI), AdGCA (48 hours, 100 MOI), Vehicle (overnight), PUGNAc (overnight, 200 μmol/L), Control siRNA (72 hours, 60 nmol/L), or GCA siRNA (72 hours, 60 nmol/L) and loaded with the mitochondrial membrane potential indicator TMRM (100 nmol/L). Cardiac myocytes were then subjected to either three hours of normoxia, or, three hours of hypoxia and one hour of reoxygenation. During the reoxygenation period, myocytes were evaluated for changes in mitochondrial membrane potential using time-lapse fluorescence microscopy. Dissipation of mitochondrial membrane potential is reflected by a loss of TMRM fluorescence. For reference purposes, the normoxic group averaged between 198 and 215 A.U. Thus, the mitochondria are not 'increasing' their fluorescence, more precisely, they are 'recovering'. Hypoxia/reoxygenation induced mitochondrial membrane potential loss. GCA overexpression attenuated the post-hypoxic mitochondrial membrane potential recovery during reoxygenation, shown by impaired recovery of TMRM fluorescence (Figure 42A-B & E). Conversely, inhibition of GCA (via PUGNAc or GCA siRNA) attenuated the loss of mitochondrial membrane potential compared to vehicle or Control siRNA, as shown by the significant restoration of TMRM

fluorescence toward that of the normoxic control, and protected cells from post-hypoxic mitochondrial dysfunction (Figure 42A, C-E).

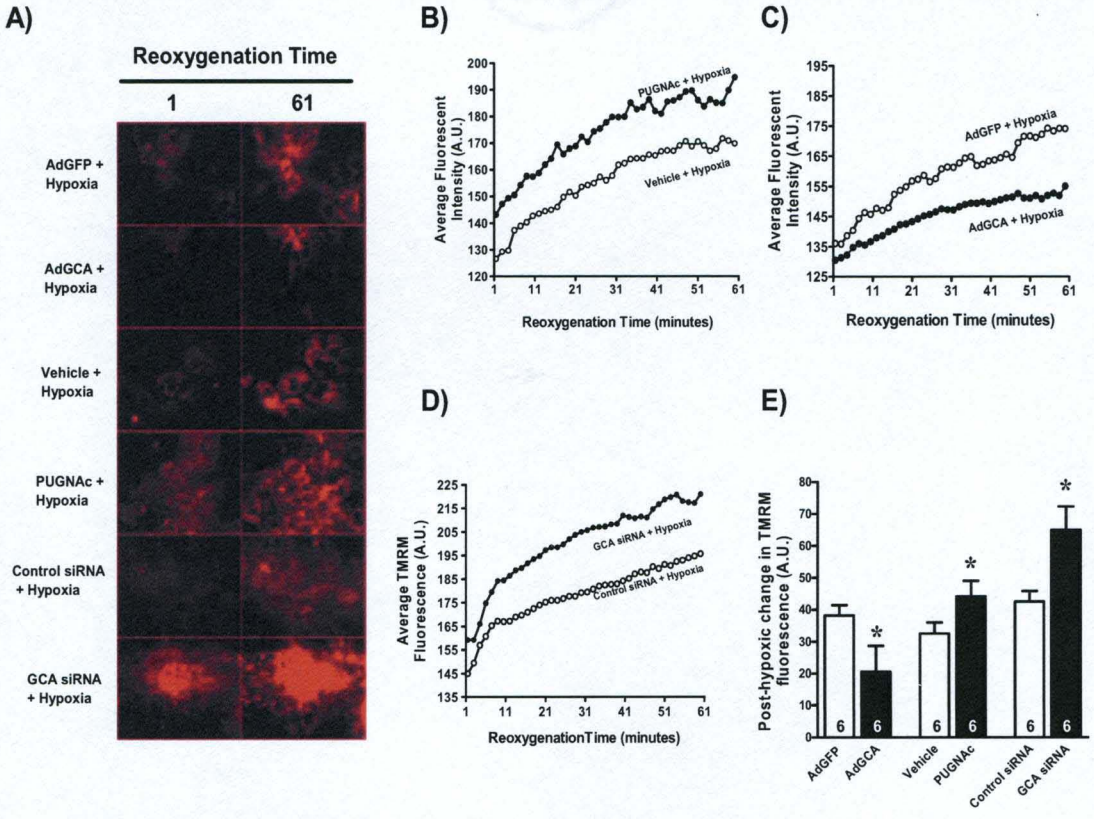

Figure 43. Assessment of post-hypoxic mitochondrial membrane potential recovery in NRCMs following manipulation of GCA. TMRM fluorescence was used to indicate mitochondrial membrane potential (n=6/group). GCA overexpression attenuated, while GCA inhibition (via PUGNAc or via GCA siRNA) enhanced mitochondrial membrane potential recovery compared to AdGFP, Vehicle or control siRNA respectively **A)** Representative montages of post-hypoxic TMRM fluorescence in cardiomyocytes. **B)** Graph showing average TMRM fluorescence for AdGFP and AdGCA infected myocytes over 60 minutes of reoxygenation as index of recovery of mitochondrial membrane potential. **C)** Graph showing average TMRM fluorescence for Vehicle and PUGNAc treated myocytes over 60 minutes of reoxygenation. **D)** Graph showing average TMRM fluorescence for Control and GCA siRNA transfected myocytes over 60 minutes of reoxygenation. **E)** Quantification of the change in relative fluorescent intensity for AdGFP, AdGCA, Vehicle, PUGNAc, Control siRNA and GCA siRNA treated myocytes. *P<0.05 vs. AdNull or Vehicle or Control siRNA.

H. TRANSLATION TO *IN VIVO* MODEL

H.1. O-GlcNAc levels change following myocardial ischemia-reperfusion:

We used the exogenous enzymatic labeling of O-GlcNAc modified proteins, Click chemistry technique to assess changes in O-GlcNAc levels in the ischemic (area at risk, n>/=4/group) and non-ischemic zones (n>/=4/group) of mice subjected to 40 minutes of myocardial ischemia (MI) via left anterior descendinf coronary artery ligation or Sham surgery and reperfused for zero, one, four or twenty four hours. O-GlcNAc levels decreased after 40 minutes of myocardial ischemia in the ischemic zone for MI group compared to sham group (Figure 43A and B). Upon reperfusion, O-GlcNAc levels were ≈1.6-fold higher than sham after 1hr, and dropped to baseline after 4hrs and 24 hrs of reperfusion (Figure 43A and B). Despite changes in O-GlcNAc levels in the ischemic zone of hearts of the MI group, there was no significant change in O-GlcNAc levels in the non-ischemic zone from both the MI and Sham groups following ischemia and during the different durations of reperfusion i.e. zero, one, four or twenty four hours(Figure 43C). Moreover, myocardial ischemia induced cellular injury which was exacerbated by reperfusion compared to Sham surgery as reflected in cardiac troponin I release (cTnI, Figure 43D). There was no significant difference in cTnI release in the Sham group at the different time points (Figure 43D).

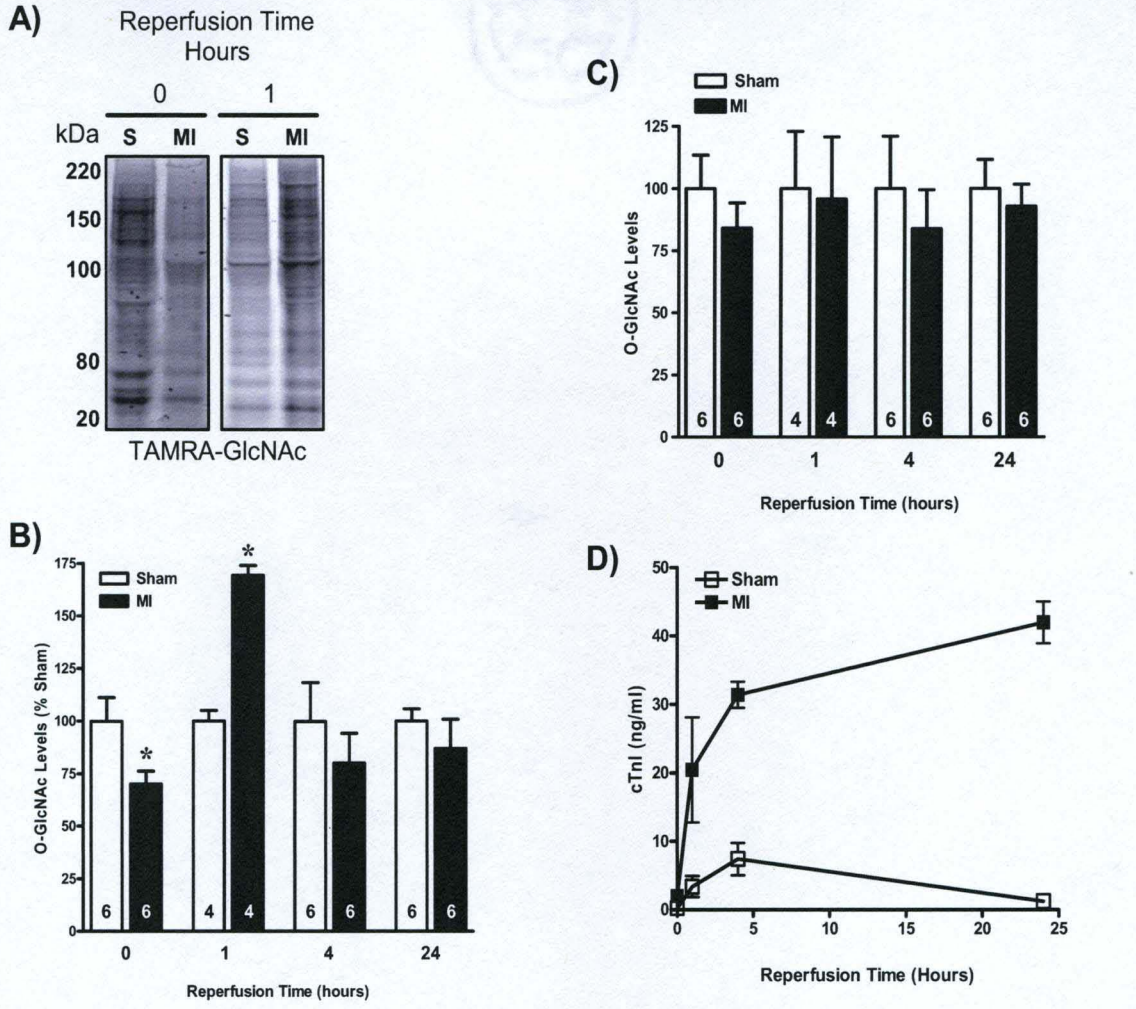

Figure 44. Effects of ischemia-reperfusion injury on O-GlcNAc levels. Adult C57 (n=4-6 per group) mice were subjected to 40 minutes of ischemia and reperfused for 0-24 hours. Evans blue dye was used to delineate ischemic zone (IZ) from non-ischemic (nIZ) zone. O-GlcNAc levels were assessed via click chemistry for the non-ischemic and ischemic zones while ischemia-reperfusion injury was assessed via serum cardiac troponin I (cTnI) levels. **A)** Representative TAMRA-GlcNAc gels for ischemic zone for time points with significant changes in O-GlcNAc levels. Ischemia induced significant decrement, while reperfusion for one hour augmented O-GlcNAc levels. **B)** Densitometric quantification of TAMRA-GlcNAc gels expressed as percent of sham for ischemic zones show significant reduction in O-GlcNAc levels following ischemia (zero hour of reperfusion), augmented O-GlcNAc levels by 1 hour of reperfusion and no change in O-GlcNAc levels by four and twenty four hours of reperfusion compared to Sham. **C)** There was no significant difference in O-GlcNAc levels in the Non-ischemic zones of MI hearts compared with sham hearts. **D)** Ischemia induced troponin I (cTnI) release. Reperfusion exacerbated ischemia-induced cTnI release. *P<0.05 vs. Sham

H.2. Reduction of myocardial infarct size by PUGNAc *in vivo*: Infarct size is a major determinant of mortality following myocardial infarction (28, 86). Reducing infarct size is therefore critical for improving survival following MI. Indeed, studies have shown that interventions that reduce infarct size reduce injury in MI (223, 243). Therefore, we ascertained whether augmentation of *O*-GlcNAc levels is sufficient to reduce infarct size *in vivo*. We intraperitoneally injected mice with 50 mg/kg of PUGNAc (*O*-GlcNAcase inhibitor) or isovolumic Vehicle eighteen hours before surgery. Several mice (n=3/group) not undergoing surgery were also euthanized to determine whether the dosing regimen of PUGNAc was sufficient to increase cardiac *O*-GlcNAc levels. As shown in Figure 44A, such treatment significantly augmented myocardial *O*-GlcNAc levels compared with Vehicle treatement. Additional mice (n>/=8/group) were treated similarly and subjected to 40 minutes of ischemia via left anterior descending coronary artery ligation and 24 hours of reperfusion. At the end of reperfusion, Evans blue dye and 2,3,5-triphenyltetrazolium chloride were used to define the area at risk (ischemic zone) and infarct size, respectively (Figure 44B). There was no difference in ratio of the area at risk (AAR) to left ventricle (LV) for PUGNAc-treated mice compared to the Vehicle-treated mice indicating that the occlusion point was same for both group (Figure 44C). PUGNAc treatment significantly reduced infarct size when normalized to the area at risk or left ventricukar area compared with Vehicle (Figure 44D).

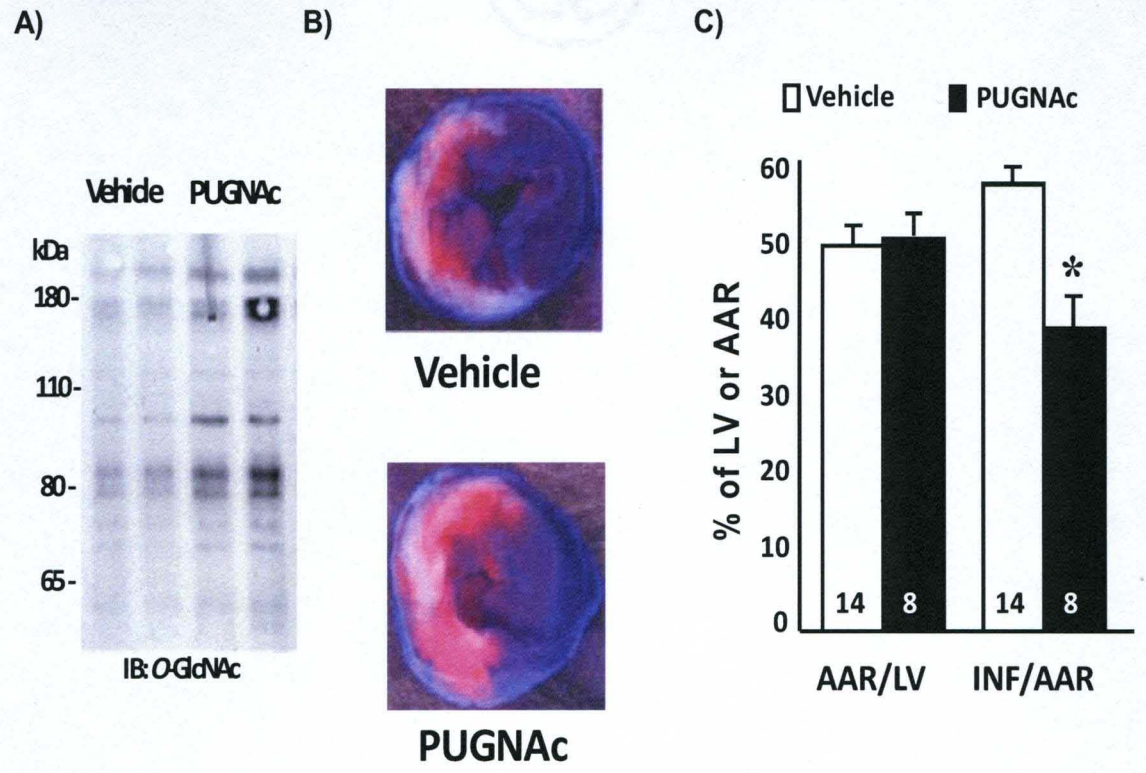

Figure 45. Mice were treated with 50 mg/kg PUGNAc or saline Vehicle for eighteen hours. **A)** To one group (n=3 per group) of PUGNAc or Vehicle-treated mice, total cellular protein was isolated from the hearts and western blotting for O-GlcNAc performed to confirm the ability of PUGNAc to augment O-GlcNAc levels in the hearts. PUGNAc treatment significantly augmented O-GlcNAc levels in the heart. **B)** Representative photomicrographs of mouse hearts treated with Vehicle or PUGNAc, subjected to 40 minutes of left coronary artery occlusion, 24 hours of reperfusion and infarct staining. The amount of dead tissue (white) in the representative PUGNAc heart is reduced compared with Vehicle. **C)** Summary data of hearts exposed to the myocardial ischemia/reperfusion protocol. LV indicates left ventricle. Infarct (INF) size with respect to the area at risk (AAR) was significantly reduced in the PUGNAc (n=8) group compared with Vehicle (n=12). *P<0.05 vs. Vehicle.

H.3. Effects of manipulaiton of O-GlcNAc levels on cardiovascular hemodynamics: One potential explanation for the cardioprotective effects may be that PUGNAc favorably affects cardiovascular hemodynamics, thereby reducing oxygen demand and by extension, infarct size. Accordingly, we measured blood pressure in mice treated with Vehicle (n=3) or PUGNAc (n=3) and found no significant differences in mean arterial blood pressure (Table 5). Furthermore, we evaluated LV end diastolic diameter, LV end systolic diameter, LV fractional shortening, and heart rate and found no differences between the two groups (Table 5). Similarly, PUGNAc did not alter blood glucose levels in the mice (143 ± 18 mg/dL) compared to Vehicle treatment (147 ± 20 mg/dL). Such data indicate that there were no gross reductions in myocardial work or circulating glucose levels that would explain the salubrious effects of PUGNAc during myocardial ischemia. Collectively, these findings provide a clinically-relevant counterpart to our more detailed and mechanistic *in vitro* studies.

Table 5: Cardiovascular hemodynamics data

Index	Vehicle (n=3)	PUGNAc (n=3)
Mean arterial blood Pressure (mmHg)	80 ± 3	78 ± 2
LV end diastolic diameter (LVEDD, mm)	3.33 ± 0.03	3.34 ± 0.24
LV end systolic diameter (LVESD, mm)	2.30 ± 0.06	2.30 ± 0.20
LV fractional shortening (LVFS, %)	30.1 ± 2.4	31.0 ± 2.6
Heart rate (HR, bpm)	360 ± 23	421 ± 33

CHAPTER VI

DISCUSSION

The purpose of this study was to determine whether the post-translational sugar modification, O-GlcNAc, plays a role in the pathogenesis of myocardial ischemia-reperfusion injury.

First, we determined if O-GlcNAc signaling changes following *in vitro* oxidative stress, hypoxia-reoxygenation, or ER stress, and *in vivo* myocardial ischemia. Oxidative stress and ER stress transiently augmented O-GlcNAc signaling, while hypoxia alone and ischemia alone reduced O-GlcNAc signaling. Characterizing O-GlcNAc profiles following short-term oxidative stress induction revealed that O-GlcNAc levels increased early and start decreasing 40 minutes post-oxidative stress. Hypoxia reduced O-GlcNAc levels, while reperfusion induced time dependent augmentation of O-GlcNAc levels peaking after six hours of reoxygenation. Our present characterization of the changes in O-GlcNAc signaling following hypoxia-reoxygenation in cardiomyocytes differs from that described by Champattanachai *et al* (33, 34). These studies revealed that *O*-GlcNAc levels rise following four hours of hypoxia and early reoxygenation (33, 34). Such disparity raises the possibility that changes in O-GlcNAc levels

following hypoxia might be dependent on the severity of hypoxia (anoxia vs. hypoxia) and the composition of the hypoxic medium. In the intact myocardium, we show that myocardial ischemia caused decrement in GlcNAc levels; while upon reperfusion, O-GlcNAc levels increased after 1 hour and were back at baseline by four and by 24 hours of reperfusion in the ischemic zone. Interestingly, O-GlcNAc signaling did not change in the non-ischemic zone of the mice subjected to myocardial ischemia-reperfusion injury. Such changes in O-GlcNAc levels *in vivo* support our *in vitro* hypoxia-reoxygenation findings. The decrement in O-GlcNAc levels observed following hypoxia/ischemia could be due to decreased substrate (glucose) availability. Moreover, hypoxic or ischemic stress could lead to decreased OGT activity and/or augmented GCA activity. Studies in isolated perfused rat hearts from Chatham's group reveal that simulated ischemia alone augments UDP-GlcNAc and O-GlcNAc levels early in the low-flow phase and then decline by the end of low flow and during reflow(83, 191). The changes in O-GlcNAc signaling following oxidative, hypoxic, ER stress or ischemic stress highlight the role of O-GlcNAc as a stress response in the heart. Moreover, these data support previous findings by Zachara *et al.* showing that O-GlcNAc signaling acts as a stress signal (333).

Next, we determined whether manipulation of O-GlcNAc levels affects oxidative stress, ER stress, hypoxia and ischemia-mediated cell death. In oxidative stress, enhanced O-GlcNAc signaling with PUGNAc (GCA inhibitor) delayed oxidative stress-induced decrease in O-GlcNAc signaling as well as attenuated the severity of the oxidative stress-mediated cardiomyocyte death.

Moreover, during ER stress, augmented O-GlcNAc levels via elevating OGT levels and O-GlcNAcase inhibition (with PUGNAc), attenuated ER stress-mediated cardiomyocyte death even though decrement of O-GlcNAc levels via elevation of GCA levels did not affect ER stress-mediated cardiomyocyte death. Additionally, during hypoxia-reoxygenation, elevated O-GlcNAc levels via OGT overexpression and O-GlcNAcase inhibition (siRNA or pharmacologically with PUGNAc) favored O-GlcNAc modification and mitigated cardiomyocyte death following hypoxia. Conversely, reducing global O-GlcNAc modification via OGT inhibition (using siRNA, cre-lox, or pharmacologically with TT04 and TT40) and O-GlcNAcase overexpression reduced O-GlcNAc levels and exacerbated post-hypoxic cardiac myocyte death. Therefore, this project provides evidence that pharmacologic or genetic manipulation of OGT and O-GlcNAcase affects cardiac myocyte survival following oxidative stress, ER stress, and hypoxia. Moreover, the present data suggest that OGT is a critical survival protein, while O-GlcNAcase antagonizes cardiac myocyte survival. Such pro-survival effects of enhanced O-GlcNAc modification are supported by data from Champathanachi *et al.* in which adenoviral (Ad) overexpression of OGT reduced post-hypoxic H_2O_2-induced cardiac myocyte death (34), while short interfering RNA against OGT sensitized NRCMs to hypoxia-induced apoptosis (34). On the other hand, evidence supporting the antagonistic role O-GlcNAcase on cardiomyocyte survival following lethal stress is seen several studies by Champattanachai *et al.* showing that O-GlcNAcase inhibition (with PUGNAc or NButGT) attenuated cardiac myocyte death following hypoxia and oxidative stress (33, 34, 190).

Better still, PUGNAc administration early in the reflow phase has been shown to improve cardiac functional recovery, reduce troponin release and calpain-mediated proteolysis of α-fodrin and Ca^{2+}/calmodulin-dependent protein kinase II compared to untreated Controls in isolated perfused hearts(190). Here, we show that the cytoprotective effects of enhanced O-GlcNAc signaling seen in NRCMs and isolated perfused heart, are relevant in an *in vivo* setting. Enhanced O-GlcNAc levels reduced infarct size in mice subjected to ischemia-reperfusion injury. Thus, enhanced O-GlcNAcylation of proteins seems essential in the ability of the cardiac myocytes, and hence the intact myocardium to withstand lethal stressors. Such collective insights during oxidant stress, ER stress, hypoxia, and ischemia are reminiscent of original findings by *Zachara et al.* of augmented *O*-GlcNAc signaling during cell stress (333).

Outside the common connections between cellular stress and *O*-GlcNAc levels, there is a body of data indicating that flux through the hexosamine biosynthetic pathway can augment *O*-GlcNAc levels and exert cytoprotection *in vitro* (33, 34, 82, 189-191) and *in vivo* (322, 337). In one *in vitro* study, hyperglycemia or treatment of cells with glucosamine (to increase HBP flux), augmented O-GlcNAcylation of proteins and was associated with increased cellular viability(33). Because the hyperglycemia-mediated increase in post-hypoxic *O*-GlcNAc levels was blocked by azerserine (a GFAT inhibitor), it seemed that the protective effect required HBP flux and subsequent *O*-GlcNAc modification of proteins. In addition, *in vivo* augmentation of O-GlcNAc levels using glucosamine after severe injury such as hemorrhagic shock has been

shown to improve cardiac function and peripheral organ perfusion in rats. Thus, the myocardium, like various tissues and cell lines, possesses the ability to recruit *O*-GlcNAc signaling system in times of stress. Such a conserved and stress-responsive system suggests an endogenous self-defense system operative in the heart.

To determine how O-GlcNAc confers cardioprotection, we first identified candidate proteins modified by O-GlcNAc in the heart. Based on the list of 13 proteins identified (table 3), voltage dependent anionic channel (VDAC) was most interesting because it is an outer mitochondrial membrane protein and a putative member of the mPTP. On this premise, we hypothesized that enhanced O-GlcNAc protein modification may act (at least partially) on the mitochondria to effect protection. Ca^{2+} accumulation in the mitochondrial matrix and increased ROS generation are prominent features of post-ischemic and hypoxic injury, and favor mPTP formation. Hence, it was logical to determine whether manipulation of O-GlcNAc signaling affect post-hypoxic Ca^{2+} overload and ROS generation. Genetic (AdOGT) and pharmacologic (O-GlcNAcase inhibition with PUGNAc) augmentation of O-GlcNAc levels attenuated hypoxia-induced Ca^{2+} overload compared to Vehicle. Conversely, diminished O-GlcNAc levels (AdGCA) exacerbated hypoxia-induced Ca^{2+} overload. These data supports previous findings by Nagy *et al.* showing that enhanced O-GlcNAc signaling via increased HBP flux or inhibition of GCA (PUGNAc) in neonatal cardiomyocytes, blocked angiotensin II-induced cytosolic Ca^{2+} elevation (222). On the other hand, inhibition of OGT (with alloxan) abrogated the glucosamine

mediated inhibition of angiotensin II-induced cytosolic Ca^{2+} overload(222). How O-GlcNAc attenuates Ca^{2+} overload in acute stress is unknown. Since the primary source for the rise in intracellular Ca^{2+} during/following ischemia or hypoxia might be via reverse functioning NCX(143), it is possible that enhanced O-GlcNAc levels mitigate hypoxia-induced Ca^{2+} overload via glycosylation of NCX. Another possible mechanism may be enhanced SERCA2a activity and/or decreased phospholamban binding to SERCA2a. Such hypothesis is supported by several studies from Dillmann's group showing that hyperglycemic cardiomyocytes and hearts from STZ-induced diabetic mice with elevated O-GlcNAc levels exhibited prolonged Ca^{2+} transients. In addition, these hyperglycemic myocytes and diabetic hearts showed diminished SERCA2a expression and phosphorylated phospholamban (PLB)(48, 135). Interestingly, overexpression of GCA (AdGCA) improved Ca^{2+} transients and augmented SERCA2a expression(48, 135), hence raising the possibility that O-GlcNAc signaling might infere with calcium handling by affecting SERCA2a expression and/or activity. If this is true, it is likely that O-GlcNAc signaling acts directly via glyocsylation of SERCA2a or indirectly by modifying an upstream kinase. Another question is whether manipulation of O-GlcNAc signaling affects SERCA2a expression and PLB phosphorylation at baseline (non-pathological conditions) in the heart. We also show that manipulation of O-GlcNAc signaling affects mitochondrial Ca^{2+} overload. Ca^{2+} likely enters the mitochondria via mitochondrial uniporter. Because there exist a mitochondrial OGT isoform (mOGT)(198) which is thought to be membrane bound(115), it is possible that

mOGT interacts with mitochondrial Ca^{2+} uniporter preventing Ca^{2+} uptake into the mitochondria. Such a hypothesis remains to be tested.

In addition to its roles in signal transduction and in regulation of redox cell signaling, ROS generation contributes to myocardial ischemia-reperfusion injury (183). Therefore, we ascertained whether manipulation of O-GlcNAc levels attenuated post-hypoxic ROS generation. Enhanced O-GlcNAc levels (AdOGT and PUGNAc) blocked hypoxia-mediated ROS generation while GCA overexpression (AdGCA) exacerbated hypoxia-induced ROS generation. One might hypothesize that O-GlcNAc signaling attenuates hypoxia-induced ROS generation by upregulating the expression and/or activity of antioxidant enzymes: catalase (Cat), glutathione peroxidase (GPX), and superoxide dismutase (SOD). Transcription of oxidative stress responsive enzymes, catalase and MnSOD (SOD2) is regulated by forkhead box O1 (FoxO1). FoxO1 is a nutrient and stress sensor known to play a regulatory role in diabetes. Recently, FoxO1 was shown to be O-GlcNAc modified. O-GlcNAc modification of FoxO1 activates FoxO1 and can in turn lead to activation of transcription of oxidative stress response enzymes Cat and MnSOD. Therefore, we evaluated whether manipulation of O-GlcNAc levels alter mRNA expression of catalase, superoxide dismutase or glutathione peroxidase in normoxia. Neither augmented O-GlcNAc (AdOGT and PUGNAc) nor diminished (AdGCA) O-GlcNAc levels significantly altered baseline mRNA levels of superoxide dismutase and glutathione peroxidase. However, inhibition of GCA (PUGNAc) augmented, while overexpression of GCA, reduced baseline catalase mRNA levels despite no change in catalase protein levels.

Because our hypoxia-reoxygenation studies last less than twenty four hours we do not believe the reduction in post-hypoxic ROS generation seen with augmented O-GlcNAc levels involves *de novo* synthesis of antioxidant enzymes. Instead, if O-GlcNAc signaling affects antioxidant enzymes SOD and GPX, we expect it to be at the level of the enzyme activity. The alteration in Cat expression with GCA manipulation partially explains the exacerbated post-hypoxic ROS generation with GCA expression and reduced ROS generation with GCA inhibition. Another possible hypothesis could be that O-GlcNAc signaling enhances oxidative phosphorylation. Studies show that augmenting glucose flux improves ischemic tolerance of the heart, potentially through an elevation in glycolytic ATP production and reduction of fatty acid oxidation (65, 274). The present data involve alterations in a glucose-derived metabolic signal, *O*-GlcNAc, leading one to question whether its manipulation would affect ATP levels. Such questions might be justified because of the present data indicating mitochondrial (including VDAC) and metabolic (e.g. glyceraldehyde-3-phosphate dehydrogenase, fructose-bisphosphate aldolase, pyruvate kinase as an *O*-GlcNAc target) proteins are *O*-GlcNAc modified. If alteration in *O*-GlcNAc modification of these enzymes affects their function, then it might be reasonable to expect changes in cellular ATP levels. Moreover, one of VDAC's physiological functions is to facilitate ATP transport across the outer mitochondrial membrane. However, because the HBP normally uses less than 5% cellular glucose, minimal changes in glycolytic ATP (via fructose-6-phosphate) should occur, assuming *O*-GlcNAc modification of such enzymes would not affect their activity. We show

that inhibition of OGT (via TT04) did not affect ATP levels in cardiac myocytes [0 μM TT04 (26.3 ± 15.3 nmol/L/mg protein) vs. 2.5 μM TT04 dose (26.3 ± 11.9 nmol/L/mg)]. In agreement with this notion, Champattanachai *et al.* found that glucosamine treatment in cardiac myocytes did not significantly affect ATP levels(33). The effects of altered O-GlcNAc signaling on post-hypoxic cardiac mitochondrial respiration remain to be tested. Though the present data suggest that decrement of OGlcNAc levels did not affect cellular ATP levels, Hu *et al.* recently identified components of mitochondrial respiratory chain complex I, III and IV to be O-GlcNAc modified (137). Moreover, Hu *et al.* showed that hyperglycemia augmented O-GlcNAcylation of components of mitochondrial respiratory chain complex I, III and IV, reduced their activity and decreased cellular ATP content in neonatal cardiomyocytes (137). Overexpression of GCA restored the activity of these complexes as well as the cellular ATP content (137). Therefore, determining whether such findings in chronic stress are similar in acute myocardial stress is critical. In addition, addressing whether baseline manipulation of OGT and GCA alter the activity of mitochondrial ETC complexes is critical. Since mitochondrial ROS is generated during electron transport in complex I and III, and components of complex I and III are known to be O-GlcNAc modified, it is possible that during myocardial ischemia/hypoxia, there is reduced O-GlcNAcylation of complex I and III components leading to augment ROS generation. Therefore, elevated O-GlcNAc signaling might diminish post-ischemic or post-hypoxic ROS generation via enhanced O-GlcNAcylation of components of complex I and III.

Mitochondria are key mediators and regulators of cell death in myocardial ischemia-reperfusion injury. The mPTP in particular appears to be a critical for the transition from reversible to irreversible myocardial ischemia-reperfusion injury(62). The mPTP is activated by ROS and Ca^{2+}, and both of these are elevated during myocardial ischemia and reperfusion. Numerous cardioprotective pathways work primarily by inhibition of mPTP formation directly or by preventing the conditions that promote mPTP formation. Consequently, we tested the hypothesis that O-GlcNAc signaling mitigated hypoxia/ischemia mediated mPTP formation. Augmented O-GlcNAc signaling (PUGNAc) attenuated Ca^{2+}-induced mitochondrial swelling while diminished O-GlcNAc levels sensitized cardiac mitochondria to Ca^{2+}-induced swelling. Because mitochondrial Ca^{2+} overload and ROS production favor mPTP (63, 141), it is possible that O-GlcNAc signaling might mitigate mPTP formation indirectly by attenuated Ca^{2+} overload and/or ROS generation. Because, VDAC, a putative component of mPTP is O-GlcNAc modified, we hypothesized that GlcNAcylation of VDAC would prevent its interaction with other mPTP components and hence block mPTP formation. One might dispute such a hypothesis based on recent findings by Baines *et al.* showing that mitochondria for VDAC null mice undergo mPTP (11). However, there is no evidence that cardiac mitochondria deficient of all three VDAC isoforms undergo mPTP.

Several models of mPTP have been proposed by different groups. In the model proposed by Halestrap's group, CyP-D when activated by augmented mitochondrial Ca^{2+} binds to ANT and undergoes conformational changes to form

mPTP (57, 58, 318). CsA blocks mPTP formation by inhibiting the peptidyl-prolyl cis-trans isomerase (PPIase) activity of CyP-D and also preventing the binding of CyP-D to ANT(58, 93, 105, 106). Based on this model, O-GlcNAc might mitigate mPTP formation by GlcNAcylation of CyP-D, inhibiting the PPIase activity of CyP-D and/or inhibition of the binding of CyP-D to ANT. In the model proposed by Lemaster's group(128), mPTP could be formed by aggregation of misfolded integral membrane proteins damaged by oxidant and other stressors and is blocked by CsA. In this model, CyP-D prevented protein aggregation normally by binding these proteins (as chaperone) but when activated by augmented mitochondrial Ca^{2+}, dissociated from these proteins. Hence, O-GlcNAc signaling might attenuate mPTP formation by enhanced CyP-D chaperone function. Whether CyP-D and ANT are O-GlcNAc modified is unknown.

Opening of mPTP is characterized by the loss of $\Delta\Psi_m$, massive mitochondrial swelling, rupture of outer mitochondrial membrane, and the release of intermembrane components such as cytochrome c(62). Dissipation of $\Delta\psi_m$ is a critical event early in the process of cell death(175), hence, we tested the hypothesis that manipulation of O-GlcNAc signaling affects post-hypoxic recovery $\Delta\Psi_m$. The present data reveals that augmented O-GlcNAc levels enhanced post-hypoxic $\Delta\Psi_m$ recovery, while reduced O-GlcNAc signaling diminished $\Delta\Psi_m$ recovery. Therefore, inhibition of $\Delta\Psi_m$ loss by O-GlcNAc signaling may be mediated by prevention of Ca^{2+} overload or ROS production in mitochondria, such that PTP never opens.

In addition to Ca^{2+} overload and increased ROS generation, endoplasmic reticulum (ER) stress has emerged as a potentially critical element of ischemia/hypoxia –induced injury. Consequently, we focused on the potential ability of O-GlcNAc signaling to directly attenuate ER stress-induced cell death (in the absence of the confounding condition of hypoxia). Here, we show that augmented O-GlcNAc levels (via overexpression of OGT or inhibition of O-GlcNAcase) attenuated the activation of maladaptive ER stress response and mitigated ER stress-induced cardiac myocyte death. On the otherhand, overexpression of GCA did not alter BfA or TM-mediated activation of maladaptive ER stress response. A notable finding in the present study is the augmentation of O-GlcNAc signaling during ER stress. It will be interesting to ascertain the cause for augmented O-GlcNAcylation during ER stress. One might conjecture that augmented O-GlcNAc levels may be due to elevated OGT and/or reduced O-GlcNAcase activities. Regardless of the mechanism, we hypothesized that such a response was a pro-adaptive but insufficient response to the induction of ER stress. The induction of O-GlcNAc signaling during ER stress might be predicted from the significant literature supporting the role of O-GlcNAc as an acute stress or alarm signal (228, 333). The present demonstration of O-GlcNAc signaling may reflect a partially pro-adaptive response during ER stress. Clearly, augmentation of O-GlcNAc signaling rescued cardiomyocytes from ER stress-induced cell death. The new question relates to the mechanism operative during O-GlcNAc signaling-mediated rescue of cells undergoing the UPR. The data related to OGT overexpression and O-

GlcNAcase inhibition (via PUGNAc) are clear in that there is robust attenuation of ER stress-mediated cell death (with either BfA or TM). In addition, it also appears that such maneuvers designed to augment O-GlcNAc signaling might limit the severity of the induction of ER stress, as indicated by the general limitation of the markers of ER stress activation. In this regard, augmented O-GlcNAc signaling might function as a regulator of the initiation/propagation of ER stress and indirectly attenuate cell death. In addition, enhanced O-GlcNAc signaling may directly attenuate cell death, which may be independent of ER stress mitigation. Conversely, the data from O-GlcNAcase could initially be viewed as ambiguous. Overexpression of O-GlcNAcase (AdGCA) did not exaggerate any of the ER stress indicators. Interestingly, AdGCA exacerbated ER stress-mediated cell death when BfA, but not TM, was used as the inducer of ER stress. Although the precise reason for the apparently discrepant response is not clear, we hypothesize that the dose of TM used in our system produces somewhat greater induction of ER stress (as evidenced by the larger increase in the ER stress markers in the TM experiments) and that AdGCA is unable to exacerbate this response.

The UPR initially attempts to support restoration of ER homoeostasis and protect cells from stress. In fact, Vitadello *et al.* first demonstrated that overexpression of Grp94 reduces ischemia-induced cardiomyocyte death(305). Moreover, Thuerauf *et al.* showed that subjecting cardiac myocytes to hypoxia activated XBP1 and XBP1 contributed to protecting post-hypoxic cardiomyocytes (293). However, prolonged ER stress activates cell death. Induction of the pro-

apoptotic transcription factor CHOP is a hallmark of ER stress-mediated cell death. Here, BfA or TM-induced CHOP expression was attenuated by genetic/pharmacologic elevation of O-GlcNAc levels (via OGT overexpression and O-GlcNAcase inhibition). The exact mechanism through which O-GlcNAc signaling blocks CHOP activation is unknown. It is known that p38 MAPK phosphorylates CHOP, which increases its activity(284). Accordingly, O-GlcNAc signaling may block CHOP phosphorylation, independent of absolute reductions in protein expression, thereby reducing its activity and subsequent cardiomyocyte death. Targeting eukaryotic initiation factor-2 (eIF-2) represents another potential mechanism in the context of ER stress. Its activity is regulated by phosphorylation and indirectly by O-GlcNAcylation. A 67kDa polypeptide (p67) binds to eIF-2 blocking its phosphorylation and subsequently inhibits protein synthesis(32). It is plausible that enhanced p67 glycosylation (i.e. with AdOGT) binds to and blocks eIF-2 phosphorylation by eIF-2 kinase. Although transient reduction in protein synthesis may be pro-adaptive during the early stages of ER stress, prolonged blockade of protein synthesis is not viable. Therefore, one might predict that augmenting O-GlcNAc levels promotes p67 glycosylation and subsequent blockade of eIF-2 phosphorylation, as one potential mechanism in the present study. Such possibilities remain to be evaluated.

Although the present study focuses on the acute effects of altered *O*-GlcNAc signaling, other studies interrogated the role of chronic elevation of *O*-GlcNAc levels and its possible role in diabetes. Several groups have shown that prolonged elevation of *O*-GlcNAc levels attenuates insulin signaling(307, 313),

though this issue is far from reconciled (29). In the heart, several studies have linked chronic elevation of O-GlcNAc levels to abnormal cardiomyocyte function. Clark *et al.* reported that in neonatal cardiomyocytes enhancing O-GlcNAc signaling with hyperglycemia, glucosamine, or OGT overexpression prolonged Ca^{2+} transient decays whereas diminishing O-GlcNAc signaling via overexpression of GCA, improved Ca^{2+} transients in cells subjected to hyperglycemia. Moreover, hyperglycemia decreased SERCA mRNA and protein expression and this was prevented by GCA overexpression(48). Subsequently, Hu *et al.* showed that hearts from STZ-induced diabetic mice have increased OGT expression and O-GlcNAc levels, accompanied by cardiomyocytes dysfunction. GCA overexpression significantly reduced O-GlcNAc levels, increased SERCA expression, and improved function in both isolated cardiomyocyte and intact hearts compared to diabetic controls(135). More recently, Hu *et al.* showed that several proteins of the mitochondrial ETC are O-GlcNAc modified (138). Moreover, hyperglycemia augmented glycosylation of mitochondrial ETC proteins and impaired mitochondrial function while overexpression of O-GlcNAcase reduced glycosylation of ETC proteins and reversed the hyperglycemia-mediated mitochondrial dysfunction(138). Such efforts support the emerging notion that *O*-GlcNAc signaling participates in the pathogenesis of diabetes. Thus, acute and chronic effects of altered *O*-GlcNAc levels may have significantly different implications in the heart. One explanation for these potentially contradictory effects of enhanced O-GlcNAc signaling in the acute and chronic settings in the heart may be that acute increases in O-GlcNAc

signaling may be protective while chronic activation of O-GlcNAc signaling may produce adverse effects. Moreover, target proteins for O-GlcNAcylation in response to short-term increase in O-GlcNAc levels may be different from that due to sustained increases in O-GlcNAc signaling. Another possible explanation is based on the concept of allostasis. The theory of allostasis suggests that the initial biological response to an acute stress is the activation of processes that are protective and improve survival, however, as the allostatic load is increased; the stress becomes more frequent and/or continuous such that activation of the same pathways results in the development of pathology. Therefore, if augmented O-GlcNAc signaling is an acute survival response, the development of pathphysiology in chronic diseases like diabetes may be partially due to chronic activation of O-GlcNAc signaling.

CHAPTER VII

SUMMARY OF FINDINGS AND FUTURE DIRECTIONS

Summary of Findings

Prior to this study, very few studies addressed the role of O-GlcNAc in the heart in general, and more so, no literature was available on its role in acute myocardial ischemia. The few studies that examined the role of O-GlcNAc in the heart were focused on its contribution to the development of diabetic cardiomyopathy.

Our study provides evidence that the heart recruits *O*-GlcNAc signaling system in times of stress (Figure 45). Oxidative and ER stress induced transient increases in O-GlcNAc signaling, while hypoxic/ ischemic stress trigger an initial decrease in O-GlcNAc signaling. This notion supports recent findings by several other groups showing that O-GlcNAc is a stress response signal. Moreover, we show that pharmacologic or genetic enhancement of O-GlcNAc signaling attenuated stress induced cellular damage while pharmacologic or genetic decrement exacerbated stress-mediated cell death. Therefore, acute increases in O-GlcNAc signaling in the heart promote resistance to stress, while short-term reduction in O-GlcNAc signaling sensitizes cells to stress-induced death.

We identified potential mechanisms through which enhanced O-GlcNAc confers cardioprotection. We show that O-GlcNAc mitigates components of mitochondrial mediated death pathway. As show in Figures 35 and 36, augmented O-GlcNAc signaling attenuates Ca^{2+} overload, ROS generation and subsequent mitochondrial permeability transition pore formation and loss of mitochondrial trans inner membrane potential. Besides mitigating mitochondrial induced death pathway, we show that O-GlcNAc signaling may confer cardioprotection via attenuating the activation of maladaptive unfolded protein response (Figure 45). Our proposed mechanisms are not the only likely mechanisms through which O-GlcNAc cardioprotects because numerous proteins are O-GlcNAc modified in the heart.

Finally, we show that *in vivo* enhancement of O-GlcNAc levels reduce infarct size after ischemia-reperfusion in mice. Such data provide strong evidence that the protective effect seen associated with increasing O-GlcNAc levels at the cellular level and supported in isolated organ studies by Chatham's group can be translated to the *in vivo* environment.

Although one limitation of this project is the use of young, healthy, isolated cardiomyocytes, such a reductionist approach was necessary to identify the role of the key enzymes that regulate O-GlcNAc modification, OGT and GCA, *per se*, and maintain the ability to elevate and reduce OGT and GCA activity.

In conclusion, complete understanding of the protective role of O-GlcNAc in the heart may yield viable therapeutic options to combat post-ischemic myocardial injury. Moreover, the present study lays the groundwork for

understanding the role of O-GlcNAc in more complex cardiovascular phenotypes such as diabetes, hypertension, obesity, and other pathologies that predispose patients to heart disease.

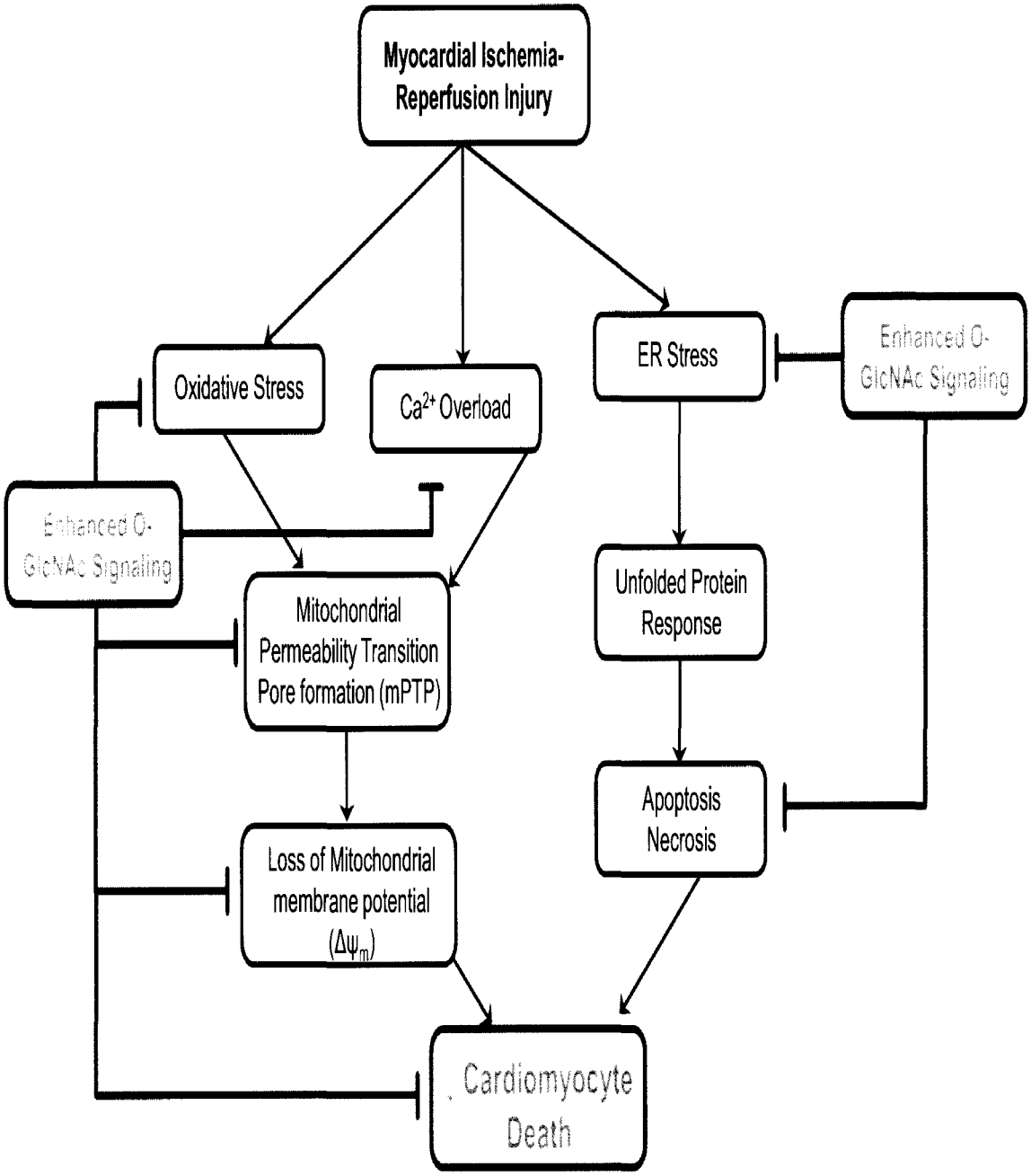

Figure 45. Summary Scheme

Future Directions

Further investigation is necessary to elucidate more fully how O-GlcNAc signaling confers cardioprotection at the level of the mitochondria and ER.

For mitochondrial-mediated cardioprotective mechanism, future studies will focus on understanding the potential interaction between O-GlcNAc signaling, ROS generation, and mitochondria. Moreover, identifying specific proteins that are involved with O-GlcNAc-mediated reductions in Ca^{2+} overload is critical for the complete understanding of O-GlcNAc mediated cardioprotection. We will also determine if other components of the mPTP are O-GlcNAc modified.

With respect to cardioprotection at the level of the ER, future studies will be geared towards identifying proteins involved with UPR that are O-GlcNAc modified. In addition, we will determine the mechanism through which O-GlcNAc attenuates ER stress.

REFERENCE

1. National Hospital Ambulatory Medical Care Survey, 1996 (CDC/NCHS).

2. Phase I, National Heath and Nutrition Examination Survey III, 1988-91.

3. **Abdallah Y, Gkatzoflia A, Gligorievski D, Kasseckert S, Euler G, Schluter KD, Schafer M, Piper HM, and Schafer C.** Insulin protects cardiomyocytes against reoxygenation-induced hypercontracture by a survival pathway targeting SR Ca2+ storage. *Cardiovasc Res* 70: 346-353, 2006.

4. **Akao M, O'Rourke B, Kusuoka H, Teshima Y, Jones SP, and Marban E.** Differential Actions of Cardioprotective Agents on the Mitochondrial Death Pathway. *Circ Res* 92: 195-202, 2003.

5. **Akao M, Ohler A, O'Rourke B, and Marban E.** Mitochondrial ATP-Sensitive Potassium Channels Inhibit Apoptosis Induced by Oxidative Stress in Cardiac Cells. *Circ Res* 88: 1267-1275, 2001.

6. **Ala-Rami A, Ylitalo KV, and Hassinen IE.** Ischaemic preconditioning and a mitochondrial KATP channel opener both produce cardioprotection accompanied by F1F0-ATPase inhibition in early ischaemia. *Basic Res Cardiol* 98: 250-258, 2003.

7. **Ambrosio G, Becker LC, Hutchins GM, Weisman HF, and Weisfeldt ML.** Reduction in experimental infarct size by recombinant human superoxide dismutase: insights into the pathophysiology of reperfusion injury. *Circulation* 74: 1424-1433, 1986.

8. **Arnold CS, Johnson GV, Cole RN, Dong DL, Lee M, and Hart GW.** The microtubule-associated protein tau is extensively modified with O-linked N-acetylglucosamine. *J Biol Chem* 271: 28741-28744, 1996.

9. **Arroyo CM, Kramer JH, Dickens BF, and Weglicki WB.** Identification of free radicals in myocardial ischemia/reperfusion by spin trapping with nitrone DMPO. *FEBS letters* 221: 101-104, 1987.

10. **Baines CP, Kaiser RA, Purcell NH, Blair NS, Osinska H, Hambleton MA, Brunskill EW, Sayen MR, Gottlieb RA, Dorn GW, Robbins J, and Molkentin JD.** Loss of cyclophilin D reveals a critical role for mitochondrial permeability transition in cell death. *Nature* 434: 658-662, 2005.

11. **Baines CP, Kaiser RA, Sheiko T, Craigen WJ, and Molkentin JD.** Voltage-dependent anion channels are dispensable for mitochondrial-dependent cell death. *Nat Cell Biol* 9: 550-555, 2007.

12. **Basso E, Fante L, Fowlkes J, Petronilli V, Forte MA, and Bernardi P.** Properties of the permeability transition pore in mitochondria devoid of Cyclophilin D. *J Biol Chem* 280: 18558-18561, 2005.

13. **Beck M, Brickley K, Wilkinson HL, Sharma S, Smith M, Chazot PL, Pollard S, and Stephenson FA.** Identification, molecular cloning, and characterization of a novel GABAA receptor-associated protein, GRIF-1. *J Biol Chem* 277: 30079-30090, 2002.

14. **Becker LB, vanden Hoek TL, Shao ZH, Li CQ, and Schumacker PT.** Generation of superoxide in cardiomyocytes during ischemia before reperfusion. *Am J Physiol* 277: H2240-2246, 1999.

15. **Bekheit S, Isber N, Jani H, Butrous G, Boutjdir M, and el-Sherif N.** Reduction of ischemia-induced electrophysiologic abnormalities by glucose-insulin infusion. *J Am Coll Cardiol* 22: 1214-1222, 1993.

16. **Bernardi P.** Mitochondrial transport of cations: channels, exchangers, and permeability transition. *Physiol Rev* 79: 1127-1155, 1999.

17. **Bernardi P, Vassanelli S, Veronese P, Colonna R, Szabo I, and Zoratti M.** Modulation of the mitochondrial permeability transition pore. Effect of protons and divalent cations. *J Biol Chem* 267: 2934-2939, 1992.

18. **Bers DM.** Cardiac excitation-contraction coupling. *Nature* 415: 198-205, 2002.

19. **Bishopric NH, Zeng G-Q, Sato B, and Webster KA.** Adenovirus E1A Inhibits Cardiac Myocyte-specific Gene Expression through Its Amino Terminus. *J Biol Chem* 272: 20584-20594, 1997.

20. **Blobel G.** Protein targeting. *Biosci Rep* 20: 303-344, 2000.

21. **Boehmelt G, Wakeham A, Elia A, Sasaki T, Plyte S, Potter J, Yang Y, Tsang E, Ruland J, Iscove NN, Dennis JW, and Mak TW.** Decreased UDP-GlcNAc levels abrogate proliferation control in EMeg32-deficient cells. *EMBO J* 19: 5092-5104, 2000.

22. **Bolli R.** Causative role of oxyradicals in myocardial stunning: a proven hypothesis. A brief review of the evidence demonstrating a major role of reactive oxygen species in several forms of postischemic dysfunction. *Basic Res Cardiol* 93: 156-162, 1998.

23. **Booth C and Koch GL.** Perturbation of cellular calcium induces secretion of luminal ER proteins. *Cell* 59: 729-737, 1989.

24. **Broekemeier KM, Dempsey ME, and Pfeiffer DR.** Cyclosporin A is a potent inhibitor of the inner membrane permeability transition in liver mitochondria. *J Biol Chem* 264: 7826-7830, 1989.

25. **Broekemeier KM and Pfeiffer DR.** Inhibition of the mitochondrial permeability transition by cyclosporin A during long time frame experiments: relationship between pore opening and the activity of mitochondrial phospholipases. *Biochemistry* 34: 16440-16449, 1995.

26. **Brosius FC, 3rd, Liu Y, Nguyen N, Sun D, Bartlett J, and Schwaiger M.** Persistent myocardial ischemia increases GLUT1 glucose transporter expression in both ischemic and non-ischemic heart regions. *Journal of molecular and cellular cardiology* 29: 1675-1685, 1997.

27. **Burkart V, Wang ZQ, Radons J, Heller B, Herceg Z, Stingl L, Wagner EF, and Kolb H.** Mice lacking the poly(ADP-ribose) polymerase gene are resistant to pancreatic beta-cell destruction and diabetes development induced by streptozocin. *Nat Med* 5: 314-319, 1999.

28. **Burns RJ, Gibbons RJ, Yi Q, Roberts RS, Miller TD, Schaer GL, Anderson JL, and Yusuf S.** The relationships of left ventricular ejection fraction, end-systolic volume index and infarct size to six-month mortality after hospital discharge following myocardial infarction treated by thrombolysis. *J Am Coll Cardiol* 39: 30-36, 2002.

29. **Buse MG.** Hexosamines, insulin resistance, and the complications of diabetes: current status. *Am J Physiol Endocrinol Metab* 290: E1-E8, 2006.

30. **Cai Z and Semenza GL.** PTEN activity is modulated during ischemia and reperfusion: involvement in the induction and decay of preconditioning. *Circ Res* 97: 1351-1359, 2005.

31. **Castilho RF, Kowaltowski AJ, Meinicke AR, Bechara EJ, and Vercesi AE.** Permeabilization of the inner mitochondrial membrane by Ca2+ ions is stimulated by t-butyl hydroperoxide and mediated by reactive oxygen species generated by mitochondria. *Free Radic Biol Med* 18: 479-486, 1995.

32. **Chakraborty A, Saha D, Bose A, Chatterjee M, and Gupta NK.** Regulation of eIF-2 alpha-subunit phosphorylation in reticulocyte lysate. *Biochemistry* 33: 6700-6706, 1994.

33. **Champattanachai V, Marchase RB, and Chatham JC.** Glucosamine protects neonatal cardiomyocytes from ischemia-reperfusion injury via increased protein-associated O-GlcNAc. *Am J Physiol Cell Physiol* 292: C178-187, 2007.

34. **Champattanachai V, Marchase RB, and Chatham JC.** Glucosamine protects neonatal cardiomyocytes from ischemia-reperfusion injury via increased protein O-

GlcNAc and increased mitochondrial Bcl-2. *Am J Physiol Cell Physiol* 294: C1509-1520, 2008.

35. **Chang Q, Su K, Baker JR, Yang X, Paterson AJ, and Kudlow JE.** Phosphorylation of human glutamine:fructose-6-phosphate amidotransferase by cAMP-dependent protein kinase at serine 205 blocks the enzyme activity. *J Biol Chem* 275: 21981-21987, 2000.

36. **Chang SC, Wooden SK, Nakaki T, Kim YK, Lin AY, Kung L, Attenello JW, and Lee AS.** Rat gene encoding the 78-kDa glucose-regulated protein GRP78: its regulatory sequences and the effect of protein glycosylation on its expression. *Proceedings of the National Academy of Sciences of the United States of America* 84: 680-684, 1987.

37. **Chen X, Zhang X, Kubo H, Harris DM, Mills GD, Moyer J, Berretta R, Potts ST, Marsh JD, and Houser SR.** Ca2+ influx-induced sarcoplasmic reticulum Ca2+ overload causes mitochondrial-dependent apoptosis in ventricular myocytes. *Circ Res* 97: 1009-1017, 2005.

38. **Cheng EH, Sheiko TV, Fisher JK, Craigen WJ, and Korsmeyer SJ.** VDAC2 inhibits BAK activation and mitochondrial apoptosis. *Science* 301: 513-517, 2003.

39. **Cheng X, Cole RN, Zaia J, and Hart GW.** Alternative O-glycosylation/O-phosphorylation of the murine estrogen receptor beta. *Biochemistry* 39: 11609-11620, 2000.

40. **Chernyak BV and Bernardi P.** The mitochondrial permeability transition pore is modulated by oxidative agents through both pyridine nucleotides and glutathione at two separate sites. *Eur J Biochem* 238: 623-630, 1996.

41. **Cheung WD and Hart GW.** AMP-activated protein kinase and p38 MAPK activate O-GlcNAcylation of neuronal proteins during glucose deprivation. *J Biol Chem* 283: 13009-13020, 2008.

42. **Cheung WD, Sakabe K, Housley MP, Dias WB, and Hart GW.** O-linked beta-N-acetylglucosaminyltransferase substrate specificity is regulated by myosin phosphatase targeting and other interacting proteins. *J Biol Chem* 283: 33935-33941, 2008.

43. **Chi LG, Tamura Y, Hoff PT, Macha M, Gallagher KP, Schork MA, and Lucchesi BR.** Effect of superoxide dismutase on myocardial infarct size in the canine heart after 6 hours of regional ischemia and reperfusion: a demonstration of myocardial salvage. *Circ Res* 64: 665-675, 1989.

44. **Chou CF and Omary MB.** Mitotic arrest-associated enhancement of O-linked glycosylation and phosphorylation of human keratins 8 and 18. *J Biol Chem* 268: 4465-4472, 1993.

45. **Chou CF, Smith AJ, and Omary MB.** Characterization and dynamics of O-linked glycosylation of human cytokeratin 8 and 18. *J Biol Chem* 267: 3901-3906, 1992.

46. **Chou TY, Dang CV, and Hart GW.** Glycosylation of the c-Myc transactivation domain. *Proceedings of the National Academy of Sciences of the United States of America* 92: 4417-4421, 1995.

47. **Chou TY, Hart GW, and Dang CV.** c-Myc is glycosylated at threonine 58, a known phosphorylation site and a mutational hot spot in lymphomas. *J Biol Chem* 270: 18961-18965, 1995.

48. **Clark RJ, McDonough PM, Swanson E, Trost SU, Suzuki M, Fukuda M, and Dillmann WH.** Diabetes and the Accompanying Hyperglycemia Impairs Cardiomyocyte Calcium Cycling through Increased Nuclear O-GlcNAcylation. *J Biol Chem* 278: 44230-44237, 2003.

49. **Cohen MV, Yang XM, and Downey JM.** The pH hypothesis of postconditioning: staccato reperfusion reintroduces oxygen and perpetuates myocardial acidosis. *Circulation* 115: 1895-1903, 2007.

50. **Cole RN and Hart GW.** Glycosylation sites flank phosphorylation sites on synapsin I: O-linked N-acetylglucosamine residues are localized within domains mediating synapsin I interactions. *J Neurochem* 73: 418-428, 1999.

51. **Colombini M.** Structure and mode of action of a voltage dependent anion-selective channel (VDAC) located in the outer mitochondrial membrane. *Ann N Y Acad Sci* 341: 552-563, 1980.

52. **Comelli M, Metelli G, and Mavelli I.** Downmodulation of mitochondrial F0F1 ATP synthase by diazoxide in cardiac myoblasts: a dual effect of the drug. *Am J Physiol Heart Circ Physiol* 292: H820-829, 2007.

53. **Comer FI and Hart GW.** Reciprocity between O-GlcNAc and O-Phosphate on the Carboxyl Terminal Domain of RNA Polymerase II. *Biochemistry* 40: 7845-7852, 2001.

54. **Comer FI, Vosseller K, Wells L, Accavitti MA, and Hart GW.** Characterization of a mouse monoclonal antibody specific for O-linked N-acetylglucosamine. *Anal Biochem* 293: 169-177, 2001.

55. **Comtesse N, Heckel D, Racz A, Brass N, Glass B, and Meese E.** Five novel immunogenic antigens in meningioma: cloning, expression analysis, and chromosomal mapping. *Clin Cancer Res* 5: 3560-3568, 1999.

56. **Comtesse N, Maldener E, and Meese E.** Identification of a nuclear variant of MGEA5, a cytoplasmic hyaluronidase and a beta-N-acetylglucosaminidase. *Biochemical and Biophysical Research Communications* 283: 634-640, 2001.

57. **Connern CP and Halestrap AP.** Chaotropic agents and increased matrix volume enhance binding of mitochondrial cyclophilin to the inner mitochondrial membrane and sensitize the mitochondrial permeability transition to [Ca2+]. *Biochemistry* 35: 8172-8180, 1996.

58. **Connern CP and Halestrap AP.** Recruitment of mitochondrial cyclophilin to the mitochondrial inner membrane under conditions of oxidative stress that enhance the opening of a calcium-sensitive non-specific channel. *Biochem J* 302 (Pt 2): 321-324, 1994.

59. **Contessi S, Metelli G, Mavelli I, and Lippe G.** Diazoxide affects the IF1 inhibitor protein binding to F1 sector of beef heart F0F1ATPsynthase. *Biochem Pharmacol* 67: 1843-1851, 2004.

60. **Costantini P, Chernyak BV, Petronilli V, and Bernardi P.** Modulation of the mitochondrial permeability transition pore by pyridine nucleotides and dithiol oxidation at two separate sites. *J Biol Chem* 271: 6746-6751, 1996.

61. **Costantini P, Chernyak BV, Petronilli V, and Bernardi P.** Selective inhibition of the mitochondrial permeability transition pore at the oxidation-reduction sensitive dithiol by monobromobimane. *FEBS letters* 362: 239-242, 1995.

62. **Crompton M.** The mitochondrial permeability transition pore and its role in cell death. *The Biochemical journal* 341 233-249, 1999.

63. **Crompton M, Costi A, and Hayat L.** Evidence for the presence of a reversible Ca2+-dependent pore activated by oxidative stress in heart mitochondria. *Biochem J* 245: 915-918, 1987.

64. **Crompton M, Ellinger H, and Costi A.** Inhibition by cyclosporin A of a Ca2+-dependent pore in heart mitochondria activated by inorganic phosphate and oxidative stress. *Biochem J* 255: 357-360, 1988.

65. **Cross HR, Opie LH, Radda GK, and Clarke K.** Is a High Glycogen Content Beneficial or Detrimental to the Ischemic Rat Heart? : A Controversy Resolved. *Circ Res* 78: 482-491, 1996.

66. **Davidson SM, Hausenloy D, Duchen MR, and Yellon DM.** Signalling via the reperfusion injury signalling kinase (RISK) pathway links closure of the mitochondrial permeability transition pore to cardioprotection. *Int J Biochem Cell Biol* 38: 414-419, 2006.

67. **Davies KJ.** Oxidative stress: the paradox of aerobic life. *Biochem Soc Symp* 61: 1-31, 1995.

68. **Di Lisa F and Bernardi P.** Mitochondria and ischemia-reperfusion injury of the heart: fixing a hole. *Cardiovasc Res* 70: 191-199, 2006.

69. **Di Lisa F, Blank PS, Colonna R, Gambassi G, Silverman HS, Stern MD, and Hansford RG.** Mitochondrial membrane potential in single living adult rat cardiac myocytes exposed to anoxia or metabolic inhibition. *J Physiol* 486 (Pt 1): 1-13, 1995.

70. **Dong DL and Hart GW.** Purification and characterization of an O-GlcNAc selective N-acetyl- beta-D-glucosaminidase from rat spleen cytosol. *J Biol Chem* 269: 19321-19330, 1994.

71. **Dorfmueller HC, Borodkin VS, Schimpl M, Shepherd SM, Shpiro NA, and van Aalten DM.** GlcNAcstatin: a picomolar, selective O-GlcNAcase inhibitor that modulates intracellular O-glcNAcylation levels. *Journal of the American Chemical Society* 128: 16484-16485, 2006.

72. **Dorner AJ, Wasley LC, Raney P, Haugejorden S, Green M, and Kaufman RJ.** The stress response in Chinese hamster ovary cells. Regulation of ERp72 and protein disulfide isomerase expression and secretion. *J Biol Chem* 265: 22029-22034, 1990.

73. **Drake MT, Shenoy SK, and Lefkowitz RJ.** Trafficking of G protein-coupled receptors. *Circ Res* 99: 570-582, 2006.

74. **Du XL, Edelstein D, Dimmeler S, Ju Q, Sui C, and Brownlee M.** Hyperglycemia inhibits endothelial nitric oxide synthase activity by posttranslational modification at the Akt site. *J Clin Invest* 108: 1341-1348, 2001.

75. **Duilio C, Ambrosio G, Kuppusamy P, DiPaula A, Becker LC, and Zweier JL.** Neutrophils are primary source of O2 radicals during reperfusion after prolonged myocardial ischemia. *Am J Physiol Heart Circ Physiol* 280: H2649-2657, 2001.

76. **Eberli FR, Weinberg EO, Grice WN, Horowitz GL, and Apstein CS.** Protective effect of increased glycolytic substrate against systolic and diastolic dysfunction and increased coronary resistance from prolonged global underperfusion and reperfusion in isolated rabbit hearts perfused with erythrocyte suspensions. *Circ Res* 68: 466-481, 1991.

77. **Eisner DA, Choi HS, Diaz ME, O'Neill SC, and Trafford AW.** Integrative analysis of calcium cycling in cardiac muscle. *Circ Res* 87: 1087-1094, 2000.

78. **Farook VS, Bogardus C, and Prochazka M.** Analysis of MGEA5 on 10q24.1-q24.3 encoding the beta-O-linked N-acetylglucosaminidase as a candidate gene for type 2 diabetes mellitus in Pima Indians. *Mol Genet Metab* 77: 189-193, 2002.

79. **Favreau C, Worman HJ, Wozniak RW, Frappier T, and Courvalin JC.** Cell cycle-dependent phosphorylation of nucleoporins and nuclear pore membrane protein Gp210. *Biochemistry* 35: 8035-8044, 1996.

80. **Forsythe ME, Love DC, Lazarus BD, Kim EJ, Prinz WA, Ashwell G, Krause MW, and Hanover JA.** Caenorhabditis elegans ortholog of a diabetes susceptibility locus: oga-1 (O-GlcNAcase) knockout impacts O-GlcNAc cycling, metabolism, and dauer. *Proceedings of the National Academy of Sciences of the United States of America* 103: 11952-11957, 2006.

81. **Fujiwara T, Oda K, Yokota S, Takatsuki A, and Ikehara Y.** Brefeldin A causes disassembly of the Golgi complex and accumulation of secretory proteins in the endoplasmic reticulum. *J Biol Chem* 263: 18545-18552, 1988.

82. **Fulop N, Marchase RB, and Chatham JC.** Role of protein O-linked N-acetyl-glucosamine in mediating cell function and survival in the cardiovascular system. *Cardiovasc Res*, 2006.

83. **Fulop N, Zhang Z, Marchase RB, and Chatham JC.** Glucosamine cardioprotection in perfused rat hearts associated with increased O-linked N-acetylglucosamine protein modification and altered p38 activation. *Am J Physiol Heart Circ Physiol* 292: H2227-2236, 2007.

84. **Gao Y, Wells L, Comer FI, Parker GJ, and Hart GW.** Dynamic O-Glycosylation of Nuclear and Cytosolic Proteins. Cloning and characterization of a neutral, cytosolic beta -N-Acetylglucosaminidase from human brain. *J Biol Chem* 276: 9838-9845, 2001.

85. **Gewinner C, Hart G, Zachara N, Cole R, Beisenherz-Huss C, and Groner B.** The coactivator of transcription CREB-binding protein interacts preferentially with the glycosylated form of Stat5. *J Biol Chem* 279: 3563-3572, 2004.

86. **Gibbons RJ, Valeti US, Araoz PA, and Jaffe AS.** The quantification of infarct size. *J Am Coll Cardiol* 44: 1533-1542, 2004.

87. **Giordano FJ.** Oxygen, oxidative stress, hypoxia, and heart failure. *J Clin Invest* 115: 500-508, 2005.

88. **Graack HR, Cinque U, and Kress H.** Functional regulation of glutamine:fructose-6-phosphate aminotransferase 1 (GFAT1) of Drosophila melanogaster in a UDP-N-acetylglucosamine and cAMP-dependent manner. *Biochem J* 360: 401-412, 2001.

89. **Green DW, Murray HN, Sleph PG, Wang FL, Baird AJ, Rogers WL, and Grover GJ.** Preconditioning in rat hearts is independent of mitochondrial F1F0 ATPase inhibition. *Am J Physiol* 274: H90-97, 1998.

90. **Griffith LS, Mathes M, and Schmitz B.** Beta-amyloid precursor protein is modified with O-linked N-acetylglucosamine. *J Neurosci Res* 41: 270-278, 1995.

91. **Griffith LS and Schmitz B.** O-linked N-acetylglucosamine is upregulated in Alzheimer brains. *Biochemical and Biophysical Research Communications* 213: 424-431, 1995.

92. **Griffiths E, Halestrap, AP.** Mitochondrial non-specific pores remain closed during cardiac ischaemia, but open upon reperfusion. *The Biochemical Journal* 307.1: 93-98, 1995.

93. **Griffiths EJ and Halestrap AP.** Further evidence that cyclosporin A protects mitochondria from calcium overload by inhibiting a matrix peptidyl-prolyl cis-trans isomerase. Implications for the immunosuppressive and toxic effects of cyclosporin. *Biochem J* 274 (Pt 2): 611-614, 1991.

94. **Griffiths EJ, Ocampo CJ, Savage JS, Rutter GA, Hansford RG, Stern MD, and Silverman HS.** Mitochondrial calcium transporting pathways during hypoxia and reoxygenation in single rat cardiomyocytes. *Cardiovasc Res* 39: 423-433, 1998.

95. **Griffiths EJ, Ocampo CJ, Savage JS, Stern MD, and Silverman HS.** Protective effects of low and high doses of cyclosporin A against reoxygenation injury in isolated rat cardiomyocytes are associated with differential effects on mitochondrial calcium levels. *Cell Calcium* 27: 87-95, 2000.

96. **Gross BJ, Kraybill BC, and Walker S.** Discovery of O-GlcNAc transferase inhibitors. *Journal of the American Chemical Society* 127: 14588-14589, 2005.

97. **Grover GJ, Atwal KS, Sleph PG, Wang FL, Monshizadegan H, Monticello T, and Green DW.** Excessive ATP hydrolysis in ischemic myocardium by mitochondrial F1F0-ATPase: effect of selective pharmacological inhibition of mitochondrial ATPase hydrolase activity. *Am J Physiol Heart Circ Physiol* 287: H1747-1755, 2004.

98. **Gurcel C, Vercoutter-Edouart AS, Fonbonne C, Mortuaire M, Salvador A, Michalski JC, and Lemoine J.** Identification of new O-GlcNAc modified proteins using a click-chemistry-based tagging. *Anal Bioanal Chem* 390: 2089-2097, 2008.

99. **Guth BD, Wisneski JA, Neese RA, White FC, Heusch G, Mazer CD, and Gertz EW.** Myocardial lactate release during ischemia in swine. Relation to regional blood flow. *Circulation* 81: 1948-1958, 1990.

100. **Guzy RD, Hoyos B, Robin E, Chen H, Liu L, Mansfield KD, Simon MC, Hammerling U, and Schumacker PT.** Mitochondrial complex III is required for hypoxia-induced ROS production and cellular oxygen sensing. *Cell Metab* 1: 401-408, 2005.

101. **Halestrap AP.** Calcium, mitochondria and reperfusion injury: a pore way to die. *Biochem Soc Trans* 34: 232-237, 2006.

102. **Halestrap AP.** Mitochondrial permeability: dual role for the ADP/ATP translocator? *Nature* 430: 1 p following 983, 2004.

103. **Halestrap AP.** The regulation of the oxidation of fatty acids and other substrates in rat heart mitochondria by changes in the matrix volume induced by osmotic strength, valinomycin and Ca2+. *The Biochemical Journal* 244.1: 159-164, 1987.

104. **Halestrap AP, Clarke SJ, and Javadov SA.** Mitochondrial permeability transition pore opening during myocardial reperfusion--a target for cardioprotection. *Cardiovasc Res* 61: 372-385, 2004.

105. **Halestrap AP, Connern CP, Griffiths EJ, and Kerr PM.** Cyclosporin A binding to mitochondrial cyclophilin inhibits the permeability transition pore and protects hearts from ischaemia/reperfusion injury. *Mol Cell Biochem* 174: 167-172, 1997.

106. **Halestrap AP and Davidson AM.** Inhibition of Ca2(+)-induced large-amplitude swelling of liver and heart mitochondria by cyclosporin is probably caused by the inhibitor binding to mitochondrial-matrix peptidyl-prolyl cis-trans isomerase and preventing it interacting with the adenine nucleotide translocase. *Biochem J* 268: 153-160, 1990.

107. **Halestrap AP, Kerr PM, Javadov S, and Woodfield KY.** Elucidating the molecular mechanism of the permeability transition pore and its role in reperfusion injury of the heart. *Biochimica et Biophysica Acta* 1366: 79-94, 1998.

108. **Halestrap AP, McStay GP, and Clarke SJ.** The permeability transition pore complex: another view. *Biochimie* 84: 153-166, 2002.

109. **Hall JL, Matter CM, Wang X, and Gibbons GH.** Hyperglycemia inhibits vascular smooth muscle cell apoptosis through a protein kinase C-dependent pathway. *Circ Res* 87: 574-580, 2000.

110. **Haltiwanger RS, Blomberg MA, and Hart GW.** Glycosylation of nuclear and cytoplasmic proteins. Purification and characterization of a uridine diphospho-N-acetylglucosamine:polypeptide beta-N-acetylglucosaminyltransferase. *J Biol Chem* 267: 9005-9013, 1992.

111. **Haltiwanger RS GK, Philipsberg GA.** Modulation of O-Linked N-Acetylglucosamine Levels on Nuclear and Cytoplasmic Proteins in Vivo Using the Peptide O-GlcNAc-beta -N-acetylglucosaminidase Inhibitor O-(2-Acetamido-2-deoxy-Dglucopyranosylidene)amino-N-phenylcarbamate. *J Biol Chem* 273: 3611-3617, 1998.

112. **Haltiwanger RS, Holt GD, and Hart GW.** Enzymatic addition of O-GlcNAc to nuclear and cytoplasmic proteins. Identification of a uridine diphospho-N-acetylglucosamine:peptide beta-N-acetylglucosaminyltransferase. *J Biol Chem* 265: 2563-2568, 1990.

113. **Han I and Kudlow JE.** Reduced O glycosylation of Sp1 is associated with increased proteasome susceptibility. *Molecular and Cellular Biology* 17: 2550-2558, 1997.

114. **Hanover JA, Cohen CK, Willingham MC, and Park MK.** O-linked N-acetylglucosamine is attached to proteins of the nuclear pore. Evidence for cytoplasmic and nucleoplasmic glycoproteins. *J Biol Chem* 262: 9887-9894, 1987.

115. **Hanover JA, Yu S, Lubas WB, Shin S-H, Ragano-Caracciola M, Kochran J, and Love DC.** Mitochondrial and nucleocytoplasmic isoforms of O-linked GlcNAc transferase encoded by a single mammalian gene. *Archives of Biochemistry and Biophysics* 409: 287-297, 2003.

116. **Hardy J and Selkoe DJ.** The amyloid hypothesis of Alzheimer's disease: progress and problems on the road to therapeutics. *Science* 297: 353-356, 2002.

117. **Harpster MH, Bandyopadhyay S, Thomas DP, Ivanov PS, Keele JA, Pineguina N, Gao B, Amarendran V, Gomelsky M, McCormick RJ, and Stayton MM.** Earliest changes in the left ventricular transcriptome postmyocardial infarction. *Mamm Genome* 17: 701-715, 2006.

118. **Hart GW.** Glycosylation. *Curr Opin Cell Biol* 4: 1017-1023, 1992.

119. **Hart GW, Greis KD, Dong LY, Blomberg MA, Chou TY, Jiang MS, Roquemore EP, Snow DM, Kreppel LK, Cole RN, and et al.** O-linked N-acetylglucosamine: the "yin-yang" of Ser/Thr phosphorylation? Nuclear and cytoplasmic glycosylation. *Advances in Experimental Medicine and Biology* 376: 115-123, 1995.

120. **Hart GW, Kreppel LK, Comer FI, Arnold CS, Snow DM, Ye Z, Cheng X, DellaManna D, Caine DS, Earles BJ, Akimoto Y, Cole RN, and Hayes BK.** O-GlcNAcylation of key nuclear and cytoskeletal proteins: reciprocity with O-phosphorylation and putative roles in protein multimerization. *Glycobiology* 6: 711-716, 1996.

121. **Hartweck LM, Scott CL, and Olszewski NE.** Two O-linked N-acetylglucosamine transferase genes of Arabidopsis thaliana L. Heynh. have overlapping functions necessary for gamete and seed development. *Genetics* 161: 1279-1291, 2002.

122. **Hausenloy DJ, Duchen MR, and Yellon DM.** Inhibiting mitochondrial permeability transition pore opening at reperfusion protects against ischaemia-reperfusion injury. *Cardiovasc Res* 60: 617-625, 2003.

123. **Hausenloy DJ, Maddock HL, Baxter GF, and Yellon DM.** Inhibiting mitochondrial permeability transition pore opening: a new paradigm for myocardial preconditioning? *Cardiovasc Res* 55: 534-543, 2002.

124. **Hausenloy DJ, Tsang A, and Yellon DM.** The reperfusion injury salvage kinase pathway: a common target for both ischemic preconditioning and postconditioning. *Trends Cardiovasc Med* 15: 69-75, 2005.

125. **Hausenloy DJ and Yellon DM.** The mitochondrial permeability transition pore: its fundamental role in mediating cell death during ischaemia and reperfusion. *Journal of molecular and cellular cardiology* 35: 339-341, 2003.

126. **Hausenloy DJ and Yellon DM.** New directions for protecting the heart against ischaemia-reperfusion injury: targeting the Reperfusion Injury Salvage Kinase (RISK)-pathway. *Cardiovasc Res* 61: 448-460, 2004.

127. **Hausenloy DJ and Yellon DM.** Reperfusion injury salvage kinase signalling: taking a RISK for cardioprotection. *Heart Fail Rev* 12: 217-234, 2007.

128. **He L and Lemasters JJ.** Regulated and unregulated mitochondrial permeability transition pores: a new paradigm of pore structure and function? *FEBS letters* 512: 1-7, 2002.

129. **Heart E, Choi WS, and Sung CK.** Glucosamine-induced insulin resistance in 3T3-L1 adipocytes. *Am J Physiol Endocrinol Metab* 278: E103-112, 2000.

130. **Heckel D, Comtesse N, Brass N, Blin N, Zang KD, and Meese E.** Novel immunogenic antigen homologous to hyaluronidase in meningioma. *Hum Mol Genet* 7: 1859-1872, 1998.

131. **Heese-Peck A, Cole RN, Borkhsenious ON, Hart GW, and Raikhel NV.** Plant nuclear pore complex proteins are modified by novel oligosaccharides with terminal N-acetylglucosamine. *Plant Cell* 7: 1459-1471, 1995.

132. **Heese-Peck A and Raikhel NV.** A glycoprotein modified with terminal N-acetylglucosamine and localized at the nuclear rim shows sequence similarity to aldose-1-epimerases. *Plant Cell* 10: 599-612, 1998.

133. **Holt GD, Snow CM, Senior A, Haltiwanger RS, Gerace L, and Hart GW.** Nuclear pore complex glycoproteins contain cytoplasmically disposed O-linked N-acetylglucosamine. *J Cell Biol* 104: 1157-1164, 1987.

134. **Horsch M, Hoesch L, Vasella A, and Rast DM.** N-acetylglucosaminono-1,5-lactone oxime and the corresponding (phenylcarbamoyl)oxime. Novel and potent inhibitors of beta-N-acetylglucosaminidase. *Eur J Biochem* 197: 815-818, 1991.

135. **Hu Y, Belke D, Suarez J, Swanson E, Clark R, Hoshijima M, Dillmann WH.** Adenovirus-mediated overexpression of O-GlcNAcase improves contractile function in the diabetic heart. *Circulation Research* 96.9: 1006-1013, 2005.

136. **Hu Y, Riesland L, Paterson AJ, and Kudlow JE.** Phosphorylation of mouse glutamine-fructose-6-phosphate amidotransferase 2 (GFAT2) by cAMP-dependent protein kinase increases the enzyme activity. *J Biol Chem* 279: 29988-29993, 2004.

137. **Hu Y, Suarez J, Fricovsky E, Wang H, Scott BT, Trauger SA, Han W, Oyeleye MO, and Dillmann WH.** Increased enzymatic O-GlcNAcylation of mitochondrial proteins impairs mitochondrial function in cardiac myocytes exposed to high glucose. *J Biol Chem* 284: 547-555, 2009.

138. **Hu Y, Suarez J, Fricovsky E, Wang H, Scott BT, Trauger SA, Han W, Oyeleye MO, and Dillmann WH.** Increased enzymatic O-GlcNAcylation of mitochondrial proteins impairs mitochondrial function in cardiac myocytes exposed to high glucose. *J Biol Chem*, 2008.

139. **Hunt KJ, Lehman DM, Arya R, Fowler S, Leach RJ, Goring HH, Almasy L, Blangero J, Dyer TD, Duggirala R, and Stern MP.** Genome-wide linkage analyses of type 2 diabetes in Mexican Americans: the San Antonio Family Diabetes/Gallbladder Study. *Diabetes* 54: 2655-2662, 2005.

140. **Hunter DR and Haworth RA.** The Ca2+-induced membrane transition in mitochondria. I. The protective mechanisms. *Archives of Biochemistry and Biophysics* 195: 453-459, 1979.

141. **Hunter DR and Haworth RA.** The Ca2+-induced membrane transition in mitochondria. III. Transitional Ca2+ release. *Archives of Biochemistry and Biophysics* 195: 468-477, 1979.

142. **Ide T, Tsutsui H, Kinugawa S, Utsumi H, Kang D, Hattori N, Uchida K, Arimura K, Egashira K, and Takeshita A.** Mitochondrial electron transport complex I is a potential source of oxygen free radicals in the failing myocardium. *Circ Res* 85: 357-363, 1999.

143. **Imahashi K, Pott C, Goldhaber JI, Steenbergen C, Philipson KD, and Murphy E.** Cardiac-specific ablation of the Na+-Ca2+ exchanger confers protection against ischemia/reperfusion injury. *Circ Res* 97: 916-921, 2005.

144. **Iyer SP, Akimoto Y, and Hart GW.** Identification and cloning of a novel family of coiled-coil domain proteins that interact with O-GlcNAc transferase. *J Biol Chem* 278: 5399-5409, 2003.

145. **Iyer SP and Hart GW.** Roles of the tetratricopeptide repeat domain in O-GlcNAc transferase targeting and protein substrate specificity. *J Biol Chem* 278: 24608-24616, 2003.

146. **Jackson SP and Tjian R.** O-glycosylation of eukaryotic transcription factors: implications for mechanisms of transcriptional regulation. *Cell* 55: 125-133, 1988.

147. **Janier MF, Vanoverschelde JL, and Bergmann SR.** Ischemic preconditioning stimulates anaerobic glycolysis in the isolated rabbit heart. *Am J Physiol* 267: H1353-1360, 1994.

148. **Javadov SA, Clarke S, Das M, Griffiths EJ, Lim KH, and Halestrap AP.** Ischaemic preconditioning inhibits opening of mitochondrial permeability transition pores in the reperfused rat heart. *J Physiol* 549: 513-524, 2003.

149. **Jennings RB, Reimer KA, and Steenbergen C.** Effect of inhibition of the mitochondrial ATPase on net myocardial ATP in total ischemia. *Journal of molecular and cellular cardiology* 23: 1383-1395, 1991.

150. **Jensen ON, Wilm M, Shevchenko A, and Mann M.** Sample preparation methods for mass spectrometric peptide mapping directly from 2-DE gels. *Methods Mol Biol* 112: 513-530, 1999.

151. **Jinek M, Rehwinkel J, Lazarus BD, Izaurralde E, Hanover JA, and Conti E.** The superhelical TPR-repeat domain of O-linked GlcNAc transferase exhibits structural similarities to importin alpha. *Nat Struct Mol Biol* 11: 1001-1007, 2004.

152. **Jones SP and Bolli R.** The ubiquitous role of nitric oxide in cardioprotection. *Journal of Molecular and Cellular Cardiology* 40: 16-23, 2006.

153. **Jones SP, Girod WG, Palazzo AJ, Granger DN, Grisham MB, Jourd'Heuil D, Huang PL, and Lefer DJ.** Myocardial ischemia-reperfusion injury is exacerbated in absence of endothelial cell nitric oxide synthase. *Am J Physiol Heart Circ Physiol* 276: H1567-1573, 1999.

154. **Jones SP, Greer JJ, van Haperen R, Duncker DJ, de Crom R, and Lefer DJ.** Endothelial nitric oxide synthase overexpression attenuates congestive heart failure in mice. *Proceedings of the National Academy of Sciences of the United States of America* 100: 4891-4896, 2003.

155. **Jones SP, Greer JJM, Kakkar AK, Ware PD, Turnage RH, Hicks M, van Haperen R, de Crom R, Kawashima S, Yokoyama M, and Lefer DJ.** Endothelial nitric oxide synthase overexpression attenuates myocardial reperfusion injury. *Am J Physiol Cell Physiol* 286: H276-282, 2004.

156. **Jones SP, Greer JJM, Ware PD, Yang J, Walsh K, and Lefer DJ.** Deficiency of iNOS does not attenuate severe congestive heart failure in mice. *Am J Physiol Heart Circ Physiol* 288: H365-370, 2005.

157. **Jones SP, Hoffmeyer MR, Sharp BR, Ho YS, and Lefer DJ.** Role of intracellular antioxidant enzymes after in vivo myocardial ischemia and reperfusion. *Am J Physiol Heart Circ Physiol* 284: H277-282, 2003.

158. **Jones SP, Teshima Y, Akao M, and Marban E.** Simvastatin Attenuates Oxidant-Induced Mitochondrial Dysfunction in Cardiac Myocytes. *Circ Res* 93: 697-699, 2003.

159. **Kadenbach B.** Intrinsic and extrinsic uncoupling of oxidative phosphorylation. *Biochimica et Biophysica Acta* 1604: 77-94, 2003.

160. **Kamemura K and Hart GW.** Dynamic interplay between O-glycosylation and O-phosphorylation of nucleocytoplasmic proteins: a new paradigm for metabolic control of signal transduction and transcription. *Progress in nucleic acid research and molecular biology* 73: 107-136, 2003.

161. **Kang J, Lemaire HG, Unterbeck A, Salbaum JM, Masters CL, Grzeschik KH, Multhaup G, Beyreuther K, and Muller-Hill B.** The precursor of Alzheimer's disease amyloid A4 protein resembles a cell-surface receptor. *Nature* 325: 733-736, 1987.

162. **Karmazyn M.** Amiloride enhances postischemic ventricular recovery: possible role of Na+-H+ exchange. *Am J Physiol* 255: H608-615, 1988.

163. **Kaufman RJ.** Stress signaling from the lumen of the endoplasmic reticulum: coordination of gene transcriptional and translational controls. *Genes Dev* 13: 1211-1233, 1999.

164. **Kelly BD HS HK, et al** Cell Type-specific Regulation of Angiogenic Growth Factor Gene Expression and Induction of Angiogenesis in Nonischemic Tissue by a Constitutively Active form of Hypoxia-inducible Factor 1. *Circ Res* 93: 1074-1081, 2003.

165. **Kelly WG, Dahmus ME, and Hart GW.** RNA polymerase II is a glycoprotein. Modification of the COOH-terminal domain by O-GlcNAc. *J Biol Chem* 268: 10416-10424, 1993.

166. **Kevin LG, Camara AK, Riess ML, Novalija E, and Stowe DF.** Ischemic preconditioning alters real-time measure of O2 radicals in intact hearts with ischemia and reperfusion. *Am J Physiol Heart Circ Physiol* 284: H566-574, 2003.

167. **Kiang JG and Tsokos GC.** Heat shock protein 70 kDa: molecular biology, biochemistry, and physiology. *Pharmacol Ther* 80: 183-201, 1998.

168. **Kilgore KS, Friedrichs GS, Johnson CR, Schasteen CS, Riley DP, Weiss RH, Ryan U, and Lucchesi BR.** Protective effects of the SOD-mimetic SC-52608 against ischemia/reperfusion damage in the rabbit isolated heart. *Journal of Molelcular and Cellullar Cardiology* 26: 995-1006, 1994.

169. **Kokoszka JE, Waymire KG, Levy SE, Sligh JE, Cai J, Jones DP, MacGregor GR, and Wallace DC.** The ADP/ATP translocator is not essential for the mitochondrial permeability transition pore. *Nature* 427: 461-465, 2004.

170. **Konrad RJ, Zhang F, Hale JE, Knierman MD, Becker GW, and Kudlow JE.** Alloxan is an inhibitor of the enzyme O-linked N-acetylglucosamine transferase. *Biochemical and Biophysical Research Communications* 293: 207-212, 2002.

171. **Krauskopf A, Eriksson O, Craigen WJ, Forte MA, and Bernardi P.** Properties of the permeability transition in VDAC1(-/-) mitochondria. *Biochimica et Biophysica Acta* 1757: 590-595, 2006.

172. **Kregel KC.** Heat shock proteins: modifying factors in physiological stress responses and acquired thermotolerance. *J Appl Physiol* 92: 2177-2186, 2002.

173. **Kreppel LK, Blomberg MA, and Hart GW.** Dynamic Glycosylation of Nuclear and Cytosolic Proteins. Cloning and characterization of a unique O-GlcNAc transferase with multiple tetratricopeptide repeat. *J Biol Chem* 272: 9308-9315, 1997.

174. **Kreppel LK and Hart GW.** Regulation of a Cytosolic and Nuclear O-GlcNAc Transferase. Role of the tetratricopeptide repeats. *J Biol Chem* 274: 32015-32022, 1999.

175. **Kroemer G, Dallaporta B, and Resche-Rigon M.** The mitochondrial death/life regulator in apoptosis and necrosis. *Annu Rev Physiol* 60: 619-642, 1998.

176. **Ku NO and Omary MB.** Expression, glycosylation, and phosphorylation of human keratins 8 and 18 in insect cells. *Exp Cell Res* 211: 24-35, 1994.

177. **Laderoute KR and Webster KA.** Hypoxia/reoxygenation stimulates Jun kinase activity through redox signaling in cardiac myocytes. *Circ Res* 80: 336-344, 1997.

178. **Lamarre-Vincent N and Hsieh-Wilson LC.** Dynamic glycosylation of the transcription factor CREB: a potential role in gene regulation. *Journal of the American Chemical Society* 125: 6612-6613, 2003.

179. **Lapidus RG and Sokolove PM.** Spermine inhibition of the permeability transition of isolated rat liver mitochondria: an investigation of mechanism. *Archives of Biochemistry and Biophysics* 306: 246-253, 1993.

180. **Le Quoc K and Le Quoc D.** Involvement of the ADP/ATP carrier in calcium-induced perturbations of the mitochondrial inner membrane permeability: importance of the orientation of the nucleotide binding site. *Archives of Biochemistry and Biophysics* 265: 249-257, 1988.

181. **Lee TN, Alborn WE, Knierman MD, and Konrad RJ.** Alloxan is an inhibitor of O-GlcNAc-selective N-acetyl-beta-D-glucosaminidase. *Biochemical and Biophysical Research Communications* 350: 1038-1043, 2006.

182. **Lefebvre T, Ferreira S, Dupont-Wallois L, Bussiere T, Dupire MJ, Delacourte A, Michalski JC, and Caillet-Boudin ML.** Evidence of a balance between

phosphorylation and O-GlcNAc glycosylation of Tau proteins--a role in nuclear localization. *Biochimica et Biophysica Acta* 1619: 167-176, 2003.

183. **Lefer DJ and Granger DN.** Oxidative stress and cardiac disease. *Am J Med* 109: 315-323, 2000.

184. **Lehman DM, Fu DJ, Freeman AB, Hunt KJ, Leach RJ, Johnson-Pais T, Hamlington J, Dyer TD, Arya R, Abboud H, Goring HH, Duggirala R, Blangero J, Konrad RJ, and Stern MP.** A single nucleotide polymorphism in MGEA5 encoding O-GlcNAc-selective N-acetyl-beta-D glucosaminidase is associated with type 2 diabetes in Mexican Americans. *Diabetes* 54: 1214-1221, 2005.

185. **Leroy E, Boyer R, Auburger G, Leube B, Ulm G, Mezey E, Harta G, Brownstein MJ, Jonnalagada S, Chernova T, Dehejia A, Lavedan C, Gasser T, Steinbach PJ, Wilkinson KD, and Polymeropoulos MH.** The ubiquitin pathway in Parkinson's disease. *Nature* 395: 451-452, 1998.

186. **Lesnefsky EJ, Chen Q, Moghaddas S, Hassan MO, Tandler B, and Hoppel CL.** Blockade of electron transport during ischemia protects cardiac mitochondria. *J Biol Chem* 279: 47961-47967, 2004.

187. **Leyssens A, Nowicky AV, Patterson L, Crompton M, and Duchen MR.** The relationship between mitochondrial state, ATP hydrolysis, [Mg2+]i and [Ca2+]i studied in isolated rat cardiomyocytes. *J Physiol* 496 (Pt 1): 111-128, 1996.

188. **Lin Z, Weinberg JM, Malhotra R, Merritt SE, Holzman LB, and Brosius FC, 3rd.** GLUT-1 reduces hypoxia-induced apoptosis and JNK pathway activation. *Am J Physiol Endocrinol Metab* 278: E958-966, 2000.

189. **Liu J, Marchase RB, and Chatham JC.** Glutamine-induced protection of isolated rat heart from ischemia/reperfusion injury is mediated via the hexosamine biosynthesis pathway and increased protein O-GlcNAc levels. *J Mol and Cell Cardiol* 42: 177-185, 2007.

190. **Liu J, Marchase RB, and Chatham JC.** Increased O-GlcNAc levels during reperfusion leads to improved functional recovery and reduced calpain-proteolysis. *Am J Physiol Heart Circ Physiol*: 00285.02007, 2007.

191. **Liu J, Pang Y, Chang T, Bounelis P, Chatham JC, and Marchase RB.** Increased hexosamine biosynthesis and protein O-GlcNAc levels associated with myocardial protection against calcium paradox and ischemia. *Journal of molecular and cellular cardiology* 40: 303-312, 2006.

192. **Liu K, Paterson AJ, Zhang F, McAndrew J, Fukuchi K, Wyss JM, Peng L, Hu Y, and Kudlow JE.** Accumulation of protein O-GlcNAc modification inhibits proteasomes in the brain and coincides with neuronal apoptosis in brain areas with high O-GlcNAc metabolism. *J Neurochem* 89: 1044-1055, 2004.

193. **Liu W, Schoenkerman A, and Lowe WL, Jr.** Activation of members of the mitogen-activated protein kinase family by glucose in endothelial cells. *Am J Physiol Endocrinol Metab* 279: E782-790, 2000.

194. **Livak KJ and Schmittgen TD.** Analysis of relative gene expression data using real-time quantitative PCR and the 2(-Delta Delta C(T)) Method. *Methods* 25: 402-408, 2001.

195. **Lodish HF and Kong N.** Perturbation of cellular calcium blocks exit of secretory proteins from the rough endoplasmic reticulum. *J Biol Chem* 265: 10893-10899, 1990.

196. **Lopaschuk GD, Collins-Nakai RL, and Itoi T.** Developmental changes in energy substrate use by the heart. *Cardiovasc Res* 26: 1172-1180, 1992.

197. **Lorenz JN and Robbins J.** Measurement of intraventricular pressure and cardiac performance in the intact closed-chest anesthetized mouse. *Am J Physiol* 272: H1137-1146, 1997.

198. **Love DC, Kochran J, Cathey RL, Shin S-H, and Hanover JA.** Mitochondrial and nucleocytoplasmic targeting of O-linked GlcNAc transferase. *J Cell Sci* 116: 647-654, 2003.

199. **Lubas WA and Hanover JA.** Functional expression of O-linked GlcNAc transferase. Domain structure and substrate specificity. *J Biol Chem* 275: 10983-10988, 2000.

200. **Macauley MS, Whitworth GE, Debowski AW, Chin D, and Vocadlo DJ.** O-GlcNAcase uses substrate-assisted catalysis: kinetic analysis and development of highly selective mechanism-inspired inhibitors. *J Biol Chem* 280: 25313-25322, 2005.

201. **Malhotra R and Brosius FC, 3rd.** Glucose uptake and glycolysis reduce hypoxia-induced apoptosis in cultured neonatal rat cardiac myocytes. *J Biol Chem* 274: 12567-12575, 1999.

202. **Maraganore DM, Farrer MJ, Hardy JA, Lincoln SJ, McDonnell SK, and Rocca WA.** Case-control study of the ubiquitin carboxy-terminal hydrolase L1 gene in Parkinson's disease. *Neurology* 53: 1858-1860, 1999.

203. **Marshall S, Bacote V, and Traxinger RR.** Discovery of a metabolic pathway mediating glucose-induced desensitization of the glucose transport system. Role of hexosamine biosynthesis in the induction of insulin resistance. *J Biol Chem* 266: 4706-4712, 1991.

204. **Marshall S, Nadeau O, and Yamasaki K.** Dynamic actions of glucose and glucosamine on hexosamine biosynthesis in isolated adipocytes: differential effects on glucosamine 6-phosphate, UDP-N-acetylglucosamine, and ATP levels. *J Biol Chem* 279: 35313-35319, 2004.

205. **Marzo I, Brenner C, Zamzami N, Susin SA, Beutner G, Brdiczka D, Remy R, Xie ZH, Reed JC, and Kroemer G.** The permeability transition pore complex: a target for apoptosis regulation by caspases and bcl-2-related proteins. *J Exp Med* 187: 1261-1271, 1998.

206. **Mathupala SP, Ko YH, and Pedersen PL.** Hexokinase II: cancer's double-edged sword acting as both facilitator and gatekeeper of malignancy when bound to mitochondria. *Oncogene* 25: 4777-4786, 2006.

207. **Matsumoto-Ida M, Akao M, Takeda T, Kato M, and Kita T.** Real-time 2-photon imaging of mitochondrial function in perfused rat hearts subjected to ischemia/reperfusion. *Circulation* 114: 1497-1503, 2006.

208. **McClain DA.** Hexosamines as mediators of nutrient sensing and regulation in diabetes. *J Diabetes Complications* 16: 72-80, 2002.

209. **McClain DA and Crook ED.** Hexosamines and insulin resistance. *Diabetes* 45: 1003-1009, 1996.

210. **McClain DA, Lubas WA, Cooksey RC, Hazel M, Parker GJ, Love DC, and Hanover JA.** Altered glycan-dependent signaling induces insulin resistance and hyperleptinemia. *Proceedings of the National Academy of Sciences of the United States of America* 99: 10695-10699, 2002.

211. **McCord JM.** Free radicals and myocardial ischemia: overview and outlook. *Free Radic Biol Med* 4: 9-14, 1988.

212. **McFalls EO, Murad B, Liow JS, Gannon MC, Haspel HC, Lange A, Marx D, Sikora J, and Ward HB.** Glucose uptake and glycogen levels are increased in pig heart after repetitive ischemia. *Am J Physiol Heart Circ Physiol* 282: H205-211, 2002.

213. **McGuinness O, Yafei N, Costi A, and Crompton M.** The presence of two classes of high-affinity cyclosporin A binding sites in mitochondria. Evidence that the minor component is involved in the opening of an inner-membrane Ca(2+)-dependent pore. *Eur J Biochem* 194: 671-679, 1990.

214. **Medina L, Grove K, and Haltiwanger RS.** SV40 large T antigen is modified with O-linked N-acetylglucosamine but not with other forms of glycosylation. *Glycobiology* 8: 383-391, 1998.

215. **Milewski S.** Glucosamine-6-phosphate synthase--the multi-facets enzyme. *Biochimica et Biophysica Acta* 1597: 173-192, 2002.

216. **Moley KH and Mueckler MM.** Glucose transport and apoptosis. *Apoptosis* 5: 99-105, 2000.

217. **Montessuit C, Papageorgiou I, Remondino-Muller A, Tardy I, and Lerch R.** Post-ischemic stimulation of 2-deoxyglucose uptake in rat myocardium: role of translocation of Glut-4. *Journal of molecular and cellular cardiology* 30: 393-403, 1998.

218. **Murata M, Akao M, O'Rourke B, and Marban E.** Mitochondrial ATP-sensitive potassium channels attenuate matrix Ca(2+) overload during simulated ischemia and reperfusion: possible mechanism of cardioprotection. *Circ Res* 89: 891-898, 2001.

219. **Murphy E, Perlman M, London RE, and Steenbergen C.** Amiloride delays the ischemia-induced rise in cytosolic free calcium. *Circ Res* 68: 1250-1258, 1991.

220. **Murry CE, Jennings RB, and Reimer KA.** Preconditioning with ischemia: a delay of lethal cell injury in ischemic myocardium. *Circulation* 74: 1124-1136, 1986.

221. **Murry CE, Richard VJ, Reimer KA, and Jennings RB.** Ischemic preconditioning slows energy metabolism and delays ultrastructural damage during a sustained ischemic episode. *Circ Res* 66: 913-931, 1990.

222. **Nagy T, Champattanachai V, Marchase RB, and Chatham JC.** Glucosamine inhibits angiotensin II-induced cytoplasmic Ca2+ elevation in neonatal cardiomyocytes via protein-associated O-linked N-acetylglucosamine. *Am J Physiol Cell Physiol* 290: C57-65, 2006.

223. **Nakagawa T, Shimizu S, Watanabe T, Yamaguchi O, Otsu K, Yamagata H, Inohara H, Kubo T, and Tsujimoto Y.** Cyclophilin D-dependent mitochondrial permeability transition regulates some necrotic but not apoptotic cell death. *Nature* 434: 652-658, 2005.

224. **Namekata I, Shimada H, Kawanishi T, Tanaka H, and Shigenobu K.** Reduction by SEA0400 of myocardial ischemia-induced cytoplasmic and mitochondrial Ca2+ overload. *Eur J Pharmacol* 543: 108-115, 2006.

225. **Nanashima N, Asano J, Hayakari M, Nakamura T, Nakano H, Yamada T, Shimizu T, Akita M, Fan Y, and Tsuchida S.** Nuclear localization of STAT5A modified with O-linked N-acetylglucosamine and early involution in the mammary gland of Hirosaki hairless rat. *J Biol Chem* 280: 43010-43016, 2005.

226. **Nandi A, Sprung R, Barma DK, Zhao Y, Kim SC, Falck JR, and Zhao Y.** Global identification of O-GlcNAc-modified proteins. *Analytical chemistry* 78: 452-458, 2006.

227. **Nazareth W, Yafei N, and Crompton M.** Inhibition of anoxia-induced injury in heart myocytes by cyclosporin A. *Journal of molecular and cellular cardiology* 23: 1351-1354, 1991.

228. **Ngoh GA and Jones SP.** New insights into metabolic signaling and cell survival: the role of beta-O-linkage of N-acetylglucosamine. *J Pharmacol Exp Ther* 327: 602-609, 2008.

229. **Nichols CG and Lederer WJ.** The role of ATP in energy-deprivation contractures in unloaded rat ventricular myocytes. *Can J Physiol Pharmacol* 68: 183-194, 1990.

230. **Nickson P, Toth A, and Erhardt P.** PUMA is critical for neonatal cardiomyocyte apoptosis induced by endoplasmic reticulum stress. *Cardiovasc Res* 73: 48-56, 2007.

231. **Nicolli A, Basso E, Petronilli V, Wenger RM, and Bernardi P.** Interactions of cyclophilin with the mitochondrial inner membrane and regulation of the permeability transition pore, and cyclosporin A-sensitive channel. *J Biol Chem* 271: 2185-2192, 1996.

232. **Nolte D and Muller U.** Human O-GlcNAc transferase (OGT): genomic structure, analysis of splice variants, fine mapping in Xq13.1. *Mamm Genome* 13: 62-64, 2002.

233. **Nunan J, Shearman MS, Checler F, Cappai R, Evin G, Beyreuther K, Masters CL, and Small DH.** The C-terminal fragment of the Alzheimer's disease amyloid protein precursor is degraded by a proteasome-dependent mechanism distinct from gamma-secretase. *Eur J Biochem* 268: 5329-5336, 2001.

234. **O'Donnell N, Zachara NE, Hart GW, and Marth JD.** Ogt-dependent X-chromosome-linked protein glycosylation is a requisite modification in somatic cell function and embryo viability. *Molecular and Cellular Biology* 24: 1680-1690, 2004.

235. **Opie LH.** Metabolic response during impending myocardial infarction. I. Relevance of studies of glucose and fatty acid metabolism in animals. *Circulation* 45: 483-490, 1972.

236. **Owen P, Dennis S, and Opie LH.** Glucose flux rate regulates onset of ischemic contracture in globally underperfused rat hearts. *Circ Res* 66: 344-354, 1990.

237. **Pang Y, Hunton DL, Bounelis P, and Marchase RB.** Hyperglycemia inhibits capacitative calcium entry and hypertrophy in neonatal cardiomyocytes. *Diabetes* 51: 3461-3467, 2002.

238. **Pappin DJ, Hojrup P, and Bleasby AJ.** Rapid identification of proteins by peptide-mass fingerprinting. *Curr Biol* 3: 327-332, 1993.

239. **Park MK, D'Onofrio M, Willingham MC, and Hanover JA.** A monoclonal antibody against a family of nuclear pore proteins (nucleoporins): O-linked N-acetylglucosamine is part of the immunodeterminant. *Proc Natl Acad Sci U S A* 84: 6462-6466, 1987.

240. **Pasternak CA, Aiyathurai JE, Makinde V, Davies A, Baldwin SA, Konieczko EM, and Widnell CC.** Regulation of glucose uptake by stressed cells. *J Cell Physiol* 149: 324-331, 1991.

241. **Paterson AJ and Kudlow JE.** Regulation of glutamine:fructose-6-phosphate amidotransferase gene transcription by epidermal growth factor and glucose. *Endocrinology* 136: 2809-2816, 1995.

242. **Petronilli V, Cola C, Massari S, Colonna R, and Bernardi P.** Physiological effectors modify voltage sensing by the cyclosporin A-sensitive permeability transition pore of mitochondria. *J Biol Chem* 268: 21939-21945, 1993.

243. **Piot C, Croisille P, Staat P, Thibault H, Rioufol G, Mewton N, Elbelghiti R, Cung TT, Bonnefoy E, Angoulvant D, Macia C, Raczka F, Sportouch C, Gahide G, Finet G, Andre-Fouet X, Revel D, Kirkorian G, Monassier JP, Derumeaux G, and Ovize M.** Effect of cyclosporine on reperfusion injury in acute myocardial infarction. *N Engl J Med* 359: 473-481, 2008.

244. **Piper HM, Abdallah Y, and Schafer C.** The first minutes of reperfusion: a window of opportunity for cardioprotection. *Cardiovasc Res* 61: 365-371, 2004.

245. **Piper HM, Garcia-Dorado D, and Ovize M.** A fresh look at reperfusion injury. *Cardiovasc Res* 38: 291-300, 1998.

246. **Piper HM, Kasseckert S, and Abdallah Y.** The sarcoplasmic reticulum as the primary target of reperfusion protection. *Cardiovasc Res* 70: 170-173, 2006.

247. **Piper HM, Spahr R, and Probst I.** Glucose, lactate, and palmitate as substrates for the resting cardiac myocyte. *Basic Res Cardiol* 80 Suppl 2: 97-101, 1985.

248. **Piper HM, Spahr R, Schweickhardt C, Hunneman DH, and Probst I.** Importance of endogenous substrates for cultured adult rat cardiac myocytes. *Biochimica et Biophysica Acta* 883: 531-541, 1986.

249. **Qi X, Vallentin A, Churchill E, and Mochly-Rosen D.** deltaPKC participates in the endoplasmic reticulum stress-induced response in cultured cardiac myocytes and ischemic heart. *Journal of molecular and cellular cardiology* 43: 420-428, 2007.

250. **Rao RV, Castro-Obregon S, Frankowski H, Schuler M, Stoka V, del Rio G, Bredesen DE, and Ellerby HM.** Coupling endoplasmic reticulum stress to the cell death program. An Apaf-1-independent intrinsic pathway. *J Biol Chem* 277: 21836-21842, 2002.

251. **Renstrom B, Liedtke AJ, and Nellis SH.** Mechanisms of substrate preference for oxidative metabolism during early myocardial reperfusion. *Am J Physiol* 259: H317-323, 1990.

252. **Renstrom B, Nellis SH, and Liedtke AJ.** Metabolic oxidation of glucose during early myocardial reperfusion. *Circ Res* 65: 1094-1101, 1989.

253. **Rigobello MP, Barzon E, Marin O, and Bindoli A.** Effect of polycation peptides on mitochondrial permeability transition. *Biochemical and Biophysical Research Communications* 217: 144-149, 1995.

254. **Roos MD, Xie W, Su K, Clark JA, Yang X, Chin E, Paterson AJ, and Kudlow JE.** Streptozotocin, an analog of N-acetylglucosamine, blocks the removal of O-GlcNAc from intracellular proteins. *Proceedings of the Association of American Physicians* 110: 422-432, 1998.

255. **Roquemore EP, Chevrier MR, Cotter RJ, and Hart GW.** Dynamic O-GlcNAcylation of the small heat shock protein alpha B-crystallin. *Biochemistry* 35: 3578-3586, 1996.

256. **Roquemore EP, Dell A, Morris HR, Panico M, Reason AJ, Savoy LA, Wistow GJ, Zigler JS, Jr., Earles BJ, and Hart GW.** Vertebrate lens alpha-crystallins are modified by O-linked N-acetylglucosamine. *J Biol Chem* 267: 555-563, 1992.

257. **Ross SA, Chen X, Hope HR, Sun S, McMahon EG, Broschat K, and Gulve EA.** Development and comparison of two 3T3-L1 adipocyte models of insulin resistance: increased glucose flux vs glucosamine treatment. *Biochemical and Biophysical Research Communications* 273: 1033-1041, 2000.

258. **Rostovtseva T and Colombini M.** ATP flux is controlled by a voltage-gated channel from the mitochondrial outer membrane. *J Biol Chem* 271: 28006-28008, 1996.

259. **Ruck A, Dolder M, Wallimann T, and Brdiczka D.** Reconstituted adenine nucleotide translocase forms a channel for small molecules comparable to the mitochondrial permeability transition pore. *FEBS letters* 426: 97-101, 1998.

260. **Ruiz-Meana M, Garcia-Dorado D, Miro-Casas E, Abellan A, and Soler-Soler J.** Mitochondrial Ca2+ uptake during simulated ischemia does not affect permeability transition pore opening upon simulated reperfusion. *Cardiovasc Res* 71: 715-724, 2006.

261. **Rutkowski DT and Kaufman RJ.** A trip to the ER: coping with stress. *Trends in Cell Biology* 14: 20-28, 2004.

262. **Schafer C, Ladilov Y, Inserte J, Schafer M, Haffner S, Garcia-Dorado D, and Piper HM.** Role of the reverse mode of the Na+/Ca2+ exchanger in reoxygenation-induced cardiomyocyte injury. *Cardiovasc Res* 51: 241-250, 2001.

263. **Schein SJ, Colombini M, and Finkelstein A.** Reconstitution in planar lipid bilayers of a voltage-dependent anion-selective channel obtained from paramecium mitochondria. *J Membr Biol* 30: 99-120, 1976.

264. **Schinzel AC, Takeuchi O, Huang Z, Fisher JK, Zhou Z, Rubens J, Hetz C, Danial NN, Moskowitz MA, and Korsmeyer SJ.** Cyclophilin D is a component of mitochondrial permeability transition and mediates neuronal cell death after focal cerebral ischemia. *Proceedings of the National Academy of Sciences of the United States of America* 102: 12005-12010, 2005.

265. **Schlattner U, Dolder M, Wallimann T, and Tokarska-Schlattner M.** Mitochondrial creatine kinase and mitochondrial outer membrane porin show a direct interaction that is modulated by calcium. *J Biol Chem* 276: 48027-48030, 2001.

266. **Schwaiger M, Neese RA, Araujo L, Wyns W, Wisneski JA, Sochor H, Swank S, Kulber D, Selin C, Phelps M, and et al.** Sustained nonoxidative glucose utilization and depletion of glycogen in reperfused canine myocardium. *J Am Coll Cardiol* 13: 745-754, 1989.

267. **Scorrano L, Nicolli A, Basso E, Petronilli V, and Bernardi P.** Two modes of activation of the permeability transition pore: the role of mitochondrial cyclophilin. *Mol Cell Biochem* 174: 181-184, 1997.

268. **Shafi R, Iyer SPN, Ellies LG, O'Donnell N, Marek KW, Chui D, Hart GW, and Marth JD.** The O-GlcNAc transferase gene resides on the X chromosome and is essential for embryonic stem cell viability and mouse ontogeny. *PNAS* 97: 5735-5739, 2000.

269. **Shimizu S, Matsuoka Y, Shinohara Y, Yoneda Y, and Tsujimoto Y.** Essential role of voltage-dependent anion channel in various forms of apoptosis in mammalian cells. *J Cell Biol* 152: 237-250, 2001.

270. **Shimizu S, Narita M, and Tsujimoto Y.** Bcl-2 family proteins regulate the release of apoptogenic cytochrome c by the mitochondrial channel VDAC. *Nature* 399: 483-487, 1999.

271. **Siegmund B, Schlack W, Ladilov YV, Balser C, and Piper HM.** Halothane protects cardiomyocytes against reoxygenation-induced hypercontracture. *Circulation* 96: 4372-4379, 1997.

272. **Snow CM, Senior A, and Gerace L.** Monoclonal antibodies identify a group of nuclear pore complex glycoproteins. *The Journal of Cell Biology* 104: 1143-1156, 1987.

273. **Stanley WC, Lopaschuk GD, Hall JL, and McCormack JG.** Regulation of myocardial carbohydrate metabolism under normal and ischaemic conditions. Potential for pharmacological interventions. *Cardiovasc Res* 33: 243-257, 1997.

274. **Stanley WC, Lopaschuk GD, Hall JL, and McCormack JG.** Regulation of myocardial carbohydrate metabolism under normal and ischaemic conditions: Potential for pharmacological interventions. *Cardiovascular Research* 33: 243-257, 1997.

275. **Starling RC, Hammer DF, and Altschuld RA.** Human myocardial ATP content and in vivo contractile function. *Mol Cell Biochem* 180: 171-177, 1998.

276. **Steenbergen C, Murphy E, Levy L, and London RE.** Elevation in cytosolic free calcium concentration early in myocardial ischemia in perfused rat heart. *Circ Res* 60: 700-707, 1987.

277. **Steenbergen C, Murphy E, Watts JA, and London RE.** Correlation between cytosolic free calcium, contracture, ATP, and irreversible ischemic injury in perfused rat heart. *Circ Res* 66: 135-146, 1990.

278. **Steenbergen C, Perlman ME, London RE, and Murphy E.** Mechanism of preconditioning. Ionic alterations. *Circ Res* 72: 112-125, 1993.

279. **Su K, Roos MD, Yang X, Han I, Paterson AJ, and Kudlow JE.** An N-terminal region of Sp1 targets its proteasome-dependent degradation in vitro. *J Biol Chem* 274: 15194-15202, 1999.

280. **Su K, Yang X, Roos MD, Paterson AJ, and Kudlow JE.** Human Sug1/p45 is involved in the proteasome-dependent degradation of Sp1. *Biochem J* 348 Pt 2: 281-289, 2000.

281. **Sun D, Nguyen N, DeGrado TR, Schwaiger M, and Brosius FC, 3rd.** Ischemia induces translocation of the insulin-responsive glucose transporter GLUT4 to the plasma membrane of cardiac myocytes. *Circulation* 89: 793-798, 1994.

282. **Sviderskaya EV, Jazrawi E, Baldwin SA, Widnell CC, and Pasternak CA.** Cellular stress causes accumulation of the glucose transporter at the surface of cells independently of their insulin sensitivity. *J Membr Biol* 149: 133-140, 1996.

283. **Szegezdi E, Duffy A, O'Mahoney ME, Logue SE, Mylotte LA, O'Brien T, and Samali A.** ER stress contributes to ischemia-induced cardiomyocyte apoptosis. *Biochemical and Biophysical Research Communications* 349: 1406-1411, 2006.

284. **Szegezdi E, Logue SE, Gorman AM, and Samali A.** Mediators of endoplasmic reticulum stress-induced apoptosis. *EMBO Rep* 7: 880-885, 2006.

285. **Szkudelski T.** The mechanism of alloxan and streptozotocin action in B cells of the rat pancreas. *Physiol Res* 50: 537-546, 2001.

286. **Takagi H, Matsui Y, and Sadoshima J.** The role of autophagy in mediating cell survival and death during ischemia and reperfusion in the heart. *Antioxid Redox Signal* 9: 1373-1381, 2007.

287. **Taylor JP, Hardy J, and Fischbeck KH.** Toxic proteins in neurodegenerative disease. *Science* 296: 1991-1995, 2002.

288. **Taylor RP, Parker GJ, Hazel MW, Soesanto Y, Fuller W, Yazzie MJ, and McClain DA.** Glucose deprivation stimulates O-GlcNAc modification of proteins through up-regulation of O-linked N-acetylglucosaminyltransferase. *J Biol Chem* 283: 6050-6057, 2008.

289. **Terai K, Hiramoto Y, Masaki M, Sugiyama S, Kuroda T, Hori M, Kawase I, and Hirota H.** AMP-activated protein kinase protects cardiomyocytes against hypoxic injury through attenuation of endoplasmic reticulum stress. *Molecular and Cellular Biology* 25: 9554-9575, 2005.

290. **Teshima Y, Akao M, Jones SP, and Marban E.** Cariporide (HOE642), a Selective Na+-H+ Exchange Inhibitor, Inhibits the Mitochondrial Death Pathway. *Circulation* 108: 2275-2281, 2003.

291. **Teshima Y, Akao M, Jones SP, and Marban E.** Uncoupling Protein-2 Overexpression Inhibits Mitochondrial Death Pathway in Cardiomyocytes. *Circ Res* 93: 192-200, 2003.

292. **Thornton J, Striplin S, Liu GS, Swafford A, Stanley AW, Van Winkle DM, and Downey JM.** Inhibition of protein synthesis does not block myocardial protection afforded by preconditioning. *Am J Physiol* 259: H1822-1825, 1990.

293. **Thuerauf DJ, Marcinko M, Gude N, Rubio M, Sussman MA, and Glembotski CC.** Activation of the unfolded protein response in infarcted mouse heart and hypoxic cultured cardiac myocytes. *Circ Res* 99: 275-282, 2006.

294. **Toleman C, Paterson AJ, Shin R, and Kudlow JE.** Streptozotocin inhibits O-GlcNAcase via the production of a transition state analog. *Biochemical and Biophysical Research Communications* 340: 526-534, 2006.

295. **Toleman C, Paterson AJ, Whisenhunt TR, and Kudlow JE.** Characterization of the histone acetyltransferase (HAT) domain of a bifunctional protein with activable O-GlcNAcase and HAT activities. *J Biol Chem* 279: 53665-53673, 2004.

296. **Tong H, Chen W, London RE, Murphy E, and Steenbergen C.** Preconditioning enhanced glucose uptake is mediated by p38 MAP kinase not by phosphatidylinositol 3-kinase. *J Biol Chem* 275: 11981-11986, 2000.

297. **Tong H, Chen W, Steenbergen C, and Murphy E.** Ischemic preconditioning activates phosphatidylinositol-3-kinase upstream of protein kinase C. *Circ Res* 87: 309-315, 2000.

298. **Tong H, Rockman HA, Koch WJ, Steenbergen C, and Murphy E.** G protein-coupled receptor internalization signaling is required for cardioprotection in ischemic preconditioning. *Circ Res* 94: 1133-1141, 2004.

299. **Torres C and Hart G.** Topography and polypeptide distribution of terminal N-acetylglucosamine residues on the surfaces of intact lymphocytes. Evidence for O-linked GlcNAc. *J Biol Chem* 259: 3308-3317, 1984.

300. **Torres CR and Hart GW.** Topography and polypeptide distribution of terminal N-acetylglucosamine residues on the surfaces of intact lymphocytes. Evidence for O-linked GlcNAc. *J Biol Chem* 259: 3308-3317, 1984.

301. **Vanden Hoek T, Becker LB, Shao ZH, Li CQ, and Schumacker PT.** Preconditioning in cardiomyocytes protects by attenuating oxidant stress at reperfusion. *Circ Res* 86: 541-548, 2000.

302. **Vanden Hoek TL, Shao Z, Li C, Zak R, Schumacker PT, and Becker LB.** Reperfusion injury on cardiac myocytes after simulated ischemia. *Am J Physiol* 270: H1334-1341, 1996.

303. **Vander Heide RS, Hill ML, Reimer KA, and Jennings RB.** Effect of reversible ischemia on the activity of the mitochondrial ATPase: relationship to ischemic preconditioning. *Journal of molecular and cellular cardiology* 28: 103-112, 1996.

304. **Vander Heiden MG, Li XX, Gottleib E, Hill RB, Thompson CB, and Colombini M.** Bcl-xL promotes the open configuration of the voltage-dependent anion channel and metabolite passage through the outer mitochondrial membrane. *J Biol Chem* 276: 19414-19419, 2001.

305. **Vitadello M, Penzo D, Petronilli V, Michieli G, Gomirato S, Menabo R, Di Lisa F, and Gorza L.** Overexpression of the stress protein Grp94 reduces cardiomyocyte necrosis due to calcium overload and simulated ischemia. *FASEB J* 17: 923-925, 2003.

306. **Vocadlo DJ, Hang HC, Kim EJ, Hanover JA, and Bertozzi CR.** A chemical approach for identifying O-GlcNAc-modified proteins in cells. *Proc Natl Acad Sci U S A* 100: 9116-9121, 2003.

307. **Vosseller K, Wells L, Lane MD, and Hart GW.** Elevated nucleocytoplasmic glycosylation by O-GlcNAc results in insulin resistance associated with defects in Akt activation in 3T3-L1 adipocytes. *Proc Natl Acad Sci U S A* 99: 5313-5318, 2002.

308. **Wang Y, Meyer JW, Ashraf M, and Shull GE.** Mice with a null mutation in the NHE1 Na+-H+ exchanger are resistant to cardiac ischemia-reperfusion injury. *Circ Res* 93: 776-782, 2003.

309. **Weiss RG, de Albuquerque CP, Vandegaer K, Chacko VP, and Gerstenblith G.** Attenuated glycogenolysis reduces glycolytic catabolite accumulation during ischemia in preconditioned rat hearts. *Circ Res* 79: 435-446, 1996.

310. **Wells L, Gao Y, Mahoney JA, Vosseller K, Chen C, Rosen A, and Hart GW.** Dynamic O-Glycosylation of Nuclear and Cytosolic Proteins. Further characterization of

the nucleocytoplasmic beta -N-Acetylglucosaminidase, O-GlcNAcase. *J Biol Chem* 277: 1755-1761, 2002.

311. **Wells L, Kreppel LK, Comer FI, Wadzinski BE, and Hart GW.** O-GlcNAc transferase is in a functional complex with protein phosphatase 1 catalytic subunits. *J Biol Chem* 279: 38466-38470, 2004.

312. **Wells L, Vosseller K, Cole RN, Cronshaw JM, Matunis MJ, and Hart GW.** Mapping sites of O-GlcNAc modification using affinity tags for serine and threonine post-translational modifications. *Mol Cell Proteomics* 1: 791-804, 2002.

313. **Wells L, Vosseller K, and Hart GW.** A role for N-acetylglucosamine as a nutrient sensor and mediator of insulin resistance. *Cell Mol Life Sci* 60: 222-228, 2003.

314. **Werns SW and Lucchesi BR.** Myocardial ischemia and reperfusion: the role of oxygen radicals in tissue injury. *Cardiovasc Drugs Ther* 2: 761-769, 1989.

315. **Whelan SA and Hart GW.** Proteomic approaches to analyze the dynamic relationships between nucleocytoplasmic protein glycosylation and phosphorylation. *Circ Res* 93: 1047-1058, 2003.

316. **Whelan SA, Lane MD, and Hart GW.** Regulation of the O-linked beta-N-acetylglucosamine transferase by insulin signaling. *J Biol Chem* 283: 21411-21417, 2008.

317. **Whitworth GE, Macauley MS, Stubbs KA, Dennis RJ, Taylor EJ, Davies GJ, Greig IR, and Vocadlo DJ.** Analysis of PUGNAc and NAG-thiazoline as Transition State Analogues for Human O-GlcNAcase: Mechanistic and Structural Insights into Inhibitor Selectivity and Transition State Poise. *J Am Chem Soc* 129: 635-644, 2007.

318. **Woodfield K, Ruck A, Brdiczka D, and Halestrap AP.** Direct demonstration of a specific interaction between cyclophilin-D and the adenine nucleotide translocase confirms their role in the mitochondrial permeability transition. *Biochem J* 336 (Pt 2): 287-290, 1998.

319. **Wrabl JO and Grishin NV.** Homology between O-linked GlcNAc transferases and proteins of the glycogen phosphorylase superfamily. *J Mol Biol* 314: 365-374, 2001.

320. **Xu M, Wang Y, Hirai K, Ayub A, and Ashraf M.** Calcium preconditioning inhibits mitochondrial permeability transition and apoptosis. *Am J Physiol Heart Circ Physiol* 280: H899-908, 2001.

321. **Yamamoto K, Tsuji T, Matsumoto I, and Osawa T.** Structural requirements for the binding of oligosaccharides and glycopeptides to immobilized wheat germ agglutinin. *Biochemistry* 20: 5894-5899, 1981.

322. **Yang S, Zou LY, Bounelis P, Chaudry I, Chatham JC, and Marchase RB.** Glucosamine administration during resuscitation improves organ function after trauma hemorrhage. *Shock* 25: 600-607, 2006.

323. **Yang WH, Kim JE, Nam HW, Ju JW, Kim HS, Kim YS, and Cho JW.** Modification of p53 with O-linked N-acetylglucosamine regulates p53 activity and stability. *Nat Cell Biol* 8: 1074-1083, 2006.

324. **Yang X, Ongusaha PP, Miles PD, Havstad JC, Zhang F, So WV, Kudlow JE, Michell RH, Olefsky JM, Field SJ, and Evans RM.** Phosphoinositide signalling links O-GlcNAc transferase to insulin resistance. *Nature* 451: 964-969, 2008.

325. **Yang X, Su K, Roos MD, Chang Q, Paterson AJ, and Kudlow JE.** O-linkage of N-acetylglucosamine to Sp1 activation domain inhibits its transcriptional capability. *Proceedings of the National Academy of Sciences of the United States of America* 98: 6611-6616, 2001.

326. **Yang X, Zhang F, and Kudlow JE.** Recruitment of O-GlcNAc transferase to promoters by corepressor mSin3A: coupling protein O-GlcNAcylation to transcriptional repression. *Cell* 110: 69-80, 2002.

327. **Yellon DM and Baxter GF.** Reperfusion injury revisited: is there a role for growth factor signaling in limiting lethal reperfusion injury? *Trends Cardiovasc Med* 9: 245-249, 1999.

328. **Ylitalo KV, Ala-Rami A, Liimatta EV, Peuhkurinen KJ, and Hassinen IE.** Intracellular free calcium and mitochondrial membrane potential in ischemia/reperfusion and preconditioning. *Journal of molecular and cellular cardiology* 32: 1223-1238, 2000.

329. **Yusuf S, Hawken S, Ounpuu S, Dans T, Avezum A, Lanas F, McQueen M, Budaj A, Pais P, Varigos J, and Lisheng L.** Effect of potentially modifiable risk factors associated with myocardial infarction in 52 countries (the INTERHEART study): case-control study. *Lancet* 364: 937-952, 2004.

330. **Yuzwa SA, Macauley MS, Heinonen JE, Shan X, Dennis RJ, He Y, Whitworth GE, Stubbs KA, McEachern EJ, Davies GJ, and Vocadlo DJ.** A potent mechanism-inspired O-GlcNAcase inhibitor that blocks phosphorylation of tau in vivo. *Nature chemical biology* 4: 483-490, 2008.

331. **Zachara NE and Hart GW.** Cell signaling, the essential role of O-GlcNAc! *Biochimica et Biophysica Acta* 1761: 599-617, 2006.

332. **Zachara NE and Hart GW.** O-GlcNAc a sensor of cellular state: the role of nucleocytoplasmic glycosylation in modulating cellular function in response to nutrition and stress. *Biochimica et Biophysica Acta* 1673: 13-28, 2004.

333. **Zachara NE, O'Donnell N, Cheung WD, Mercer JJ, Marth JD, and Hart GW.** Dynamic O-GlcNAc modification of nucleocytoplasmic proteins in response to stress. A survival response of mammalian cells. *J Biol Chem* 279: 30133-30142, 2004.

334. **Zhang F, Su K, Yang X, Bowe DB, Paterson AJ, and Kudlow JE.** O-GlcNAc modification is an endogenous inhibitor of the proteasome. *Cell* 115: 715-725, 2003.

335. **Zhao ZQ, Corvera JS, Halkos ME, Kerendi F, Wang NP, Guyton RA, and Vinten-Johansen J.** Inhibition of myocardial injury by ischemic postconditioning during reperfusion: comparison with ischemic preconditioning. *Am J Physiol Heart Circ Physiol* 285: H579-588, 2003.

336. **Zhao ZQ and Vinten-Johansen J.** Postconditioning: reduction of reperfusion-induced injury. *Cardiovasc Res* 70: 200-211, 2006.

337. **Zou L, Yang S, Champattanachai V, Hu S, Chaudry IH, Marchase RB, and Chatham JC.** Glucosamine improves cardiac function following trauma-hemorrhage by increased protein O-GlcNAcylation and attenuation of NF-{kappa}B signaling. *Am J Physiol Heart Circ Physiol* 296: H515-523, 2009.

338. **Zou L, Yang S, Hu S, Chaudry IH, Marchase RB, and Chatham JC.** The protective effects of PUGNAc on cardiac function after trauma-hemorrhage are mediated via increased protein O-GlcNAc levels. *Shock* 27: 402-408, 2007.

339. **Zweier JL.** Measurement of superoxide-derived free radicals in the reperfused heart. Evidence for a free radical mechanism of reperfusion injury. *J Biol Chem* 263: 1353-1357, 1988.

340. **Zweier JL, Flaherty JT, and Weisfeldt ML.** Direct measurement of free radical generation following reperfusion of ischemic myocardium. *Proceedings of the National Academy of Sciences of the United States of America* 84: 1404-1407, 1987.

CURRICULUM VITAE

GLADYS AFOR NGOH

PHD student

Professional Address: Department of Medicine - Division of Cardiovascular Medicine

Institute of Molecular Cardiology
University of Louisville School of Medicine
580 South Preston Street
Baxter II- 409
Louisville, KY 40202
Phone: 502-852-8071
Fax: 502-852-8070
Email: gnafor01@gwise.louisville.edu

Place of birth: Yaoundé, Central Province, Cameroon.

Visa Status: Permanent Resident, USA

Education & training: Division of Cardiovascular Medicine (Dr. Steven P. Jones)

University of Louisville, KY
Ph.D. in Physiology
Anticipated Graduation - December 2009

Department of Life Sciences
University of Buea, Cameroon
B.S. in Microbiology, 2001-2004

Professional appointment:

2005-Present	Doctoral Student, Department of Physiology and Biophysics University of Louisville

Award and Honors

2007 – 2009	American Heart Association Predoctoral Fellowship Grant Award – Great Rivers Affiliate (0715493B)
2008	American Society for Pharmacology and Experimental Therapeutics Cardiovascular Division Young Investigator Finalist
2005 – 2007	Integrated Programs in Biomedical Sciences (IPIBS) Doctoral Fellowship
2006	American Heart Association Basic Cardiovascular Sciences Minority Travel Grant Awards
2004	Best Female Science Student, graduating class of 2004 by Les Brasseries du Cameroon
2003	Financial Aid for outstanding performance by Ministry for Higher Education, Cameroon
2002	Financial Aid for outstanding performance by Ministry for Higher Education, Cameroon

Manuscripts

1) **Ngoh G A**, Facundo H T, and Jones S P. O-GlcNAc Signaling in the Cardiovascular System. *2009. (Review Circ Res, in preparation)*

2) **Ngoh G A,** Watson L J and Jones S P. O-GlcNAc Signaling Modulates Hypoxia-Induced Calcium Overload and Oxidative Stress. 2009. *(in preparation)*

3) **Ngoh G A,** Schaller S A and Jones S P. TRO40303 Attenuates Oxidant-Induced Mitochondrial Dysfunction. *2009. (JPET in review)*

4) Watson L J, Facundo H T, **Ngoh G A**, Prabhu S D, Xuan Y T, Jones S P. Hexosamine Signaling is Indispensable in the Failing Heart. *2009. (PNAS, in revision)*

5) Facundo H T, Watson L J, Brainard R E, **Ngoh G A**, and Jones S P. O-Glycosylation Contributes to Peroxisome Proliferator-Activated Receptor-gamma Coactivator (PGC)-1alpha Suppression During Cardiac Hypertrophy. *2009. (Circ Res, in revision)*

6) **Ngoh G A**, Tariq H, Prabhu S D, and Jones S P. O-GlcNAc Signaling Attenuates ER Stress-Induced Cardiomyocyte Death. *2009. (AJP, in press)*

7) **Ngoh G A**, Hamid T, Facundo H T, Dillmann W, Zachara N E, Jones S P. Unique Hexosaminidase Reduces Metabolic Survival Signal and Sensitizes Cardiac Myocytes to Hypoxia-Reoxygenation Injury. *2009. Circ Res. 104(1):41-9*

8) **Ngoh G A**, Jones S P. New Insights into Metabolic Signaling and Cell Survival: The Role of O-GlcNAc. 2008. *J Pharmacol Exp Ther. 327(3):602-9*

9) **Ngoh G A**, Watson L J, Facundo H T, Dillmann W, Jones S P. Noncanonical Glycosyltransferase *Modulates* Post-Hypoxic Cardiac Myocyte Death And Mitochondrial Permeability Transition. 2008. *J Mol Cell Cardiol. 45(2):313-25.9*

10) Jones S P, Zachara N E, **Ngoh G A**, Hill B G, Teshima Y, Bhatnagar A, Hart G W, Marbán E. Cardioprotection by N-acetylglucosamine Linkage to Cellular Proteins. 2008. *Circulation 117: 1172-1182*

Abstracts

1) **Ngoh G A** and Jones S P. O-GlcNAc Signaling Attenuates Post-Hypoxic Calcium Overload and Oxidative Stress in Cardiac Myocytes. *Circulation in press.*

2) **Ngoh G A**, Tariq H, Prabhu S D, and Jones S P. Hexosamine Signaling Reduces ER Stress Induced Cardiomyocyte Death. *FASEB J. 2009 23:991.7.*

3) **Ngoh G A,** Schaller S A. and Jones S P. TRO40303 Attenuates Oxidant-Induced Mitochondrial Dysfunction. *FASEB J. 2009 23:LB71.*

4) **Ngoh G A** and Jones S P. O-GlcNAc Signaling Attenuates Mitochondrial Mediated Post-Hypoxic Cardiac myocyte Injury. *2009 KIEC Annual Conference.*

5) Tariq H, **Ngoh G A**, Robertson A L, Prabhu S D, and Jones S P. Metabolic Survival Signal Rescues Cardiac Myocytes from ER Stress-Induced Death. *Circulation. 2008. 118: S_272.*

6) Watson L J, Facundo H T, **Ngoh G A**, Hamid T, Prabhu S D, Xuan Y-T, Jones S P. O-GlcNAc Transferase is Indispensable in Heart Failure. *Circulation.* 2008. *118: S_442.*

7) **Ngoh G A** and Jones S P. *O*-GlcNAc Signaling Attenuates Mitochondrial Permeability Transition. *FASEB J.* 2008. 22:1130.8.

8) **Ngoh G A**, Watson L J, and Jones S P. Loss of *O*-GlcNAc Transferase Activity Sensitizes Cardiac Myocytes to Post-Hypoxic Death. *FASEB J. 2008. 22:750.10.*

9) Watson L J, **Ngoh G A**, Zhu Y, Campbell A, Xuan Y-T, Jones S P. Paradoxical Reduction in Glycosylation Sensitizes the Diabetic Heart to Mitochondrial Permeability Transition. *Circulation.* 2007. *116: II_121.*

10) **Ngoh G A**, Watson L J, Jones S P. *O*-GlcNAc Transferase is a Pro-Survival Enzyme in Post-Hypoxic Cardiac Myocytes. *FASEB J.* 2007. *21:726.6.*

11) **Ngoh G A**, Watson L J, Jones S P. *O*-GlcNAcase Exacerbates Post-Hypoxic Cardiac Myocyte Death. *FASEB J.* 2007. *21:959.9.*

12) **Ngoh G A**, Watson L J, Harrison L T, Jones S P. Degradation of Metabolic Post-Translational Modification Sensitizes Cardiac Myocytes to Hypoxia. *Circulation* 2006. *114: 114: II_99.*

Professional Memberships

- American Heart Association (Basic Sciences Council)
- American Physiological Society (Cardiovascular)
- American Society of Pharmacology & Experimental Therapeutics (Cardiovascular)

Invited Presentations *(includes abstract oral presentations)*

10/09/2008: Presented "O-GlcNAc Signaling: Novel Cardioprotective Signal" at the Research Seminar Series, Department of Physiology and Biophysics, University of Louisville School of Medicine, Louisville, KY.

04/09/2008: Presented "O-GlcNAc Signaling Attenuates Mitochondrial Permeability Transition" at the "Mitochondria in Life and Death: From Biogenesis to Autophagy" symposium. Experimental Biology Meeting. San Diego, CA.

04/08/2008: Presented "O-GlcNAc Signaling Attenuates Mitochondrial Permeability Transition" at the 2008 ASPET Cardiovascular Division Graduate Student Best Abstract Competition. Experimental Biology Meeting. San Diego, CA

01/22/2008: Presented "The Role of O-GlcNAc Signaling in Acute Myocardial Ischemia" at the Research Seminar Series, Department of Physiology and Biophysics, University of Louisville School of Medicine, Louisville, KY.

09/01/2009: Presented "Glycosylation and Myocardial Ischemia-Reperfusion Injury" at the Research Seminar Series, Department of Physiology and Biophysics, University of Louisville School of Medicine, Louisville, KY.